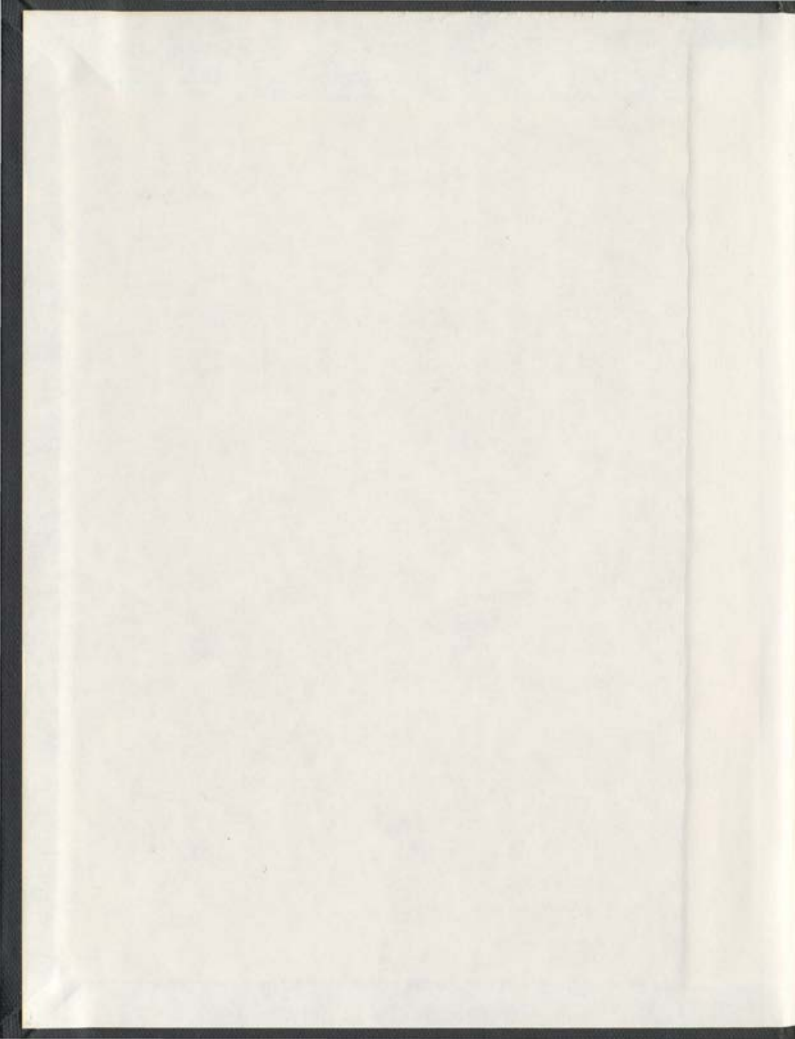
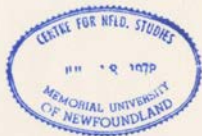


ROLE OF LYMPHATIC SYSTEM IN THE PERSISTENCE  
AND PATHOGENESIS OF WOODCHUCK HEPATITIS  
VIRUS INFECTION

SHASHI ASHOK GUJAR



001311



**ROLE OF LYMPHATIC SYSTEM IN THE PERSISTENCE AND  
PATHOGENESIS OF WOODCHUCK HEPATITIS VIRUS INFECTION**

©

by

**SHASHI ASHOK GUJAR**

**A thesis submitted to the School of Graduate Studies in partial fulfilment of  
the requirements for the degree of**

**Doctor of Philosophy**

**Faculty of Medicine**

**Memorial University of Newfoundland**

**September 2008**

**St. John's**

**Newfoundland**

## ABSTRACT

Hepatitis B virus (HBV) causes acute liver inflammation that apparently resolves completely or advances to chronic hepatitis, cirrhosis and hepatocellular carcinoma. These differential outcomes of HBV infection are orchestrated to a large extent by the virus-specific T cell responses, which characteristically appear late after exposure to hepadnavirus. In this context, the objective of this study was to delineate the kinetics and understand inter-relationships between virus-specific and non-specific T cell proliferative, humoral as well as innate cytokine responses, along with serological and molecular markers of hepadnaviral infection induced after exposure and re-exposure to liver pathogenic or nonpathogenic doses of woodchuck hepatitis virus (WHV). Our results revealed that infection of woodchucks with either a liver pathogenic ( $>10^3$  virions) or nonpathogenic ( $<10^3$  virions) dose of WHV induced strong, but delayed, virus-specific T cell responses with comparable kinetics. Interestingly, immediately after exposure to virus, the non-specific proliferative capacity of lymphocytes in response to mitogenic stimulation was heightened and then subsided preceding the appearance of WHV-specific T cell response. This augmented non-specific proliferative reactivity was accompanied by the increased expression of interferon-alpha (IFN- $\alpha$ ), interleukin-12 (IL-12) and IL-2 in circulating lymphoid cells; while its decline was associated with activation-induced cell death of lymphocytes. Importantly, the postponement of virus-specific T cell response coincided with the absence of TNF- $\alpha$  expression, while its rise was marked by

synchronously elevated expression of TNF- $\alpha$ , IFN- $\alpha$ , IFN- $\gamma$ , IL-2, IL-12, and IL-10 in lymphoid cells. Nonetheless, the virus-specific T cell responses induced during low-dose (occult) infection, in contrast to infection caused by liver pathogenic dose, did not provide protection against viral hepatitis.

We conclude that hepadnavirus infections induce delayed virus-specific T cell proliferative responses irrespective of the dose of invading virus and symptomatic or asymptomatic outcome of the infection. This postponement of anti-viral T cell responses is preceded by the aberrant activation of lymphocyte and innate cytokine responses. Such an impaired activation of immune responses following hepadnavirus infection represents a possible mechanism that allows evasion of initial clearance and subsequent elimination of virus, permits its dissemination, and contributes to the establishment of persistence.

## ACKNOWLEDGEMENTS

It is difficult to explain my gratitude towards my mentor, Dr. Thomas Michalak. He not only supervised my Ph.D. work with a great enthusiasm and dedication, but also shaped my outlook on science and on my life. His encouragement, sound advice and constructive criticism has greatly inspired me, without which this work simply would not have been possible. I thank him from the bottom of my heart.

I wish to express my sincere regards and thanks to my supervisory committee members, Dr. Michael Grant and Dr. Sheila Drover, for their continuous support and scientific advice. I would also like to thank School of Graduate Studies and Faculty of Medicine at Memorial University for a financial contribution to my fellowship.

I wish to thank my fellow friends, Trish, Jinguo, Tram, Cliff, Adam and Mohamed for their help, support and friendship. I want to extend my acknowledgements to Norma Churchill for her help and, to Collen Trelegan for her animal care expertise.

I express very hearty thanks to Sonya, who has always gone the distance to help me in every possible way, both at work and in my life; and I deeply appreciate and cherish her friendship.

Since my arrival in Canada in year 2001, many people have helped me in many different ways to make me feel like I was home. Apart from all lovely Newfoundlanders that I have met, my humble thanks to Krista and my extended

Locke family, who have played an important part in my "Canadian" life. They gave me "home away from home" and have been there for me with their unconditional love, for which I will always be indebted to them.

I also wish to convey the deepest appreciation to my loving parents, Aai and Bhau, grandparents, Aai and Dada, and my brother, Sachin. They have been through a lot of hardships in their lives just to see me here. Without their love and support, I would not be where I am today, and for that I owe them everything that I have in my life. To them I dedicate this thesis.

## TABLE OF CONTENTS

### ACKNOWLEDGEMENTS

### LIST OF TABLES

### LIST OF FIGURES

### ABBREVIATIONS AND SYMBOLS

### LIST OF APPENDICES

### CO-AUTHORSHIP STATEMENT

### CHAPTER ONE: INTRODUCTION

1.1 HISTORICAL BACKGROUND OF VIRAL HEPATITIS.....	1
1.2 EPIDEMIOLOGY OF HBV INFECTION.....	2
1.3 HBV AND OTHER MEMBERS OF HEPADNAVIRUS FAMILY.....	5
1.4 GENERAL ORGANIZATION OF HEPADNAVIRUSES.....	6
1.4.1 Genome organization.....	6
1.4.2 Viral proteins.....	10
1.5 REPLICATION OF HEPADNAVIRUSES.....	13
1.6 MODELS OF HBV INFECTION.....	14
1.6.1 Woodchuck model of HBV infection.....	14
1.6.2 Other natural models of hepatitis B infection.....	17
1.6.3 HBV transgenic mouse model.....	17
1.7 THE COURSE OF HEPADNAVIRAL-INDUCED LIVER DISEASE.....	20
1.7.1 Serologically evident infection.....	20
1.7.2 Occult infection.....	22
1.8 IMMUNOLOGY OF HEPADNAVIRUS INFECTION.....	24
1.8.1 General concepts in immunity to viruses.....	24
1.8.1.1 Innate immune response.....	25
1.8.1.2 Adaptive Immune response.....	27
1.8.1.2.1 T cell immunity.....	27
1.8.1.2.2 B cell immunity.....	28

1.8.1.3 Cytokines.....	29
1.8.2 Immune responses to hepadnavirus infection.....	30
1.8.2.1 Innate immunity against hepadnavirus infections.....	30
1.8.2.1.1 Granulocytes.....	30
1.8.2.1.2 NK cells.....	31
1.8.2.1.3 NKT cells.....	36
1.8.2.1.4 Antigen presenting cells.....	39
1.8.2.2 Adaptive immunity against hepadnaviruses.....	40
1.8.2.2.1 Cellular immunity.....	40
1.8.2.2.1.1 CD8 T cell response.....	40
1.8.2.2.1.2 CD4 T cell response.....	45
1.8.2.2.2 Humoral immunity.....	48
1.8.2.3 Cytokine responses during hepadnavirus infection.....	51
1.9 PURPOSE OF THE STUDY.....	55
<b>CHAPTER TWO:GENERAL MATERIALS AND METHODS.....</b>	<b>58</b>
2.1 ANIMALS AND VIRUS INOCULUM.....	58
2.1.1 Woodchucks.....	58
2.1.2 WHV inocula.....	59
2.1.3 Infection of woodchucks.....	59
2.2 SAMPLE COLLECTION.....	59
2.2.1 Blood collection.....	59
2.2.2 Serum isolation.....	60
2.2.3 Isolation and storage of peripheral blood mononuclear cells.....	60
2.2.4 Liver biopsies.....	61
2.2.5 Collection of specimens at autopsy.....	61
2.3 ASSAYS FOR THE SEROLOGICAL MARKERS OF WHV INFECTION.....	62
2.3.1 Detection of WHV DNA.....	62
2.3.1.1 Isolation of WHV DNA.....	62
2.3.1.2 Amplification of WHV DNA.....	62
2.3.1.3 Detection of WHV DNA.....	64
2.3.1.3.1 Agarose gel electrophoresis.....	64
2.3.1.3.2 Southern blot hybridization.....	64
2.3.2 Detection of WHV surface antigen (WHsAg).....	66
2.3.3 Detection of antibodies to WHV surface antigen (anti-WHs).....	66
2.3.4 Detection of antibodies to WHV core antigen (anti-WHc).....	68
2.3.5 Measurement of sorbitol dehydrogenase (SDH).....	69
2.4 PRODUCTION OF RECOMBINANT WHV PROTEINS.....	71

2.4.1	Cloning of cDNAs encoding for WHV proteins in plasmid vectors..	71
2.4.1.1	Cloning of WHc, WHe and WHx cDNAs in PCR II vector.	71
2.4.1.2	Plasmid isolation and enzymatic manipulations.....	72
2.4.1.3	Restriction enzyme digestion analysis.....	74
2.4.1.4	Purification of WHV gene inserts.....	75
2.4.1.5	Subcloning to generate recombinant WHV proteins.....	75
2.4.2	Expression and purification of recombinant WHV proteins.....	76
2.4.2.1	Induction of recombinant protein expression in <i>E. Coli</i> .....	76
2.4.2.2	Preparation of inclusion bodies.....	77
2.4.2.3	SDS-PAGE and Western blotting.....	77
2.4.2.4	Affinity chromatography purification.....	79
2.4.2.5	Refolding of purified recombinant proteins.....	80
2.4.2.6	Quantitation of recombinant proteins.....	80
2.5	PROCUREMENT OF OTHER WHV ANTIGENS AND MITOGENS.....	81
2.5.1	Purification of WHsAg.....	81
2.5.2	Immunodominant WHc <sub>97-110</sub> peptide.....	83
2.5.3	Mitogens.....	83
2.6	REAL TIME POLYMERASE CHAIN REACTION (PCR).....	83
2.6.1	Isolation of RNA.....	84
2.6.2	Preparation of cDNA.....	85
2.6.3	Real time PCR.....	85
2.7	HISTOLOGICAL EXAMINATION OF LIVER TISSUE SAMPLES.....	86
<b>CHAPTER 3: FLOW CYTOMETRIC QUANTITATION OF T CELL PROLIFERATION AND DIVISION KINETICS IN WOODCHUCK MODEL OF HEPATITIS B.....</b>		<b>88</b>
3.0	SUMMARY.....	88
3.1	INTRODUCTION.....	89
3.2	MATERIALS AND METHODS.....	92
3.2.1	Animals.....	92
3.2.2	PBMC isolation.....	93
3.2.3	Mitogens and antigens.....	94
3.2.4	Cell CFSE labeling and culture.....	94
3.2.5	Flow cytometry analysis.....	95
3.2.6	Adenine incorporation lymphocyte proliferation assay.....	96
3.3	RESULTS.....	97

3.3.1	Effects of CFSE on woodchuck PBMC survival.....	97
3.3.2	Comparison of CFSE profiles of woodchuck and human PBMC....	98
3.3.3	Assessment of analytical suitability of CFSE-labelled woodchuck lymphocytes.....	99
3.3.4	Determination of optimal culture time of CFSE-labelled PBMC....	102
3.3.5	Determination of optimal mitogen concentrations for assessing CFSE-labelled lymphocyte proliferation.....	105
3.3.6	Measurement of WHV-specific lymphocyte proliferation.....	111
3.3.7	Evaluation of WHV-specific T cell responses using CFSE assay.....	114
3.3.8	Comparison of CFSE and <sup>3</sup> H-adenine incorporation assay.....	118
3.4	DISCUSSION.....	122
<b>CHAPTER 4: CHARACTERIZATION OF BIOACTIVE RECOMBINANT WOODCHUCK INTERLEUKIN-2 AMPLIFIED BY RLM-RACE AND PRODUCED IN EUKARYOTIC EXPRESSION SYSTEM.....</b>		<b>127</b>
4.0	SUMMARY.....	127
4.1	INTRODUCTION.....	128
4.2	MATERIALS AND METHODS.....	131
4.2.1	Source of wL-2 RNA.....	131
4.2.2	Amplification of wL-2 cDNA fragment.....	131
4.2.3	Generation of full-length wL-2 cDNA by RLM-RACE and determination of its sequence.....	132
4.2.4	Expression of rwL-2 in <i>E. coli</i> .....	133
4.2.5	Expression of rwL-2 in insect cells.....	135
4.2.6	Assays measuring rwL-2-induced T cell proliferation.....	139
4.2.7	Assay with CTLL-2 cells.....	140
4.2.8	Production of anti-rwL-2 antibodies.....	141
4.2.9	SDS-PAGE and Western blot analyses.....	141
4.3	RESULTS.....	142
4.3.1	Determination of the complete wL-2 cDNA sequence.....	142
4.3.2	Expression of mature rwL-2 in <i>E. coli</i> .....	147
4.3.3	Expression of precursor rwL-2 in the baculovirus-insect cell system.....	151
4.3.4	Induction of woodchuck T cell proliferation by bac-rwL-2.....	154
4.3.5	Survival of IL-2-dependent CTLL-2 cells in the presence of bac-rwL-2.....	158
4.4	DISCUSSION.....	158

<b>CHAPTER 5: ABERRANT LYMPHOCYTE ACTIVATION PRECEDES DELAYED VIRUS-SPECIFIC T CELL RESPONSE AFTER BOTH PRIMARY INFECTION AND SECONDARY EXPOSURE TO HEPADNAVIRUS IN WOODCHUCK MODEL OF HEPATITIS B</b> .....	166
5.0 SUMMARY.....	166
5.1 INTRODUCTION.....	167
5.2 MATERIALS AND METHODS.....	170
5.2.1 Animals and WHV inoculations.....	170
5.2.2 Sample collection.....	172
5.2.3 Serological and WHV DNA detection assays.....	172
5.2.4 WHV antigens and mitogens for T cell proliferation assays.....	173
5.2.5 Adenine-incorporation T cell proliferation assay.....	173
5.2.6 CFSE-flow cytometry T cell proliferation assay.....	175
5.2.7 CFSE/annexin-V-PE/7-AAD assay for simultaneous detection of T cell proliferation and apoptosis.....	176
5.2.8 Real-time RT-PCR.....	177
5.2.9 Statistical analysis.....	178
5.3 RESULTS.....	178
5.3.1 Serological and WHV DNA profiles after primary and multiple exposures to WHV.....	178
5.3.2 Both primary infection and challenge with WHV induce delayed virus-specific T cell response.....	184
5.3.3 Lymphocyte generalized proliferative capacity increases immediately after primary and subsequent exposures to WHV.....	185
5.3.4 Immediate augmented lymphocyte generalized proliferative and delayed virus-specific T cell responses are consistently induced by WHV infection.....	193
5.3.5 Decline in T cell generalized proliferation capacity coincides with increased activation-induced cell death.....	197
5.3.6 Cytokine and cell marker gene expression profiles in unmanipulated circulating lymphoid cells.....	200
5.3.7 WHV replication peaks in lymphoid cells after their increased susceptibility to activation-induced death subsides.....	205
5.4 DISCUSSION.....	208

**CHAPTER 6: PRIMARY OCCULT HEPADNAVIRUS INFECTION INDUCES**

<b>VIRUS-SPECIFIC T CELL PROLIFERATIVE AND ABERRANT CYTOKINE RESPONSES IN THE WOODCHUCK MODEL OF HEPATITIS B</b> .....	220
6.0 SUMMARY.....	220
6.1 INTRODUCTION.....	221
6.2 MATERIALS AND METHODS.....	228
6.2.1 Animals.....	228
6.2.2 Inoculation, challenge and re-challenge with WHV.....	228
6.2.3 Sample collection and PBMC isolation.....	231
6.2.4 Serological and molecular markers of WHV infection.....	232
6.2.5 Liver biopsies and histopathology.....	232
6.2.6 WHV antigens and T cell mitogens.....	233
6.2.7 CFSE-based flow cytometry T cell proliferation assay.....	234
6.2.8 Adenine incorporation T lymphocyte proliferation assay.....	235
6.2.9 Real time RT-PCR analysis of gene expression.....	236
6.2.10 Statistical analysis.....	237
6.3 RESULTS.....	237
6.3.1 Infection with low WHV dose induces serologically silent but WHV DNA evident primary occult infection.....	237
6.3.2 POI is accompanied by delayed WHV-specific T cell response similarly as in symptomatic WHV infection.....	244
6.3.3 Heightened T cell proliferation in response to mitogenic stimuli follows inoculation with WHV independently of virus dose administered.....	251
6.3.4 Induction of POI and subsequent challenge with WHV are accompanied by aberrant expression of cytokines in peripheral lymphoid cells.....	258
6.3.5 Hepatic expression of IFN- $\alpha$ but not IFN- $\gamma$ or TNF- $\alpha$ is upregulated during POI.....	263
6.4 DISCUSSION.....	266
<b>CHAPTER 7: SUMMARY AND FUTURE DIRECTIONS</b> .....	277
7.1 SUMMARY.....	277
7.2 FUTURE DIRECTIONS.....	292
<b>REFERENCES</b> .....	296

**APPENDIX A:** Complete cDNA sequence of woodchuck interleukin-2 (wIL-2)  
discovered during this study.....326

**APPENDIX B:** Frequently used molecular biology buffers and reagents.....327

## LIST OF TABLES

<b>Table 5.1</b> Sequences of WHV and woodchuck gene-specific PCR primers used in this study.....	179
---	-----

## LIST OF FIGURES

<b>Figure 1.1</b> Schematic representations of HBV and WHV genomic structures.....	8
<b>Figure 3.1</b> Comparison of flow cytometric profiles of human and woodchuck PBMC labeled with CFSE.....	100
<b>Figure 3.2</b> Flow cytometric quantification of proliferation and daughter cell generations of mitogen-stimulated woodchuck lymphocytes.....	103
<b>Figure 3.3</b> Determination of optimal culture time for CFSE-labeled woodchuck lymphocytes.....	106
<b>Figure 3.4</b> Determination of optimum concentration ranges of mitogens to evaluate proliferative potency of CFSE-labelled woodchuck lymphocytes.....	108
<b>Figure 3.5</b> WHV-specific T lymphocyte proliferation profiles determined by flow cytometry.....	112
<b>Figure 3.6</b> Evaluation of WHV-specific T cell responses using CFSE assay.....	115
<b>Figure 3.7</b> Comparison of sensitivity of CFSE and $^3\text{H}$ -adenine incorporation assays in detecting T cell proliferation responses.....	119
<b>Figure 4.1</b> Schematic comparison of IL-2 sequences and their structural organizations in different mammalian species.....	137
<b>Figure 4.2</b> Alignments of woodchuck IL-2 nucleotide and amino acid sequences with those of human, mouse and rabbit IL-2.....	144
<b>Figure 4.3</b> SDS-PAGE and Western blot analyses of <i>ec-rwIL-2</i> produced in <i>E. coli</i> expression system.....	149
<b>Figure 4.4</b> PCR and Western blot analyses of <i>bac-rwIL-2</i> DNA or <i>bac-rwIL-2</i> protein in culture supernatants from Sf9 insect cells.....	152
<b>Figure 4.5</b> Proliferation and daughter cell generation in woodchuck T lymphocytes treated with <i>bac-rwIL-2</i> .....	156
<b>Figure 4.6</b> Quantification of <i>bac-rwIL-2</i> activity in bioassay with CTLL-2 cells.....	159
<b>Figure 5.1</b> General outline of the experimental protocols showing time points of	

injections with WHV, serum, PBMC and liver biopsy collections, serological markers of WHV infection and serum WHV DNA detected, hepatic WHV loads, and the results on liver histology after primary infection and challenge with WHV.....	181
<b>Figure 5.2</b> The kinetics of WHV-specific T cell proliferative responses against WHV antigens in woodchucks belonging to study Group A which were infected, challenged and re-challenged with WHV.....	186
<b>Figure 5.3</b> The kinetics of mitogen-induced (generalized) T lymphocyte proliferation in woodchucks after primary infection, challenge and re-challenge with WHV.....	189
<b>Figure 5.4</b> Discordance between the kinetics of WHV-specific and generalized T cell proliferative responses during primary WHV infection and after challenge and re-challenge with WHV.....	191
<b>Figure 5.5</b> Patterns of WHV-specific and ConA-induced T cell responses in Group B woodchucks during self-limited acute WHV infection.....	196
<b>Figure 5.6</b> Activation-induced apoptosis of lymphoid cells during progression of acute WHV infection.....	198
<b>Figure 5.7</b> Expression profiles of genes encoding cytokines and immune cell surface markers in serial unmanipulated PBMC samples collected from the woodchucks investigated.....	202
<b>Figure 5.8</b> WHV mRNA loads in serial,unmanipulated lymphoid cell samples collected during different phases of acute WHV infection from Group B animals.....	206
<b>Figure 6.1</b> Schematic representation of the experimental protocol used to infect and challenge woodchucks with liver pathogenic (Group A) and liver nonpathogenic (Group B) doses of WHV.....	229
<b>Figure 6.2</b> The profiles of serological markers of WHV infection and WHV DNA detection in sera and liver tissue samples in animals belonging to Group A and Group B.....	238
<b>Figure 6.3</b> The kinetics of WHV-specific T cell proliferative responses in woodchucks infected with liver pathogenic and nonpathogenic doses of WHV.....	245

<b>Figure 6.4</b> The comparative kinetics of mitogen-induced (virus nonspecific) and WHV-specific T cell proliferative responses in woodchucks infected with high (liver pathogenic) and low (liver nonpathogenic) doses of WHV.....	255
<b>Figure 6.5</b> A quantitative analysis of cytokine gene expression in circulating lymphoid cells in animals during different phases of WHV POI and their subsequent challenge with either low (liver nonpathogenic) or high (liver pathogenic) dose of WHV.....	260
<b>Figure 6.6</b> The hepatic expression of selected cytokines and CD3 during POI and after challenge with either high or low dose of WHV or injection with PBS.....	264
<b>Figure 7.1</b> A proposed model depicting impaired immune responses occurring during hepadnavirus infection.....	284

## ABBREVIATIONS AND SYMBOLS

ADCC	antibody-dependent cellular cytotoxicity
AH	acute hepatitis
ALT	alanine aminotransaminase
anti-wL-2	antibodies to woodchuck interleukin-2
anti-HBc	antibodies to hepatitis B virus core antigen
anti-HBe	antibodies to hepatitis B virus e antigen
anti-HBs	antibodies to hepatitis B virus surface antigen
anti-WHc	antibodies to woodchuck hepatitis virus core antigen
anti-WHe	antibodies to woodchuck hepatitis virus e antigen
anti-WHs	antibodies to woodchuck hepatitis virus surface antigen
APC	antigen presenting cell
ASGPR	asialoglycoprotein receptor
AST	aspartate aminotransferase
bp	base pairs
C	core gene of HBV or WHV
cccDNA	covalently closed circular DNA
CD	cluster of differentiation
CFSE	5-(and-6)-carboxyfluorescein diacetate succinimidyl ester
CH	chronic hepatitis
CMV	cytomegalovirus
cpm	counts per minute
CTL	cytotoxic T lymphocyte
DC	dendritic cells
DHBV	duck hepatitis B virus
DMSO	dimethyl sulfoxide
dNTP	deoxynucleotide triphosphate
EB	ethidium bromide
EBV	Epstein-Barr virus
EDTA	ethylenediaminetetraacetic acid
ELISA	enzyme-linked immunosorbent assay
ER	endoplasmic reticulum
FasL	Fas ligand
FACS	fluorescence activated cell sorting
FCS	fetal calf serum
FITC	fluorescein isothiocyanate
<i>g</i>	gravity units of force (9.8 m/s <sup>2</sup> )
GM-CSF	granulocyte-monocyte colony-stimulating factor
GSHV	ground squirrel hepatitis virus
hr	hour
HBcAg	hepatitis B virus core antigen
HBeAg	hepatitis B virus e antigen
HBsAg	hepatitis B virus surface antigen

HBSS	Hanks' balanced salt solution
HBV	hepatitis B virus
HCC	hepatocellular carcinoma
HCV	hepatitis C virus
HIV	human immunodeficiency virus
HPV	human papilloma virus
HRPO	horseradish peroxidase
HSV	herpes simplex virus
IFN $\alpha$	interferon alpha
IFN $\beta$	interferon beta
IFN $\gamma$	interferon gamma
Ig	immunoglobulin
IL	interleukin
i.v.	intravenous
kb	kilobase pairs
LCMV	lymphocytic choriomeningitis virus
MAMP	microbe-associated molecular patterns
MCMV	murine cytomegalovirus
MHC	major histocompatibility complex
min	minute
MMLV-RT	Moloney murine leukemia virus- reverse transcriptase
mo	months
NK	natural killer cell
nm	nanometres
ORF	open reading frame
P	polymerase gene of HBV or WHV
PBMC	peripheral blood mononuclear cells
PBS	phosphate buffered saline
PCR	polymerase chain reaction
PCR/NAH	nested PCR followed by Southern blot nucleic acid hybridization
p.i.	post-infection
POI	primary occult infection
preS1	large surface protein
preS2	middle surface protein
PRR	pattern recognition receptor
rcDNA	relaxed circular DNA
rpm	revolutions per minute
RT	reverse transcriptase
rWHV DNA	recombinant woodchuck hepatitis virus DNA
S	surface/envelope gene of HBV or WHV
SDH	sorbitol dehydrogenase
sec	seconds
SEM	standard error mean

SLAH	self-limited acute hepatitis
SOI	secondary occult infection
SSC	standard saline citrate
ss	single stranded
sssDNA	sonicated salmon sperm DNA
TCR	T-cell receptor
Th	helper T cell
Th1	T helper type 1
Th2	T helper type 2
TLR	toll-like receptor
TNF $\alpha$	tumor necrosis factor alpha
TRAIL	TNF-related apoptosis-inducing ligand
U	units
UV	ultraviolet
vge	virus genome equivalents
VZV	varicella-zoster virus
WHcAg	woodchuck hepatitis virus core antigen
WHeAg	woodchuck hepatitis virus e antigen
WHsAg	woodchuck hepatitis virus surface antigen
WHV	woodchuck hepatitis virus
X	X gene of HBV or WHV

## CO-AUTHORSHIP STATEMENT

All the research work presented in this thesis was primarily performed by the author that comprised of designing the research proposal and protocols in collaboration with the supervisor, performing experiments, collecting and analyzing the data and, writing the manuscripts. Most of the work described here has been published in peer reviewed articles, except for data presented in chapter 6. The publication details on these articles are mentioned in respective chapters and, the contribution of co-authors is acknowledged in this statement. Chapter 3 entitled "**Flow cytometric quantitation of T cell proliferation and division kinetics in woodchuck model of hepatitis B**" by S. A. Gujar and T. I. Michalak, was published in *Immunological Investigations* volume 34, issue 2 in May 2005. Chapter 4 entitled "**Characterization of bioactive recombinant woodchuck interleukin-2 amplified by RLM-RACE and produced in eukaryotic expression system**" by S. A. Gujar and T. I. Michalak, was published in August 2006 in *Veterinary Immunology and Immunopathology*, volume 112, issue 3-4. The work from chapter 5 entitled "**Aberrant lymphocyte activation precedes delayed virus-specific T cell response after both primary infection and secondary exposure to hepadnavirus in woodchuck model of hepatitis B**" by S. A. Gujar, A. K. Jenkins, C. S. Guy, J. Wang, and T. I. Michalak, was published in *Journal of Virology*, volume 82, issue 14 in July

2008. I wish to acknowledge the contribution of co-authors of chapter 5. Adam Jenkins and Clifford Guy performed apoptosis assays with lymphocytes and RT-PCR analysis in liver samples, respectively, while, Jinguo Wang provided the expression plasmids encoding for WHV-specific proteins.

## CHAPTER 1: INTRODUCTION

### 1.1 HISTORICAL BACKGROUND OF VIRAL HEPATITIS

In the 1940s, a British liver disease specialist, Dr. F.O. MacCallum, coined the term "hepatitis B" for the form of a liver disease which was transmitted through exposure to contaminated blood. The infectious agent which caused this form of hepatitis, later named as hepatitis B virus (HBV), was accidentally discovered by Dr. Baruch Blumberg's laboratory in 1967 while studying the inherited genetics of disease susceptibility (Blumberg, 2002). He and his colleagues found a protein antigen in the serum of an Australian aborigine which reacted with the antibodies from a hemophiliac patient convalescent from hepatitis who had received multiple blood transfusions. This protein, which was named as an Australia (Au) antigen, is now recognized as a HBV envelope protein that carries reactivity of the virus surface antigen (HBsAg). Further in 1969, Dr. Blumberg along with Dr. Irving Millman isolated HBsAg particles from the serum of HBV-infected patients and used it for successful immunization of high-risk patients. This finding laid the foundation of the modern day anti-HBV vaccine. For his work on HBV, Dr. Blumberg received a Nobel Prize in 1976.

In 1970, using blood from HBV-infected patients, Dr. David Dane distinguished 42-nm viral particles (known as "Dane particles") containing the HBV genome, as opposed to 22-nm non-infectious, subviral particles discovered by Blumberg. These Dane particles were further identified to be HBV virions.

These findings prompted the constitution of new laws in 1972 in the United States and other countries regarding the screening of donor blood for the presence of HBsAg. In 1982-1984, Dr. Hilleman and colleagues produced the first subunit vaccine using HBsAg isolated from serum of HBV-infected individuals. Later, between 1983 and 1986, Dr. Router and colleagues developed the first recombinant subunit vaccine in yeast, which was capable of inducing protective immunity against HBV infection. These hallmark studies and numerous others in the following years dissected the molecular structure of HBV and identified this virus as an etiological agent of acute and chronic viral hepatitis type B, and further associated this viral infection with the development of primary liver cancer, hepatocellular carcinoma (HCC).

## **1.2 EPIDEMIOLOGY OF HBV INFECTION**

HBV infection causes acute and chronic hepatitis, persistent asymptomatic (occult) infection, cirrhosis and HCC. It is the tenth leading cause of deaths worldwide. As reported by the World Health Organization (WHO) in 2004, 2 billion people in the world are infected with HBV, out of which more than 370 million people are serum HBsAg-positive chronic carriers of the virus (Lavanchy, 2004). It is estimated that each year more than 4 million clinical cases of acute HBV infection are reported, while approximately 1 million people die from liver failure due to chronic hepatitis, cirrhosis or liver cancer.

The highest prevalence of HBV infection is in the developing countries of

Asia and Africa, where the incidence of serum HBsAg-positive infection is as high as 10-15% of the entire population. Based on the percentile of people that are serum HBsAg-positive, the worldwide HBV prevalence is classified into three categories: high (8% and above), intermediate (2 - 8%), and low (less than 2%). Only 12% of people worldwide live in the areas where HBV endemicity is low, while 45% and 43% of people live in intermediate and high endemic areas, respectively (WHO report, 2004). In Western countries, the infection is relatively infrequent and is acquired mostly during adulthood, while in parts of Asia and Africa, it is usually acquired perinatally (Lavanchy, 2004).

HBV is classified into 8 genotypes (A-H) depending on intergroup genome sequence divergence of 8% or more. Each genotype has a distinct geographical distribution. Genotype A, F, G and H are more prevalent in Europe and North America, while genotype B, C and A, D are the major genotypes seen in China and Southeast Asia, respectively. Genotype E is mostly observed in West Africa.

In Canada, pertaining to the heterogeneity of the population, the rate of HBV prevalence has been estimated between 0.5 to 1.0 %. The highest rate (6-7%) of HBsAg positivity is observed in immigrants and Innuits, intermediate (0.3-0.6%) between First nations, adolescents, STD clinic visitors and residents of long-term care facilities, and the lowest amongst the general population (Zang *et al.*, 2001).

A safe and effective vaccine against HBV has been available since 1982, and its global implementation in mass immunization has helped in decreasing the

rate of hepatitis B prevalence in some countries. The efficacy of anti-HBV vaccination has been demonstrated in a population-based study performed in Taiwan (Hsu *et al.*, 1999), when mass immunization reduced the serum HBsAg occurrence from 10% to 1%. Unfortunately, despite the availability of a vaccine for more than two decades, the global reservoir of HBV-infected people is growing, most likely due to the limited access to this relatively expensive vaccine and socioeconomic conditions.

The transmission of HBV occurs through contaminated blood and blood products (percutaneous), from infected mothers to babies (perinatal), via unprotected sexual contacts, and using unsterilized medical devices and needles. Since HBV is transmitted through contaminated blood products, the testing of blood donors for the presence of HBsAg, antibodies to HBV core antigen (anti-HBc), and most recently, HBV DNA has become mandatory in many countries.

Most adults (80-90%) resolve acute hepatitis B (AH), while the remaining 10-15% develop chronic hepatitis B (CH). Diagnosis of CH is based on the presence of HBsAg in serum for more than 6 months. Patients with CH are 100-200 times more likely to develop HCC than their healthy counterparts (Beasley *et al.*, 1981). In contrast, children who acquire HBV infection perinatally or during early childhood develop CH at a very high rate (80-90%). Nonetheless, it has become evident in recent years that the individuals who acquire HBV infection become carriers of the virus for their life-time irrespective of the outcome of

serologically evident infection and hepatitis. The individuals who recover from AH harbor low levels of virus for decades in the liver as well as in the lymphatic system (Michalak *et al.*, 1994, Reherrmann *et al.*, 1996, Yuki *et al.*, 2003, Raimando *et al.*, 2006, Michalak, 2007).

### 1.3 HBV AND OTHER MEMBERS OF HEPADNAVIRUS FAMILY

HBV belongs to a family of hepatotropic viruses called *Hepadnaviridae*. The name "hepadnaviridae" is derived from the latin word 'hepa' meaning liver and pertains to the liver tropism of this group of DNA viruses. The hepadnavirus family contains two genera, namely *Orthohepadnaviridae* and *Avihepadnaviridae*. HBV is a prototype of mammalian hepadnaviruses, which also include other viruses, such as woodchuck hepatitis virus (WHV) (Summers *et al.*, 1978), ground squirrel hepatitis virus (GSHV) (Marion *et al.*, 1980) and arctic squirrel hepatitis virus (ASHV) (Testut *et al.*, 1996). On the other hand, duck hepatitis B virus (DHBV) (Mason *et al.*, 1980), heron hepatitis B virus (HHBV) (Sprengel *et al.*, 1988) and Ross' and snow goose hepatitis B virus (RGHBV and SGHBV, respectively) belong to genus *Avihepadnaviridae* (Chang *et al.*, 1999).

The members of *Orthohepadnaviridae* genus, HBV and WHV, both have a very narrow host range. Thus, HBV infects humans, chimpanzees, African green monkeys and, rhesus and woolly monkeys, while WHV infects woodchucks (*Marmota monax*) and ground squirrels.

## 1.4 GENERAL ORGANIZATION OF HEPADNAVIRUSES

HBV and WHV are small, partially double-stranded DNA viruses with an approximate genome size of 3.2 kilobases (Kb) and 3.3 Kb, respectively. Both these viruses are enveloped and possess the smallest genomes of all the double-stranded DNA viruses. Their virion sizes are 42 nm and 45 nm respectively. The outer envelope lipoproteins of HBV and WHV, carry surface antigen reactivity (HBsAg and WHsAg, respectively) and share significant antigenic cross-reactivity with each other. These envelope proteins form the empty spherical subviral particles and filaments (20-25 nm in diameter) which along with infectious virions, circulate freely. Serum HBsAg and WHsAg represent the hallmark markers of hepadnaviral infection and are detectable during the acute and/or chronic phase of hepatitis B. The envelope proteins surround the icosahedral nucleocapsid which is composed of proteins carrying core (HBcAg and WHcAg) and e (HBeAg and WHeAg) antigen reactivities. These nucleocapsid particles contain the viral genome and genome-associated polymerase essential for hepadnaviral replication.

### 1.4.1 Genome organization

Genomes of hepadnaviruses are formed by partially double stranded, relaxed circular DNA molecules. These DNA molecules contain two complementary (plus and minus) strands which are unequal in length. The minus-strand is complete and has a nick at a fixed position, while the

complementary plus strand is incomplete with variable length that is usually more than 50% of the complete positive-strand. Both strands have short cohesive overlapping regions at the 5'-end which maintain the circular structure of hepadnavirus genome. The minus-strand contains 4 major, overlapping open reading frames (ORFs), which encode four viral proteins and are highly homologous with each others counterparts from HBV and WHV. The HBV mRNA transcripts are either genome-size transcripts (3.5 Kb) or subgenomic transcripts (2.4, 2.1 and 0.7 Kb). The genomic transcripts serve as a template for the reverse transcription of the HBV minus-strand DNA. In contrast, only two species of polyadenylated mRNAs of 3.7 and 2.1 Kb have been identified for WHV. These genomic transcripts also transcribe the mRNAs for the translation of pre-core (preC), core (C) and polymerase (P) proteins, while subgenomic transcripts transcribe the mRNA templates encoding envelope and the X proteins (Couillin *et al.*, 1999).

The polymerase ORF, which encodes for DNA polymerase polyprotein, is the longest and overlaps all other ORFs. The nucleocapsid ORF contains two in frame start codons and encodes for longer precore and shorter core protein. Similarly, envelope ORF consists of three in frame ATG start codons which initiate the translation of large (preS1), middle (preS2) and small (S) envelope proteins. The X protein is encoded by X ORF and is the smallest of all the ORFs (Figure 1.1).

The appropriate expression of these viral ORFs is regulated by four

**Figure 1.1** Schematic representations of HBV and WHV genomic structures. For both HBV and WHV, double stranded DNA is shown with black bold-line circles, while repective viral proteins are depicted as black arrows. The viral transcripts are indicated with colored lines at the outer circle. The promoters, enhancers and direct repeats (DR1 and DR2) are shown as colored-filled eclipses, open color eclipses and purple rectangles, respectively. The nucleotide positions in both genomes are relative to a unique *EcoRI* site arbitrarily set as 1 (Adapted from Wang and Michalak, Doctoral thesis submitted to Memorial University of Newfoundland, 2007).



promoter elements. The nucleocapsid or core promoter is located within the nucleocapsid ORF, directs the transcription of the 3.5 kb HBV transcript, and is transcriptionally active in HBV-infected tissues. It also aids the tissue-specific HBV gene expression (Yee *et al.*, 1989). The transcription of the envelope gene is regulated by two different promoters, i.e. relatively silent preS and very active S promoter (see Figure 1.1). The preS promoter drives the transcription of the 2.4-kb envelope transcript, which subsequently is translated into large envelope protein called preS1 protein. This promoter is located just upstream from the first start codon for this protein. Transcriptionally active S promoter drives the expression of the 2.4-kb transcript, which is eventually translated into preS2 and S envelope proteins. This promoter is located just before the ATG codon that initiates expression of the middle envelope protein. Finally, X promoter strictly controls the expression of X protein and hence is transcriptionally silent. Apart from four promoter sequences, HBV gene expression is also regulated by two enhancer elements (E1 and E2) which aid in enhanced promoter activity. The E1 enhancer is located between preS1 and S ORFs, while the E2 enhancer is located within the X gene sequence. The WHV genome consists of the four homologous promoter sequences as in the HBV genome, but contains only E2 enhancer element.

#### **1.4.2 Viral Proteins**

In total, the hepadnaviral genome encodes for four major viral proteins.

Envelope proteins of HBV and WHV are type II transmembrane proteins and are encoded by three in-frame translation initiation codons present at the beginning of preS1, preS2 and S regions within a single ORF (see Figure 1.1). These envelope proteins differ in N-terminal amino acid sequences, but share the same C-terminal sequences. The preS1 protein is the largest of these three envelope proteins and is known to interact with nucleocapsid protein and facilitates the enveloping of virion particles. Further, preS1 protein is also hypothesized to contain the binding site responsible for binding of the virus to the unidentified cellular receptor (Bruss *et al.*, 1996a). The S protein is the smallest, but the most abundant of all the three hepadnaviral envelope proteins, and is the major component of both Dane particles and freely circulating subviral particles. The preS2 protein is least abundant in serum but is expressed at higher density in virions derived from woodchuck livers (Michalak and Lin, 1994). All the hepadnaviral envelope proteins exist in glycosylated or non-glycosylated forms (Feitelson *et al.*, 1983) and can be visualized by Western blot analysis as polypeptides of different molecular weights pertaining to the state of glycosylation as: 42 and 39 kDa for preS1, 36 and 33 kDa for preS2, and 26, 23 and 19 kDa for S protein. The studies have shown that the infectivity of HBV requires the myristylation of the large envelope protein and is independent of the glycosylation of any of the three proteins (Bruss *et al.*, 1996b).

Similar to the envelope proteins, two hepadnaviral nucleocapsid polypeptides are also encoded by two in-frame initiation codons located within C

ORF. The translation beginning at the first start codon produces precore polypeptide, which subsequently gets transported in endoplasmic reticulum (ER), undergoes partial proteolysis and appropriate glycosylation and then is secreted as e protein. The second start codon initiates the translation of core protein which has an arginine rich carboxyl domain. The N-terminus of the core protein mediates the self assembly of these proteins into core particles in the cytoplasm, while the arginine-rich carboxyl domain can bind to negatively charged hepadnaviral DNA essential for packaging of virions. The WHe (24 kDa) protein differs from WHc (22 kDa) in that it is truncated of the N-terminal signal peptide as well as the arginine-rich carboxyl terminal residues. Clinically, presence of HBeAg in the circulation is associated with actively progressing HBV infection, while the appearance of antibodies to HBeAg (anti-HBe) is considered as a good prognostic marker.

The X protein, encoded by X ORF, is 154-aa and 141-aa long for HBV (HBx) and WHV (WHx), respectively. Even though the exact role of X protein in hepadnaviral replication and pathogenesis is unknown, it has been shown that the intact WHV X gene is essential for the initiation of WHV infection (Zoulim *et al.*, 1994). The X protein is shown to activate proliferation, to induce apoptosis of infected cells, and is possibly involved in mediating the development of HCC.

Hepadnaviral DNA P is the largest of all the four proteins and is composed of 845-aa for HBV and 879-aa for WHV. It is encoded by P ORF, which overlaps with the other three ORFs and displays DNA-dependent DNA polymerase,

reverse transcriptase, and RNase H enzyme activities. The N-terminal domain of the P protein provides a primer for the initiation of reverse transcription of HBV DNA negative strand.

### 1.5 REPLICATION OF HEPADNAVIRUSES

After the entry into a susceptible target cell, viral polymerase repairs the incomplete DNA plus strand of the hepadnavirus genome, which is then joined with the minus strand to generate the covalently closed circular DNA (cccDNA). The cccDNA is then transported to the nucleus of the infected cells within the core particles. Inside the nucleus, cccDNA serves as the template for the transcription of the viral pregenomic and messenger RNAs using host RNA polymerase II enzyme. These transcripts are polyadenylated and then transported back to the cytoplasm where they are eventually translated into different viral proteins. Newly formed pregenomic RNA is transported into the cytoplasm, where it becomes associated with viral P protein complex and is encapsidated by core particles. The reverse transcriptase reactivity of polymerase synthesizes a new minus strand DNA using protein primer from the N-terminal domain of the polymerase protein, after which, RNase H degrades the pregenomic RNA. This minus strand DNA serves as a template for the synthesis of a plus strand and, thus, completes the formation of viral genome inside the core particles. Some of these newly formed core particles are transported back into the nucleus, where they replenish the hepadnaviral

genome pool, while the remaining particles are transported into the ER where they associate with envelope protein and are secreted into the extracellular spaces through non-cytopathic secretory mechanisms (Seeger and Mason, 2000). These secreted mature virions were first described by Dr. Dane and are known as "Dane particles".

### 1.6 ANIMAL MODELS OF HBV INFECTION

The experimental studies on HBV infection are hampered by the fact that HBV is strictly host specific and, at the same time, only with great difficulty, can be propagated in culture because of its inability to infect cells efficiently *in vitro*. Further, in most of the clinical situations, it is difficult to determine the precise time of the infection and to obtain samples during the pre-acute phase, i.e., prior to the appearance of clinical symptoms. These constraints have forced a search for natural models of hepadnaviral infection in lower species and the development of surrogate systems in transgenic animals. The animal models which most prominently contributed to our better understanding of HBV replication and pathobiology include HBV-infected chimpanzees, woodchucks and ducks infected with WHV and DHBV, respectively, as well as the transgenic mouse HBV models. In particular, WHV infection in eastern Northern American woodchucks (*Marmota monax*) is recognized as the most relevant natural mammalian model of human HBV infection.

### 1.6.1 Woodchuck model of HBV infection

In 1978, WHV was discovered in the colony of woodchucks at Penrose Research Laboratory at Zoological Gardens in Philadelphia, where high rates of CH and HCC accompanied by the presence of Dane-like particles were found. Following this observation, an experimental animal model of HBV infection was established at Cornell University using woodchucks infected with WHV (Tenant and Gerin, 2001; Tenant *et al.*, 2004). The nucleotide sequences of WHV and HBV share considerable homology with each other and they are ultrastructurally indistinguishable. Infection of woodchucks with WHV induces similar profiles of tissue tropism, immunological events, hepatic pathogenesis, disease outcome patterns as well as virus-induced hepatocarcinogenesis as those observed during HBV infection in humans.

Unlike chimpanzees, woodchucks are relatively easily accessible and less expensive to maintain. The biggest inconvenience in utilizing this model is the unavailability of research reagents, however, recent efforts focused on production of woodchuck-specific immune cell markers, functionally active recombinant proteins and different bioassays have provided new tools for investigations in this model.

Similar to HBV, the natural transmission of WHV occurs through either parenteral, i.e., exposure to infected blood or bodily fluids, or perinatal, i.e., from infected mother to the offspring. After exposure to WHV, most of the adult woodchucks (approximately 85-90%) display characteristic AH and then

successfully resolve hepatitis, while the remaining 10% develop chronic infection. The rate of development of CH in neonates infected at birth is higher and ranges between 60-90% (Cote *et al.*, 2000). These outcome statistics are very similar to those observed in humans infected with HBV.

Infection of woodchucks with a liver-pathogenic dose of WHV (i.e. >1000 virions) (Michalak *et al.*, 2004) induces characteristic WHsAg-positive, symptomatic infection. The incubation period of WHV measured by the appearance of WHV DNA in serum and peripheral blood lymphoid cells (PBMC) is as short as 10-20 days. It is followed by appearance of WHsAg in circulation between 4-10 weeks post-infection (w.p.i.). Usually, the anti-WHc appears between 6-10 w.p.i., while neutralizing anti-WHs appear after the disappearance of WHsAg from the serum. This correlates with the decreasing severity of hepatic inflammation and recovery. The resolution of WHV-induced AH is followed by long-term persistence of low level virus replication in the liver and lymphatic system and anti-WHc antibodies.

Woodchucks carrying CH display higher virus loads (up to  $10^{11}$  virus genome equivalent [vge]/ml) and presence of WHsAg in serum for at least 6 months. Additionally, they are serum WHeAg positive and fail to seroconvert to anti-WHe. It is believed that the presence of higher quantities of WHsAg and WHeAg in the circulation may tolerize virus-specific T and B lymphocytes, leading to unsuccessful or weaker anti-viral immune responses. Contrary to HBV-infected humans, male woodchucks do not display higher rates of CH and

subsequent HCC development.

### 1.6.2 Other natural models of HBV infections

Chimpanzees infected with HBV display compatible profiles of liver pathology and anti-viral immunological responses, and so far have provided valuable information regarding HBV immunopathology (reviewed in Bertoletti and Gehring, 2006; Chisari, 2000). However, since chimpanzees are rarely available, hard to breed and very expensive to maintain under laboratory conditions, the implementation of this very valuable animal model poses major problems.

Some of the important findings regarding viral entry and hepadnavirus replication have come from the studies performed in DHBV-infected ducks. Primary duck hepatocytes can be easily isolated from the duck embryos, cultured, and infected with DHBV. Thus they provide a relatively easy *in vitro* system. However, DHBV genome lacks the homologous counterpart of HBV X gene and encodes only two envelope proteins. Further, DHBV does not induce liver pathology, cirrhosis or HCC. Additionally, the avian immune system is different than that of humans and, hence, this model is a less attractive option to study the immunopathological aspects of HBV infection (reviewed in Funk *et al.*, 2007).

### 1.6.3 HBV transgenic mouse model

HBV does not infect mouse. However, using embryo microinjection

technology, complete or partial copies of HBV genome have been expressed in mice. Different HBV transgenic mouse models generated this way have several advantages. The mouse immune system is very well characterized and most of the reagents and assays are commercially available to carry out experiments. Further, unlike any other animal model of HBV infection, the genetic homogeneity of the mice can be easily controlled by using inbred animals (Chisari and Ferrari, 1995).

The transgenic mice expressing the HBV envelope (S) gene under liver-specific promoters or the endogenous virus promoters (Babinet *et al.*, 1985; Burk *et al.*, 1988; Chisari *et al.*, 1985; Chisari, 1995) were shown to produce envelope protein in the liver as well as in extrahepatic tissues, such as kidney and testes (DeLoia *et al.*, 1989). When the albumin promoter was used to drive the expression of large envelope protein (preS1), the intracellular accumulation of HBsAg was observed within hepatocytes, which causes expansion of the ER and, subsequently liver injury. This HBsAg leads to the ground glass appearance of hepatocytes, as observed in patients with CH (Chisari *et al.*, 1987). Thus, the transgenic mouse model has demonstrated that viral envelope proteins can be toxic to the hepatocytes under certain conditions (Chisari, 1996). When HBcAg and HBeAg were expressed in transgenic mice, these antigens were expressed in the nucleus or found in the circulation, respectively (Milich *et al.*, 1994; Reifenberg *et al.*, 1997; Takashima *et al.*, 1992). Similarly, after expressing nonstructural X protein in transgenic mice, some groups confirmed the

involvement of this transactivator in the development of HCC (Koike *et al.*, 1994), while others showed contradictory results (Lee *et al.*, 1990).

The complete genome of HBV has also been expressed in transgenic mice under an endogenous viral promoter (Araki *et al.*, 1989; Burk *et al.*, 1988; Choo *et al.*, 1991; Farza *et al.*, 1988; Guidotti *et al.*, 1995). These mice assembled HBV virions in hepatic as well as extrahepatic tissues, e.g. kidneys, and released them into circulation. Furthermore, circulating HBV virions from transgenic mice were able to produce infection in chimpanzees (Heise *et al.*, 1999). However, HBV replicative cccDNA was not detected in these mice.

The immunological studies carried out in the HBV transgenic mouse models have strengthened the concepts of the immunological basis of liver pathology induced by HBV infection. The understanding of the importance of HBV-specific CD8+ CTLs or CD4+ T cell responses was further advanced in this model. Nonetheless, the HBV transgenic model has also emphasized that CTLs may not be able to target the cells which reside outside of the liver and express the HBV gene products, most probably due to the microvascular barrier that exists in these tissues (Chisari, 1996, Guidotti and Chisari, 2001). This finding has an implication in understanding the mechanism of HBV persistence in the face of an otherwise successful and vigorous immune response. It has been hypothesized that the extrahepatic HBV replication sites not only act as a reservoir of the virus but also generate enough antigenic stimulus for the maintenance of the HBV-specific memory responses, as those observed in

patients long after recovery (Rehermann *et al.*, 1996). However, the results from the transgenic mouse model should be interpreted with caution since HBV does not infect mouse cells, including liver and lymphoid tissues.

## **1.7 THE COURSE OF HEPADNAVIRUS-INDUCED LIVER DISEASE**

HBV infection can be broadly classified in two subcategories: serologically evident, symptomatic infection and serologically silent, asymptomatic or occult infection.

### **1.7.1 Serologically evident symptomatic HBV infection**

Infection with HBV displays an array of symptoms and variable outcomes. After exposure to the virus, HBV infection can progress through any of the following phases: incubation period or asymptomatic subclinical phase, acute hepatitis (AH), fulminant hepatitis, apparent resolution of infection or serum HBsAg-positive chronic hepatitis (CH).

The incubation period of HBV varies from 4-24 weeks post-infection and is accompanied by detectable levels of HBV DNA in the circulation. During this phase of HBV infection, patients show mild symptoms such as fatigue, nausea, anorexia and slight fever, while in some cases mild jaundice is also apparent. Sometimes, this incubation period could also be asymptomatic. Exposure to HBV induces asymptomatic infection in an estimated 70% of immunocompetent adults (Chisari and Ferrari, 1995), while the remaining 30% display typical

symptomatic, clinically evident hepatitis. Approximately, 1% of adults also develop a very severe form of the disease known as fulminant hepatitis, which is characterized by massive, rapid destruction of hepatocytes resulting in loss of liver function and subsequent encephalopathy leading to coma.

After infection, anti-HBc antibodies of IgM type appear between 4-10 weeks post-infection. These antibodies can be used as a diagnostic marker of a recent exposure to HBV. The peak in serum HBV DNA level is usually accompanied by HBsAg in circulation and is usually followed by elevated levels of liver enzymes, such as alanine transaminase (ALT) and aspartate aminotransferase (AST), indicating hepatic injury. Patients who recover from AH and clear HBsAg from serum, develop anti-HBs antibodies that are protective and neutralizing in nature. Now, it has been widely accepted that, apparent clinical recovery from symptomatic viral hepatitis is always followed by low level HBV carriage in the liver as well as in the lymphatic system for decades (Michalak *et al.*, 1994; Yuki *et al.*, 2003; Raimondo *et al.*, 2006; Mulrooney and Michalak, 2007).

The remaining patients who develop chronic hepatitis B display the presence of HBsAg in the circulation for at least 6 months or more along with persistent presence of anti-HBc and elevated levels of liver enzymes. This is usually accompanied by high levels of circulating HBV virions. The development of CH is determined by the age of the individual at the time of exposure. After HBV infection, 80-90% of adults resolve AH, while the remaining 10% progress

to CH. However, the percentage chronicity development is up to 90% in neonatally infected children, as compared to 30-60% in that of children infected before the age of 4 years (Okada *et al.*, 1976). The CH occurs in two different histopathological forms: active (aggressive) CH and mild (persistent) CH. In addition, HBsAg-positive healthy carrier states without apparent liver injury or alterations in the levels of ALT and AST are encountered (Hoofnagle *et al.*, 1984). Patients with CH display continuous liver inflammation which frequently leads to cirrhosis and HCC.

Even though the exact mechanisms responsible for initiation of HCC are not well understood, the progressive and constant inflammation associated with continuous regeneration of injured tissue are believed to be involved in the initiation of the oncogenic process. Further, it has been well documented that, the HBV genome or fragments of subviral DNA can be integrated into the host genome, and possibly deregulate cell growth control pathways. The integration of HBV DNA in host genome, especially that of the X gene, which has many transactivating functions, has been shown to cause the activation of proto-oncogenes, such as n-ras and c-myc, or disruption of tumor suppressor genes, such as p53, potentially leading to oncogenesis (Diao *et al.*, 2001; Elmore *et al.*, 1997).

### **1.7.2 Occult HBV infection**

Occult HBV infection is defined by the presence of HBV DNA in serum,

lymphatic tissues and/or liver in the absence of serum HBsAg (Mulrooney and Michalak, 2007). Most of the adults who resolve symptomatic AH, carry low levels of virus for decades after apparent complete recovery from HBV infection (Michalak *et al.*, 1994; Rehermann *et al.*, 1996; Yuki *et al.*, 2003; Raimondo *et al.*, 2006). This low level carriage of HBV is called secondary occult infection (SOI) and is typically accompanied by anti-HBc antibodies in serum. Regardless of strong HBV-specific T cell response and circulating anti-HBc and anti-HBs antibodies, the HBV genome can be detected in the serum, PBMC and liver samples from patients years after recovery from AH (Michalak *et al.*, 1994; Rehermann *et al.*, 1996).

Detailed characteristics of residual SOI have been recognized in the woodchuck model of hepatitis B following apparent complete resolution of experimentally induced WHV AH. Serial sera, PBMC and liver samples collected after resolution of the acute phase of WHV infection indicated the persistence of viral DNA when analyzed by very sensitive PCR/ nucleic acid hybridization (NAH) assays. Additionally, WHV replicative intermediates, e.g., WHV mRNA and cccDNA were consistently detected in hepatic as well as lymphatic tissues, indicating low level active replication of WHV. This residual infection is associated with the development of HCC in 20% of the recovered woodchucks (Korba *et al.*, 1989, Michalak *et al.*, 1999).

More recently, another form of occult infection has been identified and characterized. The infection of woodchucks with low doses of WHV (<1000

virions) induces serologically undetectable, but WHV DNA positive infection (Michalak *et al.*, 2004). This form of low-level persistent hepadnavirus infection is called primary occult infection (POI) (Michalak, 2000; Michalak *et al.*, 2004; Mulrooney and Michalak, 2007; Michalak, 2007; Michalak *et al.*, 2007). The same studies also confirmed that WHV invades not only the liver but also the lymphatic system, and that the cells of the lymphatic system are a reservoir for long-term persisting virus. It has been recently shown that virus found in liver and lymphatic system is not enriched with any particular variant of WHV (Mulrooney and Michalak, 2008). Further, it was also determined that the amount of the virus predetermines whether the infection is silent and confined to the lymphatic system or serologically evident and liver pathogenic. However, the exact mechanisms and kinetics of immune responses determining the outcome of infection and the extent to which these responses provide protection against reinfection is not fully understood.

The presence of POI in humans is still not thoroughly investigated. However, detection of HBV DNA in the blood or liver samples obtained from patients with no history of HBV exposure or anti-HBc/anti-HBs antibody-positivity, suggests the existence of this form of infection. It is estimated that, 7-19% of the blood donors from endemic areas show the presence of occult infection. In Western countries, this prevalence is estimated to be between 0-9% (Matsumoto *et al.*, 1997; Iizuka *et al.*, 1992; Douglas *et al.*, 1993; Weienberger *et al.*, 2000).

## **1.8 IMMUNOLOGY OF HEPADNAVIRUS INFECTION**

### **1.8.1 General concepts in immunity to viruses**

The mammalian immune system is comprised of a variety of recognition systems capable of recognizing the invading pathogens, and is broadly divided into two different arms: the innate and adaptive immune systems. The innate immune system provides the first line of defense, but does not have the ability to identify a particular pathogen with antigenic specificity. On the other hand, the adaptive immune response develops secondary to innate immunity and recognizes a pathogen in an antigen-specific manner. Additionally, this adaptive immune response also generates the antigen-specific memory responses that protect the immune host against re-infection with the same pathogen.

#### **1.8.1.1 Innate immune response**

The invasion by pathogens activates innate immunity through inflammatory responses. The first phase of the immune response occurs between 0-4 hours (h) post-infection and is known as immediate innate immune response. During this phase, the infectious agent is identified by preformed non-specific effectors which cause either removal of the pathogen or otherwise lead to the development of the second phase of immune response. One of the components of the early innate immune response is the complement system. Complements are small plasma proteins, most of which are proteases, which opsonize the infectious agent and then induce different pro-inflammatory

responses, facilitating the phagocytosis or lysis of the pathogen itself. This system can be directly activated by a pathogen or indirectly by pathogen-antibody complexes.

The second phase of innate immunity is called early induced response, which is activated when microbe-associated molecular patterns (MAMPs) are recognized by host pattern recognition receptors (PRRs) expressed on the cells such as dendritic cells (DCs), natural killer (NK) cells, macrophages, etc.. The best example of this type of receptors is toll like receptors (TLRs), which recognize characteristic components on pathogenic microorganisms, e.g., lipopolysaccharide (LPS), and then trigger the production of different chemokines and pro-inflammatory cytokines. The identification of the MAMPs on an invading pathogen induces the expression of a range of cytokines, such as tumor necrosis factor-alpha (TNF- $\alpha$ ), IL-1 $\beta$ , IL-2, IL-6, IL-12, and chemokine IL-8. This inflammatory response heightens antigen presentation capability and co-stimulatory molecule expression on the APCs, that further initiates the adaptive immune response in an antigen-specific manner (Akira *et al.*, 2001; Janeway and Medzhitov, 2002; Kawai and Akira, 2006).

The infection of cells, especially with viruses, also stimulates the production of interferon proteins. Interferons are divided in two major categories: type 1, i.e., interferon-alpha (IFN- $\alpha$ ) and IFN-beta (IFN- $\beta$ ) and type 2, i.e., IFN-gamma (IFN- $\gamma$ ). The double stranded RNA, which is a replication intermediate for many viruses, is recognized by TLR-3 and is a potent inducer of type 1

interferons (Andoniou *et al.*, 2005; Kawai and Akira, 2006). The induction of these interferons in cells inhibits viral replication and increases major histocompatibility complex (MHC) class I expression. The binding of type 1 interferons to their cognate receptors induces the synthesis of several host proteins, including endoribonuclease, PKR kinase and Mx protein, which contribute to the inhibition of viral replication. These type I interferons, along with TNF- $\alpha$ , IL-2 and IL-12 activate NK cells as well as APCs, including DCs. Activated NK cells bear potent cytotoxic properties and are very efficient in restricting virus replication and spread of infection.

#### **1.8.1.2 Adaptive immune response**

Professional APCs capture the antigens, process them and then present the antigenic peptides in the context of MHC class I or II molecules to circulating T cells.

##### **1.8.1.2.1 T cell immunity**

T cells are broadly divided into two types: CD8+ and CD4+ T cells. CD4+ T cells, also called T helper (Th) cells, identify antigen in the context of MHC class II molecules, while CD8+ T cells, also called cytotoxic T cells (CTL) are MHC class I restricted. The CD4+ T helper cells are further divided into type 1 (Th1) and type 2 (Th2) cells, depending upon the type of cytokines produced.

The activation of T cells in an antigen-specific manner leads to the

proliferation and differentiation of T cells into effector T cells. Effector CD4+ T cells play a central role in providing help to CD8+ lymphocytes T and B lymphocytes. Additionally, Th1 CD4+ T cells secrete cytokines such as IFN- $\gamma$ , TNF- $\alpha$ , IL-2, IL-3 and granulocyte monocyte colony stimulating factor (GM-CSF), which drive the proliferation of T cells and activation of macrophages. On the other hand, Th2 CD4+ T cells are known to produce cytokines, such as IL-10 and IL-4, which have antagonistic effects on Th1 T cell responses. Upon activation, CD8+ T cells kill infected cells through FasL and perforin pathways and eliminate the replication niche of the pathogen. Further, these CD8+ T cells can also produce IFN- $\gamma$  and TNF- $\alpha$ , which can inhibit viral replication in a non-cytopathic way (Guidotti and Chisari, 2001). Some of the effector T and B lymphocytes further develop into a memory phenotype, which are rapidly activated after a secondary encounter with the same pathogen. They are responsible for providing protection against re-infection/challenge.

#### **1.8.1.2.2 B cell immunity**

When a naive B cell encounters an antigen-specific CD4+ T cell in lymphoid tissue, the initiation of humoral immune response occurs. Activated B cells undergo proliferation, become plasma cells and then secrete antigen-specific antibodies. The antibodies directed against external virion proteins can block the binding of the virus to its receptor on the cell surface and thus prevent entry and subsequent infection. These neutralizing antibodies have proven their

importance in providing protection against viral infections caused by HBV, influenza virus, measles virus and others. Further, antibodies bound to the surface of pathogen can activate Fc receptors on phagocytic cells, such as macrophages, DCs and granulocytes which, in turn, ingest and kill the pathogen. Antibodies can also activate the complement system which can either induce phagocytosis, recruit more inflammatory cells to the site of infection or directly destroy the pathogen (Gasque, 2004; Tarlinton *et al.*, 2008).

### 1.8.1.3 Cytokines

Cytokines are small protein molecules made by cells which act as immunomodulators and chemical mediators and affect the function of the immune cells. They are important signaling molecules in the development and maintenance of innate and adaptive immunity. Both haemopoietic and non-haemopoietic cells can produce cytokines that can function in either an autocrine, paracrine or even an endocrine manner. They can directly inhibit viral replication and spread, activate different immune cells and cause tissue injury.

Activated macrophages secrete a range of cytokines, such as IL-1 $\beta$ , IL-6, IL-12, TNF- $\alpha$ , and a myriad of chemokines including IL-8. IL-8 is a potent chemokine that attracts inflammatory granulocytes, such as neutrophils, to the site of infection. TNF- $\alpha$  is involved in local containment of the infection as well as in differentiation and activation of DCs, however, its systemic release can cause septic shock. Neutrophils exposed to chemokines and TNF- $\alpha$  produce a

respiratory burst that generates oxygen radicals and nitric oxide, and release stored lysosomal granules, contributing to the death of the pathogen as well as tissue destruction. IL-12, IFN- $\alpha$  and IFN- $\gamma$  are efficient NK cell activators which further aid in the development of adaptive T cell response.

After infection, naive CD8+ and CD4+ T cells undergo differentiation and become activated to produce distinct profiles of cytokines after the recognition of cognate antigen presented through MHC complex. Activated CD8+ T cells can kill pathogen-infected cells either directly through perforin, granzyme and FasL pathways or indirectly in a non-cytopathic fashion by producing IFN- $\gamma$ , TNF- $\beta$  and TNF- $\alpha$ . On the other hand, CD4+ T cells can produce two distinct profiles of cytokines and are accordingly classified as Type 1 (Th1) and type 2 (Th2) cells. Thus, Th1 cells mainly produce IFN- $\gamma$ , TNF- $\alpha$ , and IL-2 which have macrophage activating properties, while CD4+ T cells of Th2 type are known to express IL-4, IL-10 and TGF- $\beta$  that promote the activation of a humoral immune response.

## **1.8.2 Immune responses to hepadnavirus infection**

### **1.8.2.1 Innate immunity against hepadnavirus infection**

Similar to any other viral infection, exposure to HBV stimulates different components of innate immunity, that involves priming of granulocytes, NK cells, NKT cells, macrophages, dendritic cells and production of anti-viral cytokines such as interferons and TNF- $\alpha$ .

#### 1.8.2.1.1 Granulocytes

Granulocytes are a group of short lived phagocytic cells which include neutrophils, eosinophils and basophils. Although the role of the granulocytes during hepadnaviral infection is unclear, the role of neutrophil-mediated recruitment of non-specific innate immune cells in the liver during the acute phase of HBV infection has been demonstrated in the HBV transgenic mouse model (Sitia *et al.*, 2002). In these mice, the neutrophils were depleted by targeting Ly-6G receptor (Gr-1), that is expressed on bone marrow granulocytes, peripheral neutrophils, plasmacytoid DCs and certain subsets of monocytes. Such a depletion of neutrophils inhibited the recruitment of the antigen non-specific inflammatory cells to the liver and resultant severity of liver injury without affecting virus-specific CTL responses (Sitia *et al.*, 2002). These Gr-1<sup>+</sup> cells also produce matrix-degrading metallo-proteinases (MMPs), which facilitate the leucocyte trafficking through solid organs, such as liver (Sternlicht and Werb, 2001). These MMPs are rapidly induced in livers of the HBV-transgenic mice after injection of HBV-specific CTLs and their expression is associated with intra-hepatic recruitment of inflammatory cells. However, administration of anti-Gr-1<sup>+</sup> antibody in these transgenic mice inhibits the trafficking of non-specific innate cells in the liver, suggesting the role of neutrophils in recruitment of inflammatory cells during the acute phase of HBV infection (Sitia *et al.*, 2002).

#### 1.8.2.1.2 NK cells

NK cells constitute 2% of peripheral and 30% of intra-hepatic T lymphocyte population in the mouse liver, while these percentages are variable in humans (Doherty and O'Farrelly, 2000). Patients infected with HBV show an increased number of circulating NK cells during the pre-acute phase of the infection (Webster *et al.*, 2000). This study regarding the dynamics of immune response during early phases of infection in humans has shown the highest frequency of NK cells in the periphery before the development of AH and preceding the HBV-specific adaptive CD4 and CD8 T cell immune response (Webster *et al.*, 2000). Further, these NK cells show increased cytotoxic potential and elevated expression of IL-2 that eventually subsides to normal levels during recovery phase (Echevarria *et al.*, 1991, Monsalve-De *et al.*, 2002). It is believed that NK cell-mediated cytotoxicity is the major mechanism that keeps HBV replication in check during the pre-acute phase of infection and before the development of virus-specific adaptive immunity. In woodchucks infected with WHV, the acute phase of infection is characterized by the increased ability of PBMC to kill NK cell-susceptible target cells through the perforin pathway, indirectly suggesting the heightened activation of NK cells (Hodgson *et al.*, 1999).

Hepatitis C virus (HCV) encodes protein E2, that binds to CD81 molecules on the surface of NK cells and consequently inhibits the NK cell-mediated anti-HCV immune functions. Whether HBV targets the NK cells in this manner and inhibits its cellular function in order to persist is not yet known. Interestingly,

Chemin and colleagues have shown that PBMC isolated from patients with CHB showed HBsAg and HBcAg expressing CD56+ NK cells (Chemin *et al.*, 1994), suggesting that HBV can infect these cells *in vivo*.

Mouse liver contains high numbers of NK and NKT cells, which constitutes 60-70% of the total intra-hepatic lymphoid cells, while the remaining one third is constituted by conventional lymphocytes (Doherty and O'Farrelly, 2000). Since hepatocytes have low expression of the MHC class I molecules, NK cells might be the main effector cell types early after infection and before upregulated MHC class I expression as observed during AH (Michalak *et al.*, 2000). The activation of NKT and APCs can indirectly activate NK cells which has the potential to inhibit hepadnaviral replication. It is believed that intrahepatic NK and NKT cells, which become activated after HBV infection, are the major producers of IFN- $\gamma$  during AH. The inhibition of NK cell recruitment to the liver by blocking either chemokines such as IP-10 and Mig, or by depleting the neutrophils (Sitia *et al.*, 2002), ameliorates the liver injury (Kakimi *et al.*, 2001), suggesting that these cells have the capacity to mediate hepatic injury.

In chimpanzees infected with HBV, an increased number of intra-hepatic NK and NKT cells, along with elevated IFN- $\gamma$  and TNF- $\alpha$  expression, is accompanied by decreased HBV replication (Thimme *et al.*, 2003; Weiland *et al.*, 2004). The findings in this report were supported by the observation in HBV-transgenic mice, wherein IL-18- or IL-12-mediated activation of NK cells leads to the inhibition of HBV transcripts and replicative intermediates in the liver as well

as extra-hepatic tissues, i.e., kidney (Cavanaugh *et al.*, 1997; Kimura *et al.*, 2002a). Interestingly, the superinfection of HBV-transgenic mice with *Schistosoma mansoni* or *Plasmodium* (malaria) parasites (Pasquetto *et al.*, 2000), both of which activate the intrahepatic NK cells, suppresses HBV gene replication in the liver as a secondary effect of the intrahepatic immune response. The HBsAg-carrier transgenic mice, which have high prevalence of HCC development, had a decreased number of intrahepatic NK cells (Chen *et al.*, 2005). These NK cells also displayed lowered cytotoxic potential and were poorly activated after poly (I:C) stimulation (Chen *et al.*, 2005).

Additionally, NK-cell derived IFN- $\gamma$  non-cytopathically restricts the virus spread in hepatocytes early after infection and upregulates the expression of MHC class I molecules on their surface, facilitating the enhanced antigen recognition by virus-specific CTLs (Guidotti and Chisari, 2006). In transgenic mice, IFN- $\gamma$  and TNF- $\alpha$  inhibit the HBV gene expression and replication in hepatocytes probably by destabilizing the viral RNA in the nucleus of the infected cell and accelerating its degradation, without destroying the cell itself (Guidotti and Chisari, 2001). This phenomenon of non-destructive viral purging is also validated in human hepatocytes (Suri 2001).

IL-2-stimulated NK cells, also called lymphokine activated killer (LAK) cells, have a higher potential to secrete anti-viral cytokines and kill the target cells. The increased levels of IL-2, observed during AH, showed a positive correlation with the increased cytotoxicity of NK cells and better virus control

(Monsalve-De *et al.*, 2002). Further, during CH, NK cells had impaired functional capabilities, which was partly attributed to the detached IL-2 receptor alpha chain in activated cells (Monsalve-De *et al.*, 2002). Interestingly, administration of IL-2 in HBV-transgenic mice inhibits the viral gene expression in a TNF- $\alpha$  dependent manner (Guilhot *et al.*, 1993; Guidotti *et al.*, 1994; Uprichard *et al.*, 2003). Since hepatocytes are not known to express receptors for IL-2 (Smith, 1988), the IL-2-driven inhibitory effect is believed to originate from the immune cells that traffic through the liver, express the IL-2R and produce high amount of TNF- $\alpha$  upon activation, such as NK cells and macrophages.

Apart from direct activation by HBV, the NK cells can also be indirectly activated by action of other immune cells and cytokines. In the HBV transgenic mouse model, administration of  $\alpha$ -galactoceramide activates NKT cells to produce IFN- $\gamma$  and IFN- $\alpha/\beta$ , that subsequently recruit NK cells into the liver. Similarly, anti-CD40 antibody-activated intrahepatic APCs produce IL-12 and TNF- $\alpha$  and trigger IFN- $\gamma$  production by NK and T cells, which further mediates the inhibition of HBV replication in the livers of transgenic mice (Kimura *et al.*, 2002b).

Because of the difficulty in obtaining liver samples from healthy individuals or HBV infected patients, most of the studies related to intrahepatic NK cells are carried out in animal models. Similarly, insight into the involvement of NK cells in the pathogenesis of hepadnavirus infection comes from studies performed in HBV transgenic mice or chimpanzees. Since there is an inherent difference

between the composition of intrahepatic lymphocytes between mouse and humans (Doherty and O'Farrelly, 2000), the data derived from the mouse model has its own limitations. Nonetheless, it provides valuable basic information on the involvement of NK cells in the disease progression and virus control during hepatotropic virus infection.

#### 1.8.2.1.3 NKT cells

NKT cells are non-classical T cells that share partial characteristics of conventional T and NK cells and express  $\alpha\beta$  T cell receptors (TCRs) which are restricted by MHC-like CD1d molecules that present glycolipid molecules. NKT cells are derived from a separate hemopoietic lineage than conventional T cells. Both human and mouse NKT cells are autoreactive with CD1d expressing cells and identify marine sponge-derived glycolipid  $\alpha$ -galactoceramide, a microbial  $\alpha$ -glycuronylceramides and autoantigen isoglobotrihexosylceramide in the context of CD1d (Bendelac *et al.*, 2007; Swann *et al.*, 2007; Behar and Porcelli, 2007). In mice, NKT cells make up approximately 0.5% in peripheral blood and lymph nodes, 2.5% in spleen, and almost 30% of total lymphocytes in liver (Doherty and O'Farrelly, 2000, Bendelac *et al.*, 2007). In humans the frequencies of NKT cell occurrence in different lymphoid organs vary between individuals, but overall, they seem to be 10 times less frequent than in mice, in all the locations. CD1d is constitutively expressed on DCs, macrophages, B cells, Kuffer cells and endothelial cells. Interestingly, hepatocytes constitutively express CD1d on their

surface in mice and not in humans (De alla *et al.*, 2004). However, during an inflammatory process, such as viral hepatitis, human hepatocytes also constitutively express CD1d (De lalla *et al.*, 2004). This constitutive expression on hepatocytes and other intrahepatic cells makes them effective, CD1d-bearing antigen presenting cells capable of presenting antigenic glycolipids to NKT cells in the liver. NKT cells are activated when CD1d bearing cells present the proper glycolipid antigen. In consequence, they express CD40L and produce massive amounts of IL-4, followed by a burst of IFN- $\gamma$ . Then, NKT cells undergo apoptosis within 3-4 days.

Pertaining to their high prevalence in hepatic tissue, NKT cells have been implicated in the immunopathogenesis of HBV infection. Using the HBV transgenic mouse model, it has been shown that the intravenous injection of  $\alpha$ -galactoceramide activates intrahepatic NKT cells to produce IL-4 and IFN- $\gamma$  simultaneously (Kakimi *et al.*, 2000). These activated NKT cells rapidly disappear from the liver, most probably due to activation-induced cell death (AICD), but activate and recruit NK cells which produce IFN- $\gamma$  and IFN- $\alpha/\beta$ , causing inhibition of the HBV replication. A similar study also showed that the  $\alpha$ -galactoceramide-induced NKT-mediated inhibition of HBV replication was diminished in IFN- $\gamma$  and IFN- $\alpha/\beta$  KO mice, but was unaffected after depletion of CD4+ and CD8+ T cells. This suggested that NKT-mediated inhibition of HBV replication was interferon-dependent, but T cell independent (Kakimi *et al.*, 2000).

Human hepatoma cell line, Hep3b, derived from HBV-induced HCC, induces tumors in athymic nude mice. Recent studies in this model have shown that adoptive transfer of NKT cells, activated in the presence of either tumor-specific or HBV-specific antigen (HBsAg), can inhibit the development of tumors in these mice (Shibolet *et al.*, 2003, Margalit *et al.*, 2005).

When HBV transgenic mice, expressing HBsAg in their liver were backcrossed with immune deficient Rag *-/-* mice and were adoptively transferred with naive splenocytes, they developed AH within 2-3 days post-transfer (Baron 2002). The analysis of the intrahepatic cell population in these animals showed that the livers from the HBV-Env x Rag-1*-/-* mice were infiltrated with a large number of NKT cells expressing IL-4 and IFN- $\gamma$ , suggesting their activation (Baron *et al.*, 2002). Further, depletion of NK 1.1+ cells from the naive splenocytes ameliorated the early acute hepatitis, while exclusive transfer of sorted NK 1.1+ cells augmented liver pathology. Additionally, hepatitis was induced in the animals which expressed transgenic HBV envelope gene only, while mice that did not carry the transgene remained unaffected after the transfer of naive splenocytes, suggesting the role of NKT cells in mediating hepatitis.

The studies so far have acknowledged the involvement of NKT cells in the inhibition of virus replication during HBV infection. However, the nature of molecules on hepatocytes that are recognized by these cells during this HBV infection are unknown. Since NKT cells are known to identify hydrophobic ligands, it is hypothesized that the possible ligands for NKT cells include the

myristylated part or hydrophobic peptides of HBV envelope protein expressed by HBV-infected hepatocytes (Baron *et al.*, 2002). It is also believed that infection with HBV might trigger the aberrant processing of endogenous host lipids and glycolipids and induce their presentation as hydrophobic ligands (Bendelac *et al.*, 1997; Chiu *et al.*, 1999).

#### **1.8.2.1.4 Antigen presenting cells**

Even though the involvement of APCs in mediating innate immune response has been demonstrated in HBV-transgenic mice, it has not been entirely recognized during natural HBV infection. In the HBV transgenic mouse model, a single i.v. injection of anti-CD40 antibody recruits activated APCs in the liver and causes noncytopathic inhibition of HBV replication. However, the depletion of APCs by liposome-encapsulated dichloromethylene diphosphonate (L-MDP) that causes apoptosis of macrophages and DCs, but not of T cells, abolishes the antiviral effects associated with anti-CD40 activation. This suggests the possible role of activated APCs in inhibiting HBV replication in a T cell-independent way.

Different viruses are also known to target APCs as a strategy to evade the host immune response. Measles virus infects DCs, affects their maturation, induces TRAIL expression leading to apoptosis in interacting T cells and subsequently causes the generalized immune suppression in infected patients (Vidalain *et al.*, 2000). On the same note, different studies have shown that

HBV also can infect DCs. The presence of HBV DNA and RNA has been documented in DCs from patients with CH. These HBV-infected DCs are known to have impaired immunological functions, such as antigen presentation, cytokine secretion and initiation of T cell response (Arima *et al.*, 2003; Beckebaum *et al.*, 2003). These findings in human studies are also supported in the woodchuck model wherein the WHV DNA and cccDNA was demonstrated in monocyte derived DCs (Michalak and Mulrooney, personal communication).

#### **1.8.2.2 Adaptive immunity against hepadnaviruses**

Although innate immune responses contain the initial viral replication and spread, cellular immunity governed by virus-specific T and B lymphocytes maintain long-term anti-viral immunity as well as rapid secondary memory immune response upon re-exposure to the same virus.

##### **1.8.2.2.1 Cellular Immunity**

Hepadnavirus-specific cellular immunity is mediated by two major subsets of conventional CD8+ and CD4+ T cells. Although, the kinetics of these cellular responses immediately after HBV infection are not delineated, studies have shown that the strength and breadth of these T cell responses during AH, determine the outcome of the infection.

###### **1.8.2.2.1.1 CD8+ T cells:**

Activated HBV-specific CD8+ T cells identify the virally infected cells and kill them in a highly precise, MHC class I-restricted manner. The qualitative attributes of this virus-specific CD8+ T cell response appear to orchestrate the outcome of hepadnaviral infection. HBV-infected patients who develop strong, multispecific and polyclonal CD8+ T cell responses during AH, inhibit the infection and recover from hepatitis (Chisari, 1997; Rehermann *et al.*, 1996). In contrast, patients with weak, narrow and oligoclonal virus-specific CTL responses develop a HBsAg-positive CH (Ferrari *et al.*, 1990; Bertoletti and Ferarri, 2003; Guidotti and Chisari, 2006).

The analysis of HBV-specific CD8+ T cell responses during AH that progresses to resolution shows the successful generation of CTL responses against HBV core, envelope and polymerase proteins. (Rehermann *et al.*, 1995; Rehermann *et al.*, 1996; Bertoni *et al.*, 1997). The analysis of HLA-A2-HBV tetramer-positive CD8+ T cells obtained during AH indicated the quantitative hierarchy for HBV core, polymerase and envelope antigens in CD8+ T cells (Maini *et al.*, 1999). The direct quantitation of HBV-specific CD8+ T cells in the circulation further revealed that HBcAg<sub>19-27</sub>-specific CD8+ T cells comprised 1.3% of total CD8 T cells and were accompanied by CD8+ T cells that were specific for other epitopes of HBV. This hierarchy and multispecificity of HBV-specific CD8+ T cells was detectable even one year after the resolution of acute infection, but was almost undetectable in the patients with CH (Maini *et al.*, 1999).

During multispecific CD8+ T cell response, the CTL repertoire is directed

against different HBV antigens, while the polyclonal T cell response recognizes a single HBV antigen in the context of diverse TCRs. Bertoletti *et al.*, 1994, had shown that, patients with CH displayed a monospecific CTL response to HBC<sub>18-27</sub> epitope without mounting stronger reactivity to any other HBV antigenic epitopes. The sequence analysis of the HBV from these patients revealed that the virus genome was mutated at HBC<sub>18-27</sub> epitope, suggesting that the epitope was no longer recognized by the prevalent CTL response. It is believed that the polyclonality of the CTL response provides a practical advantage since CTLs with different TCRs directed with similar specificity could easily identify substituted residues within the epitope (Maini and Bertoletti, 2000) . These findings suggest that multispecificity and polyclonality of anti-HBV CTL response prevents the development of escape mutants and subsequently determines a favorable outcome from the infection.

The activation of a virus-specific T cell response is delayed after primary exposure to hepadnavirus and is detectable only after 8-12 w.p.i. (Menne *et al.*, 2002a; Bertoletti and Ferrari, 2003; Webster *et al.*, 2000). This delayed appearance of a virus-specific T cell response is a hallmark characteristic of hepadnavirus infection since other viral infections, such as SIV, HIV or cytomegalovirus activate similar responses after 1-2 w.p.i. (reviewed in Wherry *et al.*, 2004). Although, the reasons behind this characteristic, delayed arise of a virus-specific T cell response are poorly understood, it is believed that the impaired innate responses early after hepadnaviral exposure may postpone the

appearance of HBV-specific T cells. On the same note, the peak frequency of HBV-specific CD8+ T cells during AH does not exceed 1% of circulating CD8+ T cells, which is again lower than that observed during other infections such as LCMV, EBV and HIV (Callan *et al.*, 1998; Ogg *et al.*, 1998).

The peak frequency of the virus-specific CD8+ T cells during AH type B infection is accompanied by the highest degree of hepatic injury, as measured by the elevation in the serum levels of liver enzymes, such as AST and ALT. The best evidence explaining the importance of the CD8+ T cells in the control of HBV infection comes from the studies in the chimpanzee HBV infection model. In this model, the depletion of CD8+ T cells using anti-CD8 antibodies during the acute phase of infection resulted in the prolonged persistence of HBV infection (Thimme *et al.*, 2003). On the contrary, some studies have suggested that the maximal reduction in hepadnavirus load during AH precedes the peak in the virus-specific T cell responses (Guidotti *et al.*, 1999; Chang and Lewin, 2007). Even though these studies challenge the concept that CTL-mediated clearance of virus-infected cells is a main mechanism of inhibition of replication of HBV, it should be remembered that these cells also produce cytokines such as IFN- $\gamma$  and TNF- $\alpha$ , which might control the infection via a non-cytopathic mechanism. Of note, after infection with HBV, not all individuals develop elevated levels of liver enzymes or display clinical symptoms of hepatitis, indicating that IFN- $\gamma$  and/or TNF- $\alpha$  mediated non-cytolytic pathway could constitute a major mechanism of clearance of HBV (Kakimi *et al.*, 2003). In transgenic mice,

adoptively transferred HBV-specific CD8 T cells can inhibit HBV gene expression non-cytopathically in the HBV transgene-replicating hepatocytes. Apart from the fact that almost 100% of hepatocytes are infected with HBV at the peak of infection (Guidotti and Chisari, 2001), only a minor percentage appears to be actually killed during resolution of hepatitis. This observation supports the notion that the non-cytopathic clearance of virus is a major anti-viral pathway after hepadnaviral infection.

The precise involvement and significance of the particular subset of T cells in the inhibition of HBV infection was delineated in a chimpanzee experiment wherein the CD8+ or CD4+ T cells were depleted using specific antibodies. In this experiment, chimpanzees were infected with  $10^8$  HBV v.g.e. and administered exclusively with either anti-CD8 or anti-CD4 antibodies during the acute phase of infection (i.e., 6 w.p.i.). In anti-CD8 antibody-treated chimpanzee, the peak HBV viremia during the acute phase of infection persisted for longer time periods, which was followed by the delayed onset of liver injury. Further, reappearance of the CD8 T cells was correlated with increased IFN- $\gamma$  mRNA and decreased HBV load in the liver, and was also accompanied by mild liver injury. Surprisingly, the dynamics of HBV infection in anti-CD4 antibody-treated chimpanzee was similar to that of control chimpanzee, which received isotype control antibody. This suggests that deletion of CD4+ T cells during the acute phase of HBV infection does not change the disease dynamics. This experiment demonstrated that the CD8+ T cells are the main mediators of

inhibition of HBV replication, as well as hepatic injury. Nonetheless, the results from this experiment should be interpreted with caution since the administration of anti-CD4 (or anti-CD8) antibodies was not performed until 6 w.p.i., which could have provided enough time for CD4+ T cells to perform their helper functions long before the depletion event.

#### 1.8.2.2.1.2 CD4+ T cells

Just like CD8+ T cells, HBV-specific CD4+ T cells are multispecific and polyclonal and show reactivity against different HBV antigens when monitored in a proliferation assay. During acute HBV infection progressing towards recovery, CD4+ T cell responses are strong, reactive against multiple HBV antigenic epitopes and are of a Th1 type. Their reactivity is accompanied by a successful virus-specific CD8+ T cell response (Ferrari *et al.*, 1990; Penna *et al.*, 1997). A population based study has shown that this multispecificity of CD4+ T cell response against multiple HBV antigens is due to heterozygosity of MHC class II alleles, and is often associated with a more favorable outcome i.e., resolution of AH (Thursz *et al.*, 1997).

The patients with AH that progress to resolution display strong anti-HBc T cell responses, while in patients with CH these responses are either weak or absent (Ferrari *et al.*, 1990). This impairment of CD4+ T cell responsiveness during serum HBsAg- as well as WHsAg-positive chronic infection can be reversed after treatment with an antiviral agent, lamivudine, suggesting that high

viral or antigen load may contribute to this characteristic hyporesponsiveness of CD4+ T cells (Livingston *et al.*, 1999; Boni *et al.*, 1998; Menne *et al.*, 2002c).

Epitope mapping studies have shown that 95% of patients in the acute phase of infection show strong antigenic reactivity against an immunodominant epitope located between 50-69 residues of HBcAg, irrespective of their human leukocyte antigen (HLA) haplotype (Ferrari *et al.*, 1991). The similar pattern of immunodominance has been observed in the woodchuck model of hepatitis B, where the majority of WHV-infected woodchucks show a response to an antigenic epitope located between 97-110 amino acid residues of WHcAg (Menne *et al.*, 1997). Overall CD4+ T cell responses generated after HBV infection are directed at the highest frequency to antigenic epitopes of core protein than to the epitopes of any other HBV protein (Penna *et al.*, 1996). It is recognized that, HBcAg can initiate the immune response in a T cell dependent, as well as, in an independent manner, which may be due to the fact that T cell immune responses to this antigen are more vigorous than to any other virus. Interestingly, these HBc-specific CD4+ T cells are known to extend help during the induction of anti-HBs antibody response (Milich *et al.*, 1986). The anti-HBs antibody response generated with the help of HBcAg-specific CD4+ T cells was believed to be responsible for the protection of HBcAg immunized chimpanzees against HBV-induced hepatitis (Murray *et al.*, 1984; Milich *et al.*, 1995). Similarly, woodchucks immunized with peptide containing an immunodominant peptide encoded within WHcAg or WHcAg-encoding plasmid were protected against

WHV-induced hepatitis (Menne *et al.*, 1997; Wang *et al.*, 2007).

Similar to HBV-specific CD8+ T cell response, reactivity of virus-specific CD4+ T cells to different HBV antigens appears at 10-12 w.p.i. in HBV-infected individuals (Bertoletti and Ferrari, 2006) and between 6-12 w.p.i. in WHV-infected woodchucks (Menne *et al.*, 2002). Again, compared to other viral infections, the appearance of virus-specific CD4+ T cell reactivity is delayed and is believed to be a consequence of the impaired early innate immune response or long incubation period of HBV. This CD4+ T cell response persists long after the resolution of AH, as measured by the proliferative capacity of lymphocytes after stimulation with HBV-specific antigens. Even though HBV-specific CD8+ T cells are assumed to be the main effector T cells during HBV infection, virus-specific CD4+ T cells provide help in developing this CTL response and thus indirectly determines the outcome of AH. Further, it is also shown that the maintenance of antigen-specific effector CD8+ T cells require CD4+ T cell help, especially of Th1 type (Cardin *et al.*, 1996; Zajac *et al.*, 1998).

It is hypothesized that, during hepadnaviral SOI, low level virus replication provides enough antigenic stimulation for the maintenance of the memory and effector HBV-specific CD4+ T cells. PBMC isolated from patients with resolved AH type B display the distinct subsets of virus-specific CD4+ T cells which carry markers of current activation or memory phenotype, indicating the continuous regeneration of effector as well as long-term maintenance of memory CD4+ T cells. The importance of this residual T cell response in controlling the virus

replication during SOI was demonstrated in a recent study carried out in the woodchuck model. In this study, woodchucks convalescent from symptomatic WHV infection and treated with the immunosuppressant agent, cyclosporin A, re-developed serum WHsAg-positive WHV infection (Menne *et al.*, 2007). These results indicate that after recovery from AH, successful anti-viral cellular immunity is essential for the long-term control of hepadnaviral replication as well as reactivation.

In the mouse model, it has been shown that, HBeAg and HBcAg can selectively elicit either Th2 or Th1 CD4+ T cell responses, respectively (Milich *et al.*, 1994 and 1998) . It was shown that, when mice were immunized with HBeAg and HBcAg together, the Th2 CD4+ T cell response induced by HBeAg was dominant over the Th1 CD4+ T cell response induced by HBcAg, resulting in the skewing of the immune response towards the Th2 type. It is hypothesized that this type of skewing of helper CD4+ T cell response to Th2 type could be one of the immune evasion mechanisms used by hepadnavirus to avoid elimination by the virus-specific immune responses and establish persistent infection.

#### **1.8.2.2 Humoral immunity**

Antibody responses directed against different HBV antigens can be detected in patients following exposure and is critical in providing protection against re-infection and maintaining active anti-viral immunity. Anti-HBV antibodies can provide an important barrier against the infection, if they are

present prior to virus invasion. The neutralizing antibodies developed after natural HBV infection, especially anti-HBs antibodies, are known to restrict cell-to-cell spread of virus and to protect against infection upon re-exposure to the virus. Apart from its protective role, anti-HBV antibodies are believed to mediate complement-mediated ADCC or phagocytosis of virally infected cells.

Unlike virus-specific T cell responses, anti-HBc antibody responses that occur during the acute phase of HBV infection that progresses to either resolution or chronicity are usually indistinguishable. In both groups of patients, the presence of anti-HBc antibodies is readily detectable. Although, anti-HBs or anti-HBe antibodies usually become detectable only in patients with resolving AH, after disappearance of serum HBsAg and HBeAg, respectively (Milich *et al.*, 1995).

The appearance of anti-HBs antibodies is considered to be a good indicator of resolution of acute HBV infection. These antibodies are not detectable by commercial assays during the early pre-acute phase or in patients with CH type B. It is believed that, during chronic HBV infection, anti-HBs antibodies form circulating immune complexes with excess HBsAg. However, when specific assays that detect traces of anti-HBs antibodies complexed to HBsAg are used, these antibodies can also be detected in patients with CH (Maruyama *et al.*, 1994). The anti-HBs antibodies are believed to prevent cell-to-cell spread by blocking the viral receptors essential for cell surface attachment (Milich *et al.*, 1995; Huang *et al.*, 2006).

Other HBV envelope proteins, i.e. preS1 and preS2 also induce antibody responses. Anti-preS1 antibodies are the first antibodies to appear during the incubation period of HBV or WHV (around 4 w.p.i.), preceding the appearance of anti-core antibodies (Klinkert *et al.*, 1986; Jin *et al.*, 1996). In contrast, anti-preS2 antibodies appear later during the acute phase of infection and can circulate simultaneously with anti-preS1 antibodies (Budkowska *et al.*, 1988). Interestingly, anti-preS2 antibodies were not detectable during AH that culminated in CH, regardless of HBeAg or anti-HBeAg status (Budkowska *et al.*, 1992; Coursaget *et al.*, 1988).

Similarly, anti-HBc antibodies of IgM type appear relatively early after HBV invasion (10-12 w.p.i), while anti-HBe antibodies are usually detectable later during HBV infection (Rehermann and Nascimbeni, 2005). Anti-HBe antibodies usually appear after the clearance of HBeAg and are associated with better prognosis and benign hepatitis. Anti-HBc antibodies of IgG class persist for life after recovery from AH and represent a reliable marker of previous exposure to the virus. In WHV-infected woodchucks, anti-WHc antibodies also persist for a life-time (Coffin *et al.*, 2004). The biological function of the anti-HBc and anti-HBe is poorly understood. Unlike anti-HBs antibodies, anti-WHc antibodies are produced at a high titer by the majority of infected patients (Milich *et al.*, 1995). Even though it is believed that anti-HBc or anti-HBe antibodies are not virus neutralizing, passive immunization of chimpanzees with anti-HBe antibodies has been shown to be protective against HBV infection (Prince *et al.*, 1983).

Antibodies to polymerase or X protein have also been detected in HBV-infected patients. Reports have shown that antibody to the c-terminus of polymerase protein can be detected during the acute phase of infection (Weimer *et al.*, 1989), while higher titers of anti-HBx antibodies have been found in patients with CH (Stemler *et al.*, 1990) but not in those with AH or resolved HBV infection.

However, anti-HBV antibodies induced during natural infection can induce pathological effects in the liver as well as extrahepatic tissues. The immune complexes formed between anti-HBs antibodies and HBsAg can cause membranoproliferative glomerulonephritis, necrotizing vasculitis and arthritis in patients with chronic hepatitis (reviewed in Milich *et al.*, 1995 and Michalak, 2004). Further, Michalak *et al.* have shown that complement dependent cytotoxicity directed against hepatocytes expressing HBcAg, HBsAg or asialoglycoprotein receptor (ASGPR) can contribute to the injury of HBV-infected hepatocytes, particularly in patients with severe CH (Diao *et al.*, 1998).

### **1.8.2.3 Cytokine responses during hepadnavirus infection**

Both *in vivo* and *in vitro* evidence suggest that cytokines, especially interferons and TNF- $\alpha$  directly inhibit HBV replication. *In vitro*, the HBV replication can be inhibited by recombinant TNF- $\alpha$  by accelerating the degradation of HBV mRNA, while virus core promoter has been shown to be sensitive to the actions of IFN- $\gamma$ , TNF- $\alpha$  and IFN- $\alpha$  (Ando *et al.*, 1994; Gilles *et*

*al.*, 1992; Tsui *et al.*, 1995). Further, the observation that intrahepatic induction of IFN- $\gamma$  and TNF- $\alpha$  triggers the degradation of preformed HBV RNA in the nucleus of the hepatocytes confirms the ability of these cytokines in controlling HBV gene expression, as observed in *in vitro* studies (Tsui *et al.*, 1995). Recent evidence suggests that IFN- $\gamma$  and TNF- $\alpha$  induce the cleavage of La autoantigen, which has function in stabilizing HBV mRNA and, thus, exposing the endonuclease-sensitive site of the HBV mRNA (Heise *et al.*, 1999).

In chimpanzees infected with  $5 \times 10^7$  HBV virions, virus DNA from serum and liver seemingly disappears in the absence of hepatic injury and long before the appearance of virus-specific T cell response during AH (Thimme *et al.*, 2003). In these chimpanzees, viral replication is almost completely abolished soon after appearance of CD3 and IFN- $\gamma$  mRNA in the liver and that this occurs several weeks before the peak of liver disease, suggesting the non-cytopathic control of HBV replication. Similarly, depletion of IFN- $\gamma$  and TNF- $\alpha$  producing CD8+ T cells during AH prolongs the duration of peak viremia in HBV-infected chimpanzees (Thimme *et al.*, 2003), further supporting the role of these cytokines in inhibiting viral replication.

The type of cytokine response, i.e., Th1 or Th2, is also associated with the outcome of HBV infection. The CD4+ T cells from patients who recover from AH display a Th1 cytokine profile, while the T cell clones generated from the PBMC of patients with CH produce predominantly Th2 type cytokines (Penna *et al.*, 1997; Bertoletti *et al.*, 1997). Further, the patients with CH, who respond to

interferon therapy produce more IL-12 and Th1 cytokines than that of interferon nonresponders (Penna *et al.*, 1997; Bertoletti *et al.*, 1997).

The best evidence suggesting the importance of different cytokines in the control of HBV replication, as well as in mediating liver injury, came from the transgenic mouse models of HBV. In these models, it has been shown that the cytokines, such as IFN- $\gamma$ , TNF- $\alpha$ , IFN- $\alpha/\beta$ , IL-12, IL-18 and IL-2 (reviewed in Guidotti and Chisari, 2001), independently or in conjunction with each other, inhibit the HBV replication. Activated HBV-specific CTLs adoptively transferred in a transgenic mouse expressing full length replicative form of HBV produce IFN- $\gamma$  and TNF- $\alpha$  and inhibit HBV gene expression in the liver, as well as mediate intrahepatic inflammation and subsequent liver damage (Guidotti *et al.*, 1994). When these transgenic mice were pre-administered with anti-IFN- $\gamma$  or anti-TNF- $\alpha$  antibodies, the adoptive transfer of HBV-specific CTLs failed to inhibit the HBV gene expression. Further, the ability of HBV-specific CTLs to inhibit the HBV replication was intact in the HBV transgenic mice which were knocked out for perforin molecules, suggesting that the inhibition of replication is not solely dependent on direct killing of hepatocytes (Guidotti *et al.*, 1999). It has been also shown that administration of recombinant murine IL-12 in HBV transgenic mice induces IFN- $\gamma$ , IFN- $\alpha/\beta$  and TNF- $\alpha$  responses in the liver, that further inhibits the HBV gene expression principally in a IFN- $\gamma$  dependent manner (Cavanaugh *et al.*, 1997). Interestingly, superinfection of HBV transgenic mice with hepatotropic pathogens, such as LCMV, cytomegalovirus, adenovirus or plasmodium parasite

induces a strong intrahepatic Th1 type cytokine response and ultimately inhibits HBV gene replication as a secondary effect (Cavanaugh *et al.*, 1998). These findings further stress the importance of the cytokine responses in the inhibition of HBV replication.

Nonetheless, the cytokines induced after HBV infection also mediate hepatic inflammation and liver injury. The hepatocytes from the HBV transgenic mouse which overexpress HBsAg in the liver have been shown to be more susceptible to lysis by IFN- $\gamma$  (Gilles *et al.*, 1992). In these mice, administration of recombinant IFN- $\gamma$  induces liver disease similar to that observed during fulminant hepatitis. The fact that this type of liver injury can be markedly reduced by pretreating mice with anti-IFN- $\gamma$  antibodies suggests the role of IFN- $\gamma$  in mediating liver injury during HBV infection. In the same mice, LPS-induced intrahepatic cytokine response and resultant severe liver inflammation is inhibited by treating the animals with anti-TNF- $\alpha$  monoclonal antibodies. Further, a liver-specific expression of IFN- $\gamma$  in a HBV transgenic mouse induces transaminases and histologically evident hepatitis similar to that observed during CH (Chen *et al.*, 2007). *In vitro*, HBV-expressing rat cell lines are susceptible to apoptosis to varied concentrations of TNF- $\alpha$ , ranging from 200-20,000 U/ml, and this susceptibility directly corresponds to the HBV gene expression (Guilhot *et al.*, 1996).

## 1.9 PURPOSE OF THE STUDY

Although the importance of virus-specific T cell and anti-viral cytokine responses in determining the outcome of hepadnaviral infection and mediating associated liver disease is acknowledged, the mechanisms behind the delayed appearance of the adaptive cellular responses in hepadnavirus infection and the inter-relationship between them and innate responses in the initial (pre-acute) phase of infection are poorly understood. Further, the features and kinetics of secondary (memory) virus-specific T cell response after the re-exposure of the virus-immune individuals or animals to different doses of the same hepadnavirus are also not well recognized. Similarly, recent studies from our laboratory, characterizing different attributes of low-level carriage of hepadnavirus during POI, have prompted questions regarding the properties of adaptive and innate immune responses that may accompany this type of virus persistence. The accomplishment of these objectives was difficult due to the unavailability of sensitive assays as well as appropriate woodchuck-specific reagents. Hence, the aims of the present study were focused on the development of the assays to monitor T cell proliferative responses and T cell susceptibility to apoptotic death and, subsequently, to determine the kinetics and inter-relationship between adaptive and innate responses during different phases of hepadnaviral infection and after challenge with virus. This project encompasses both *in vivo* and *in vitro* experimentation in the WHV-woodchuck model of hepatitis B.

In this context, the aims of the study were as follows:

1. Development of *in vitro* assays and molecular reagents for the assessment of cellular and cytokine immune responses in woodchucks infected with WHV.

1.1 Development of an *in vitro* T lymphocyte proliferation assay based on staining of dividing cells with CFSE (carboxyfluorescein di-acetate succinimidyl ester) dye to determine strength and longevity of WHV-specific and mitogen-induced T cell proliferative response in the course of WHV infection.

1.2 Cloning, sequencing and expression of the gene encoding for woodchuck IL-2 (wIL-2) to produce biologically active recombinant wIL-2 (rwIL-2) in prokaryotic and eukaryotic protein expression systems, to aid the studies on T cell responses in the woodchuck model.

2. Determination of the profiles and dissection of the kinetics of WHV-specific and generalized (mitogen-induced) T cell proliferative responses, and analysis of expression of cytokines and immune cell marker genes in PBMC and liver samples sequentially obtained after primary infection and subsequent re-exposure to WHV.

2.1 To analyze hepadnavirus-specific T cell proliferative responses against different WHV antigens during symptomatic infection induced with a liver-pathogenic dose of WHV ( $\geq 10^3$  virions) by using the traditional adenine incorporation assay and comparing the results with those obtained by applying more sensitive CFSE-based lymphocyte proliferation assay.

2.2 To determine the kinetics of the generalized immune competency of lymphocytes using their mitogen-induced proliferative capacity as a measure,

along with the gene expression of selected cytokines and immune cell surface markers in sequential PBMC samples, to elucidate the potential reasons behind the delayed appearance of virus-specific T cell response after exposure to different doses of WHV.

2.3 To investigate whether the infection of woodchucks with low, liver nonpathogenic dose ( $<10^3$  virions) of WHV evokes development of virus-specific T cell response and gene expression of cytokines and immune cell surface markers in PBMC. If so, to determine the profiles of T cell proliferative responses and to delineate their interrelationship with cytokine expression patterns, during establishment and progression of POI.

2.4 To assess the profiles of headnavirus-specific T cell proliferative responses and their relation to cytokine expression after challenge of woodchucks recovered from AH or those with established persistent POI.

## CHAPTER 2: GENERAL MATERIALS AND METHODS

### 2.1 ANIMALS AND VIRUS INOCULUM

#### 2.1.1 Woodchucks

The woodchucks (*Marmota monax*) used in these studies were maintained at the Woodchuck Viral Hepatitis Research Facility at the Health Sciences Centre, Memorial University of Newfoundland, St. John's, Newfoundland. Animals were housed under environmental and biosafety conditions specifically established for this species and the infection protocols were approved by the Institutional President's Ethics Committee.

Woodchucks infected with WHV were housed separately from non-infected, healthy animals. The healthy status of the non-infected animals was regularly monitored by evaluating the absence of WHV DNA by nested PCR followed by nucleic acid hybridization (PCR-NAH; sensitivity  $\leq 10$  vge/ml) and anti-WHc antibodies or WHsAg by ELISA, to eliminate the possibility of previous exposure with WHV.

After infection with WHV, the acute phase of infection was diagnosed when serum became positive for WHsAg and antibody to WHV core antigen (anti-WHc), but when WHs antigenemia lasted no longer than 6 months. CH was considered when WHsAg, accompanied by WHV DNA and anti-WHc, persisted for longer than a 6-month period (Hodgson and Michalak, 2001).

### 2.1.2 WHV inocula

The woodchucks were infected with well characterized WHV inocula derived from the sera of chronically infected animals. The inoculum WHV/tm3 (Genbank number AY334075, Michalak *et al.*, 2004) and WHV/tm4 were derived from sera of woodchucks with serum WHsAg-positive WHV infection and contained  $2.2 \times 10^{10}$  vge/ml and  $3.8 \times 10^{11}$  vge/ml, respectively. The comparative nucleotide sequence analysis of WHV/tm3 and WHV/tm4 showed the heterogeneity at nine nucleotides and has been described in detail elsewhere (Mulrooney-Cousins and Michalak, 2008).

### 2.1.3 Infection of woodchucks

All the infection protocols were performed after restraining the woodchucks under isoflurane-induced anaesthesia (CDMV Inc., St. Hyacinthe, Quebec). The animals were infected intravenously with the different doses of WHV as described in the Materials and Methods section for each experiment.

## 2.2 SAMPLE COLLECTION

### 2.2.1 Blood collection

Woodchucks were bled from the digitalis vein under aseptic conditions into tubes with no additives (Becton Dickinson, Rutherford, New Jersey) for serum isolation (Section 2.2.2) or into tubes containing sodium ethylenediamine tetra-acetic acid (EDTA; Becton Dickinson) for plasma and PBMC isolation. The

blood samples were processed immediately to avoid any undesired effects on the survival of PBMC.

### **2.2.2 Serum isolation**

Blood samples collected in the tubes containing no preservatives were positioned in a slanted position and allowed to clot for 2-3 h. The tubes were then spun down at 700 x *g* for 5 min and the layer of the serum from the top was carefully removed. These serum samples were aliquoted into smaller volumes and stored at -20 °C.

### **2.2.3 Isolation and storage of peripheral blood mononuclear cells (PBMC)**

PBMC were isolated from sodium EDTA-treated blood by density gradient centrifugation. In brief, whole blood was diluted with an equal volume of phosphate buffered saline, pH 7.4 (PBS) containing 1 mM EDTA (PBS-EDTA) and centrifuged through Ficoll-Paque Plus (Amersham Pharmacia Biotech, AB, Uppsala, Sweden). The top layer of the plasma was carefully removed without disturbing the underlying layer of PBMC and stored at -20 °C. The PBMC were collected, washed with PBS-EDTA, and incubated with ammonium chloride cell lysing buffer (ACK buffer, see Appendix B) for 15 minutes at room temperature to eliminate residual red blood cells (Lew and Michalak, 2001). The cells were washed with 10 mL of PBS-EDTA, assessed for viability by the trypan blue dye exclusion method and then counted in a hemocytometer. Usually, more than

99% cells were viable in the isolated PBMC.

In this study, isolated PBMC were usually used to perform the proliferation assays (see Section 3.2), while the remaining cells were resuspended in Trizol solution (Invitrogen, Auckland, New Zealand) and stored at -20 °C. These frozen PBMC samples were later processed to isolate RNA (see Section 2.6.1).

#### **2.2.4 Liver biopsies**

Woodchucks were sedated by an intramuscular injection of ketamine (23 mg/kg; Ketaset; CDMV Inc.) and xylazine (10 mg/kg; Lloyd Laboratories, Shenandoah, Iowa), and then anaesthetized using 2-4% isoflurane (CDMV Inc.). The surgical laprotomy was performed on the animals to obtain a liver biopsy sample, which was further divided aseptically into several fragments. Liver biopsy pieces of 1-2 mm<sup>3</sup> each were immediately frozen in liquid nitrogen for future nucleic acid analyses, while other fragments of about 5-mm<sup>3</sup> each were fixed in 10% buffered formalin (Fisher Scientific, Nepean, Ontario) for histological examination or embedded in HistoPrep (Fisher Scientific) and then frozen in isopentane pre-cooled in liquid nitrogen for future immunofluorescent (IFL) examination.

#### **2.2.5 Collection of specimens at autopsy**

The woodchucks were euthanized with an overdose of ketamine-xylazine and immediately blood was collected by cardiac puncture. The tissue samples

from liver, spleen, lymph nodes, bone marrow, kidneys, pancreas, and skeletal muscles were removed aseptically and preserved, as explained for liver biopsy samples (see Section 2.7).

## **2.3 ASSAYS FOR THE SEROLOGICAL AND MOLECULAR MARKERS OF WHV INFECTION**

### **2.3.1 Detection of WHV DNA**

#### **2.3.1.1 Isolation of WHV DNA**

To isolate WHV DNA, either 100  $\mu$ L of serum or 100 mg of liver tissue homogenized in 100  $\mu$ L of Hank's balanced salt solution (HBSS) were resuspended in 200  $\mu$ L of DNA lysis buffer (10 mM Tris-HCl, pH 8.0, with 10 mM NaCl, 1 mM EDTA, and 0.5% sodium dodecyl sulfate [SDS] containing 200  $\mu$ g proteinase K [Invitrogen]). The samples were incubated at 42°C overnight in a shaking incubator, then extracted two times with equal volumes of Tris-HCl-buffered phenol followed by chloroform/isoamyl alcohol (24:1). DNA was precipitated from the aqueous phase using one-tenth volume of 3 M sodium acetate and 2.5 volumes of absolute ethanol (Sigma Chemical Co.) for 12 h at -20 °C. The precipitated DNA was washed with 70% ethanol, resuspended in sterile water and quantified by measuring its absorbance at 260 nm using a DU 530 spectrophotometer (Beckman Instruments Inc., Fullerton, CA).

#### **2.3.1.2 Amplification of WHV DNA**

The presence of WHV DNA in the isolated DNA samples was detected after amplifying 1-4 µg of total genomic DNA using WHV gene-specific primers in direct PCR followed by nested PCR and Southern blot hybridization. The sequences of the oligonucleotide primers used for amplification and their location in the WHV genome have been previously reported (Coffin and Michalak, 1999; Michalak *et al.*, 1999). For direct PCR, three sets of primers amplifying fragments of WHc, WHx or WHs genes were used. To enhance sensitivity of DNA detection, the first round of direct PCR amplification was followed by another round of amplification in nested PCR using three sets of primers internal to the above mentioned direct primer pairs (Coffin and Michalak, 1999; Michalak *et al.*, 1999).

In general, direct PCR detection of WHV DNA utilized 1 X reaction buffer comprising 1.5 mM MgCl<sub>2</sub> with 50 mM KCl in 20 mM Tris-HCl buffer (pH 8.4) and 2.5 U of *Taq* DNA polymerase, 200 µM of each dNTP (all from Invitrogen), 300 ng of each oligonucleotide primer in a 100 µL total volume. The PCR reaction mixture was added with 1-4 µg of genomic DNA and overlaid with 100 µL of mineral oil (Sigma Chemical Co.) to prevent evaporation. The amplification of WHV DNA was performed in a programmable thermal cycler (TwinBlock System; Ericomp Inc., San Diego, CA) using the following steps: first step - 94 °C for 5 min, Second step - 94 °C for 30 sec, 52 °C for 30 sec and 72 °C for 30 sec; for 30 cycles, third step - 72 °C for 15 min. For each PCR reaction, a plasmid containing WHV DNA and DNA isolated from liver or serum of a WHsAg-positive

chronically infected woodchuck were used as positive controls (Coffin and Michalak, 1999; Lew and Michalak, 2001). For nested PCR, 10  $\mu$ L of the direct PCR mixture was re-amplified under the same conditions as the direct reaction. As negative controls, a water and a mock sample, containing all reagents used during the DNA extraction and PCR were included (Michalak *et al.*, 1999).

### **2.3.1.3 Detection of WHV DNA**

#### **2.3.1.3.1 Agarose gel electrophoresis**

The WHV DNA amplified in a PCR reaction was visualized on the standard 1% agarose gel. For this purpose, 1% agarose gel was prepared with 1 X TAE buffer (40 mM Tris-HCl buffer, pH 8.0, 1 mM EDTA,) containing 0.5 ng/mL of EB. Next, 18  $\mu$ L of PCR reaction was mixed with 2  $\mu$ L of DNA loading dye (10% Ficoll-400, 0.25% bromophenol blue, 0.25% xylene cyanol FF, 50 mM EDTA, 10 mM Tris-HCl buffer) (all from Sigma Chemical Co.) and loaded into the wells of a 1% agarose gel (Invitrogen) along with molecular weight standard (100 bp ladder or 1 kb ladder; Invitrogen). The electrophoresis was performed at 100 V for 50 min, the DNA bands were visualized under a UV light, and the image was recorded using an imaging system (ChemiGenius 2, Syngene; Frederick, MD).

#### **2.3.1.3.2 Southern blot hybridization**

The agarose gel containing the PCR products was denatured with 1.5 M

NaCl with 0.5 M NaOH for 30 min and then neutralized with two changes of 1.5 M NaCl in 1 M Tris-HCl buffer (pH 8.0) for 30 min each. Further, DNA from the gel was transferred on to nylon membrane (Amersham Biosciences, Uppsala, Sweden) by downward capillary transfer for 12-16 h and the membrane was baked at 80 °C in a vacuum oven for 2 h.

The nylon membrane was prehybridized at 65 °C for 1 h in a sealed glass tube using 6 mL of hybridization buffer containing 100 µg/mL sonicated salmon sperm DNA (Sigma Chemical Co.), 5 mL 6 X SSC (standard saline citrate), 0.5 mL 50 X Dendhardt's solution and 0.5 mL 10% SDS. Further, the membrane was hybridized overnight at 65 °C with radiolabeled WHV-specific DNA or oligonucleotide (Coffin and Michalak, 1999; Michalak *et al.*, 1999). Next day blots were washed twice in 2 X SSC with 0.1% SDS for 10 min at room temperature (RT) followed by two washes with 0.2 X SSC and 0.1% SDS for 10 min each. The membranes were taken out, blotted against paper towels, covered in plastic wrap and exposed to a multipurpose phosphor screen or exposed to X-ray film (MRP-1; Eastman Kodak Co., Rochester, NY) at -70 °C in autoradiography cassettes.

The relative quantity of the WHV DNA in the test samples was determined after comparing their band intensity with that of serial dilutions of recombinant WHV DNA, using either phosphoimager (Cyclone system, Canberra Packard Ltd., Montreal, Quebec) or densitometry (Gene Tools software on the ChemiGenius-2 imaging system).

### 2.3.2 Detection of WHV surface antigen (WHsAg)

Detection of WHsAg in the woodchuck serum samples was performed using an in-house ELISA. For this purpose, flat bottom 96-well plates (Linbro/Titertek; ICN Biomedicals, Aurora, OH) were coated with anti-WHs antibodies and incubated overnight at 4 °C. The plates were washed three times with PBS and blocked by adding 300 µL of 0.25% Tween-20 (Sigma Chemical Co., St. Louis, MO) in PBS (blocking buffer) at RT for 1 h. Plates were washed with PBS and 50 µL of either test serum samples or appropriate controls were added and incubated for 1 h at RT. Mouse anti-WHs was added (diluted 1:1000 in blocking buffer) and incubated for 1 h at RT. The unbound antibody was washed out and then alkaline phosphatase (AP)-conjugated goat anti-mouse antibody (Jackson Laboratories) was added (diluted 1:1000 in blocking buffer) and incubated for 1 h at RT. The assay was developed by adding 50 µL of soluble AP substrate (p-nitrophenyl phosphate; Sigma Chemical Co.) for 30 min and then terminated by adding 50 µL of 0.1 M EDTA. The absorbance of the developed reaction was measured at 400 nm using a microplate reader (BioRad Laboratories, Hercules, CA). The samples with absorbance 2.1 greater than the negative control were considered as WHsAg positive.

### 2.3.3 Detection of antibodies to WHV surface antigen (anti-WHs)

As previously described (Michalak *et al.*, 1990 and 1999), commercially available, cross-reactive anti-HBs ELISA (AUSAB EIA, Abbott Laboratories) was

used to detect anti-WHs antibodies in the serum samples. Briefly, HBsAg-coated polystyrene beads were incubated overnight with 200  $\mu$ L of either test woodchuck serum along with appropriate positive and negative control sera supplied by the manufacturer, as well as with anti-WHs positive and negative woodchuck sera. Next day, the beads were washed with water and incubated with 200  $\mu$ L of a biotin-tagged HBsAg. Rabbit anti-biotin conjugated with horseradish peroxidase (HRPO) was added for 2 h at 4  $^{\circ}$ C. The beads were washed to remove unbound conjugates, transferred to fresh tubes, and incubated with 300  $\mu$ L of freshly prepared o-phenylenediamine solution containing hydrogen peroxide for 30 min at RT. Further, the beads were transferred to fresh tubes and the HRPO reaction was stopped by addition of 1 mL of 1N  $H_2SO_4$ . Using a Quantum II dual-wavelength analyser (Abbott Laboratories), the absorbance was measured at 492 nm. The samples with absorbance values  $\geq 0.05$  cutoff value were considered positive (Michalak *et al.*, 1990 and 1999).

Alternatively, an in-house developed woodchuck-specific ELISA was also employed to detect anti-WHs antibodies. For this purpose, wells of a 96-well ELISA plate were coated with purified WHsAg at a concentration of 200 ng per well in 50  $\mu$ L of PBS and incubated overnight. Next day, wells were washed and then 300  $\mu$ L of blocking solution containing 1% milk powder and 0.05% Tween-20 in PBS, at RT was added. After 1 h, blocking solution was discarded and the plate blotted dry. Then, 50  $\mu$ L of test serum along with serum collected from

healthy animals as a negative control were added to each well, incubated at RT for 1 h and then washed with PBS three times. Next, 50  $\mu$ L of mouse anti-WHV preS2 antibody prepared in blocking solution at a dilution of 1:1000 was added to each well for 1 h, RT. Further, the wells were washed three times with PBS and a 1:1000 diluted AP-conjugated goat anti-mouse IgG (Jackson ImmunoResearch) for 1 h, RT was added. Finally, wells were washed three times with PBS and developed with 50  $\mu$ L of p-Nitrophenyl phosphate (pNPP) reagent (Sigma) for 30 min at RT. The reaction was stopped with 50  $\mu$ L of 0.1 M EDTA and absorbance was read at 405 nm. The test samples were considered positive for anti-WHs when the absorbance values from respective wells were below the cutoff values calculated as: mean of absorbance from negative control wells minus 3 standard derivations (SD).

#### **2.3.4 Detection of antibodies to WHV core antigen (anti-WHc)**

The detection of anti-WHc antibodies was performed by using a competitive ELISA previously developed in this laboratory, where in anti-WHc present in the test sample competes with HRPO-labeled anti-WHc for binding to immobilized WHcAg (Michalak *et al.*, 1999). For this purpose, a 96-well, flat-bottom plate (Linbro/Titertek; ICN Biomedicals) was coated with woodchuck anti-WHc antibodies at 1  $\mu$ g protein in 50  $\mu$ L of PBS per well and incubated at 4  $^{\circ}$ C for overnight. Next day, wells were washed three times and blocked with blocking buffer (as explained for WHsAg ELISA) for 2 h at RT. Further, 0.5  $\mu$ g

of WHcAg in 50  $\mu$ L volume was added to each well and the plate was incubated at RT for 2 h. Next, the plate was washed 4 times with PBS, blotted dry and the test serum sample or appropriate controls were added to each well and incubated with 25  $\mu$ L of anti-WHc labeled with HRPO (diluted 1:2,500 in blocking buffer) for 2 h. The wells were washed 3 times with PBS and supplemented with 50  $\mu$ L of 3,3',5,5'-tetramethylbenzidine (TMB) substrate (BioRad Laboratories). After 30 min, the reaction was stopped by adding 50  $\mu$ L of 1N sulfuric acid and absorbance at 450 nm was measured using a microplate reader (BioRad Laboratories). For this assay, serum samples collected from healthy animals served as negative controls, while sera from woodchucks chronically infected with WHV were used as positive controls. The degree to which the test sample inhibited the binding of HRPO-labeled anti-WHc was calculated as follows:

$$\text{percent inhibition} = 100 (\text{test sample optical density (OD)} \div \text{negative control OD} \times 100).$$

The assay results were accepted when the positive controls inhibited 95% of the HRPO-anti-WHc binding to WHcAg and the negative controls gave no inhibition. Samples that produced 50% inhibition were considered positive for anti-WHc.

### **2.3.5 Measurement of serum sorbitol dehydrogenase (SDH)**

The levels of SDH in serum were measured by using a standard SDH enzyme assay (Sigma Chemical Company, St. Louis, MO) with slight modifications. Briefly, 100  $\mu$ L of fresh woodchuck serum sample was added to

700  $\mu\text{L}$  of SDH buffer A (0.05 M Tris-HCl, pH 8.0, containing 100  $\mu\text{M}$  Dithiothreitol), 100  $\mu\text{L}$  of 10 mM nicotinamide adenine dinucleotide (NAD; Sigma Chemicals) and 100  $\mu\text{L}$  of 1M sorbitol in a cuvette and mixed properly. The cuvette was immediately placed in a spectrophotometer, absorbance at 340nm (A340) adjusted to 0.000 and then net A340 recorded at 30 sec intervals for 5 min. For the same serum sample, a blank assay was performed using a similar protocol, except replacing 1M sorbitol solution with 100  $\mu\text{L}$  of water. The absorbance for each test and blank sample was plotted on a graph and coefficient of absorbance per min ( $\Delta A/\text{min}$ ) was determined by determining the slope of each graph line. Further, net  $\Delta A/\text{min}$  was calculated by subtracting the slope of the blank sample from that of the test sample. The amount of SDH present in the serum sample was calculated using the formula:

$$\text{SDH [mili-International Units(mIU)/mL]} = \frac{[(\Delta A/\text{min}) \times 1 \times 60]}{[0.00622 \times 0.5]}$$

wherein:

1 = reaction volume (mL)

0.00622 = micromolar absorptivity of NAD at 340 nm

0.1 = sample volume (mL)

One International Unit (IU) of an SDH enzyme converts 1  $\mu\text{mol}$  of substrate per minute under the specified conditions of the procedure. In this assay, for healthy woodchucks the normal range of SDH in serum ranged from 0 to 20 IU/mL (Chen *et al.*, 1992, Michalak, 1998). The levels of SDH were

considered elevated when it contained more than  $2.1 \pm 3$  SD above the control values detected in the same animal prior to WHV exposure. Typically, during the acute phase of symptomatic WHV infection, SDH values in infected woodchucks ranged between 30 to 400 mIU/mL.

## 2.4 PRODUCTION OF RECOMBINANT WHV PROTEINS

### 2.4.1 Cloning of cDNAs encoding for WHV proteins in plasmid vectors

#### 2.4.1.1 Cloning of WHc, WHe and WHx cDNAs in pCR II vector

Different WHV cDNA sequences encoding for virus proteins were amplified by PCR and then cloned in an appropriate vector, as described earlier (Wang *et al.*, 2005). The following WHV proteins were amplified using respective gene-specific primer sequences: WHcAg encoded by nucleotides from 2021 to 2584 (rWHcAg), truncated WHeAg encoded by nucleotides 2021 to 2467 (rWHeAg), and X protein encoded by nucleotides 1503-1928 (rWHxAg). The nucleotide positions mentioned above refer to WHV/tm3 genome sequence as previously described (Genbank AY334075; Michalak *et al.*, 2004). The WHV gene-specific primers also contained the additional nucleotide sequences encoding for *Nde* I and *Xho* I restriction enzymes at the 5'- and 3'-ends, respectively, to facilitate the further cloning of these inserts in pET 4.1b expression vector. The PCR fragments generated were directly cloned into pCR II plasmid vector using TOPO-TA Cloning Kit (Invitrogen, Carlsbad, CA). For this purpose, 4  $\mu$ L of each PCR product was mixed with 1  $\mu$ L NaCl and 1  $\mu$ L of TOPO

pCR II and incubated at RT for 30 min. Then, 2  $\mu$ L of this reaction mixture was added to 50  $\mu$ L of thawed competent *Escherichia coli* (*E. coli*) TOP10 cells (Invitrogen) and kept on ice for 30 min. For the transformation of recombinant DNA into *E. coli*, these competent cells were heat shocked for 45 sec at 42 °C, immediately placed on ice for 2 min, added with 400  $\mu$ L of LB medium and incubated at 37 °C for 1 h in a rotator at 200 rpm. A 100  $\mu$ L aliquot of each transformation reaction mixture was then spread onto LB agar (Difco Laboratories, Detroit, MI) plates containing 50  $\mu$ g/mL of kanamycin and coated with 40  $\mu$ L of X-Gal (Sigma Chemical Co.). The plates were incubated at 37 °C for 16-24 h and the white bacterial colonies were identified as the positive colonies containing recombinant DNA insert.

#### **2.4.1.2 Plasmid isolation and enzymatic manipulations**

The white recombinant colonies obtained after transformation of *E. coli* were picked up using sterile pipette tips, labeled, transferred to 5 mL of LB broth supplemented with 50  $\mu$ g/mL kanamycin and further incubated overnight in a shaker incubator at 37 °C. The next day, a 1.5-mL aliquot of this LB broth was pelleted at 20,000  $\times g$  for 20 sec in Eppendorf tubes and the cells were resuspended in 100  $\mu$ L of glucose Tris-EDTA (GTE; see Appendix B) for 5 min at RT. The bacteria cells were lysed with 100  $\mu$ L of freshly prepared 0.2 N NaOH/1% SDS for 5 min at RT. This solution was neutralized by adding 100  $\mu$ L of pre-chilled 3 M potassium acetate (pH 5.5) on ice for 5 min which aids in the

removal of chromosomal DNA and proteins. The tubes were centrifuged at 20,000 x *g* for 5 min to pellet cell debris and chromosomal DNA. The supernatant was transferred to a fresh Eppendorf tube and plasmid DNA was precipitated with 1 mL of 95% ethanol for 10 min at RT. The plasmid pellet was centrifuged at 15,000 x *g* for 5 min, washed with 1 mL of 70% ethanol, air-dried, resuspended in 30-50  $\mu$ L of TE buffer, and stored at -20 °C until further use. The plasmids isolated this way were subjected to restriction enzyme digestion (see Section 2.4.1.3) and gel electrophoresis for the confirmation of the proper WHV gene insert.

In some instances, to obtain higher quantities of plasmid with a greater purity, large-scale plasmid DNA preparation were done using Maxi/Midi plasmid preparation kits (Qiagen). For this purpose, 1 mL of *E. coli* culture harboring appropriate recombinant plasmid insert, as judged by miniprep analysis described above, was added to 100 mL of superbroth medium supplemented with 50  $\mu$ g/mL of the appropriate antibiotic (kanamycin or ampicillin) and incubated overnight in a shaker incubator at 200 rpm, 37 °C. Next day, bacterial cells were centrifuged at 10,000 rpm for 15 min at 4 °C and resuspended in 10 mL of P1 solution (see Appendix B) supplemented with 100  $\mu$ g/mL RNase A. Next, 10 mL of P2 solution (see Appendix B) was added for 5 min at RT to lyse the bacteria, which was further neutralized with 10 mL of ice-old P3 solution (see Appendix B) on ice for 30 min. This mixture was passed through a filter cartridge provided with the kit to remove chromosomal DNA and bacterial proteins. The

filtrate was run through a column containing DNA binding resin, washed twice with QC buffer (see Appendix B), and plasmid DNA was eluted with 15 mL of QF buffer (see Appendix B). The eluted plasmid DNA was precipitated by adding 10.5 mL of isopropanol (Sigma Chemical Co.) for 5 min at RT, followed by centrifugation at 20,000 x g for 30 min. The plasmid preparation was washed with 70% ethanol, resuspended in 500  $\mu$ L of TE buffer, quantified as previously described, and stored at  $-20^{\circ}\text{C}$ .

#### **2.4.1.3 Restriction enzyme digestion analysis**

The recombinant plasmids isolated from a mini, midi or maxi preparations were analyzed by digesting them with appropriate restriction enzymes to confirm the proper WHV DNA insert. The restriction enzyme digestion was performed using either a single or double enzyme reaction. For single enzyme digestion, 0.5 - 1  $\mu$ g plasmid DNA, 10 U enzyme (usually in 1  $\mu$ L; no more than 10% of reaction volume), 2  $\mu$ L appropriate buffer and 1  $\mu$ L of RNase solution were resuspended in sterile water, to make a final volume of 20  $\mu$ L per reaction. When performing double enzyme digestion, 20  $\mu$ L of final reaction volume contained 0.5 - 1  $\mu$ g plasmid of DNA, 1  $\mu$ L of each enzyme, 2  $\mu$ L appropriate compatible buffer and 1  $\mu$ L of RNase solution in sterile water. The reaction mixture was incubated  $37^{\circ}\text{C}$  for 18-24 h and the presence of proper insert in the plasmid backbone was analyzed by performing agarose gel electrophoresis.

#### 2.4.1.4 Purification of WHV gene inserts

Since all the recombinant WHV proteins contained additional nucleotide sequences encoding for *Nde* I and *Xho* I restriction enzymes at the 5'- and 3'-ends respectively (see Section 2.4.1.1), the respective plasmids were digested with these enzymes to obtain the insert containing the WHV gene sequence. The digested plasmids were run on a 1% low melting point agarose (Invitrogen) gel, the band containing the PCR product of interest was visualised, excised, placed in a 1.5-mL Eppendorf tube and heated at 65 °C. Next, 1 mL of DNA binding resin was added to the tube, incubated at RT for 1 min and then passed through a Wizard minicolumn (Promega Corp., Madison, WI) using vacuum suction. The column was washed twice with 80% isopropanol and then centrifuged at 12,000 x g for 20 sec to remove residual alcohol. Finally, 30 µL of prewarmed TE buffer was added to a column and incubated for 2 min at RT. Next, the column was spun at 12,000 x g for 20 sec, RT to elute the insert DNA. The eluted WHV gene insert was subcloned in pET 4.1b expression vector.

#### 2.4.1.5 Subcloning to generate recombinant WHV proteins

The WHV DNA gene inserts encoding for respective proteins and containing additional *Nde* I and *Xho* I enzyme flanking sequences (see Section 2.4.1.1) were first ligated in pET 4.1b vector (Novagen, Darmstadt, Germany). For this ligation reaction, 2 µL of *Nde* I/*Xho* I digested pET 4.1b vector was added to 6 µL of WHV gene insert, 4 µL ligation buffer, 2 µL of 10 mM ATP

(Invitrogen), 1  $\mu\text{L}$  of T4 DNA ligase and 5  $\mu\text{L}$  of sterile water to make a final volume of 20  $\mu\text{L}$ . The reaction mixture was incubated at 14  $^{\circ}\text{C}$  for overnight. Next day, 10  $\mu\text{L}$  of ligation reaction mixture was transformed in *E. coli*, BL21, DE3 cells as described for TOP10 cells (section 2.4.1.1). When ligated in the proper orientation, all the WHV gene inserts also contained an additional pET 4.1b derived six histidine amino acids at the carboxyl end followed by a stop codon. The transformed *E. coli* colonies from the LB agar plates containing 100  $\mu\text{g}/\text{mL}$  of ampicillin or 50  $\mu\text{g}/\text{mL}$  of carbenicillin were picked up and cultured in the 5 mL of superbroth (see Appendix B) supplemented with similar regimen of either antibiotic, to generate the stock inoculum to be used in expression experiments.

## **2.4.2 Expression and purification of recombinant WHV proteins**

### **2.4.2.1 Induction of recombinant protein expression in *E. coli***

The expression cultures were started by adding 1 mL of stock inoculum in 100 mL of superbroth supplemented with 100  $\mu\text{g}/\text{mL}$  of ampicillin or 50  $\mu\text{g}/\text{mL}$  of carbenicillin. The cultures were incubated at 37  $^{\circ}\text{C}$  in a shaking incubator at 200 rpm until the growth density (absorbance at 600 nm) reached 2.0. At this stage, 5 mL of culture was aliquoted and cultured in a separate tube as an uninduced control. The rest of the culture was added with isopropyl  $\beta$ -D-1-thiogalactopyranoside (IPTG; Invitrogen) at the final concentration of 1  $\mu\text{M}$  to induce the expression of the recombinant proteins in the bacterial cells and

incubated for an additional 2 h. Both induced and uninduced cultures were terminated by chilling them on ice for 10 min and then centrifuging the cells at 4000 rpm, for 15 min at 4 °C. The pellets were stored at -70 °C until further use.

#### **2.4.2.2 Preparation of inclusion bodies**

The cell pellets were thawed on ice for 10-15 mins, supplemented with 1 mL of BugBuster reagent (Novagen) in the presence of 25 U/mL benzonase (Novagen). After 30 mins of incubation at RT, the pellet was centrifuged at 16,000 x g for 20 min at 4 °C to precipitate the insoluble inclusion body (IB) fraction from that of the cytoplasmic protein fraction. The cytoplasmic fraction was collected without disturbing the IB precipitate and stored at -20 °C until further analysis. Further, the IB fraction was treated with lysozyme at a final concentration of 200 µg/mL for 5 min at room temperature, followed by three washes with 1:10 diluted BugBuster reagent and then suspended in denaturing buffer B (see Appendix B) containing 8 M urea. Both IB and cytoplasmic fractions from both IPTG-induced and uninduced cultures, were then examined by sodium dodecyl sulphate-polyacrylamide gel electrophoresis (SDS-PAGE)/Western blotting to determine the presence of the recombinant proteins.

#### **2.4.2.3 SDS-PAGE and Western blot analysis**

The samples to be tested by SDS-PAGE analysis were resuspended in a

loading buffer (6X) containing 3% SDS, 5% 2-mercaptoethanol, 10% glycerol in 62.5 mM Tris-HCl buffer, pH 6.8 for 10 min at 95 °C. A denaturing 12% or 15% separating polyacrylamide gel was prepared in 37.5 mM Tris-HCl buffer, pH 8.8, with 0.1% (wt/vol) SDS along with a 3% acrylamide upper stacking gel in 12.5 mM Tris-HCl buffer, pH 6.8, with 0.1% (wt/vol) SDS and were loaded in a mini-gel apparatus (Mini-Protean II dual slab cell; Bio-Rad Laboratories, Hercules, CA). The samples along with a protein molecular weight marker ladder were loaded in the wells of the upper gel and separated in the stacking gel at a constant voltage of 200 V for about 45 min in reservoir buffer (20 mM glycine, 2.5 mM Tris base). The gel apparatus was disassembled and the polyacrylamide gel was either put in a small plastic tray containing 0.5% coomassie blue staining solution and incubated for 2-3 h or transferred onto nitrocellulose (NC) membrane for Western blotting. The stained gel was further destained with destaining solution (10% acetic acid) for 2-3 h to visualize protein bands. The molecular weights of the protein bands were determined by comparing them with that of the molecular weight ladder.

Alternatively, proteins separated by SDS-PAGE were directly transferred onto a NC membrane (Amersham) by semi-dry transfer using a Bio-Trans unit (Gelman Inc., Ann Arbor, MI). The efficiency of protein transfer was determined using a pre-stained molecular weight marker (Invitrogen). After transfer, NC blots were incubated with PBS containing 10% normal goat serum and 0.025% Tween-20 for 1 h at RT, to block nonspecific binding sites. Next, the NC blot was

incubated with mouse anti-histidine primary antibodies resuspended in blocking buffer at 1:1000 dilution for 2 h at RT or overnight at 4 °C. The NC blot was washed twice with blocking buffer and added with goat anti-mouse IgG antibody conjugated with AP at 1:5000 dilution for 1 h at RT. Again, the blot was washed twice with blocking buffer and developed for 5-10 min in a solution containing nitro-blue tetrazolium and 5-bromo-4-chloro-3-indolyl phosphate, as described in the supplier's instructions (Sigma Chemicals). The developing reaction was stopped by washing the NC blot in cold water.

#### **2.4.2.4 Affinity chromatography purification**

The IB pellet dissolved in 4 mL of buffer B was incubated at RT on a rotator for 2 h and then added to 1 mL of 50% nickel-nitriloacetic acid (Ni-NTA) slurry (Novagen). This mixture was incubated at RT for 2 h on a rotating shaker at 20-30 rpm, to insure the proper binding of the histidine residues on recombinant proteins with the Ni-NTA slurry. Next, the IB-Ni-NTA slurry mixture was loaded on a syringe column plugged with sterile wool. The mixture was allowed to run through the column without applying any force and flow-through fractions were collected. The column was washed twice with 4 mL of Buffer C (see Appendix B) and wash fractions were collected. Finally, the recombinant protein bound to resin was eluted twice with 500  $\mu$ L of Buffer E (see Appendix B), collected in sterile Eppendorf tubes and stored at -20 °C until it was analyzed by SDS-PAGE and Western blotting or refolded using gradient dialysis.

#### **2.4.2.5 Refolding of purified recombinant proteins**

Recombinant WHV proteins purified under denaturing conditions were further refolded by dialyzing them against a series of decreasing concentrations of Buffer E. Dialysis tube with molecular weight cut off value of 12000 Da was cut into pieces of 10-15 cm each and immersed in 250 mL of water containing 100 µg sodium bicarbonate and 12.5 mg EDTA, boiled for 10-15 min and allowed to cool at room temperature. A pinch of sodium azide was added and tubes were stored at 4 °C until further use. Affinity purified recombinant proteins were poured into dialysis tubes, sealed properly using thread knots, and then immersed in a flask containing 250 mL of 6 M Buffer E. Dialysis on a magnetic stirrer was performed at 4 °C for overnight. After every 18-24 h, the dialysis buffer was changed to a lower molarity (4 M, 2 M and 1 M Buffer E. Finally, 1 M Buffer E was replaced by sterile PBS and dialysis was performed for additional 2 days at 4 °C. Next, the recombinant proteins in it were collected in sterile Eppendorf tubes. Small aliquots of these proteins were used for determination of protein content, while the remaining volume was supplemented with phenylmethyl sulfonyl fluoride (PMSF, 0.1 µM final concentration; Sigma Chemicals), as a protease inhibitor, and stored at -20 °C in small (100 µL) aliquots.

#### **2.4.2.6 Quantitation of recombinant proteins**

The quantitation of proteins was done using standard bicinchoninic acid

(BCA) assay. For this purpose, one volume of copper sulfate solution was added to 50 volumes of bicinchoninic acid solution. As a standard, serial dilutions of BSA (1 mg/mL; Sigma Chemicals) in the range of 0 to 100  $\mu$ g were prepared in separate test tubes in a final volume of 100  $\mu$ L. Then, 50  $\mu$ L of each recombinant protein to be quantified was added in a separate test tube and supplemented with 50  $\mu$ L of sterile water. Each tube containing standard and test sample was mixed with 2 mL of protein determination reagent and incubated at 37 °C for 30 min. Then, the tubes were cooled at RT for 5 min and absorbance was measured at 562 nm (A562). The standard curve was obtained using A562 values of serial dilutions of BSA which were used to estimate the protein content of the test samples.

## **2.5 PROCUREMENT OF OTHER WHV ANTIGENS AND MITOGENS**

### **2.5.1 Purification of WHsAg**

A discontinuous sucrose gradient followed by a cesium chloride (CsCl) gradient were used to purify WHsAg from the serum of a woodchuck chronically infected with WHV. First, 7 mL of WHsAg-positive woodchuck serum was centrifuged at 3,000 rpm, 4 °C for 30 min to remove possible sediments. Next, 6 mL of discontinuous sucrose gradient was prepared by overlaying 1.5 mL each 20% (bottom of the gradient), 15%, 10% and 5% (top of the gradient) sucrose in 0.01M Tris-HCl buffer, pH 7.5 containing 500 mM NaCl and 1 mM EDTA. The pre-cleared woodchuck serum (7mL) was carefully laid on the top of this gradient

and centrifuged at 40,000 rpm at 4 °C for 18 h. The resulting pellet was resuspended in 1 mL of 15 mM NaCl by sonication at 9 amps for 45 sec and solid CsCl was added to make up a density of 1.30 g/cm<sup>3</sup> in a 2 mL volume. Separately, CsCl gradient solutions were prepared at different densities ranging from 1.1 to 1.35 g/cm<sup>3</sup>, in 0.01M Tris-HCl buffer, pH 7.5 containing 500 mM NaCl and 1 mM EDTA. To mount the density gradient, 2 mL of 1.35 g/cm<sup>3</sup> CsCl (bottom of the gradient) was overlaid with 2 mL each of 1.30 g/cm<sup>3</sup> CsCl-WHsAg pellet suspension and 1.25 g/cm<sup>3</sup>, 1.2 g/cm<sup>3</sup> and 1.1 g/cm<sup>3</sup> (top of the column) of CsCl solutions. The gradient was spun down at 40,000 rpm, 10 °C for 20 h. From the top of the gradient, 500 µL aliquots were collected and the pellet was saved. The presence of WHsAg in different fractions was assessed by ELISA with anti-WHsAg antibody and fractions containing peak WHsAg reactivity were pooled together. Again, solid CsCl was added to these fractions to make up a density of 1.30 g/cm<sup>3</sup> and applied on a CsCl density gradient. The second gradient was prepared by overlaying 2 mL of 1.35 g/cm<sup>3</sup> CsCl solution (as explained above; bottom of the column) with 2 mL of CsCl-WHsAg pellet and 9 mL of 1.15 g/cm<sup>3</sup> CsCl solution (top of the column) and centrifuged at 40,000 rpm at 10 °C for 20 h. Similar to the first CsCl gradient, 500 µL fractions were collected, assayed for WHsAg by ELISA and fractions containing peak WHsAg reactivities were pooled. This pool was dialyzed against 0.01M Tris-HCl buffer, pH 7.4, for 24 h at 4 °C with at least three changes of buffer. The protein content of purified WHsAg was measured using a standard BCA assay and then stored

at -20 °C in small aliquots.

### **2.5.2 Immunodominant WHc<sub>97-110</sub> peptide**

Synthetic WHV core peptide (WHc<sub>97-110</sub>), encompassing amino acids located in positions 97 to 110 of the virus nucleocapsid protein was prepared by Synprep Corporation (Dublin, CA). This peptide is known to contain an immunodominant epitope of WHc antigen recognized by the T lymphocytes from most of the WHV-infected woodchucks (Menne *et al.*, 1997) and was implemented in our experiments to evaluate WHV-specific T cell response along with other WHV antigens.

### **2.5.3 Mitogens**

Different mitogens were used as non-specific stimulators in proliferation assays to monitor generalized proliferative capability of PBMC, as an indicator of their overall immune competence. These mitogens included: Concanavalin-A (ConA; Pharmacia Fine Chemicals, Uppsala, Sweden), pokeweed mitogen (PWM, *Phytolacca americana* agglutinin; ICN Biochemicals Inc., Aurora, Ohio) and phytohemagglutinin (PHA; ICN Biochemicals Inc.). The varied concentrations of the mitogens used in different experiments have been described under respective sections in Materials and Methods sections.

## **2.6 Real time reverse transcription-polymerase chain reaction (RT-PCR)**

### 2.6.1 Isolation of RNA

Total RNA was isolated from PBMC or liver tissue samples using Trizol reagent according to the manufacturer instruction. As described in Section 2.2.3, PBMC samples already resuspended in Trizol reagent and frozen at  $-20^{\circ}\text{C}$  were thawed at RT for 10-15 min. For liver biopsy or autopsy samples, a small piece (approx.  $1\ \mu\text{g}$  in weight) was recovered from  $-80^{\circ}\text{C}$  freezers and homogenized in 1 mL of Trizol reagent. Either PBMC sample or homogenized liver tissue resuspended in 1 mL of Trizol were mixed on a rotator for 30 min, added with  $200\ \mu\text{L}$  of chloroform, shaken vigorously for 15 sec and then centrifuged at  $12,000\ \times\ g$  for 15 min at  $4^{\circ}\text{C}$ . The upper aqueous layer was collected into a fresh tube, added with  $500\ \mu\text{L}$  of isopropanol, incubated at RT for 10 min, and kept at  $-20^{\circ}\text{C}$  overnight for the precipitation of RNA. Next day, the tubes were centrifuged at  $12,000\ \times\ g$  for 10 min at  $4^{\circ}\text{C}$  to pellet the RNA. The pellet was washed in 1 mL of RNase-free 75% ethanol, dried in a vacuum chamber for 5-7 min and resuspended in  $8\ \mu\text{L}$  of autoclaved RNase-free water. Further, the possible contamination of total RNA with that of genomic DNA was eliminated by treating RNA samples with DNase I (Ambion Inc. Tx). For this purpose, to  $8\ \mu\text{L}$  of RNA sample was added  $1\ \mu\text{L}$  of DNase I and  $1\ \mu\text{L}$  of reaction buffer and incubated for 15 min at RT. The reaction was stopped by adding  $1\ \mu\text{L}$  of stop solution and incubating the samples at  $70^{\circ}\text{C}$  for 10 min. The samples were then chilled on ice for 2 min, briefly centrifuged and quantitated using a spectrophotometer. Finally,  $2\ \mu\text{g}$  of total RNA was immediately used for a

reverse transcription reaction or stored at  $-20^{\circ}\text{C}$ .

### 2.6.2 Preparation of cDNA

The total RNA isolated as above was converted in cDNA by using a reverse transcription (RT) reaction kit (Invitrogen), as per vendor's instructions. After quantitation, the concentration of total RNA was adjusted in such a way that 2  $\mu\text{g}$  of total RNA was present in a total of 8  $\mu\text{L}$  volume. To this RNA sample was added 2  $\mu\text{L}$  of random primers (100 ng/ $\mu\text{L}$ ), 4  $\mu\text{L}$  of 5X RT buffer (375 mM KCl, 15 mM  $\text{MgCl}_2$  in 250 mM Tris-HCl buffer, pH 8.3; Invitrogen), 2  $\mu\text{L}$  of dithiothreitol (DTT; 0.1 M; Invitrogen), 2  $\mu\text{L}$  of deoxynucleotide triphosphate (dNTP) mixture (10 mM dATP, dCTP, dGTP and dTTP each, all from Promega), 10 U of RNase inhibitor (RNasin; 40 U/ $\mu\text{L}$ ; Promega), and 200 U of reverse transcriptase from Moloney murine leukemia virus (Invitrogen) in a total of 20  $\mu\text{L}$  per reaction. The reaction mixture was incubated at  $37^{\circ}\text{C}$  for 1 h and then at  $95^{\circ}\text{C}$  for 5 min to convert RNA samples into cDNA. The cDNA samples prepared this way were stored at  $-70^{\circ}\text{C}$  until PCR amplification was performed.

### 2.6.3 Real time RT-PCR

A LightCycler (LC; Roche Biosciences) thermocycler instrument was used in this study to perform real time RT PCR. The 20  $\mu\text{L}$  cDNA prepared as above (see Section 2.6.2) was diluted (1:4) with 60  $\mu\text{L}$  of sterile water and 2  $\mu\text{L}$  of this diluted cDNA was used in each real time PCR reaction. The LC PCR buffer was

prepared by adding 100  $\mu\text{L}$  of 10X PCR buffer (Invitrogen), 80  $\mu\text{L}$  of  $\text{MgCl}_2$  (Invitrogen), 40  $\mu\text{L}$  of BSA (10 mg/mL) and 8  $\mu\text{L}$  of 25 mM dNTP mixture in 572  $\mu\text{L}$  sterile water. Next, 2  $\mu\text{L}$  diluted cDNA or 2  $\mu\text{L}$  water, as a negative control, or 2  $\mu\text{L}$  of appropriate plasmid with known copy number of the respective gene, as a positive control, were loaded into LC capillaries (Roche Biosciences). Each capillary was added with 16  $\mu\text{L}$  of freshly prepared LC PCR buffer, 0.2  $\mu\text{L}$  of *Taq* DNA polymerase, 0.667  $\mu\text{L}$  of 10X SYBR I dye (Invitrogen), and 2  $\mu\text{L}$  of gene-specific primer mixture containing plus and minus primers at a concentration of 5 pmol each. The primer sequences for each gene amplified in real time PCR are shown in Table 5.1 the capillaries were loaded into the LC carousel, briefly spun down and inserted into the chamber of the LC module (Roche Biosciences) to perform the reaction as per conditions established previously (Guy *et al.*, 2006). LightCycler quantification software (Roche Diagnostics) was used for enumeration of copy numbers of the respective gene amplified.

## 2.7 HISTOLOGICAL EXAMINATION OF LIVER TISSUE SAMPLES

As described previously (Michalak *et al.*, 1999, Hodgson and Michalak, 2001; Michalak *et al.*, 2004), liver tissue samples were embedded in paraffin blocks. These liver fragments were cut into 5- $\mu\text{m}$  thin sections and stained with hematoxylin and eosin, Mason-trichrome, periodic acid Schiff or impregnated with silver. The sections were examined under a microscope to assess histological lesions. Morphological alterations encountered in

hepatocellular, extrahepatocellular, intralobular and portal compartments of hepatic parenchyma were graded on a numerical scale from 0-3, as described in previous works (Michalak *et al.*, 1999, Hodgson and Michalak, 2001; Michalak *et al.*, 2004). This numerical score has been referred to herein as the histological degree of hepatitis.

**CHAPTER 3: FLOW CYTOMETRIC QUANTITATION OF T CELL  
PROLIFERATION AND DIVISION KINETICS IN WOODCHUCK MODEL OF  
HEPATITIS B**

*This study has been published in Immunological Investigations, 2005; 34(2): pp 215–236.*

### **3.0 SUMMARY**

Woodchucks infected with woodchuck hepatitis virus (WHV) represent the closest natural animal model to study the immunopathogenesis of liver injury caused by essentially noncytopathic, highly human specific hepatitis B virus (HBV). The importance of antiviral T cell response in induction of hepatitis and in control of HBV replication has been demonstrated. However, the understanding of how these responses contribute to the development of different immunomorphological forms of liver disease and their outcomes remain elusive. In this study, we established and standardized a flow cytometry assay using peripheral blood mononuclear cells labeled with carboxyfluorescein diacetate succinimidyl ester (CFSE) to assess WHV-specific and mitogen-driven T lymphocyte proliferative responses in woodchucks. The assay is of significantly greater sensitivity than the adenine incorporation assay currently used when applied to measure either WHV-specific T cell responses in acute ( $P < 0.001$ ) and chronic ( $P < 0.03$ ) viral hepatitis or those induced by mitogens in both healthy and WHV-infected animals. It also provides a new type of information, not previously available, characterizing the strength of woodchuck T cell

proliferative reactivity by measuring cell division rates. The study shows that woodchuck PBMC labeled with CFSE exhibit light scatter and fluorescence profiles compatible to those of human PBMC, allowing quantitation and deconvolution of the flow cytometric data by applying the existing analytical softwares. The availability of this novel assay should facilitate a more precise and comprehensive evaluation of hepadnavirus-specific and generalized T cell responses in experimental WHV hepatitis.

### 3.1 INTRODUCTION

Hepatitis B virus (HBV) is a noncytopathic DNA virus, the prototype of the hepadnaviral family. This pathogen infects an estimated 2 billion people, including more than 350 million persons with symptomatic chronic infection (WHO report, 2000). It contributes towards 0.5 to 1.2 million deaths annually (Lavanchy, 2004). The virus causes acute and chronic hepatitis, cirrhosis, and hepatocellular carcinoma (Chisari and Ferrari, 1995). It also induces persistent, probably lifelong, serologically silent (occult) infection (Michalak *et al.*, 1994; Rehermann *et al.*, 1996; Yuki *et al.*, 2003). A large body of evidence indicates that the host cellular immune reactions directed against HBV proteins, particularly those mediated by T lymphocytes, are crucial to the development of liver disease and, at the same time, in restriction of virus replication in hepatic tissue (Bertoletti *et al.*, 1994; Maini *et al.*, 2000; Thimme *et al.*, 2003). It also becomes apparent that the strength and breadth of the initial T helper and

cytotoxic T cell responses are important in determining the final outcome of the disease, *i.e.*, whether acute infection resolves or progresses to chronic hepatitis (reviewed in Chisari, 1997 & Michalak, 2004). Investigations of these events in humans are hampered by practical and ethical difficulties in acquisition of relevant samples, especially from individuals with acute hepatitis and with well-defined onset of the infection. Chimpanzees infected with HBV have provided valuable insights to some aspects of the T cell response kinetics, but because of their restricted usage, the data available are sparse and derived from singular animals (Bertoni *et al.*, 1998; Thimme *et al.*, 2003; Weiland *et al.* 2004). Studies in HBV transgenic mice allowed detailed characterization of T cell immune responses towards different viral protein epitopes and contribution of these responses to hepatocellular injury in mice (Moriyama *et al.*, 1990; Guidotti *et al.*, 1994; Chisari, 1996; Nakamoto *et al.*, 1998, Guidotti *et al.*, 1999); however, these observations require validation in the natural models of hepadnavirus infection.

The infection of woodchucks (*Marmota monax*) with woodchuck hepatitis virus (WHV) has a disease course and the rates of recovery or progression to chronic hepatitis similar to those seen in hepatitis B (Michalak, 1998). This animal model is accepted as the closest natural system for studies of the HBV pathobiology and the pathogenesis of liver injury in hepatitis B (Michalak, 1998; Menne and Tennant, 1999). Evaluations completed so far have shown that the dynamics of WHV-specific T cell responses in woodchucks are compatible with those observed in HBV-infected humans (Menne *et al.*, 1998; Menne *et al.*,

2002a). However, the measurement of these responses by nucleotide incorporation assays currently used is elaborate, of low sensitivity, and involves biohazardous reagents. Among others, this is due to the fact that cultured woodchuck lymphocytes have very low levels of thymidine kinase activity, making implementation of assays based on  $^3\text{H}$ -thymidine incorporation impractical (Cote and Gerin, 1995; Maschke *et al.*, 2001). Alternatively,  $^3\text{H}$ -adenine was used to overcome this problem (Kreuzfelder *et al.*, 1996). However, since this nucleotide is incorporated into RNA, stimuli which induce cell proliferation and a higher RNA transcription cause a greater adenine incorporation leading to high background values and decreased assay sensitivity.

In recent years, different cell dyes (*e.g.*, CFSE, PKH, calcein, H33342) have been applied to label lymphocytes and monitor their proliferation kinetics (Parish, 1999). Among them, 5-(and-6)-carboxyfluorescein diacetate succinimidyl ester (CFDA-SE; commonly named as CFSE) is a membrane permeant dye that covalently binds to cytoplasmic proteins forming stable fluorescent conjugates, which can be readily tracked by flow cytometry (Lyons and Parish, 1994). During each cell division, intracellular CFSE concentration is halved in daughter cell generations, allowing monitoring of the mitotic activity of proliferating cells (Nordon *et al.*, 1999; Bernard *et al.*, 2003). Studies have shown that the assays measuring lymphocyte proliferation using CFSE gave overall more consistent results and a greater sensitivity than those using radiolabeled nucleotides (Angulo and Fulcher, 1998; Fulcher and Wong, 1999;

Mannering *et al.*, 2003). Further, the CFSE assay has been successfully applied to assess division kinetics of both naturally and *in vitro* activated cells in a variety of animal and cell culture systems (Fujioka *et al.*, 1994; Hodgkins *et al.*, 1996; Fulcher and Wong, 1999; Warren, 1999; Oostendorp *et al.*, 2000; Sathiyaseelan and Baldwin, 2000; Dengler *et al.*, 2001; Miller *et al.*, 2002; Schneider *et al.*, 2002; Chen *et al.*, 2003; Li *et al.*, 2003; Mueller-Stahl *et al.*, 2003).

In this work, we developed and standardized the CFSE-based flow cytometric assay to monitor lymphocyte proliferation in the woodchuck model of HBV infection. We established conditions to measure both virus-specific and non-specific T cell proliferative responses. Furthermore, we compared the sensitivity of the CFSE assay with that of the adenine incorporation assay that is currently used. The CFSE assay, due to its superior sensitivity, reproducibility and the ability to measure kinetics of T cell division, should provide a valuable tool in more precise and comprehensive measurements of T cell responses in the woodchuck model of hepatitis B.

## **3.2 MATERIALS AND METHODS**

### **3.2.1 Animals**

Eight healthy eastern American woodchucks (*Marmota monax*) and 17 infected with WHV (11 with acute and 6 with chronic viral hepatitis) served as blood donors. WHV-positive animals were infected with  $1.1 \times 10^{10}$  DNase-protected virus genome equivalents (vge) (Michalak *et al.*, 1999; Hodgson and

Michalak, 2001). Acute infection was diagnosed when serum became positive for WHV surface antigen (WHsAg) and antibody to WHV core antigen (anti-WHc), but when WHs antigenemia lasted no longer than 6 months. Chronic WHV infection was considered when WHsAg, accompanied by WHV DNA and anti-WHc, persisted for longer than a 6-month period (Hodgson and Michalak, 2001). Serial liver biopsies obtained from these animals at yearly intervals showed histological features of chronic hepatitis, as described previously (Michalak, 1998; Michalak *et al.*, 1999). Healthy animals were negative for serological markers of WHV infection and nonreactive for WHV DNA, as determined by testing total DNA extracted from randomly selected serum, peripheral blood mononuclear cell (PBMC) and liver biopsy samples by nested PCR-Southern blot hybridization assay with WHV genome-specific PCR primers (sensitivity, 10 vge/ml) (Michalak *et al.*, 1999; Michalak *et al.*, 2004). The study protocol was approved by the Institutional President's Committee on Animal Bioethics and Care.

### **3.2.2 PBMC isolation**

PBMC were isolated from sodium ethylenediamine tetra-acetic acid (EDTA)-treated blood by density gradient centrifugation. In brief, whole blood was diluted with an equal volume of phosphate buffered saline, pH 7.4 (PBS) containing 1 mM EDTA (PBS-EDTA) and centrifuged through Ficoll-Paque Plus (Amersham Pharmacia Biotech, AB, Uppsala, Sweden). PBMC were collected,

washed with PBS-EDTA, and incubated with ammonium chloride cell lysing buffer for 15 minutes at room temperature to eliminate residual red blood cells (Lew and Michalak, 2001). PBMC viability was assessed by trypan blue exclusion and the cells were counted in a hemocytometer.

### 3.2.3 Mitogens and antigens

Concanavalin-A (ConA; Pharmacia Fine Chemicals, Uppsala, Sweden), pokeweed mitogen (PWM, *Phytolacca americana* agglutinin; ICN Biochemicals Inc., Aurora, Ohio) and phytohemagglutinin (PHA; ICN Biochemicals Inc.) were used as nonspecific stimulants of T cell proliferation. Synthetic WHV core peptide (WHC<sub>97-110</sub>), encompassing amino acids located in positions 97 to 110 of the virus nucleocapsid protein and containing a WHV core T cell immunodominant epitope (Menne *et al.*, 1997), was prepared by Synprep Corporation (Dublin, CA). This peptide was implemented to evaluate WHV-specific T cell response (Menne *et al.*, 2002b). Bovine serum albumin (BSA; Sigma Chemical Comp., St. Louis, MO) was used as an irrelevant antigen and a negative control. Two-fold serial dilutions of mitogens (0.6 - 40 µg/ml), WHC<sub>97-110</sub> peptide (1.2 - 20 µg/ml) and BSA (1.2 -10 µg/ml) were used to standardize the assay conditions and to determine optimum concentrations to measure proliferation of T lymphocytes and kinetics of their division in different animals.

### 3.2.4 Cell CFSE labeling and culture

PBMC at  $1 \times 10^7$ /ml in PBS were supplemented with  $50 \mu\text{M}$  CFSE (Molecular Probes, Eugene, Oregon) to achieve final concentrations ranging between  $0.6 \mu\text{M}$  and  $5 \mu\text{M}$  for the preliminary experiments aimed at determining the optimal CFSE labeling dose and  $1.2 \mu\text{M}$  for the final working assay. The cells were incubated at  $37^\circ\text{C}$  for 10 min and then washed twice with 10 ml of 5% fetal calf serum (FCS; GIBCO-Invitrogen Corporation, Auckland, New Zealand) in PBS (PBS-FCS). The cells were resuspended at  $1 \times 10^6$  cells/ml in complete AIM-V lymphocyte culture medium (GIBCO-Invitrogen Corporation) supplemented with 10% FCS. CFSE-stained PBMC were cultured in triplicate at  $1 \times 10^5$  cells/well in 96-well flat-bottom tissue culture plates (Becton Dickinson Labware, Franklin Lakes, NJ) in the presence of different concentrations of test mitogens, WHC<sub>97-110</sub> peptide or BSA. As controls, CFSE-labeled cells cultured with AIM-V medium alone and cells not stained with CFSE but stimulated with test mitogens or antigens were included. The plates were incubated at  $37^\circ\text{C}$  for 5 days, unless otherwise indicated. The cells from triplicate wells were pooled, supplemented with 5 ml of PBS-EDTA, spun down, resuspended in 1 ml of PBS-EDTA, and analyzed in a FACSCalibur flow cytometer (Becton Dickinson).

### 3.2.5 Flow cytometry analysis

Flow cytometry data were acquired for  $2 \times 10^4$  to  $5 \times 10^4$  events from each test sample by measuring CFSE fluorescence using an argon laser with 488 nm excitation wavelength and a 430/25 filter (FL1 channel). The woodchuck

lymphocyte population was defined by plotting total events using forward (FSC) and side (SSC) light scatter properties and normal human PBMC as the reference standard (see Figure 3.1). The woodchuck lymphocyte fraction was electronically gated to exclude cellular debris and granular cells other than lymphocytes. The kinetics of cell division were determined by deconvoluting and analyzing the reduced CFSE fluorescence using BD CellQuest Pro (Becton Dickinson) or ModFit LT (Verity Software House, Topsham, ME) softwares. Different quadrant and gate markers in BD CellQuest Pro software, which define cells with a higher (CFSE<sup>bright</sup>) and a lower (CFSE<sup>dim</sup>) fluorescence, were used to determine cell division index (C.D.I.) by applying the formula: percentage of CFSE<sup>dim</sup> cells after mitogen or antigen stimulation divided by percentage of CFSE<sup>dim</sup> cells without stimulation. Mathematical deconvolution of halved cellular CFSE fluorescence, available in the Proliferation Wizard module of ModFit LT software, was used to determine the proliferation index (P.I.) and the number of daughter cell generations. Proliferative response with C.D.I. or P.I. values greater than 3 standard deviations (SD) above the mean value from controls (*i.e.*, unstimulated PBMC from the same animal or PBMC stimulated with WHC<sub>97-110</sub> peptide from uninfected animals) was considered as positive.

### 3.2.6 Adenine incorporation lymphocyte proliferation assay

An adenine incorporation assay was applied in parallel with CFSE staining to comparatively determine the sensitivity and versatility of the CFSE assay in

detecting T lymphocyte proliferative responses in woodchucks. For this purpose, PBMC were cultured with or without test mitogen, WHc<sub>97-110</sub> or BSA, under the same conditions as in the CFSE assay. After 96-h culture, the cells were supplemented with 0.5  $\mu$ Ci of 2-<sup>3</sup>H-adenine (Amersham Pharmacia Biotech) and incubated for 12-18 h. Then, cells were harvested on a glass fibre filter membrane (Wallac Oy, Turku, Finland) using an automatic cell harvester (Harvester 96; Tomtec, Hamden, CT), and counts per minute (cpm) per well were determined in a Topcount Scintillator (Packards Bioscience Company, Meriden, CT). The average cpm counts from readings of triplicate wells, containing either stimulated or control cells, were calculated to define mean cpm values. The stimulation index (S.I.) was calculated by dividing mean cpm obtained after a mitogen or antigenic stimulation by mean cpm detected in the absence of a stimulant. An S.I. value of  $\geq 3.1$  was considered as positive.

### **3.3 RESULTS**

#### **3.3.1 Effects of CFSE on woodchuck PBMC survival**

To determine whether CFSE may affect survival of woodchuck lymphoid cells in culture, PBMC from healthy animals ( $n = 4$ ) were exposed to different concentrations of CFSE (0.6 to 5  $\mu$ M) and cultured for up to 7 days. Cells not exposed to CFSE dye (designated as 0  $\mu$ M) and those incubated with CFSE and counted immediately after labeling and washing (designated as time 0) were used as controls. Cell viability was determined at the end of each incubation

period by trypan blue exclusion and expressed as the mean percent viability  $\pm$  SD. The results showed that the survival of cultured woodchuck PBMC, either stained with CFSE or not, progressively declined over culture time, however, it was not influenced to any appreciable extent by the concentration of CFSE (data not shown). Thus, CFSE-labelled PBMC showed viability comparable to that of unstained cells or cells exposed to CFSE but not cultured (time 0). Similar results were obtained when viability of PBMC was examined by flow cytometry using cells labelled with CFSE and propidium iodide (data not shown). PBMC from animals infected with WHV showed identical CFSE labeling and survival properties as those from healthy woodchucks (data not shown). As there was no difference in % viability of cells labelled with different concentrations of CFSE and concentration of 1.2  $\mu$ M did not interfere with reading of PI fluorescence, 1.2  $\mu$ M CFSE was chosen for staining of woodchuck PBMC in subsequent experiments.

### **3.3.2 Comparison of CFSE profiles of woodchuck and human PBMC**

Freshly isolated human and woodchuck PBMC stained with 1.2  $\mu$ M CFSE were cultured with or without ConA for 5 days and analyzed by flow cytometry. As illustrated in Figure 3.1, woodchuck PBMC, either unstimulated or stimulated with mitogen, displayed comparable light scatter patterns to those of human PBMC. In Figure 3.1, lower right (LR) quadrant in dot-plots and M1 gate in histograms represent resting lymphocytes with no change in CFSE fluorescence

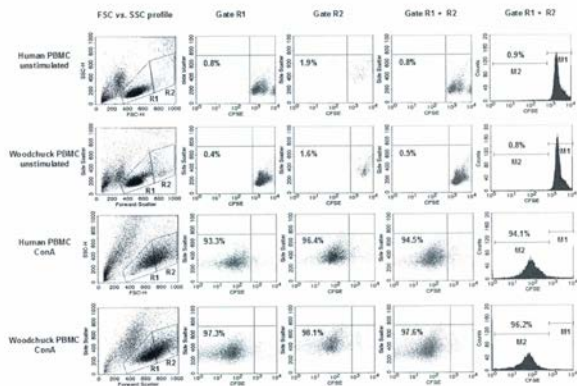
(CFSE<sup>bright</sup> cells), while lower left (LL) quadrant and M2 gate represent the dividing cells with lowered CFSE fluorescence (CFSE<sup>dim</sup> cells). As anticipated, control PBMC cultured without ConA showed no loss in CFSE fluorescence in either LL quadrant or gate M2 (1% CFSE<sup>dim</sup> cells), which indicates that most of the cells were not proliferating in the absence of the test mitogen. In contrast, ConA-stimulated cells in either LL quadrant or gate M2 showed extensive reduction in CFSE fluorescence (95% CFSE<sup>dim</sup> cells), indicating proliferation of lymphocytes and generation of daughter cells. Overall, the results revealed that woodchuck and human lymphocytes produced similar CFSE light scatter and fluorescence patterns when either cultured with or without a stimulant. It was concluded that flow cytometric parameters used for identification of human lymphocytes are also applicable for lymphocytes derived from woodchuck PBMC.

### **3.3.3 Assessment of analytical suitability of CFSE-labelled woodchuck lymphocytes**

After establishing light scatter parameters identifying CFSE-labelled woodchuck lymphocytes, the mitogen-driven proliferation of the cells was examined to determine analytical suitability of the flow cytometric data generated using different CFSE fluorescence deconvolution approaches. For this purpose, healthy PBMC were stained with CFSE and cultured with 5 µg/ml of ConA, PHA or PWM or without mitogen for 5 days. As shown in Figure 3.2, PBMC were first plotted according to the FSC-SSC pattern and gated for lymphocyte population

**Figure 3.1** Comparison of flow cytometric profiles of human and woodchuck PBMC labeled with CFSE. PBMC were stained with 1.2  $\mu$ M CFSE, cultured for 5 days without (unstimulated) or in the presence of 5  $\mu$ g/ml of ConA, and analyzed by flow cytometry. Forward (FSC) and side (SSC) light scatter properties of the cells were used to differentiate between lymphocytes and other cells using human PBMC as a standard. Lymphocytes were gated to resting (gate R1) and blastogenic (gate R2) cells. Dot-plots and histograms included lymphocytes either from R1 or R2 or from R1 + R2 gates. LL quadrant in dot-plots and M2 gated region in histograms define the proportion of proliferating lymphocytes with halved fluorescence. Percent values indicate proportion of the total lymphocytes present in each quadrant or gate.

Figure 3.1



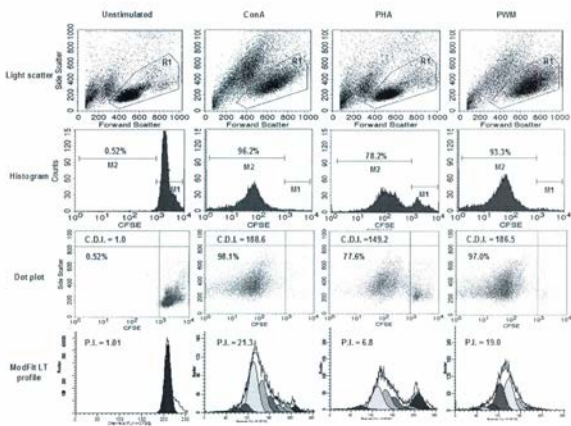
(R1 gates are equal to R1 + R2 gates in Figure 3.1). Subsequently, the cells in the R1 gate were analyzed using either BD CellQuest Pro (histograms and dot-plot profiles) or ModFit LT (ModFit LT profiles). With BD CellQuest Pro, the analysis showed that the mitogen-stimulated lymphocytes produced a large population of CFSE<sup>dim</sup> cells (>78% in either M2 gates or LL quadrants with C.D.I. >149), whereas those unstimulated exhibited the CFSE<sup>bright</sup> phenotype for most of the cells (Figure 3.2). However, while ConA, and PWM gave comparably high magnitudes of woodchuck lymphocyte proliferation (C.D.I. >186), stimulation with PHA led to relatively lower cell expansion (C.D.I. 149). Quantification of the lymphocyte division by deconvoluting CFSE fluorescence using ModFit LT demonstrated that woodchuck lymphocytes that responded to mitogen were mainly in daughter generations 4 to 6, although they could be tracked up to 6-8 generations. Also, while the calculated P.I. values for lymphocytes stimulated with ConA and PWM were similar, the value obtained for cells incubated with PHA was the lowest. This was consistent with the results from the histogram and dot-plot profile analyses. Overall, the different analytical approaches tested confirmed the versatility of the flow cytometric data generated using CFSE-stained woodchuck lymphocytes.

### **3.3.4 Determination of optimal culture time of CFSE-labelled PBMC**

After establishing that the CFSE-labelled woodchuck PBMC were suitable for the quantitative assessments of lymphocyte proliferation and division kinetics, the

**Figure 3.2** Flow cytometric quantification of proliferation and daughter cell generations of mitogen-stimulated woodchuck lymphocytes. PBMC labeled with 1.2  $\mu$ M CFSE were cultured for 5 days with 5  $\mu$ g/ml of ConA, PHA or PWM or medium alone (unstimulated), harvested, washed, and analyzed by flow cytometry. Lymphocyte population was gated using light scatter properties (R1 gate). The CFSE fluorescence data from cells in gate R1 were re-analyzed with BD CellQuest Pro (histograms and dot-plots) or ModFit LT (ModFit LT profiles). CFSE<sup>dim</sup> cells were separated from CFSE<sup>bright</sup> cells by gates in histograms and quadrant lines in dot-plots, and percent of CFSE<sup>dim</sup> cells and C.D.I. calculated, respectively. Deconvolution of CFSE fluorescence with ModFit LT separated daughter cells into generations. Using unstimulated cells to define parent generation, P.I. values were determined. Percent of CFSE<sup>dim</sup> cells and C.D.I. or P.I. values for unstimulated and stimulated PBMC are shown in respective plots.

Figure 3.2



CFSE assay conditions were standardized. In the first instance, the optimum time period for culture of CFSE-labelled lymphocytes was determined. For this purpose, CFSE-stained PBMC from healthy animals ( $n = 3$ ) were cultured for 1, 3, 5, 7 and 10 days with 5 or 10  $\mu\text{g/ml}$  of ConA or PHA or with 2.5 or 5  $\mu\text{g/ml}$  of PWM, analyzed by flow cytometry, and their C.D.I determined. As shown in Figure 3.3, lymphocytes stimulated with two concentrations of three different mitogens produced maximum mean proliferative responses on day 5. A similar result was obtained when cells were exposed to WHc<sub>97-110</sub> peptide (see Figure 3.5). Although stimulated lymphocytes gave a comparable number of CFSE<sup>dim</sup> cells when cultured for 5, 7 or 10 days (data not shown), C.D.I. values were noticeably lower for the cells cultured for longer than 5 days due to an increased proliferation of unstimulated cells in control wells. Based on these results, woodchuck PBMC labelled with CFSE were cultured for 5 days in subsequent experiments.

### **3.3.5 Determination of optimal mitogen concentrations for assessing CFSE-labelled lymphocyte proliferation**

To determine the range of mitogen concentrations which would be most appropriate for assessing the extent of woodchuck lymphocyte proliferation and their division kinetics, CFSE-labelled PBMC were cultured for 5 days with increasing 2-fold serial concentrations of ConA (1.2 - 40  $\mu\text{g/ml}$ ), PHA (1.2 - 40  $\mu\text{g/ml}$ ) or PWM (0.6 - 20  $\mu\text{g/ml}$ ). Figure 3.4A illustrates the typical patterns and

**Figure 3.3** Determination of optimal culture time for CFSE-labeled woodchuck lymphocytes. PBMC from 3 healthy animals were stained with 1.2  $\mu\text{M}$  CFSE and cultured in the presence of ConA or PHA at 5 (open symbols) or 10  $\mu\text{g}/\text{ml}$  (filled symbols) or PWM at 2.5 (open symbols) or 5  $\mu\text{g}/\text{ml}$  (filled symbols). Cells were harvested after 1, 3, 5, 7 and 10 days and analyzed by BD CellQuest Pro to determine the percent of CFSE<sup>dim</sup> cells and C.D.I. The data shown at each time point represent the C.D.I. values for 3 PBMC samples each stimulated with two concentrations of the mitogens tested. The mean C.D.I. values are marked.

Figure 3.3

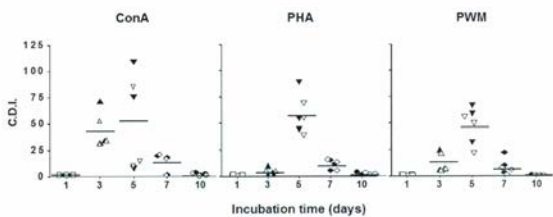


**Figure 3.4** Determination of optimum concentration ranges of mitogens to evaluate proliferative potency of CFSE-labelled woodchuck lymphocytes. Isolated PBMC were cultured for 5 days with six 2-fold serial dilutions of ConA or PHA (1.2 - 40  $\mu\text{g/ml}$ ) or PWM (0.6 - 20  $\mu\text{g/ml}$ ) or without mitogen (control), and analyzed by flow cytometry. Deconvolution of CFSE fluorescence and determination of P.I. was done using ModFit LT software. (a) Profiles of lymphocyte daughter cell generations from a single healthy woodchuck donor after stimulation with six two-fold serial concentrations of each mitogen tested. (b) Cumulative data from four independent experiments in which PBMC from 9 healthy animals were examined. The results were shown as means  $\pm$  SD.

Figure 3.4A

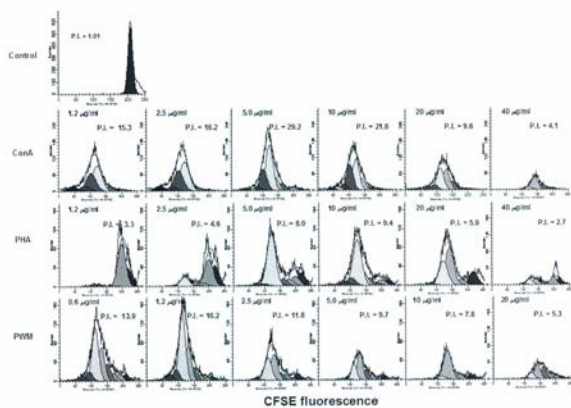
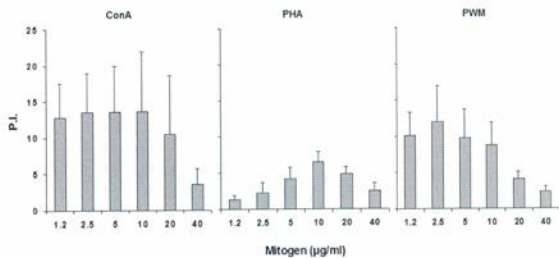


Figure 3.4B



the range of responses to different mitogen concentrations using PBMC from a single healthy woodchuck donor. Deconvolution of CFSE fluorescence into generations showed that various concentrations of the same mitogens produced variable numbers of daughter cell generations and, in consequence, P.I. values, although the highest and the lowest amounts of the mitogens usually stimulated cells to the lowest degree.

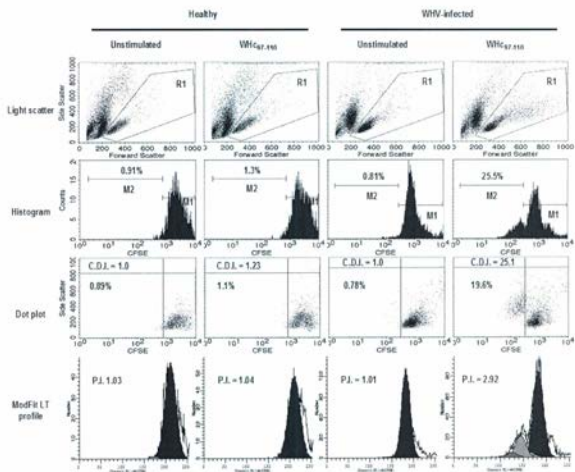
Figure 3.4B shows the cumulative data from 9 healthy animals. As depicted, any amount of ConA, PHA or PWM tested was able to stimulate, at least to some degree, proliferation of PBMC (represented by high error bars). However, overall, the greatest proliferation and the most daughter cell generations were seen when PBMC were cultured with ConA at 5  $\mu\text{g/ml}$ , PHA at 10  $\mu\text{g/ml}$  or PWM at 2.5  $\mu\text{g/ml}$  (Figure 3.4B). Among the mitogens tested, ConA gave the greatest P.I. (Figure 3.4A and Figure 3.4B) and C.D.I. (not shown) values. Nevertheless, due to fluctuations in mitogen-driven lymphocyte proliferative responses in different animals, it was concluded that five 2-fold serial dilutions of each mitogen, *i.e.*, ConA and PHA at 1.2 - 20  $\mu\text{g/ml}$  and PWM at 0.6 - 10  $\mu\text{g/ml}$ , should be routinely tested for truly thorough determination of the response in woodchucks.

### 3.3.6 Measurement of WHV-specific lymphocyte proliferation

After standardization of the conditions using non-specific mitogens, CFSE assay was applied to test WHV-specific T cell responses using synthetic peptide

**Figure 3.5** WHV-specific T lymphocyte proliferation profiles determined by flow cytometry. PBMC isolated from a healthy woodchuck and a WHV-infected animal were labeled with 1.2  $\mu$ M CFSE and cultured unstimulated or stimulated with 10  $\mu$ g/ml WHC<sub>97-110</sub> peptide for 5 days. Different analytical methods were employed to evaluate WHV-specific T lymphocyte proliferation response, as described in the legend to Figure 3.2.

Figure 3.5



WHC<sub>97-110</sub> as a virus-specific antigen. PBMC from either healthy or WHV-infected woodchucks were stimulated with the peptide (see below) and analyzed by flow cytometry. It was found that lymphocytes in response to WHV peptide gave the light scatter and CFSE fluorescence profiles comparable to those induced by mitogens (Figure 3.5). Although all methods of the cytometric data analysis used for evaluation of mitogen-induced T cell responses (see Figure 3.2) were applicable to monitor rather weak proliferation driven by WHC<sub>97-110</sub> peptide, C.D.I. values were found to define this reactivity with the highest precision. Hence, C.D.I. units were used in the subsequent experiments to quantify WHV-specific lymphocyte response.

### 3.3.7 Evaluation of WHV-specific T cell responses using CFSE assay

To determine the optimal culture period and concentrations of WHC<sub>97-110</sub> peptide, PBMC from WHV chronically infected ( $n = 4$ ) and healthy ( $n = 4$ ) animals were cultured for 3, 5, 7, 10 and 14 days with 2-fold serial dilutions of the peptide ranging between 1.2 and 10  $\mu\text{g/ml}$ . The highest proliferative response produced by a given PBMC sample against any concentration of the WHC<sub>97-110</sub> peptide or mitogen was defined as a peak response. As shown in Figure 3.6A, lymphocytes from healthy animals did not proliferate following incubation with WHC<sub>97-110</sub> peptide for any of the time periods examined. In contrast, lymphocytes from WHV-infected animals responded, producing the peak C.D.I. mean value after 5 days in culture. Similarly as it was observed with mitogen stimulations,

**Figure 3.6** Evaluation of WHV-specific T cell responses using CFSE assay. (a) PBMC from 4 healthy animals and 4 WHV-infected woodchucks were cultured with four 2-fold serial concentrations of WHC<sub>97-110</sub> peptide (1.2 - 10 µg/ml) for the time periods shown. Their CFSE fluorescence was analyzed by BD CellQuest Pro software and C.D.I. determined. The data shown represent the peak C.D.I. values given by PBMC from each animal with any of four WHC<sub>97-110</sub> concentrations tested. The mean peak C.D.I. values are marked. (b) Cumulative data from four independent experiments in which PBMC from 7 healthy animals, 11 with acute WHV hepatitis and 6 with chronic WHV hepatitis which were cultured for 5 days with four 2-fold serial concentrations of WHC<sub>97-110</sub> peptide (1.2 - 10 µg/ml). Only the peak T cell proliferation response (peak C.D.I.) against any concentration of the peptide for each test PBMC sample is shown. The mean peak C.D.I. values are marked for each group of animals. The dotted line represents the cut off value determined as described in Materials and Methods. Mann-Whitney test was used to compare the data between the groups.

Figure 3.6A

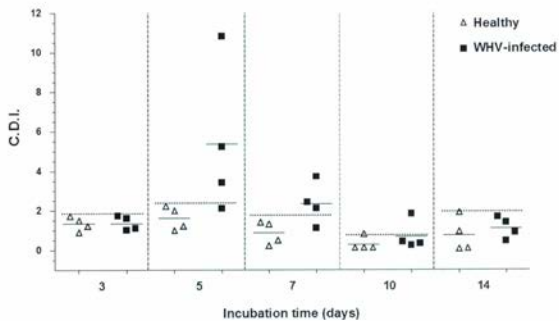
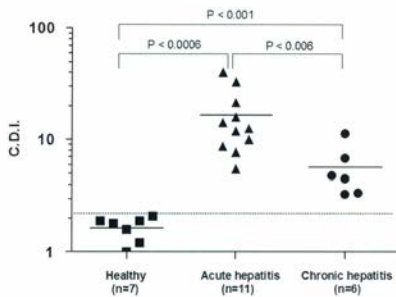


Figure 3.6B



CFSE<sup>dim</sup> cells were also abundant after 7- and 10-day culture (data not shown), but the peak C.D.I. mean values were lower than those of day 5, since unstimulated cells in control wells proliferated to a greater extent. Furthermore, there was no evident correlation between the peptide concentration and the magnitude of the response. Therefore, four 2-fold serial concentrations of the peptide ranging between 1.2 and 10 µg/ml were routinely used in subsequent tests.

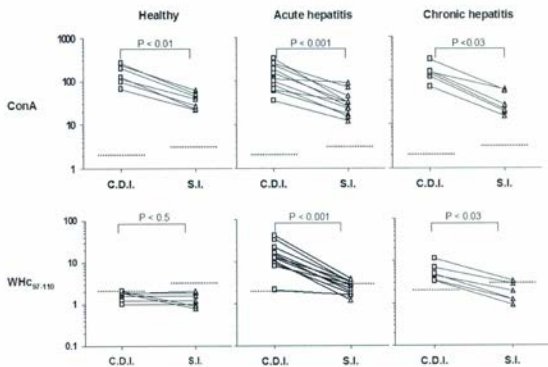
Figure 3.6B shows cumulative data from examining lymphocytes from 7 healthy animals, and from 11 woodchucks with acute and 6 with chronic WHV hepatitis using WHC<sub>97-110</sub> peptide. The woodchucks in acute phase of hepatitis showed the strongest WHV-specific T cell response (peak C.D.I. mean  $16.5 \pm$  SD 3.3), as compared to the animals with chronic hepatitis (peak C.D.I. mean  $5.7 \pm$  SD 1.2), while T lymphocytes from healthy woodchucks did not respond (peak C.D.I. mean  $1.6 \pm$  SD 0.1). Statistical analysis using nonparametric Mann-Whitney test confirmed that the lymphocyte proliferation in WHV-infected animals was significantly greater than that in healthy woodchucks and that the animals with acute hepatitis demonstrated overall a stronger response to WHC<sub>97-110</sub> peptide than those chronically infected (Figure 3.6B).

### 3.3.8 Comparison of CFSE and <sup>3</sup>H-adenine incorporation assay

Assessment of T cell proliferation was carried out simultaneously using CFSE and <sup>3</sup>H-adenine incorporation assay to compare the relative sensitivity of

**Figure 3.7** Comparison of sensitivity of CFSE and  $^3\text{H}$ -adenine incorporation assays in detecting T cell proliferation responses. PBMC from healthy animals ( $n = 7$ ) and from woodchucks with acute ( $n = 11$ ) or chronic ( $n = 6$ ) WHV hepatitis were analyzed in parallel using CFSE and  $^3\text{H}$ -adenine incorporation assays. For both assays, cells were cultured for 5 days with 2-fold serial concentrations of ConA (1.2 - 20  $\mu\text{g}/\text{ml}$ ) or WHc<sub>97-110</sub> peptide (1.2 - 10  $\mu\text{g}/\text{ml}$ ) and their proliferation responses assessed to define peak C.D.I. and S.I. values. The dotted lines represent the cut off values for each assay and group tested. The statistical analysis of data was performed using Wilcoxon signed rank test.

Figure 3.7



the assays in detecting woodchuck lymphocyte proliferation. In both assays, PBMC from healthy and WHV-infected animals were stimulated for 5 days with 2-fold serial concentrations of ConA (1.2 - 20  $\mu\text{g/ml}$ ) or WHC<sub>97-110</sub> peptide (1.2 - 10  $\mu\text{g/ml}$ ). The peak C.D.I. and S.I. were determined and compared using Wilcoxon signed rank test. As shown in Figure 3.7, stimulation with ConA gave a stronger PBMC response in all three groups of animals that was readily detectable by both assays, but the magnitude of the response was significantly greater in CFSE assay than that determined by <sup>3</sup>H-adenine incorporation assay ( $P < 0.01$ ). As expected, lymphocytes from healthy animals did not respond to stimulation with WHC<sub>97-110</sub> peptide in either CFSE or <sup>3</sup>H-adenine incorporation assay. Based on the cut off value of these assays, *i.e.*, mean C.D.I. plus 3 SD given by PBMC from healthy animals or S.I.  $\geq 3.1$ , it was found that the CFSE assay detected WHC<sub>97-110</sub> peptide-specific T cell response in 10 of 11 animals with acute hepatitis and in all 6 with chronic WHV hepatitis, while the <sup>3</sup>H-adenine incorporation assay failed to detect the response in 7 of 11 and 5 of 6, respectively. In addition, the magnitudes of the lymphocyte proliferation measured by the CFSE assay were significantly greater for both acutely ( $P < 0.001$ ) and chronically ( $P < 0.03$ ) infected woodchucks than those determined using the <sup>3</sup>H-adenine incorporation. Therefore, the data clearly showed the CFSE assay's superiority, considering both the sensitivity with which WHV-specific proliferation was detected and the magnitude of the response. In addition, the CFSE assay provided a new set of valuable data characterizing the division kinetics on the woodchuck T cells, which were not available using the <sup>3</sup>H-adenine incorporation assay.

### 3.4 DISCUSSION

In this study, the conditions to quantify woodchuck T lymphocyte responses using flow cytometry and cells stained with CFSE dye were established. Until now, different nucleotide analogues, such as adenine, uridine or bromodeoxyuridine (BrdU), have been employed for this purpose (Kreuzfelder *et al.*, 1996; Menne *et al.*, 1997; Shanmuganathan *et al.*, 1997). The present report describes a more sensitive, non-radioactive and relatively simple approach to measure both antigen-driven and mitogen-induced division of woodchuck lymphocytes.

CFSE is a cell membrane permeant dye which becomes fluorescent only after diffusing into the cells where it binds to intracellular molecules and gets sequentially halved in its intracellular concentration during each mitotic daughter cell generation (Lyons, 2000; Lyons *et al.*, 2001). It has been shown that CFSE can be incorporated into different types of lymphoid cells, including T cells (Schneider *et al.*, 2002; Givan *et al.*, 2004), B cells (Fulcher *et al.*, 1996; Cabatingan *et al.*, 2002), NK cells (Warren and Kinnear, 1999), dendritic cells (Weijer *et al.*, 2002) and hematopoietic cells (Ristevski *et al.*, 2003; Servet-Delprat *et al.*, 2002). Hence, when using this dye for monitoring lymphocyte proliferation, the electronic gating is essential to the separation of the lymphocytic population from other constituent cells of PBMC, using their differential FSC and SSC properties. Further, while gating PBMC based on their light scatter properties, it needs to be considered that resting lymphocytes have lower light

scatters than those of proliferating cells. Therefore, the extended gates are required to include blastogenic cells, which possess higher FSC vs SSC properties. As shown in this study, the comparative analysis of flow cytometric data demonstrated that woodchuck PBMC share similar, if not identical, light scatter and CFSE fluorescence patterns to those of human PBMC. These affirmative analogies led to the conclusion that the analytical methods used to deconvolute and quantify CFSE fluorescence from experiments with human PBMC (*e.g.*, Angulo and Fulcher, 1998) can also be applied for the assessment of cell proliferation rates in CFSE-labelled woodchuck PBMC.

CFSE dye has been used in a wide variety of *in vivo* and *in vitro* experimental systems for the determination of cell division. However, most of these studies report cell division rates in terms of the total number or percentage of cells with lowered CFSE fluorescence over that of the non-proliferating parent cell generation. In contrast, defining cell proliferation in terms of C.D.I. or P.I. allows for the quantification, as well as the gradient comparison of the strength of cell division. Nevertheless, magnitudes defined by these units reflect different aspects of cell proliferation. Thus, C.D.I. is a semi-quantitative measure of cell proliferation and is more useful in quantifying proliferation in response to a weak stimulus, because it does not consider different degrees of CFSE fluorescence halving in proliferating cells, but instead, all the cells with fluorescence lower than that of the parent generation cells are considered as one population. In contrast, P.I. evaluation considers the differential CFSE fluorescence halving for grouping the dividing cells into different daughter cell generations and then determines the

cell population in each generation separately. Therefore, C.D.I. units are more useful when determining relatively weak T cell proliferative responses, as seen for those against WHC<sub>97-110</sub> peptide (Figure 3.5 and 3.6), while evaluation of P.I. has a greater value when grading rather strong proliferative responses, as observed in mitogen-triggered division of woodchuck T cells (see Figure 3.4).

Mitogens are routinely employed in T cell proliferation assays as non-specific stimulants to measure the generalized competence of the cellular immune response and as positive controls in the assay evaluating antigen-specific responses. However, in most of the studies, only one or two different concentrations of any mitogen are tested. During this study, we have observed that there was no single concentration of the mitogen examined (*i.e.*, ConA, PHA or PWM), which produced uniformly maximum stimulation of PBMC derived from different animals. Considering this result, it should be mandatory to assess different concentrations of each stimulant to establish the concentration ranges producing maximum T cell responses in the majority (or preferentially in all) of PBMC samples tested. Subsequently, the pretested range of concentrations specific for each mitogen or antigenic stimulant should be routinely applied to monitor lymphocyte proliferative responses to determine their true range.

Previous studies have shown that the magnitudes of antiviral T cell proliferation produced by WHV-infected woodchuck PBMC are lower than those observed in other viral infections (Menne *et al.* 1998). Further, woodchucks progressing to or being in chronic phase of WHV hepatitis displayed even lower levels of virus-specific T cell response than those detected in animals who

resolved the infection (Menne *et al.*, 2002a). In these studies, either adenine or BrdU incorporation assays were implemented. These traditional assays measure T cell proliferation at the end of the stimulation period (*i.e.*, after 4 to 7 days of culture) by pulsing cells with nucleotide for 12-18 hours. This approach suffers from the short-time cell exposure to a marker nucleotide and from the fact that it accounts only for the cells in the S phase of division (Parish and Warren, 2001). It was also shown that lymphocyte division in response to the antigenic stimuli is followed by a wave of apoptosis (Renno *et al.*, 1999; Mannering *et al.*, 2002) and that this event occurs during the first few days of culture (Usherwood *et al.*, 1999). Therefore, cells proliferating during this initial phase are excluded from the proliferation analysis in this type of assays. On the other hand, it was shown that CFSE remains associated with apoptotic cells, which are readily traced by flow cytometry (Dumitriu *et al.*, 2001). This feature of CFSE makes possible monitoring of cell division during a prolonged stimulation period that is normally required for testing T cell proliferation in response to antigenic stimuli. Furthermore, the CFSE-based assay generates detectable magnitudes of cell proliferation even after exposure to a weak antigenic stimulant and, therefore, can be used to detect rare antigen-specific T cells and their proliferative responses (Mannering *et al.*, 2003). This property could be particularly valuable when assessing WHV-specific T cell reactivity in chronic WHV hepatitis, as it is exemplified by detection of WHC<sub>97-110</sub> peptide-specific T cell response in PBMC samples from all 6 animals chronically infected with WHV (see Figure 3.6B).

In summary, the present study shows that the flow cytometry assay applying PBMC labelled with CFSE dye offers a new approach to more sensitive and informative assessment of WHV-specific and generalized T cell response in the woodchuck model of hepatitis B. Implementation of this assay should contribute towards a better understanding of the pathogenesis of liver disease and its chronic progression in HBV infection.

CHAPTER 4: CHARACTERIZATION OF BIOACTIVE RECOMBINANT  
WOODCHUCK INTERLEUKIN-2 AMPLIFIED BY RLM-RACE AND PRODUCED  
IN EUKARYOTIC EXPRESSION SYSTEM

*This study has been published in Vet. Immunol. Immunopath. 2006;112(3-4): pp 183-198.*

#### 4.0 SUMMARY

Woodchucks (*Marmota monax*) infected with woodchuck hepatitis virus (WHV) represent a highly valuable laboratory model of hepatitis B virus (HBV) infection, in which molecular, immunological and pathological events occurring in infected humans are adequately reflected. To advance studies on T cell immune responses and propagation of hepadnavirus in T lymphocytes in this animal model, we determined the complete sequence of woodchuck interleukin-2 (wIL-2) cDNA by utilizing RNA ligase-mediated rapid amplification of cDNA ends (RLM-RACE) reaction. The wIL-2 sequence revealed a single open reading frame encoding for the predicted precursor protein comprised of a signal peptide and a 134 amino acid-long mature protein. The mature wIL-2 protein produced in the *Escherichia coli* expression system, designated as *ec-rwIL-2*, was found to be immunogenic but not biologically active. In contrast, precursor wIL-2 protein cloned into baculovirus transfer vector and expressed in Sf9 cells, designated as *bac-rwIL-2*, demonstrated functional competence. Further, *bac-rwIL-2* was able to stimulate proliferation and to induce multiple daughter cell generations in woodchuck T cells, as well as facilitated the survival of standard IL-2-dependent mouse CTLL-2 cells in culture. Western blot analysis of *bac-rwIL-2* using

antibodies generated against *ec-rwL-2* revealed a single protein band of 15.5 kDa. The availability of biologically active recombinant *wL-2* should facilitate *ex vivo* studies on functional competence of woodchuck T lymphocytes derived from different stages of hepadnaviral hepatitis and assist in recognizing their contribution to the pathogenesis of liver injury in the woodchuck model of hepatitis B.

#### 4.1 INTRODUCTION

Interleukin-2 (IL-2) was discovered while studying *in vitro* proliferation of human T cells derived from the bone marrow (Morgan *et al.*, 1976). It had been initially named as a T cell growth factor (TCGF). This cytokine is mainly produced by activated T lymphocytes (Ho *et al.*, 1999), while at smaller quantities it is also secreted by dendritic cells (Granucci *et al.*, 2001), B cells (Walker *et al.*, 1988) and NK cells. IL-2 is required for the antigen-specific primary and memory T cell proliferation and during the phenotypic maturation of type 1 and type 2 T helper cells (Miyazaki *et al.*, 1995; Frauwirth and Thompson, 2004). The cytokine also enhances cytotoxic activity of CD8<sup>+</sup> T and NK cells (Carson *et al.*, 1997), and production of antibodies by B cells (Gaffen *et al.*, 1996; Blackman *et al.*, 1986). IL-2 binds to the receptor complex, IL-2R, made up of three subunits, IL-2R $\alpha$  (CD25 or Tac antigen), which is specific for IL-2, and IL-2R $\beta$  (CD122) and IL-2R $\gamma$  (CD132), which belong to the type I cytokine receptor superfamily (Waldman, 1993; Gaffen, 2001).

IL-2 cDNA is composed of the 5'-leader sequence, open reading frame (ORF), and the 3'-trailer sequence (see Fig. 4.1). The ORF encodes for a precursor protein of 155 to 169 amino acids depending on the species origin, which contains a 20-23 amino acid-long signal peptide. This signal peptide is cleaved off prior to the secretion of the mature, functionally active cytokine from cells. In different mammals, the mature IL-2 is glycosylated to varying degrees giving molecular masses ranging between 15 to 18 kDa (Robb and Smith, 1981; Robb *et al.*, 1981; Taniguchi *et al.*, 1983; Cerretti *et al.*, 1986). Two of three cysteine residues present in the secreted protein form disulfide bonds and are essential for the cytokine's biological activity (Cerretti *et al.*, 1986). IL-2 belongs to the type I cytokines comprised of four  $\alpha$ -helical bundles, as it was shown by crystal structure analysis of human IL-2 (Bazan, 1992).

IL-2 sequences from several different species have been determined, cloned, and expressed in either prokaryotic or eukaryotic cells to generate a functionally active protein. For example, human IL-2 was produced in *Escherichia coli* (*E. coli*) (Devos *et al.*, 1983), COS cells (Cerretti *et al.*, 1986), insect cells infected with a recombinant baculovirus vector (Smith *et al.*, 1983), and in tobacco cells (Magnuson *et al.*, 1998). These studies revealed that the biological activity of IL-2 is independent of the glycosylation status and it is embraced within the extreme N-terminal 30 amino acid sequence of the mature protein, which also contains the binding site for IL-2R (Eckenberg *et al.*, 2000).

Previous attempts to determine a nucleotide sequence of woodchuck IL-2

(wL-2) led to identification of a 3'-terminal portion of the mature protein and the 3'-trailer sequence (see Figure 4.1) (Nakamura *et al.*, 1997; Hodgson and Michalak, 2001). In the present study, we determined the complete sequence of wL-2, cloned its full-length cDNA, expressed both mature and precursor wL-2 proteins and assessed their biological activity, none of which had been known or done before. In addition, specific polyclonal antibodies against wL-2 were produced.

Woodchucks (*Marmota monax*) infected with woodchuck hepatitis virus (WHV) represent a highly valuable natural model of human hepatitis B virus (HBV) infection and HBV-induced hepatocellular carcinoma (HCC) (Michalak, 1998; Menne and Tennant, 1999; Michalak, 2000). It is important to indicate that HBV is one of the most widely spread human pathogens which chronically infects 350 to 400 million people worldwide (Lavanchy, 2004). Studies in the woodchuck model significantly contributed to recognition of the mechanisms of hepadnavirus-induced liver injury (Michalak, 2004). Among others, the strength and the broadness of virus-specific T cell responses were found to be crucial in determining the outcome of hepadnaviral hepatitis (Ferrari *et al.*, 1990; Chisari and Ferrari, 1995; Menne *et al.*, 2002). It was also established that both HBV and WHV invade and replicate in cells of the immune system (Michalak, 2000; Michalak *et al.*, 2004), although immunological and pathological consequences of this infection remain unclear.

The studies in the woodchuck model of hepatitis B are hampered by the

limited availability of species-specific reagents and assays (Wang and Michalak, 2005). The present work was undertaken to generate biologically active recombinant wIL-2 (rwIL-2) to facilitate *ex vivo* experimentations with woodchuck T cells, including those infected *in vivo* or *in vitro* with WHV.

## 4.2 MATERIALS AND METHODS

### 4.2.1. Source of wIL-2 RNA

Healthy woodchucks were maintained in the Woodchuck Research and Breeding Facility at the Health Sciences Center of Memorial University, St. John's, Newfoundland, Canada. Blood samples were collected under a general inhalant anesthesia and peripheral blood mononuclear cells (PBMC) isolated by density gradient centrifugation, as described before (Gujar and Michalak, 2005). The cells viability was determined by trypan blue dye exclusion and normally exceeded 98%.

### 4.2.2 Amplification of wIL-2 cDNA fragment

Total RNA was isolated from woodchuck PBMC *in vitro* stimulated with Concanavalin (ConA). For this purpose,  $1 \times 10^7$  cells were cultured for 72 h in 10 ml of complete AIM-V medium (GIBCO-Invitrogen Corp., Auckland, New Zealand) supplemented with 10% fetal calf serum (GIBCO-Invitrogen Corp.) and 5 µg/ml of ConA (Pharmacia Fine Chemicals, Uppsala, Sweden). Total RNA was extracted using Trizol reagent (Invitrogen, Carlsbad, CA) and 2 µg of RNA was

reversely transcribed to cDNA, as described elsewhere (Hodgson and Michalak, 2001). Expression of wL-2 in the resulting cDNA preparation was determined using primers and PCR conditions reported previously (Hodgson and Michalak, 2001). For this purpose, sense primer 5'-GGAGGAAGTGCTGAATGTACC, homologous to the sequence located in a 3'-portion of the predicted mature wL-2, and antisense primer 5'-GATGTTATACACGGGAGGCACC, homologous to a fragment of the predicted 3'-trailer sequence of wL-2, were used. Based on interspecies sequence homology between IL-2 of human, rabbit and mouse, several degenerative primers (not shown) were designed in an attempt to amplify wL-2 cDNA sequence located upstream from the fragment amplified with the primers indicated above using various PCR conditions. However, all these attempts were not successful.

#### **4.2.3. Generation of full-length wL-2 cDNA by RLM-RACE and determination of its sequence**

The 5'-end of wL-2 cDNA was amplified using RNA ligase-mediated rapid amplification of cDNA ends (RLM-RACE) reaction kit (Ambion Inc. Austin, TX) following the manufacturer's instruction. Briefly, 10 µg of total RNA was treated with calf intestine alkaline phosphatase to remove the 5'-terminal phosphates from the nucleic acid sequences except the capped mRNA. Then, the RNA was treated with tobacco acid pyrophosphatase to remove the cap structures, leaving monophosphate at the 5'-ends of the full-length mRNAs. The resulting mRNAs

were ligated to a 45 base pair (bp)-RNA adapter oligonucleotide using T4 RNA ligase. The adapter-ligated RNAs were reversely transcribed to cDNAs using random primers. Subsequently, a hot-start PCR was implemented to amplify the 5'-portion of wL-2 sequence using as the template cDNA generated above. For this purpose, the adapter-specific outer sense primer provided in the kit and wL-2-specific outer antisense primer 5'-GCTTCGAGATGATGCTTTGGC were used. The PCR product was further amplified in a nested reaction with the adapter-specific inner sense primer from the RLM-RACE kit and wL-2 specific inner antisense primer 5'-GTACATTCAGCACTTCTCCA.

To determine a complete sequence of wL-2, the resulted nested PCR product was cloned into TOPO-PCR II vector using a TA cloning kit (Invitrogen) and amplified in competent Top 10 cells. Recombinant plasmid was excised and the presence of wL-2 insert confirmed after digestion with *Hind* III and *Xho* I restriction enzymes by electrophoresis in agarose gel. The full-length wL-2 sequence was determined using both the fmol DNA Sequencing System (Promega Corp., Madison, Wi) (Coffin *et al.*, 2004) and fluorescence-based automated sequencing (services provided by the Core Facility of the Department of Genetics, the Hospital for Sick Children, Toronto, Canada).

#### 4.2.4 Expression of rwL-2 in *E. coli*

Based on the complete sequence of wL-2 determined as above (also see Figure 4.2), PCR primers spanning the entire predicted sequence of mature wL-

2 were designed. For this purpose, cDNA derived from ConA-stimulated woodchuck PBMC was amplified with the pair of primers constituted by sense primer 5'-GCGCATAcatatgGCACCCACCTCCGGC and antisense primer 5'-GTGctcgagAGTGAGCTTCGAGATGATGCTTTGGC with introduced *Nde*I and *Xho*I restriction sites (indicated in lower case letters), respectively. The resulted PCR product was cloned into pET-41b(+) expression vector (Novagen, Darmstadt, Germany) and amplified in *E. coli* Top 10 cells. Kanamycin-resistant bacterial colonies were selected, their extracted DNA digested with *Nde*I and *Xho*I enzymes, and the digests screened for the presence of the rwL-2 insert. In the next step, *E. coli* BL21(DE3) cells were transformed with the recombinant plasmid isolated from a single positive colony and cells cultured overnight. Subsequently, using the obtained aliquot as the starter inoculum, a new scaled up culture was established. When OD<sub>600</sub> of the culture reached 2.0, 1 mM isopropyl-β-D-thiogalctopyranoside (IPTG) was added and incubation continued for 2 h. In parallel, an aliquot of the same cell suspension was incubated in the absence of IPTG, as an uninduced cell control. The cells were spun down, immediately frozen at -80 °C for overnight, and then lysed with BugBuster reagent (Novagen) in the presence of 20 U/ml of benzonase (Novagen). The resultant inclusion bodies and soluble cytoplasmic fractions were suspended in 8 M urea and analyzed by SDS-PAGE to assess the presence of *E. coli*-derived rwL-2, designated as *ec*-rwL-2, by comparing lysates from IPTG-induced and uninduced cells.

Because *ec-rwL-2* was tagged at the C-terminus with a polyhistidine, the purification of this recombinant protein was accomplished in the presence of 8 M urea using a Ni-NTA agarose immobilized metal affinity chromatography (IMAC) column (Qiagen Inc., Mississauga, Canada), following the procedure proposed by the manufacturer. Purified fractions were analyzed by SDS-PAGE and Western blotting (see below) using anti-histidine antibodies (Jackson ImmunoResearch Lab Inc., West Grove, Pa). The fractions containing *ec-rwL-2* were pooled and dialyzed against stepwise decreasing concentrations of urea from 6 M to 1 M and finally against phosphate-buffered saline, pH 7.4 (PBS) over a 7-day period at 4 °C. Using the same approach, unrelated recombinant WHV e antigen (*ec-rWHe*) was expressed and purified, and used as a specificity control (Wang and Michalak, 2005).

#### 4.2.5. Expression of *rwL-2* in insect cells

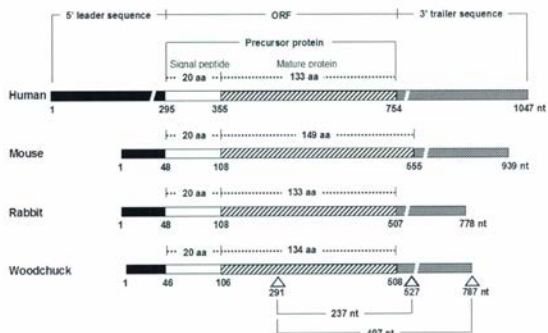
The whole precursor sequence of *wL-2*, encompassing both the mature protein and the signal peptide sequences (see Figure 4.1), was inserted into the baculovirus transfer vector pBlueBac4.5 (Invitrogen). Briefly, the fragment was amplified with sense primer 5'-GCCGctcagCTCTACCGCCATGCACACCC and antisense primer 5'-ATGCCCaagcttTCAAGTGAGCTTCGAGATG with introduced *XhoI* and *HindIII* restriction sites (indicated in lower case letters), respectively. The resulting PCR product was subcloned in pBlueBac4.5 vector and amplified in *E. coli* Top 10 cells. After confirmation of the correctness of the DNA band

pattern obtained after digestion with *Xho*I and *Hind*III enzymes by gel electrophoresis and the correct orientation of the rWIL-2 insert in pBlueBac4.5-rWIL-2 plasmid by sequence analysis, a Hi-Speed Plasmid Purification Kit (Qiagen Inc.) was used to acquire a large quantity of pBlueBac4.5-rWIL-2. This purified plasmid was co-transfected along with AcMNPV DNA (Bac-N-Blue DNA; Invitrogen) into *Spodoptera frugiperda* (Sf9) insect cells using a cationic liposome reagent, InsectinPlus (Invitrogen). Chromogenic substrate X-gal and plaque assay were used to distinguish between recombinant and wild type (WT) viral plaques. For the amplification of the recombinant and WT (control) viruses, respective plaques were collected and used to infect healthy Sf9 cultures. DNA was isolated from supernatants of these cells and screened by PCR using primers specific for baculovirus polyhedrin gene (Invitrogen) or rWIL-2. To generate a larger amount of the recombinant virus, the Sf9 cells were infected with the confirmed baculovirus-rWIL-2 construct and cultured for 8 days. The titer of the recombinant virus was determined in the plaque assay with 10-fold serial dilutions of the final supernatant and was found to be  $1.2 \times 10^8$  plaque forming units/ml.

For protein production, Sf9 cells were infected with the recombinant baculovirus carrying rWIL-2 at the multiplicity of infection (MOI) of 5 and cultured for 7 days at 27 °C. The supernatant from this culture containing secreted rWIL-2, designated as *bac*-rWIL-2, was collected and examined by Western blotting using guinea pig anti-ec-rWIL-2 antibodies prepared in the course of this study

**Figure 4.1** Schematic comparison of IL-2 sequences and their structural organizations in different mammalian species. Nucleotide and amino acid sequences for human, mouse and rabbit IL-2 were procured from GenBank (accession numbers NM000586, NM008366, and AF068057 respectively). The lengths of the complete cDNAs and their structural elements are shown as a number of nucleotides (nt) and those of the translated proteins as a number of amino acids (aa). The lengths of the complete sequence of woodchuck IL-2 cDNA identified in this study, its predicted constitutive elements, and encoded proteins are depicted at the bottom of the figure. The locations of the previously identified 237-nt (Hodgson and Michalak, 2001) and 497-nt (Nakamura *et al.*, 1997) wIL-2 sequence fragments are marked.

Figure 4.1



(See below).

#### 4.2.6. Assays measuring rwIL-2-induced T cell proliferation

Since proliferating woodchuck PBMC fail to incorporate  $^3\text{H}$ -thymidine (Maschke *et al.*, 2001), the ability of *ec*-rwIL-2 and *bac*-rwIL-2 to stimulate proliferation of normal woodchuck T cell was examined using  $^3\text{H}$ -adenine incorporation assay and a CFSE (5-and-6-carboxyfluorescein diacetate succinimidyl ester)-based flow cytometry lymphocyte proliferation assay, as described before (Gujar and Michalak, 2005). Briefly, for  $^3\text{H}$ -adenine incorporation assay, woodchuck PBMC were cultured at  $1 \times 10^5$  cells/well in triplicates in 96-well, flat-bottom tissue culture plates (Becton Dickinson Labware, Franklin Lakes, NJ) with 10-fold serial dilutions of purified *ec*-rwIL-2 or Sf9 cell supernatant containing *bac*-rwIL-2. As controls, IMAC-purified *ec*-rWHe or supernatants from non-infected Sf9 cells and from Sf9 cells infected with WT baculovirus were used. After 6 days of culture, cells were pulsed for 12-18 h with  $^3\text{H}$ -adenine (0.25  $\mu\text{Ci}$ /well) (Amersham Pharmacia Biotech AB, Uppsala, Sweden) and harvested. Stimulation index (S.I.) was defined by dividing mean counts per minute (cpm) obtained after rwIL-2 stimulation by mean cpm detected in the absence of rwIL-2 (Gujar and Michalak, 2005).

For CFSE assay, woodchuck PBMC were labeled with 1  $\mu\text{M}$  of CFSE (Molecular Probes, Eugene, Or) and then cultured as indicated for the adenine incorporation assay. After 7 days of culture, cells were harvested and CFSE

fluorescence analyzed using a BD FACSCalibur cytometer (Becton Dickinson, Franklin Lakes, NJ), as described previously (Gujar and Michalak, 2005). In this assay, supernatants from cultured non-infected Sf9 cells and from Sf9 infected with WT baculovirus cells, along with rhIL-2 (Roche Applied Sciences, Indianapolis, In), served as controls. CFSE fluorescence halving in dividing cells was evaluated using ModFit LT software (Verity Software House, Topsham, Me).

#### 4.2.7 Assay with CTLL-2 cells

To further ascertain that the generated *ec-rwIL-2* and *bac-rwIL-2* were biologically active, murine CTLL-2 cells, a cytotoxic T cell clone which depends on IL-2 for survival (Gillis and Smith, 1977), were used to quantify *wIL-2* activity. Briefly, CTLL-2 cells were maintained in complete AIM-V medium in the presence of 1:10 dilution of supernatant from ConA-stimulated rat splenocytes (Gillis and Smith, 1977; Belani and Weiner, 1999). Prior to the assay, the cells were washed with PBS containing 1 mM EDTA, counted, and seeded at a density of  $5 \times 10^4$  cells/well in a 96-well, flat-bottom tissue culture plate. Ten-fold serial dilutions of affinity-purified *ec-rwIL-2*, Sf9 cell supernatant containing *bac-rwIL-2* or supernatants from cultures of non-infected Sf9 cells and Sf9 cells infected with WT baculovirus or aliquots containing two-fold serial dilutions of recombinant human IL-2 (rhIL-2) ranging from 40 U/ml to 0.03 U/ml were added to wells in triplicates, while AIM-V medium alone was added to control wells. The cells were incubated for 24 h at 37 °C in a tissue culture incubator, then pulsed for 18 h with

$^3\text{H}$ -adenine (0.25  $\mu\text{Ci}/\text{well}$ ), and harvested. One IL-2 unit was defined as the amount of the cytokine required to induce 50% of maximal  $^3\text{H}$ -adenine incorporation (Stern *et al.*, 1984; Reeves *et al.*, 1986).

#### 4.2.8 Production of anti-rwIL-2 antibodies

Guinea pigs were immunized intramuscularly with 100  $\mu\text{g}$  of the IMAC-purified *ec*-rwIL-2 emulsified in 500  $\mu\text{l}$  of complete Freund's adjuvant. Subsequent booster injections of *ec*-rwIL-2 (50  $\mu\text{g}$  each) emulsified in incomplete Freund's adjuvant were given intramuscularly on days 21, 28 and 35 following the initial injection. One week after the final injection, the animals were sacrificed. Serum samples were collected before the first injection (preimmune serum) and at autopsy. The presence of anti-wIL-2 antibodies and their titer was determined by Western blot analysis using *ec*-rwIL-2 and unrelated *ec*-rWHe protein as a specificity control.

#### 4.2.9 SDS-PAGE and Western blot analyses

For SDS-PAGE, preparations of inclusion bodies from the IPTG-induced cultures of *E. coli* expressing *ec*-rwIL-2 or *ec*-rWHe and from cultures not induced with IPTG were separated along with pre-stained protein molecular weight markers (Invitrogen) on 12% or 15% polyacrylamide gels following procedures previously described (Michalak and Lin, 1994). Molecular weights of the proteins detected after staining with 0.5% Coomassie blue were determined

using standard curves derived from the relative electrophoretic mobilities of the pre-stained molecular weight markers.

For Western blot analysis, the recombinant proteins indicated above separated by SDS-PAGE were transferred onto a nitrocellulose membrane (Amersham Biosciences Ltd., Little Chalfon, UK) using semi-dry protein transfer method (Michalak and Lin, 1994). To eliminate possible non-specific binding, the membrane was treated with a blocking solution containing 1% normal goat serum (Sigma-Aldrich Comp., St. Louis, Mo) and 0.25% Tween-20 in PBS with 1 mM EDTA. The transferred proteins were probed with mouse monoclonal anti-histidine antibody (Jackson) and then with alkaline phosphatase-labeled goat anti-mouse IgG antibodies (Jackson). The reaction was developed with a NBT/BCIP substrate solution (Sigma-Aldrich).

Similarly, the IMAC-purified *ec-rwL-2* and culture supernatants from Sf9 cells containing *bac-rwL-2* or from Sf9 cells infected with WT baculovirus or from naive Sf9 cells, along with control unrelated *ec-rwWHe*, were analyzed by immunoblotting. The transferred proteins were probed with guinea pig anti-*ec-rwL-2* antibodies (1:100 dilution) and then exposed to alkaline phosphatase-labeled goat anti-guinea pig IgG (Jackson). Positive reactions were visualized with a NBT/BCIP substrate reagent.

## 4.3 RESULTS

### 4.3.1 Determination of the complete *wL-2* cDNA sequence

Prior to this study, only a 497 bp-long fragment of wIL-2 encompassing the 3'-portion of the predicted mature protein and the 3'-trailer sequence had been identified (Nakamura *et al.*, 1997; Hodgson and Michalak, 2001). The order of nucleotides encoding for the 5'-leader sequence, the signal peptide and the 5'-portion of the mature wIL-2 were unknown. After several attempts, in which different primer pairs and varied PCR conditions were tested, we were unable to generate the 5'-portion of wIL-2 cDNA using this approach. However, when the 5'-terminal sequence of wIL-2 cDNA was amplified by RLM-RACE reaction and the resulting product cloned, and the cloned fragment expanded, excised and sequenced, the desired sequence was obtained (Figure 4.2A). Combining this newly determined 290-bp 5'-fragment with the 237-bp sequence previously defined in this laboratory (Hodgson and Michalak, 2001), and confirmed in the course of this study, and with the 3'-terminal 260-bp fragment of the 3'-trailer sequence delineated by others (Nakamura *et al.*, 1997), we reconstructed the complete sequence of wIL-2 cDNA (Figure 4.1). The wIL-2 sequence determined in this study was submitted to GenBank under accession number DQ272238.

The alignment of the entire wIL-2 nucleotide sequence determined in this study with those of human, mouse and rabbit revealed an overall homology of 80%, 71% and 79%, accordingly (Figure 4.2A), while comparison of the predicted amino acid sequence showed compatibility of 70%, 55%, and 67%, respectively (Figure 4.2B). Further analysis, in which the results on an interspecies comparison of known IL-2 amino acid sequences were taken under

**Figure 4.2** Alignments of woodchuck IL-2 nucleotide and amino acid sequences with those of human, mouse and rabbit IL-2. (A) Nucleotide sequence comparison. The start codon of the predicted precursor protein of wIL-2 is underlined. (B) Comparison of the amino acid sequences of the precursor IL-2 proteins. Inverted triangle shows the predicted cleavage site for the mature wIL-2 protein. In consensus sequences (bottom lines), nucleotides or amino acids identical in all sequences are marked as asterisks and differences are shown as dots.



Figure 4.2B

▼

```

Woodchuck  1 MHTMPLLSCLALTLALVAHGAPTSGS-----AEETRQLEQLLLDLQMLSR
Human      1 .YR.Q...I..I...TNS...S.T-----IKTKK.QL..H.....ILN
Mouse     1 .YS.Q.A..VT...V.LVNS...S.TSSSTAEAQQQQQQQQQ.H....M...E.LS
Rabbit    1 .YKVQ...I.....LTSS...S.-----TK..QE..D.....V.LK
consensus  1 *...*...*...*...*...*...*...*...*...*...*...*...*...*...

Woodchuck  47 GVSNQENSTLTRLKFKFYPFKASDLEHLQCLEELKPLQEVNLVFPQSKNFHLKDRNF
Human     50 .IN.YK.PK....T....K..TE.KQ.....E....LA.....R-P.DL
Mouse     61 RME.YR.LK.P...T...L.KQ.TE.KD....D..G..RH..DLT...S.Q.E.AE..
Rabbit    47 ..NDYK..K.S...T....K.VTE.K.....E....LA.G..S.GGN..ES
consensus  61 .....*..*...*...*...*...*...*...*...*...*...*...*...*...

Woodchuck  107 ISNINVTVLKMGSAITFTCEYAFETANIVEFLNWTWIFCQSIISKLT-
Human     109 .....I..E...E...M...D...T....R.....T..-
Mouse     121 ...R...V...DN..E.QFDD.S.TV.D..RR..A.....TSPQ
Rabbit    107 .....E...M...-D..VT....R.....ASSS
consensus  121 ****.*...*...*...*...*...*...*...*...*...*...*...*...*...

```

consideration, predicted the existence of a single ORF in the wL-2 sequence. This ORF is comprised of a 465 bp-long sequence encoding for the wL-2 precursor with the translation initiation codon located at nucleotide 46 and the termination codon positioned at residue 508 (see Figure 4.1 and 4.2A). This precursor sequence should encode for the 20 amino acid-long signal peptide and the 134 amino acid-long mature protein with calculated molecular weights of 1.8 kDa and 15.5 kDa, respectively. The predicted mature wL-2 protein contains an alanine residue at the N-terminus (position 21) and a threonine at the C-terminus (position 154). Post factum analysis, in which the entire wL-2 nucleotide sequence was compared to the consensus sequence derived from IL-2 of human, mouse and rabbit origin, revealed that the 3'-trailer sequence, as anticipated, to be most homologous (69%), whereas the region encoding for wL-2 signal peptide to be most heterogeneous (43%). The sequences encoding for wL-2 5'-leader sequence and mature protein showed compatibility with a consensus sequence of 63% and 64%, respectively.

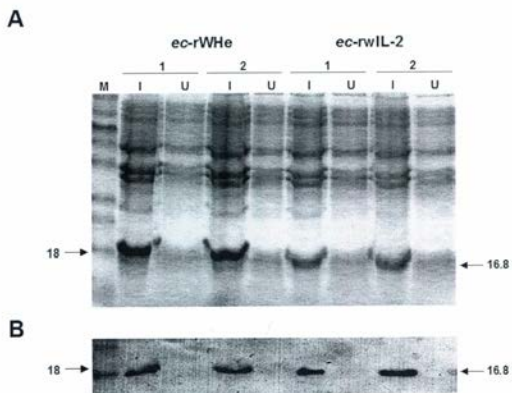
#### **4.3.2 Expression of mature rwL-2 in *E. coli***

A woodchuck cDNA fragment encoding for the predicted mature wL-2 protein was amplified by PCR, subcloned, and the construct expressed in *E. coli*. By SDS-PAGE analysis (Figure 4.3A), the presence of *ec*-rwL-2 was evident in the inclusion bodies prepared from *E. coli* cultures induced with IPTG, but not from the bacteria cultures not treated with IPTG. These inclusion bodies carried a

protein with a molecular size of 16.8 kDa, which was compatible with that calculated for the mature wL-2 based on the nucleotide sequence determined in this study plus six histidine residues added at the C-terminus along with a methionine residue at the N-terminus of the protein. In contrast, soluble cell fractions or culture supernatants collected from either IPTG-induced or non-induced cultures did not show *ec-rwL-2* presence (data not shown). An irrelevant protein, *ec-rWHe* with a molecular size of 18 kDa (Figure 4.3A), which was cloned and expressed in the same expression system (Wang and Michalak, 2005), was used as an efficacy control. To facilitate purification by IMAC, both *ec-rwL-2* and control *ec-rWHe* were tagged with polyhistidine at their C-termini. The affinity-purified *ec-rwL-2* and *ec-rWHe* showed single protein bands of 16.8 kDa and 18 kDa, respectively, when examined by SDS-PAGE (data not shown). These purified proteins were further analyzed by Western blotting using monoclonal antibody to polyhistidine as a probe. The immunoblot data confirmed the existence of a single protein band of 16.8 kDa for *ec-rwL-2*, as compared with the 18-kDa band given by *ec-rWHe* (Figure 4.3B). It was estimated that the yield of the affinity-purified *ec-rwL-2* was 40  $\mu$ g per ml of culture medium from the IPTG-induced cells. Further investigations revealed that although *ec-rwL-2* was able to induce specific antibodies in immunized animals (see Figure 4.4B), it was functionally inactive when tested in appropriate bioassays (see below).

**Figure 4.3** SDS-PAGE and Western blot analyses of *ec-rwL-2* produced in *E. coli* expression system. (A) SDS-PAGE analysis of two randomly selected *E. coli* colonies (indicated as 1 and 2) expressing *ec-rwL-2* or control *ec-rWHe*. Lanes: I, inclusion bodies from *E. coli* cell lysates after IPTG induction; U, uninduced *E. coli* cell lysates; M, pre-stained protein marker ladder. (B) Western blot analysis of IMAC-purified *ec-rwL-2* and *ec-rWHe* using anti-histidine monoclonal antibodies. Molecular sizes of the identified *ec-rwL-2* (16.8 kDa) and *ec-rWHe* (18 kDa) are marked on the right side and the left side of the panel, respectively.

Figure 4.3



#### 4.3.3 Expression of precursor rWL-2 in the baculovirus-insect cell system

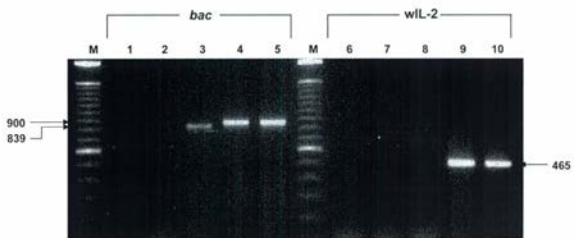
Since generation of biologically active mature wL-2 in the *E. coli* system was not successful, the predicted sequence encoding the entire wL-2 precursor protein was amplified by PCR and the purified product subcloned in pBlueBac4.5 plasmid vector using *Xho* I and *Hind* III restriction sites. The resulting recombinant plasmid, pBlueBac4.5-wL-2, along with linearized AcMNPV DNA, was co-transfected in Sf9 insect cells. Then, Sf9 cell plaques carrying the recombinant baculovirus with wL-2 sequence (*bac-rWL-2* virus) were differentiated from those carrying WT virus in the plaque assay. The correctness of the *bac-wL-2* recombination was confirmed by PCR using baculovirus polyhedrin-specific and wL-2-specific primer pairs. As shown in Figure 4.4A, DNA from culture supernatants of two randomly selected Sf9 cell plaques expressing *bac-wL-2* showed the expected DNA fragments of 900 bp or 465 bp after amplification with baculovirus or wL-2 specific primers, respectively. As anticipated, a supernatant from uninfected Sf9 cells tested did not show DNA amplification signals, whereas a supernatant from Sf9 cells infected with WT baculovirus gave a band of 839 bp with polyhedrin-specific primers but not with wL-2-specific primers (Figure 4.4A). This PCR analysis ensured that only the cell plaques expressing *bac-rWL-2* were used for further expansion and studies.

Further, the selected Sf9 cell plaque carrying *bac-rWL-2* virus, as confirmed by the PCR analysis, was expanded and its supernatant tested for the presence of rWL-2 protein, designated as *bac-rWL-2*, by SDS-PAGE and

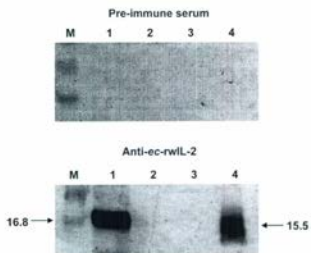
**Figure 4.4** PCR and Western blot analyses of *bac-rwL-2* DNA or *bac-rwL-2* protein in culture supernatants from Sf9 insect cells. (A) PCR-based identification and purity screening of the recombinant baculovirus DNA in supernatants from infected Sf9 cell plaques. DNA isolated from test supernatants was amplified with primers specific for either baculovirus polyhedrin gene (lanes 1-5) or *wL-2* (lanes 6-10). Lanes: M, molecular marker ladder; 1 and 6, water instead of DNA as a contamination control; 2 and 7, supernatant from uninfected Sf9 cells; 3 and 8, supernatant from Sf9 cells infected with WT baculovirus; 4, 5, 9 and 10, supernatants from two randomly selected Sf9 cell plaques transfected with recombinant baculovirus carrying *rwL-2*. Molecular sizes of PCR amplicons are indicated on sides of the panel. (B) Western blot analysis of *bac-rwL-2* protein. Supernatants from Sf9 cell plaques were probed with either guinea pig pre-immune serum (top panel) or guinea pig anti-*ec-rwL-2* antibodies (bottom panel). Lanes: M, pre-stained molecular weight markers; 1, IMAC-purified *ec-rwL-2*; 2, supernatant from uninfected Sf9 cells; 3, supernatant from Sf9 cells infected with WT baculovirus; 4, supernatant from Sf9 cells transfected with recombinant baculovirus carrying *rwL-2*. Protein bands of 16.8 kDa and 15.5 kDa correspond to *ec-rwL-2* and *bac-rwL-2*, respectively.

Figure 4.4

A



B



immunoblotting using antibodies to *ec-rwIL-2* produced in the course of this study. When analyzed by SDS-PAGE, *bac-rwIL-2* did not yield a protein band (data not shown). However, a clearly visible band of 15.5 kDa was detected when *bac-rwIL-2* was probed with anti-*ec-rwIL-2* antibodies by Western blotting (Figure 4.4B), indicating that the cytokine was produced but at the levels not detectable by standard SDS-PAGE. The same immunoblot analysis showed that anti-*ec-rwIL-2* antibodies also specifically recognized *ec-rwIL-2*, but they did not react with proteins present in supernatants from uninfected Sf9 cells or those infected with WT baculovirus (Figure 4.4B). Pre-immune serum collected from the animal that finally provided anti-*ec-rwIL-2* antibodies was not reactive with the preparations tested (Figure 4.4B).

#### 4.3.4 Induction of woodchuck T cell proliferation by *bac-rwIL-2*

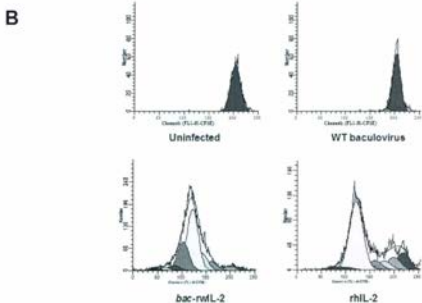
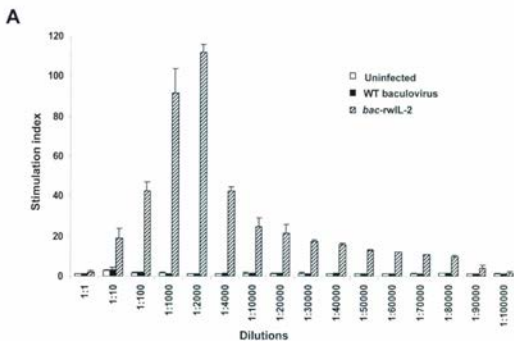
Recombinant *wIL-2* proteins, both *ec-rwIL-2* and *bac-rwIL-2*, were tested for their ability to stimulate proliferation of woodchuck T lymphocytes by using PBMC isolated from healthy animals. The proliferation was measured by a <sup>3</sup>H-adenine incorporation assay or a CFSE-based flow cytometric assay, which were previously established in this laboratory (Gujar and Michalak, 2005). The results showed that the affinity-purified *ec-rwIL-2* failed to stimulate proliferation of woodchuck T lymphocytes under any concentration and assay conditions tested (data not shown). In contrast, woodchuck PBMC cultured in the presence of 10-fold serial dilutions of the supernatant containing *bac-rwIL-2* demonstrated an

extensive, dose-dependent uptake of  $^3\text{H}$ -adenine, as shown in Figure 4.5A. The analysis revealed that *bac-rwL-2* was highly potent since measurable woodchuck T cell proliferation was found even at the supernatant dilution of 1:90,000 (Figure 4.5A). Nevertheless, the supernatant at dilutions of 1:1000 or 1:2000 consistently gave the highest T cell stimulation indices and, hence, *bac-rwL-2* at these dilutions was used in subsequent experiments. Supernatants from either uninfected Sf9 cells or those infected with WT baculovirus did not induce proliferation of woodchuck PBMC (Figure 4.5A).

In the subsequent step, division kinetics of woodchuck T lymphocytes driven by *bac-rwL-2* was examined using a CFSE flow cytometric assay (Gujar and Michalak, 2005). Deconvolution of CFSE fluorescence into daughter cell generations showed that the supernatant containing *bac-rwL-2* at 1:1000 produced up to 9 cell divisions of woodchuck lymphocytes, as shown in Figure 4.5B. When dilution 1:100 was tested, up to 7 cell divisions were seen, whereas dilutions 1:10 and 1:10,000 generated no more than 5 cell divisions (data not shown). In parallel, the effect of a commercially available rhIL-2 on proliferation of woodchuck T cells was also examined. The results showed that rhIL-2 at 5, 10 and 20 U/ml induced no more than 5 to 6 divisions of woodchuck T cells, as illustrated for *rwL-2* tested at concentration of 5 U/ml in Figure 4.5B. It is of note that *bac-rwL-2* was also able to stimulate proliferation in human T cells, but the magnitude of cell division was many fold lower than that induced by rhIL-2 (data not shown). Culture supernatants from Sf9 cells, either uninfected or infected

**Figure 4.5** Proliferation and daughter cell generation in woodchuck T lymphocytes treated with *bac-rwL-2*. (A) Proliferation of woodchuck T cells in response to increasing dilutions of *bac-rwL-2* measured by  $^3\text{H}$ -adenine incorporation assay. PBMC isolated from a healthy woodchuck were incubated in triplicates with indicated dilutions of supernatants from Sf9 plaques not infected with baculovirus (uninfected), infected with WT baculovirus or infected with the recombinant baculovirus (*bac-rwL-2*). After 5 days, cells were pulsed with  $^3\text{H}$ -adenine, proliferation of T cells measured and expressed as stimulation index, as outlined in Section 3. (B) Analysis of woodchuck T cell division kinetics using a CFSE-based flow cytometric assay. Woodchuck PBMC from a healthy woodchuck were labeled with  $1\ \mu\text{M}$  of CFSE and incubated with 1:1000 dilution of supernatants from uninfected Sf9 cells, Sf9 cells infected with WT baculovirus, Sf9 cells infected with the recombinant baculovirus (*bac-rwL2*) or with 5 U/ml of rhIL-2. After 6 days, cells were harvested and analyzed by flow cytometry. Using ModFit LT software, CFSE fluorescence halving was deconvoluted into daughter cell generations.

Figure 4.5



with WT baculovirus did not induce division of woodchuck T cells (Figure 4.5B), confirming specificity of the results obtained.

#### 4.3.5 Survival of IL-2-dependent CTLL-2 cells in the presence of *bac-rwIL-2*

To further strengthen the conclusion that *bac-rwIL-2* displays characteristics of biologically active IL-2, a classical bioassay with murine IL-2-dependent CTLL-2 cell line was performed using rhIL-2 as a reference. As shown in Figure 4.6, serial dilutions of the supernatant containing *bac-rwIL-2* and purified rhIL-2 produced comparable kinetics of cell division in CTLL-2 cells when measured by <sup>3</sup>H-adenine incorporation assay. Taking into consideration the bioactivity plot obtained for known concentrations of rhIL-2 (Figure 4.6) (Stern *et al.*, 1984), it was estimated that *bac-rwIL-2* activity was equivalent to  $5 \times 10^4$  U/ml in the culture supernatant produced.

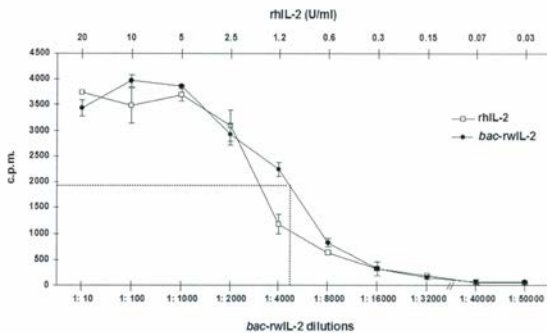
#### 4.4 DISCUSSION

In the course of this study, the complete nucleotide sequence of wIL-2 was established. We have successfully resolved the previously unknown 5'-fragment of wIL-2 cDNA encoding for the cytokine 5'-leader sequence, the cytokine signal peptide and the 5'-portion of the mature protein. We also confirmed the correctness of the previously identified segments of wIL-2 sequence. Further, the deduced mature protein and the precursor protein of wIL-2 were produced in prokaryotic and eukaryotic expressions systems,

**Figure 4.6** Quantification of *bac-rwL-2* activity in bioassay with CTLL-2 cells.

CTLL-2 cells were cultured in triplicates with indicated dilutions of Sf9 cell supernatant containing *bac-rwL-2* or with indicated amounts of rhIL-2 preparation. After 24-h incubation, cells were pulsed with  $^3\text{H}$ -adenine, harvested and incorporation of adenine determined by measuring cpm. Dotted line identifies the amount of *bac-rwL-2* needed for producing half maximal proliferation in CTLL-2 cells, as extrapolated from a standard curve given by serial dilutions of rhIL-2.

Figure 4.6



respectively, and their molecular size and biological activity were determined.

Our initial attempts were directed toward amplification of the 5'-portion of wL-2 cDNA by standard PCR using several degenerative primers. The sequences of these primers were designed based on the interspecies IL-2 sequence homology and were located up-stream from the previously identified 497-bp wL-2 fragment (see Figure 4.1) (Nakamura *et al.*, 1997; Hodgson and Michalak, 2001). However, repeated efforts using different primer combinations and PCR conditions failed to generate the anticipated sequence. Therefore, the RLM-RACE reaction was utilized to retrieve the 5'-portion of wL-2 cDNA. This approach was successful allowing for reconstruction of the entire wL-2 sequence. The alignment of the wL-2 sequence with the IL-2 consensus sequence derived from human, mouse and rabbit (Figure 4.2) showed the highest degree of heterogeneity (~57%) in the region encoding for the predicted signal peptide of the precursor protein. This may explain why efforts to amplify the 5'-portion of wL-2 cDNA using degenerative PCR primers with sequences corresponding to this region were futile.

Analysis of the wL-2 sequence indicated that the ORF identified should encode for the 154 amino acid-long precursor protein comprised of a 20 amino acid-long signal peptide and 134 amino acid-long mature protein. The previous studies demonstrated that biological activity of recombinant IL-2 derived from different species was contained within the mature protein and was independent of post-transcriptional modifications (Robb and Smith, 1981; Robb *et al.*, 1981). These recombinant proteins, which were usually produced in *E. coli* expression

system, displayed signature biological characteristics of IL-2, such as the ability to induce division in autologous T lymphocytes and to support survival of IL-2-dependent cell lines, such as CTLL-2 or BT2 cells (Miller-Edge and Splitter *et al.*, 1984; Cerretti *et al.*, 1986; Sato *et al.*, 1987; Magnuson *et al.*, 1998; Zhou *et al.*, 2005). Considering these facts, the deduced mature protein of wIL-2 was expressed in *E. coli* as a polyhistidine-tagged protein, affinity purified from bacterial cell lysate on an IMAC column, and reconstituted by gradually removing urea from the eluate. Nevertheless, although the obtained protein retained antigenic competence of wIL-2 and antibodies raised against this protein recognized both *ec*-wIL-2 and *bac*-wIL-2 by immunoblotting, it was not able to stimulate proliferation of woodchuck T cells or CTLL-2 cells in culture. This suggested that wIL-2 derived from *E. coli* was inactive or may have failed to re-fold properly during purification.

Recombinant baculovirus vector propagating in insect Sf9 or Sf21 cells is an increasingly used system in which expression of a variety of mammalian proteins has been achieved (Cochran *et al.*, 1987; Domingo and Trowbridge, 1988; Hasemann and Capra, 1990; Luckow, 1993; Barrault *et al.*, 2005), including production of recombinant woodchuck interferon gamma and tumor necrosis factor alpha in this laboratory (Wang and Michalak, 2005). This system offers an important advantage over the *E. coli* expression system in which protein post-translational modifications, folding and secretion are more compatible with those naturally occurring within mammalian cells (Kidd and Emery, 1993; Geisse

*et al.*, 1996). Furthermore, recombinant proteins generated in the baculovirus-insect cell system are devoid of potentially toxic bacterial contaminations (Stacey *et al.*, 1993; Wang and Michalak, 2005). In the current study, expression of the precursor wL-2 protein in insect cells led to secretion of the biologically active cytokine to the culture supernatant, indicating that the cells correctly processed this woodchuck protein. Western blot analysis of *bac-rwL-2* showed a single protein band of 15.5 kDa for which the molecular size was identical to that predicted from the nucleotide sequence of the mature wL-2. Of note is that the culture supernatant did not reveal a protein with the predicted molecular size of 17.3 kDa, which might have corresponded to the precursor protein, confirming that precursor protein was completely processed to mature protein within the infected insect cells prior to secretion.

The biological activity of IL-2 is traditionally evaluated by measuring its potential to induce proliferation of autologous T lymphocytes or other cells of which survival or function intimately depend on the cytokine presence. Using  $^3\text{H}$ -adenine incorporation and CFSE flow cytometric assays, the specificity and magnitude of cell division induced by *bac-rwL-2* in samples of normal woodchuck PBMC were examined. The data from these evaluations showed that the culture supernatants from either uninfected insect cells or those infected with WT baculovirus did not stimulate woodchuck T cells, whereas that containing *bac-rwL-2* induced measurable proliferation of the cells even at very high dilutions which corresponded to estimated cytokine concentrations of as low

as 0.05 U/ml. Parallel testing of *bac-rwIL-2* and rhIL-2 by CFSE-based flow cytometry proliferation assay revealed that *bac-rwIL-2* examined at the functionally optimal dilutions was consistently more potent and induced more daughter cell generations in woodchuck T lymphocytes than rhIL-2. Moreover, deconvolution of CFSE fluorescence showed that there was a smaller percentage (<1 %) of undivided parent cells in woodchuck T cells stimulated with *bac-rwIL-2* than in those exposed to rhIL-2 (5-10%). Together, these data demonstrated that there was a significant degree of cross-reactivity in biological activity between human and woodchuck IL-2, as it was also noticed by others (Menne *et al.*, 1998), but *bac-rwIL-2* was consistently more effective in inducing woodchuck T cell proliferation *ex vivo* than rhIL-2.

To further validate functional capacity of *bac-rwIL-2* produced in this study and, at the same time, to quantify its biological activity, the cytokine was tested in parallel with a well characterized preparation of rhIL-2 using a standard bioassay in which murine IL-2-dependent CTLL-2 cells are used as targets (Stern *et al.*, 1984; Sato *et al.*, 1987). It was found that *bac-rwIL-2* supported survival of CTLL-2 cells as well as stimulated their proliferation in a dose dependent manner giving a profile similar to that induced by rhIL-2. Based on the compatibility in the proliferation kinetics of CTLL-2 cells in response to serial dilutions of rhIL-2 and *bac-rwIL-2*, the biological activity of *bac-rwIL-2* in the Sf9 cell culture supernatant was estimated. This activity was found to be similar to or greater than that for recombinant IL-2 preparations reported in other studies (Taniguchi *et al.*, 1983;

Cerretti *et al.*, 1986; Reeves *et al.*, 1986; Sato *et al.*, 1987; Magnuson *et al.*, 1998;).

The availability of biologically active wIL-2 should facilitate further research on hepadnavirus-specific T cell responses in the woodchuck model of hepatitis B and aid in the development of WHV-specific T cell clones. It should also contribute to the elucidation of a role of hepadnavirus replication in lymphoid cells in the natural course of hepatitis and help to establish long-term cultures of woodchuck T lymphocytes susceptible to and supporting WHV infection *in vitro*.

**CHAPTER 5: ABERRANT LYMPHOCYTE ACTIVATION PRECEDES  
DELAYED VIRUS-SPECIFIC T CELL RESPONSE AFTER BOTH PRIMARY  
INFECTION AND SECONDARY EXPOSURE TO HEPADNAVIRUS IN  
WOODCHUCK MODEL OF HEPATITIS B**

*This study has been published in J. Virol. 2008; 82(14): pp 6992-7008.*

**5.0 SUMMARY**

The contribution of virus-specific T lymphocytes to the outcome of acute hepadnaviral hepatitis is well recognized, but a reason behind the consistent postponement of this response remains unknown. Also characteristics of T cell reactivity following re-exposure to hepadnavirus are not thoroughly recognized. To investigate these issues, healthy woodchucks were infected with liver-pathogenic doses of woodchuck hepatitis virus (WHV) and investigated unchallenged or after challenge with the same virus. As expected, WHV-specific T cell response appeared late, 6 to 7 weeks post-infection, remained high during acute disease, and then declined but remained detectable long after resolution of hepatitis. Interestingly, almost immediately after infection, lymphocytes acquired a heightened capacity to proliferate in response to mitogenic (nonspecific) stimuli. This reactivity subsided before WHV-specific T cell response appeared and its decline coincided with the cells augmented susceptibility to activation-induced death. Analysis of cytokine expression profiles confirmed early *in vivo* activation of circulating immune cells and revealed impaired transcription of

tumor necrosis factor-alpha (TNF- $\alpha$ ) and gamma interferon (IFN- $\gamma$ ). Strikingly, re-exposure of the immune animals to WHV swiftly induced hyper-responsiveness to nonspecific stimuli followed again by the delayed virus-specific response. Our data show that both primary and secondary exposures to hepadnavirus induce aberrant activation of lymphocytes preceding virus-specific T cell response. They suggest that this deviant activation and augmented death of the cells activated, accompanied by a defective expression of cytokines pivotal for effective T cell priming, postpone adaptive T cell response. These impairments likely hamper initial recognition and clearance of hepadnavirus permitting its dissemination in the early phase of infection.

## 5.1 INTRODUCTION

Hepatitis B virus (HBV) causes acute liver inflammation which may advance to chronic hepatitis, cirrhosis and hepatocellular carcinoma (Chisari, 2000). In the majority of adults, immune responses induced by HBV are sufficient to resolve acute hepatitis (AH), although they commonly fail to eliminate the virus entirely leading to an indefinitely long persistence of trace virus replication in the liver and cells of the immune system (Rehermann *et al.*, 1996; Raimondo *et al.*, 2006; Michalak, 2007; Michalak *et al.*, 2007). This residual virus carriage, termed as secondary occult HBV infection (SOI) (Michalak *et al.*, 2004), is accompanied by protracted HBV-specific T cell proliferative and cytotoxic T lymphocyte (CTL) responses (Rehermann *et al.*, 1996; Thimme *et al.*, 2003; Guidotti and Chisari,

2006) and by persistently elevated intrahepatic transcription of gamma interferon (IFN- $\gamma$ ) and tumor necrosis factor alpha (TNF- $\alpha$ ), and residual liver inflammation in woodchucks convalescent from AH (Michalak *et al.*, 1990; Hodgson and Michalak, 2001). The contribution of the innate and adaptive immunity to the control of HBV infection has been overall well delineated (Guidotti and Chisari, 2001). Among others, it was established that the recovery from AH is accompanied by a robust polyclonal and multispecific HBV-specific T helper type 1 (Th1) proliferative and CTL responses (Ferrari *et al.*, 1990). These virus-specific reactivities were found to be preceded by upregulated hepatic expression of IFN- $\gamma$  and TNF- $\alpha$ , suggesting activation of the local innate immunity (Guidotti *et al.*, 1999; Thimme *et al.*, 2003). However, contrary to infections with other viruses, HBV is seemingly ignored by the CD4+ and CD8+ T cells for about two months after primary infection, even when the infection is finally resolved (Bertoletti and Ferrari, 2003). This delay is accompanied by a very low frequency of HBV-specific CTL, which usually does not exceed 1% of circulating CD8+ T cells during acute phase of self-limiting infection (Maini *et al.*, 1999). This contrasts with infections with other viral pathogens where the primary adaptive T cell responses can be detected as early as 5-10 days post-infection and in which up to 10% of the peripheral CD8+ T cells might consist of virus-specific CTL (Koup *et al.*, 1994; Rentenaar *et al.*, 2000). A reason behind this delay in the appearance and in the relative weakness of virus-specific T cell response in hepadnaviral infection is unknown. Nonetheless, it is likely that this situation may

hinder the initial control of viremia and the complete clearance of hepadnavirus, as evidenced by the common occurrence of persistent low-level (occult) infection continuing after resolution of acute hepatitis (Michalak *et al.*, 1994; Mulrooney-Cousins and Michalak, 2007). Furthermore, it is generally accepted that the recovery from acute hepatitis B is associated with a complete protection from re-occurrence of HBV infection. However, the nature and characteristics of the cellular immune responses following re-exposure to hepadnavirus are not defined and a primary protective role for anti-HBV antibodies in this regard is acknowledged (Yuki *et al.*, 2003; Rehermann and Nascimbeni, 2005; Sjogren, 2005; Bertoletti and Gehring, 2006).

Woodchucks (*Marmota monax*) infected with woodchuck hepatitis virus (WHV) represents a highly valuable natural model of HBV infection in which sequella of virological and molecular events, and the patterns of virus-induced liver disease closely resemble those occurring in humans (Michalak, 1998; Michalak *et al.*, 2004; Menne and Cote, 2007). A significant degree of antigenic cross-reactivity between HBV and WHV and similarities in the profiles of immune responses induced by both infections, make investigations in the woodchuck-WHV model highly relevant to the recognition of immunological events occurring after the primary exposure and subsequent re-exposures to HBV.

In the present study, we dissected the profiles of hepadnavirus-specific and generalized (nonspecific, mitogen-induced) proliferative T cell responses during pre-acute and acute phases of WHV infection and after challenge and re-

challenge with the same virus, along with the expression of cytokines affiliated with immune cell activation. We also investigated lymphoid cell susceptibility to undergo apoptotic death during progressing acute infection. We have found that lymphocytes after primary and secondary exposures to WHV acquire almost immediately a strongly augmented capacity to proliferate in response to virus-nonspecific (mitogenic) stimuli, which each time precedes the delayed appearance of virus-specific T cell response. This *ex vivo* evident hyper-reactivity coincides with the augmented expression of cytokines in unmanipulated, circulating lymphoid cells indicative of their *in vivo* activation and with an inhibited expression of TNF- $\alpha$  and IFN- $\gamma$  suggesting their impaired function. These findings provide new insights into the properties of T cell reactivity during the early stages of hepadnaviral infection and after re-exposure to pathogenic hepadnavirus. They raise a possibility that a strong aberrant activation of lymphocytes occurring immediately after exposure to hepadnavirus contributes to the postponement of virus-specific primary as well as secondary T cell responses. These events may hinder recognition and elimination of the virus facilitating its dissemination in the prodromal phase of infection.

## **5.2 MATERIALS AND METHODS**

### **5.2.1 Animals and WHV inoculations**

Ten healthy, adult woodchucks housed in the Woodchuck Hepatitis Research Facility at Memorial University, St. John's, Canada were infected with

large, liver pathogenic doses of WHV. Prior exposure to WHV was excluded based on negative serological markers for WHV infection and by the absence of WHV DNA in randomly selected serum, peripheral blood mononuclear cell (PBMC) and liver biopsy samples assessed by nested polymerase chain reaction-nucleic acid hybridization (PCR-NAH) assays (sensitivity <10 virus genome equivalents [vge]/mL) (Michalak *et al.*, 1999; Coffin *et al.*, 2004). The animals were divided into three groups. Four animals (Group A) were investigated in the first phase to determine overall features of T cell proliferative responses accompanying primary infection and subsequent exposures to hepadnavirus. The animals were intravenously (i.v.) injected with  $1.9 \times 10^{11}$  DNase-protected vge of WHV/tm4 inoculum carrying the wild-type WHV, as determined by the whole genome sequence analysis (P.M. Mulrooney-Cousins and T.I. Michalak, unpublished data). They were followed for 65 weeks post-primary infection (w.p.p.i.), then challenged with the same dose of WHV/tm4 and re-challenged 15 weeks later with either  $1.9 \times 10^{11}$  vge (1/F and 2/F animals) or  $1.9 \times 10^2$  vge (3/F and 4/M) of the inoculum (see Figure 5.1A). Four other woodchucks constituted study Group B. These animals were injected once with WHV, followed for 16 w.p.p.i., and investigated to recognize an interdependence between heightened T lymphocyte proliferate capacity occurring immediately after WHV exposure identified in the first study and the lymphocyte susceptibility to apoptotic death, delayed WHV-specific T cell response, and expression of selected proinflammatory and antiviral cytokines in lymphoid cells. In this group, two

animals (5/M and 6/M) were infected with  $1.9 \times 10^{11}$  vge of WHV/tm4, while other two (7/M and 8/M) with WHV/tm3 inoculum (GenBank accession number AY334075) (Michalak *et al.*, 2004) at  $1.1 \times 10^{10}$  DNase-protected vge per dose (see Figure 5.1B). In addition, two woodchucks, each injected with a single dose of WHV/tm4 at  $1.9 \times 10^{11}$  vge, were examined for 112 w.p.i. as controls. The study protocol was approved by the Institutional President's Committee on Animal Bioethics and Care.

### 5.2.2 Sample collection

Animals were bled at the time points indicated in Figure 5.1. Sera were collected and preserved. PBMC were isolated as described before (Gujar and Michalak, 2005). Their viability normally exceeded 98%, as determined by trypan blue dye exclusion. Liver biopsies were obtained by surgical laparotomy at time points showed in Figure 5.1, and examined for WHV DNA load and histological lesions using the scoring criteria reported before (Michalak *et al.*, 1999; Hodgson and Michalak, 2001; Michalak *et al.*, 2004).

### 5.2.3 Serological and WHV DNA detection assays

Serial serum samples were tested for WHV surface antigen (WHsAg), antibodies to WHV core antigen (anti-WHc) and antibodies to WHsAg (anti-WHs) by in-house specific enzyme-linked immunoassays reported before (Michalak *et al.*, 1999; Coffin *et al.*, 2004; Michalak *et al.*, 2004). WHV DNA in sera and liver

biopsies was quantified by real-time PCR (Michalak *et al.*, 2004) and, when negative, by PCR-NAH assay, as reported (Michalak *et al.*, 1999).

#### 5.2.4 WHV antigens and mitogens for T cell proliferation assays

Recombinant WHV core, e and X proteins, designated as rWHc, rWHe and rWHx, respectively, and used to measure WHV-specific T cell proliferation *in vitro*, were produced in the pET41b(+) *Escherichia coli* expression system (Novagen, Darmstadt, Germany) and affinity purified, as recently reported (Wallace *et al.*, 1999). They were extensively tested for nonspecific T cell proliferation against potential bacterial contaminants and found entirely devoid of such activity (Wallace *et al.*, 1999). In addition, a synthetic WHV peptide, containing the immuno-dominant epitope corresponding to amino acids 97 to 110 (WHc<sub>97-110</sub>) of the virus nucleocapsid protein (Menne *et al.*, 1997) was synthesized. WHV envelope particles carrying WHsAg specificity were purified from pooled sera of a chronic WHV carrier, as described (Michalak *et al.*, 1999; Michalak *et al.*, 2004). As inducers of generalized, nonspecific, polyclonal lymphocyte response, concanavalin A (ConA; Pharmacia Fine Chemicals, Uppsala, Sweden), pokeweed mitogen (PWM, *Phytolacca americana* agglutinin; ICN Biochemicals Inc., Aurora, OH) and phytohemagglutinin (PHA; ICN Biochemicals) were used (see below).

#### 5.2.5 Adenine-incorporation T cell proliferation assay

<sup>3</sup>H-adenine incorporation T lymphocyte proliferation assay was applied to examine WHV-specific and mitogen-induced T cell responsiveness and performed as described elsewhere (Kreuzfelder *et al.*, 1996; Gujar and Michalak, 2005). Briefly, freshly isolated PBMC were cultured in 96-well flat-bottom plates (Becton Dickinson Labware, Franklin Lakes, NJ) at a density of  $1 \times 10^5$  cells/well in complete AIM-V lymphocyte culture medium (Gibco-Invitrogen Corp., Auckland, New Zealand) with 10% fetal calf serum (Gibco-Invitrogen). Recombinant WHV proteins and WHsAg were added in triplicate at 1  $\mu$ g/mL and 2  $\mu$ g/mL, whereas WHC<sub>97-110</sub> peptide was used at five two-fold dilutions from 1.25  $\mu$ g/mL to 20  $\mu$ g/mL. Similarly, to assess the generalized lymphocyte response, each PBMC sample was exposed in triplicate to five two-fold dilutions of ConA or PHA from 1.25  $\mu$ g/mL to 20  $\mu$ g/mL and PWM from 0.6  $\mu$ g/mL to 10  $\mu$ g/mL or to medium alone as a control. The cultures were incubated for 96 hours at 37 °C, pulsed with 0.5  $\mu$ Ci of 2-<sup>3</sup>H-adenine (Amersham Pharmacia Biotech, AB, Uppsala, Sweden) per well, and incubated for an additional 12-18 hours. Then, the cells were harvested and their radioactivity counts per minute (cpm) in each well were determined (Gujar and Michalak, 2005). The mean cpm values for either stimulated or control cells were calculated by averaging the counts in the respective triplicate wells. The stimulation index (S.I.) was calculated by dividing mean cpm obtained either after WHV antigen or mitogen stimulation by mean cpm detected in control, unstimulated wells. S.I. values of  $\geq 3.1$  for rWHC, rWHE and rWHx and  $\geq 2.1$  for WHC<sub>97-110</sub> and WHsAg were considered as positive based on the cut off values

given by three standard deviations (S.D.) above the mean values obtained from control wells. Mean mitogenic stimulation index (M.M.S.I.) was determined by averaging the S.I. values obtained for all five concentrations of a given mitogen, as described (Gujar and Michalak, 2005).

#### **5.2.6 CFSE-flow cytometry T cell proliferation assay**

Since WHV-specific T cell response examined by the  $^3\text{H}$ -adenine incorporation assay gave readings in samples collected after the third injection with WHV, *i.e.*, 80 w.p.p.i., at the detection limit of the assay and to confirm the observations made in study Group A in Group B animals, a more sensitive flow cytometric assay with 5-and-6-carboxyfluorescein diacetate succinimidyl ester (CFSE; Molecular Probes, Eugene, Oregon) was employed, as recently reported (Gujar and Michalak, 2005). Briefly, woodchuck PBMC were labeled with  $1\ \mu\text{M}$  of CFSE and either stimulated with WHV antigens or WHC<sub>97-110</sub> at the same concentrations as those in the adenine incorporation assay or left unstimulated as controls. The plates were incubated for 5 days. The cells were harvested and analyzed in a FACSCalibur flow cytometer (Becton Dickinson, Franklin Lakes, NJ). The halved CFSE fluorescence in dividing PBMC was determined by applying CellQuest Pro software (Becton Dickinson). The cell division index (C.D.I.) was defined by dividing the percentage of cells showing halved CFSE-fluorescence after stimulation with WHV antigens by that of cells with halved CFSE-fluorescence cultured in the absence of stimulation, as we described

before (Gujar and Michalak, 2005). The highest C.D.I. value found at a given time point for any concentration of WHV protein/peptide tested was taken as a measure of WHV-specific T cell response. The cut off C.D.I. values of  $\geq 3.1$  were considered to represent a positive WHV-specific response (Gujar and Michalak, 2005).

### **5.2.7 CFSE/annexin-V-PE/7-AAD assay for simultaneous detection of T cell proliferation and apoptosis**

The assay simultaneously measuring lymphocyte proliferation and their apoptotic death was adopted using ConA and rWHe as stimulators, and as three-color CFSE/annexin-V-PE/7-AAD assay. Briefly, freshly isolated PBMC were labeled with 1  $\mu$ M of CFSE, cultured at a density of  $5 \times 10^5$  cells per well in 48-well tissue culture plate, and stimulated with either ConA (2.5 and 5  $\mu$ g/ml) or rWHe (1 and 2  $\mu$ g/ml) as indicated above. The cells were harvested, washed with annexin-labeling buffer (5 mM NaCl, 5 mM KCl and 2 mM  $\text{CaCl}_2$  in 10 mM HEPES), stained for 30 min on ice with 50  $\mu$ g/ml of 7-actinomycin-D (7-AAD; Molecular Probes) and 50  $\mu$ l/ml of R-PE-conjugated recombinant human annexin-V (annexin-V-PE; Caltag Laboratories, Burlingame, CA), and analyzed by flow cytometry. In addition, to monitor death of lymphoid cells potentially occurring *in vivo*, freshly isolated PBMC were directly labeled with annexin-V/7-AAD, without preceding stimulation with ConA or rWHe, and analyzed. The authenticity of specific binding of annexin-V and 7-AAD was verified by visualizing intracellular

fluorescence distribution (see Figure 5.6A) using an Olympus BX 50WI confocal microscopy system (Olympus America Inc., Center Valley, PA).

The C.D.I. was defined by dividing percentage of CFSE<sup>dim</sup> cells after stimulation with rWHe or ConA by CFSE<sup>dim</sup> cells without any stimulation (medium only), as indicated above. The C.D.I. of  $\geq 3.1$  after rWHe or ConA stimulation was accepted as a positive T cell response. The cell apoptosis was assessed by using CellQuestPro software (Becton Dickinson) by separating test cells into four quadrants as: live cells, *i.e.*, annexin-V/7-AAD-negative (lower left quadrant), early apoptotic, *i.e.*, annexin-V- positive only (lower right quadrant), late apoptotic, *i.e.*, annexin-V and 7-AAD-positive (upper right quadrant), and necrotic, *i.e.*, 7-AAD-positive only (upper left quadrant), as illustrated in Figure 5.6A. The total percentage of apoptotic cells was determined by adding the percentages of early apoptotic, late apoptotic and necrotic cells.

### 5.2.8 Real-time RT-PCR

PBMC and liver biopsy samples collected prior to and during WHV infection were analyzed for expression of selected cytokines and cell marker genes by real time RT-PCR using a LightCycler (Roche Diagnostics, Mannheim, Germany). For this purpose,  $5 \times 10^5$  -  $1 \times 10^6$  PBMC were resuspended immediately after isolation in 1 mL of Trizol reagent (Invitrogen, Auckland, New Zealand) and stored at -20°C. After collection of all experimental samples, RNA was extracted and 2- $\mu$ g RNA samples were reversely transcribed to cDNA, as

reported (Coffin *et al.*, 2004). The expression of woodchuck IFN- $\alpha$ , IFN- $\gamma$ , TNF- $\alpha$ , IL-2, IL-4, IL-10, IL-12, CD3, CD4, CD14 and CD56 was quantified using equivalent of 50 ng of total RNA and gene-specific primer pairs shown in Table 5.1 and their transcription normalized against that of woodchuck  $\beta$ -actin.

To quantify WHV mRNA, cDNA derived from equivalent of 50 ng RNA, along with serial 10-fold dilutions of complete recombinant WHV DNA (rWHV DNA) as standards (Michalak *et al.*, 1999), was amplified by real-time PCR using WHV core gene-specific primers (Table 5.1). When WHV RNA was undetectable, 2  $\mu$ g of cDNA was analyzed by nested PCR/NAH) using WHV-specific primers and conditions described before (Michalak *et al.*, 2004).

### 5.2.9 Statistical analysis

Two-tailed, unpaired Student *t* test with 95% confidence interval was applied to compare the means of sample groups investigated and *P* values of < 0.05 were considered as statistically significant. Differences marked with one asterisk were significant at  $P < 0.05$ , with two at  $P < 0.005$ , and with three at  $P < 0.0001$ .

## 5.3 RESULTS

### 5.3.1 Serological and WHV DNA profiles after primary and multiple exposures to WHV

Among animals belonging to study Group A, three woodchucks developed

**Table 5.1 Sequences of WHV and woodchuck gene-specific PCR primers used in this study**

Gene	GenBank number	Primer sequence	Amplicon size (bp)
WHV mRNA	AY334075	Forward 5'- ATGCACCCATTCTCTCGAC	221
		Reverse 5'- CTGAGCAGCTTGGTTAGAGT	
IFN $\alpha$	AF425778	Forward 5'- CTCCATGAGATGACCC	204
		Reverse 5'- GGTAGACAGTGATCCT	
IFN $\gamma$	AF232728	Forward 5'- AGGAGCATGGACACCATCA	215
		Reverse 5'- CCGACCCCGAATCGAAG	
TNF $\alpha$	AF333967	Forward 5'- TGAGCACTGAAAGTATGATCC	283
		Reverse 5'- TGCTACAACATGGGCTACAG	
IL-2	DQ272238	Forward 5'- AAGGCTTCTGACCTGG	185
		Reverse 5'- CGGGCGTACTCACAA	
IL-4	AF333965	Forward 5'- TTTGCTGTCCCAAGAAC	200
		Reverse 5'- CCTGGATTCACTCAOGG	
IL-10	AF012909	Forward 5'- AGGCCGTACAGCAAGTGAAG	200
		Reverse 5'- ACAACCCTGAGCCAGATTTT	
IL-12	X97019	Forward 5'- TTGGATTGGCACCCCTGACAC	198
		Reverse 5'- GCATCTGGCTCAGAACCTCAC	
CD3	AF232727	Forward 5'- CTGGGACTCTGCCTCTTATC	536
		Reverse 5'- GCTGGCCTTTCCGGATGGGCTC	
CD4	EF621765	Forward 5'- GGAGAATAAGAAGATAGAGG	560
		Reverse 5'- TCAAGAGTCACAGTCAGG	
CD14	EF621769	Forward 5'- ACTGTCTGACAATCCT	187
		Reverse 5'- CGAGCATCGAGTTGTG	
CD56	EF621771	Forward 5'- CATCTACAACGCCAATATCG	187
		Reverse 5'- GGGAGCTGACCACATC	
$\beta$ -actin	AF232730	Forward 5'- CAACCGTGAGAAGATGACC	338
		Reverse 5'- ATCTCCTGCTCGAAGTCC	

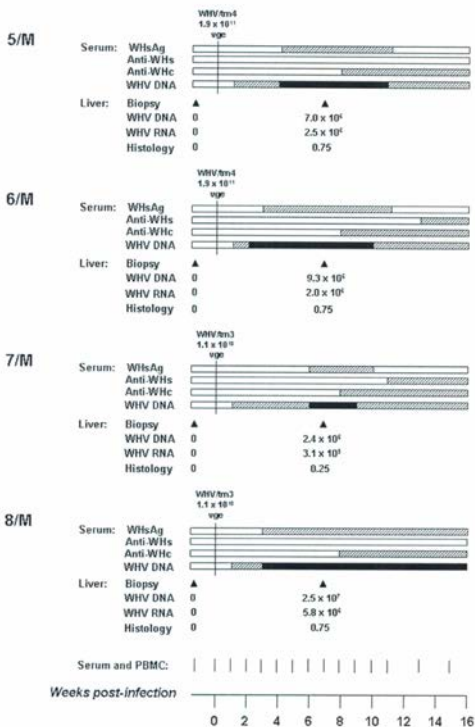
classical self-limited AH with WHsAg detectable in serum between 3 and 7 w.p.i. (Figure 5.1A). Woodchucks 1/F, 2/F and 3/F seroconverted to anti-WHs between 8 and 12 w.p.i., while 4/M became transiently anti-WHs reactive one week after challenge with WHV, *i.e.*, at 66 w.p.i. (Figure 5.1A). Anti-WHc appeared at 6 w.p.i. and remained detectable during the entire follow-up period in all animals. The level of anti-WHc did not fluctuate noticeably after challenge or re-challenge with WHV. Serum WHV DNA became detectable from one w.p.i. and persisted until the end of follow-up in all 4 woodchucks. After clearance of serum WHsAg, the level of circulating WHV DNA declined and usually did not exceed  $10^2$  vge/mL thereafter, as it has been previously reported for animals with SOI continuing after resolution of AH. Serum WHV DNA remained at a similar low level after the second and third injections with WHV (Figure 5.1A). Hepatic WHV loads were at  $2 \times 10^3$  -  $8 \times 10^3$  vge/ $\mu$ g of total liver DNA during AH, then subsided to about  $3 \times 10^2$  vge/ $\mu$ g and persisted at an approximately similar level until the end of follow-up (Figure 5.1A), as previously observed (Michalak *et al.*, 1999; Cote *et al.*, 2000; Michalak *et al.*, 2004).

In study Group B, 3 animals infected with WHV/tm3 or WHV/tm4 developed immunovirological and WHV DNA profiles indicative of a self-limiting episode of AH which were closely comparable to those seen in animals in Group A (Figure 5.1B), while 8/M developed histologically evident mild protracted hepatitis. In this animal, serum WHsAg appeared 3 weeks post-infection (w.p.i.) and persisted until the end of follow-up, *i.e.*, 16 w.p.i. Anti-WHs became

**Figure 5.1** General outline of the experimental protocols showing time points of injections with WHV, serum, PBMC and liver biopsy collections, serological markers of WHV infection and serum WHV DNA detected, hepatic WHV loads, and the results on liver histology after primary infection and challenge with WHV. (A) Four woodchucks (study Group A) were infected (time 0) with  $1.9 \times 10^{11}$  DNase-protected virions of WHV/tm4 inoculum, challenged with same dose of WHV at week 65 and then re-challenged with either  $1.9 \times 10^{11}$  (1/F and 2/F animals) or  $1.9 \times 10^2$  virions (3/F and 4/M) at week 80. (B) Four woodchucks (study Group B) were infected (time 0) with  $1.9 \times 10^{11}$  virions of WHV/tm4 (5/M and 6/M animals) or with  $1.1 \times 10^{10}$  virions of WHV/tm3 (7/M and 8/M animals) and followed for 16 weeks after infection. The appearance and the duration of WHsAg, anti-WHs and anti-WHc and serum WHV DNA are shown by horizontal bars. The estimated levels of serum WHV DNA are depicted as black bars ( $>10^3$  vge/ml), hatched bars ( $<10^3$  vge/ml) or white bars (not detectable). The PBMC collected at the time points marked by the short vertical lines at the bottom of A and B panels were analyzed for WHV-specific and generalized T cell proliferative responses. Samples marked with \* were obtained from all woodchucks except 1/F. WHV DNA load in liver biopsies collected at the time points indicated by solid arrow heads is presented as the estimated WHV DNA vge/ $\mu$ g of total liver DNA. Liver morphological alterations are presented as the histological degree of hepatitis graded on the scale of 0 to 3.



Figure 5.2B



detectable in 6/M and 7/M after clearance of WHsAg from serum around 13 and 10 w.p.i., respectively. Liver biopsies collected at 7 w.p.i. contained WHV DNA loads ranging from  $2.4 \times 10^6$  to  $2.5 \times 10^7$  vge/ $\mu$ g of total DNA (mean  $1.1 \times 10^7 \pm 4.9 \times 10^6$  vge/ $\mu$ g) and WHV mRNA at  $3.1 \times 10^5$  to  $5.5 \times 10^6$  copies/ $\mu$ g of total RNA (mean  $2.7 \times 10^6 \pm 1.1 \times 10^6$  copies/ $\mu$ g).

### **5.3.2 Both primary infection and challenge with WHV induce delayed virus-specific T cell response**

In animals from Group A, the WHV-specific T cell proliferation against WHV antigens or WHC<sub>97-110</sub> peptide measured by <sup>3</sup>H-adenine incorporation assay was multispecific and of relatively high magnitude between 10 and 14 w.p.i. (Figure 5.2). Persistently detectable virus-specific proliferative response to rWHe, rWHx and WHC<sub>97-110</sub> peptide first appeared around 6-8 w.p.i. and preceded that against rWHc and WHsAg, which became detectable at 10-14 w.p.i. However, it is of note that a transient T cell reactivity of very low-magnitude towards rWHe, WHC<sub>97-110</sub> and WHsAg was also evident at 3 w.p.i. The strong WHV-specific response was evident for up to 30 w.p.i., then subsided and became intermittently detectable by <sup>3</sup>H-adenine incorporation assay until challenge at 65 w.p.i. (Figure 5.2). In two control animals, the pattern of WHV-specific response during acute phase of infection was similar to that described above and the reactivity remained detectable until termination of the experiment at 112 w.p.i. (data not shown). Overall, the virus-specific T cell response was strong and

multispecific during the acute phase of primary infection, with the greatest magnitudes after *ex vivo* stimulation with rWHe followed by rWHc or rWHx and the lowest after stimulation with WHc<sub>97-110</sub> or WHsAg.

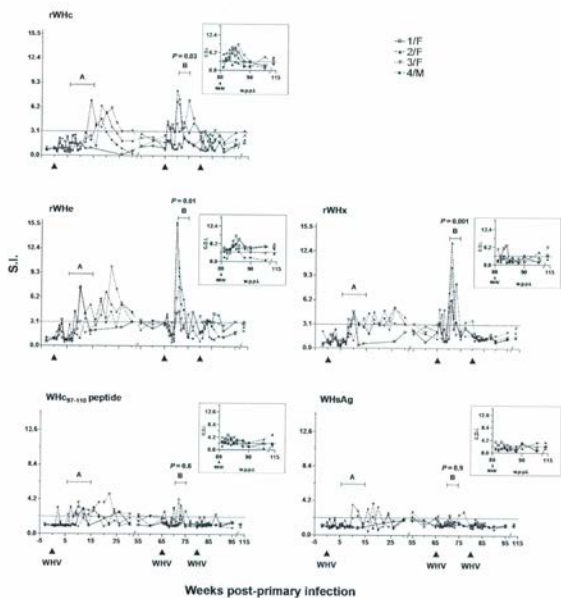
Challenge of the convalescent woodchucks with the same  $1.9 \times 10^{11}$  vge dose of WHV/tm4 did not induce the expected immediate memory virus-specific T cell response (Figure 5.2). However, a strong T cell response to WHV antigens was found in all animals between 5 and 10 weeks after challenge, *i.e.*, 70-75 w.p.i. The magnitudes of the secondary response to rWHe ( $P = 0.01$ ), rWHc ( $P = 0.03$ ) and rWHx ( $P = 0.001$ ) were significantly greater than those during the primary infection (Figure 5.2). In contrast, the levels of secondary T cell response against WHc<sub>97-110</sub> peptide ( $P = 0.6$ ) and WHsAg ( $P = 0.9$ ) were comparable to those detected in the primary infection. After re-challenge with either high (1/F and 2/F) or low (3/F and 4/M) dose of WHV/tm4, all animals demonstrated minuscule or undetectable virus-specific T cell reactivity when tested by <sup>3</sup>H-adenine incorporation assay (Figure 5.2). However, a transient increase in the magnitude of WHV-specific T cell proliferation was evident when more sensitive CFSE-flow cytometric assay was applied (Figure 5.2; insets).

### **5.3.3 Lymphocyte generalized proliferative capacity increases immediately after primary and subsequent exposures to WHV**

Almost immediately after the primary injection with WHV, *i.e.*, 1-3 w.p.i., the lymphocytes acquired from animals in study Group A showed strongly

**Figure 5.2** The kinetics of WHV-specific T cell proliferative responses against WHV antigens in woodchucks belonging to study Group A which were infected, challenged and re-challenged with WHV. The animals were injected with WHV at the time points indicated by solid arrow heads. Freshly isolated PBMC were stimulated *in vitro* with rWHc, rWHe, rWHx, WHc<sub>97-110</sub> peptide or WHsAg, and their proliferation measured by <sup>3</sup>H-adenine incorporation assay. The results are presented as stimulation index (S.I.). *P* values were calculated for peak T cell reactivity against each WHV antigen in each animal observed during primary (A) and secondary (B) virus exposures in the time periods marked by vertical short lines. The insets show T cell proliferative responses against the same WHV antigens after re-challenge with WHV as measured by CFSE-flow cytometry assay with the results presented as cell division index (C.D.I.). The cut-off values for positive responses against rWHc, rWHe and rWHx were  $\geq 3.1$  and against WHc<sub>97-110</sub> peptide and WHsAg  $\geq 2.1$ , as indicated by horizontal dotted lines.

Figure 5.2

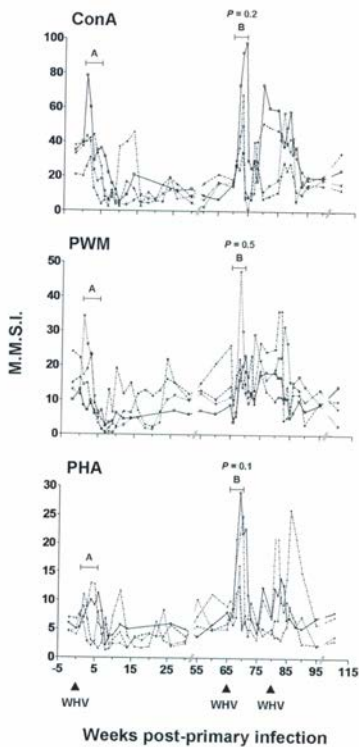


heightened capacity to proliferate in response to ConA, PWM and PHA (Figure 5.3). Then, the response subsided between 6 and 30 w.p.i., at the time when the WHV-specific T cell response appeared and endured at high levels (see Figure 5.4). The exception was 4/M with serum WHsAg-negative, but anti-WHc and WHV DNA-positive infection in which the nonspecific lymphocyte reactivity after the initial lowering increased between 10 and 14 w.p.i. During the phase of the lowered responsiveness to mitogenic stimuli, temporal increases in this T cell response occurred. Interestingly, these periodic increases appeared to be synchronized in all animals, as recapitulated in Figure 5.4. It also is of note that ConA, PHA and PWM induced similar profiles of the proliferative response (Figure 5.3), suggesting that no particular lymphocyte subset was predominantly involved in the periodic increases.

After challenge with WHV at 65 w.p.i., this non-specific T cell proliferative reactivity was again augmented in all animals with the peak occurring between one and 3 weeks following challenge, *i.e.*, 66 and 68 w.p.i. (Figures 5.3 and 5.4). However, the magnitudes of the cell proliferation in response to ConA ( $P = 0.2$ ), PWM ( $P = 0.5$ ) and PHA ( $P = 0.1$ ) were not significantly different from those detected after the first injection with WHV (Figure 5.3). This heightened response to mitogens subsided between 68 and 75 w.p.i., which coincided again with arise of the secondary WHV-specific T cell response (Figure 5.3 and 5.4). Subsequently, when the virus-specific T cell reactivity progressively decreased, the T cell proliferative capacity in response to mitogens rebounded and remained

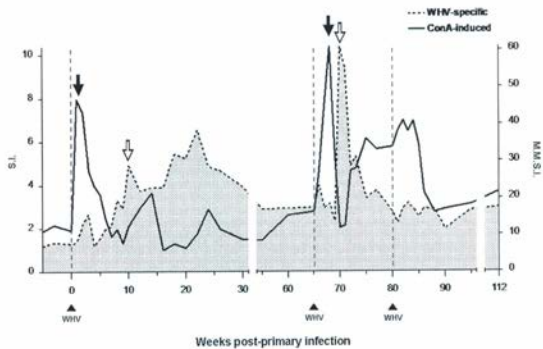
**Figure 5.3** The kinetics of mitogen-induced (generalized) T lymphocyte proliferation in woodchucks after primary infection, challenge and re-challenge with WHV. The same animals shown in Figure 5.2 (study Group A) were injected with WHV at the time points indicated by solid arrow heads. The T cell proliferation was measured in response to five different concentrations of ConA, PWM or PHA by  $^3\text{H}$ -adenine incorporation assay. The M.M.S.I. values were calculated for each mitogen in each animal at indicated time points as explained in Materials and Methods. *P* values were determined as in Figure 5.2.

Figure 5.3



**Figure 5.4** Discordance between the kinetics of WHV-specific and generalized T cell proliferative responses during primary WHV infection and after challenge and re-challenge with WHV. The profiles are compiled from the data generated using  $^3\text{H}$ -adenine incorporation assay measuring T cell proliferation in response to rWHc, rWHe, rWHx, WHc<sub>97-110</sub> peptide and WHsAg (S.I. values) and in response to five concentrations of ConA (M.M.S.I. values). The mean of the highest S.I. given by any WHV antigen or that of M.M.S.I. in response to any ConA concentration from each of 4 animals constituting study Group A were used to construct the profiles of the WHV-specific and generalized T cell responses, respectively. Solid and open downward arrows depict peaks of mitogen-induced or WHV-specific T cell responsiveness, respectively, after primary infection and challenge with WHV. Solid upward arrow heads mark injections with WHV.

Figure 5.4



at a high level until 80 w.p.i. when the animals were re-challenged with WHV (Figure 5.4). The third injection with either a high or low WHV dose induced another, although lower in magnitude, immediate increase in the T cell generalized proliferative response (Figure 5.3 and 5.4).

#### **5.3.4 Immediate augmented lymphocyte generalized proliferative and delayed virus-specific T cell responses are consistently induced by WHV infection**

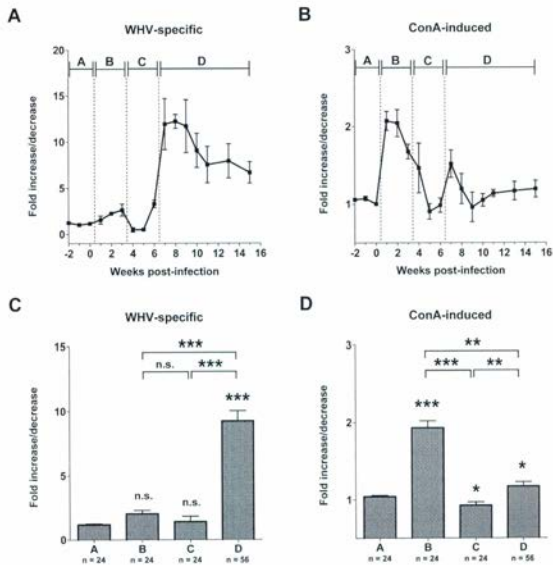
To confirm findings made in the first study by assessing WHV-specific response using CFSE-flow cytometric assay, as well as to test if another WHV inoculum will induce the same effects on T cell responses and to systematically evaluate lymphoid cell predisposition to apoptotic death after exposure to WHV, weekly PBMC samples collected from animals constituting study Group B were investigated. Thus, the CFSE-based lymphocyte proliferation assay with rWHe confirmed that the primary exposure to WHV induces delayed virus-specific T cell response which appeared from 7 w.p.i. and persisted until the end of the 16-week follow-up (Figure 5.5A). Further, the lymphoid cell capacity to proliferate in response to stimulation with mitogenic stimulus (ConA) was evident again immediately after exposure to WHV, *i.e.*, as early as one w.p.i. This response rapidly subsided between 4 and 6 w.p.i., then transiently increased between 7-8 w.p.i., and receded to approximately pre-infection levels thereafter (Figure 5.5B). All 4 animals belonging to study Group B displayed closely comparable patterns

of both WHV-specific and ConA-induced T cell proliferative responses, including 8/M animal which developed protracted infection suggesting progression to chronic hepatitis.

Considering distinct and, for the most part, opposing kinetics of the generalized, mitogen-induced and WHV-specific T cell proliferative responses, the progression of acute WHV infection was divided into phases (Figures 5.5A and 5.5B). Thus, phase A corresponded to the time period prior to WHV infection; phase B or pre-acute phase occurred between one and 3 w.p.i. and was characterized by heightened nonspecific and essentially absent WHV-specific T cell response; phase C or early-acute phase between 4 and 6 w.p.i. was accompanied by subsiding nonspecific and absent virus-specific T cell response, and phase D or acute phase (7 w.p.i. onwards) was associated with the initially slightly increasing but then normalized mitogen-induced proliferative capacity and with significantly augmented WHV-specific T cell response. As shown in Figure 5.5C, the magnitude of WHV-specific T cell reactivity during acute infection (phase D) was significantly ( $P < 0.0001$ ) greater when compared to those detected during pre-acute (phase B) and early-acute (phase C) periods of WHV infection. In contrast, PBMC displayed significantly ( $P < 0.0001$ ) increased magnitudes of mitogen-induced proliferation immediately after exposure to WHV (Figure 5.5D), *i.e.*, during the pre-acute period (phase B). This reactivity declined during the early-acute period (phase C) by displaying a mean response lower ( $P = 0.02$ ) than that observed prior to infection (phase A), and subsequently

**Figure 5.5** Patterns of WHV-specific and ConA-induced T cell responses in Group B woodchucks during self-limited acute WHV infection. (A) WHV-specific T cell response was measured by CFSE-based flow cytometric assay against rWHe. The data are presented as the mean  $\pm$  SEM of cell division indices (CDI) obtained from all 4 animals measured at 1 and 2  $\mu\text{g}/\text{mL}$  rWHe at each time point indicated. (B) ConA-induced T cell proliferative response was measured in the same samples by adenine incorporation assay using two-fold dilutions of ConA ranging from 1.25 to 20  $\mu\text{g}/\text{mL}$ . The mean mitogenic stimulation index (MMSI) was calculated by averaging the SI from all five ConA concentrations for all 4 animals at each time point showed. The CDI or MMSI values detected after infection with WHV were compared with those before infection (phase A) from the same animal and expressed as fold increase or decrease. Each data point represents the mean  $\pm$  SEM of fold increases/decreases from all 4 animals. Pre-infection period (phase A) and stages of WHV infection (phases B to D) are marked as defined in Materials and Methods. The cumulative data on (C) WHV-specific and (D) ConA-induced T cell proliferative responses detected during indicated phases of WHV infection are presented as mean  $\pm$  SEM for fold increase or decrease. The data presented as bars B, C and D were compared with either those presented by bar A or with each other. Differences marked with stars are significant at *P* values as indicated in Materials and Methods.

Figure 5.5



rebounded in the acute phase (phase D) to a mean level greater ( $P = 0.03$ ) than that prior to infection (phase A), but still significantly ( $P < 0.005$ ) lower than that characterizing phase B.

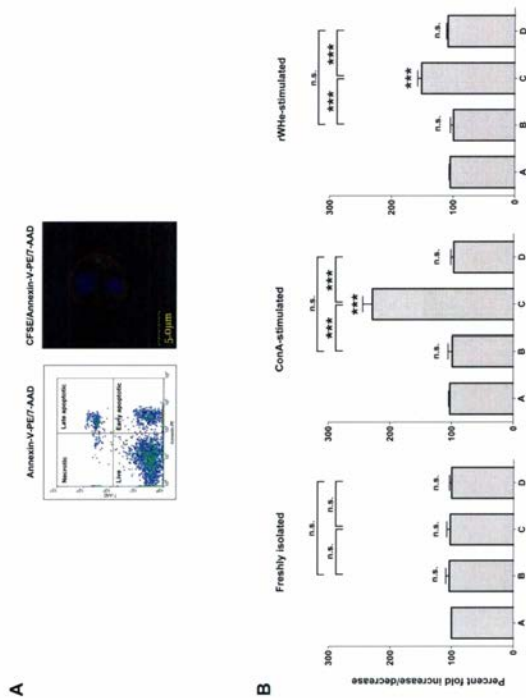
### **5.3.5 Decline in T cell generalized proliferation capacity coincides with increased activation-induced cell death**

To recognize a possible reason behind the observed rapid decline in the T cell proliferative response to mitogenic stimuli seen during the early-acute period (phase C) of WHV infection, the rate of apoptotic death of lymphomononuclear cells was evaluated in weekly PBMC samples from Group B animals by the assay employing staining with annexin-V-PE, 7-AAD and CFSE. In preliminary experiments, the authenticity of staining of woodchuck lymphoid cells with recombinant human annexin-V-PE and 7-AAD was verified by visualizing appropriate subcellular compartments under confocal microscopy. As illustrated in Figure 5.6A, annexin-V, 7-AAD and CFSE produced cell surface, nuclear and cytoplasmic staining, respectively, in woodchuck lymphocytes undergoing apoptosis.

To assess whether naturally circulating lymphocytes from different phases of acute WHV infection (Figure 5.5) might be differentially predisposed to apoptosis, freshly isolated, unmanipulated, weekly PBMC samples were stained with annexin-V and 7-AAD. The results showed that the fresh cells from different phases did not display any noticeable variations in mean percentage of apoptotic

**Figure 5.6** Activation-induced apoptosis of lymphoid cells during progression of acute WHV infection. (A) A representative flow cytometry dot-plot and a confocal microscopy micrograph showing annexin-V-PE and 7-AAD labeling patterns in circulating woodchuck lymphoid cells. (B) Freshly isolated or ConA- or rWHe-stimulated PBMC samples collected prior to inoculation with WHV (phase A) from Group B animals or weekly during progression of acute infection were analyzed for the rate of apoptosis by flow cytometry with annexin-V and 7-AAD. The percentage of apoptotic cells was determined in each weekly sample from 4 animals, averaged to find the mean percentage of apoptosis for each phase of infection (phases B to D), and compared with that calculated for PBMC collected prior to WHV infection (phase A) which was taken as 100%. The bars represent the mean  $\pm$  SEM of percent fold increase or decrease in apoptosis for freshly isolated PBMC or those stimulated with ConA at 2.5 and 5  $\mu$ g/mL or with rWHe at 1 and 2  $\mu$ g/mL. Differences between data bars are marked as outlined in Materials and Methods.

Figure 5.6



cells in comparison to the cells collected prior to infection (Figure 5.6B). However, when the rate of apoptosis was measured in the same cell samples after stimulation with ConA or rWHe, significantly greater rates and infection phase-dependent changes in apoptotic death were identified (Figure 5.6B). Overall, the results indicated that lymphocytes derived from the early-acute period (phase C) of WHV infection, when nonspecific T cell responsiveness profoundly declined but WHV-specific response had not yet occurred, were significantly more prone to activation-induced death than the cells collected immediately after infection (phase B) or during AH (phase D).

#### **5.3.6 Cytokine and cell marker gene expression profiles in unmanipulated circulating lymphoid cells**

Since the expression patterns of anti-viral and pro-inflammatory cytokines in peripheral lymphoid cells after primary hepadnaviral infection have been described (Guidotti *et al.*, 1999; Thimme *et al.*, 2003), initially (study Group A), we examined the kinetics of this expression after re-exposure to WHV. We found that following challenge of animals convalescent from AH with WHV, the heightened expression of IFN- $\alpha$  became immediately evident in sequential PBMC samples collected after challenge, *i.e.*, between 66-69 w.p.i. This cytokine transcription then subsided and increased again, but to a lower level, around the time of re-challenge with the same virus inoculum (Figure 5.7A). This significantly increased ( $P < 0.0001$ ) expression of IFN- $\alpha$  coincided with the phase of

augmented T cell proliferative responsiveness to mitogen stimuli (Figure 5.7A and Figure 5.3, respectively). The transcription of TNF- $\alpha$  ( $P < 0.0001$ ) and, to some extent, IFN- $\gamma$  ( $P = 0.015$ ) was transiently enhanced between 68-69 w.p.p.i.. The mRNA levels of IFN- $\alpha$ , IFN- $\gamma$ , TNF- $\alpha$  and, to a lesser degree, CD3 subsided 5 weeks later, *i.e.*, around 70 w.p.p.i. In general, the enhanced expression of IFN- $\alpha$ , IFN- $\gamma$  and TNF- $\alpha$  coincided with highly augmented T cell nonspecific proliferative capacity and clearly preceded the re-appearance of WHV-specific T cell proliferative response, which occurred between weeks 70 and 75 post infection (Figure 5.7A and Figure 5.2, respectively). The expression profiles of IL-2 and IL-4 did not correlate with the magnitudes of either specific or nonspecific T cell responses, except for 4/M which displayed increased expression of both these cytokines at the time of greater expression of IFN- $\gamma$  and TNF- $\alpha$ . CD14 and CD56 transcription levels measured in serial PBMC samples showed unremarkable profiles (data not shown). Overall, the data revealed a close association between the augmented expression of IFN- $\alpha$ , TNF- $\alpha$  and, to a lesser extent, IFN- $\gamma$  in circulating unmanipulated lymphoid cells and their heightened proliferative capacity in response to mitogenic, but not virus-specific, stimuli after challenge with WHV.

To further recognize events accompanying distinctive phases of WHV-specific and nonspecific T cell proliferative responses accompanying acute WHV infection, transcriptional activity of genes encoding selected cytokines and immune cell subtype-specific markers was quantified by real-time RT-PCR in

**Figure 5.7** Expression profiles of genes encoding cytokines and immune cell surface markers in serial unmanipulated PBMC samples collected from the woodchucks investigated. (A) Expression of IFN- $\alpha$ , IFN- $\gamma$ , TNF- $\alpha$ , IL-4, IL-2 and CD3 in lymphomononuclear cell samples collected from Group A animals after challenge and re-challenge with WHV. The solid arrow heads mark the time points of challenge or re-challenge with WHV/tm4. The peak expression of IFN- $\alpha$  (66-69 w.p.p.i.), and IFN- $\gamma$  and TNF- $\alpha$  (68-69 w.p.p.i.) was compared with that during enhanced WHV-specific response (70-74 w.p.p.i.) and *P* values were calculated as indicated in the legend to Figure 5.2 and differences marked as outlined in Materials and Methods. (B) Transcription levels of IFN- $\alpha$ , TNF- $\alpha$ , IFN- $\gamma$ , IL-12, IL-2, IL-10, IL-4, CD3, CD4 and CD56 in circulating lymphoid cells in different phase of acute WHV infection characterized by distinctive rWHe-specific and Con-A-induced T cell responses in Group B animals. The fold increase/decrease for each gene tested in a given phase of infection was calculated and statistically compared as outlined in Materials and Methods.

Figure 5.7A

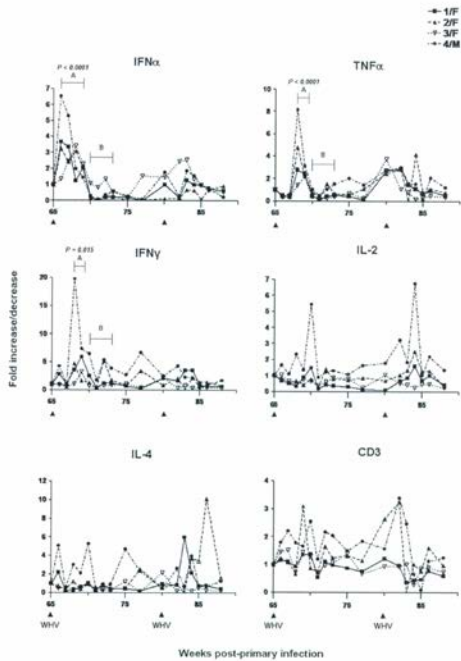
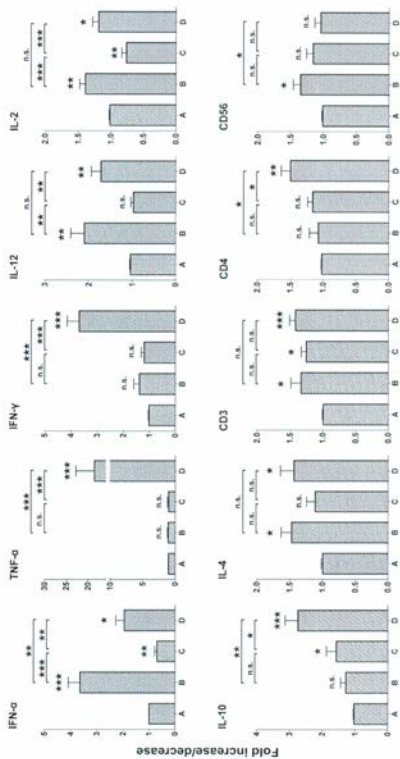


Figure 5.7B

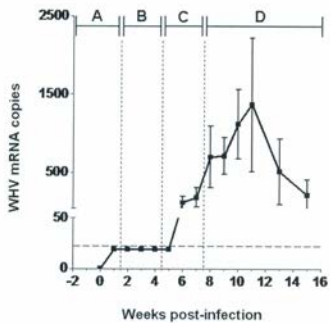


unmanipulated PBMC weekly collected from animals belonging to study Group B. As shown in Figure 5.7B, the significantly augmented expression of IFN- $\alpha$  ( $P = 0.0001$ ), IL-12 ( $P = 0.005$ ), IL-2 ( $P = 0.005$ ) and IL-4 ( $P = 0.01$ ) was evident almost immediately after primary exposure to WHV (phase B), as compared to the levels detected prior to infection (phase A). This coincided with the elevated expression of CD3 ( $P = 0.04$ ) and CD56 ( $P = 0.01$ ). This selective upregulation of pro-growth lymphoid cell cytokines, along with NK and T cell-specific markers, was associated with the significantly heightened lymphocyte proliferative responsiveness to stimulation with ConA but not to WHV (see Figures 5.5C and 5.5D). However, these elevated expressions of the cytokines and cell markers indicated above became drastically reduced during the early-acute period (phase C), which coincided with the augmented susceptibility of lymphoid cells to undergo activation-induced apoptosis (Figure 5.6B). It is important to note that WHV infection failed to induce the expression of either TNF- $\alpha$  or IFN- $\gamma$  in lymphoid cells during both pre-acute (phase B) and early-acute (phase C) periods (Figure 5.7B). Finally, during acute WHV infection (phase D), expression of IFN- $\alpha$ , TNF- $\alpha$ , IFN- $\gamma$ , IL-12, IL-2, IL-10 and IL-4 was synchronously upregulated along with significantly greater expression of CD3 ( $P < 0.0001$ ) and CD4 ( $P < 0.0001$ ), which coincided with the appearance of strong WHV-specific T cell response (Figure 5.5A).

### 5.3.7 WHV replication peaks in lymphoid cells after their increased

**Figure 5.8** WHV mRNA loads in serial, unmanipulated lymphoid cell samples collected during different phases of acute WHV infection from Group B animals. The total RNA isolated from weekly PBMC samples collected before (phase A) and after inoculation with WHV was reverse transcribed and virus-specific transcripts quantified by real time PCR. The data are represented as means  $\pm$  SEM for WHV RNA loads detected in all 4 woodchucks at each time point indicated. The horizontal line represents the detection limit of real-time RT-PCR (~20 copies/0.1  $\mu$ g of total RNA). When negative by real-time RT-PCR, samples were further analyzed by nested RT-PCR/NAH assay (sensitivity 2.5-5 copies/ $\mu$ g of total RNA).

Figure 5.8



### **susceptibility to activation-induced death subsides**

As shown in Figure 5.8 for animals from study Group B, the WHV mRNA was detectable in serial PBMC samples beginning from the first week p.i. at levels not exceeding 200 copies/ $\mu$ g of total RNA. From 5 w.p.i., *i.e.*, at the time of termination of the cells' increased susceptibility to activation-induced apoptosis, WHV mRNA levels progressively increased in circulating lymphoid cells, peaked around 11 w.p.i., and then subsided until the end of follow-up. Overall, the results revealed that WHV replication in peripheral lymphoid cells is established as early as one week post exposure to a large, liver pathogenic dose of WHV and persists at a low level until the serologically and histologically evident acute infection (phase D).

## **5.4 DISCUSSION**

In the present study, the lymphocyte capacity to proliferate in response to hepadnaviral antigens and mitogenic stimuli was measured during the pre-acute and acute phases of experimental WHV infection, and after challenge and re-challenge with the same virus. In addition, predisposition of lymphoid cells to undergo activation-induced apoptotic death and the expression of the cytokines affiliated with activation of immune cells were quantified in serial samples of circulating lymphoid cells. The study revealed several previously unidentified features of T cell response accompanying a self-limiting course of hepadnaviral AH and re-exposure of the immune host to pathogenic hepadnavirus. Thus, it

was found that: (1) A strong lymphocyte activation, evidenced by the heightened proliferative responsiveness against nonspecific stimuli, appears soon after both primary invasion and challenge and, in both situations, prior to the arise of virus-specific T cell response; (2) This temporal lymphocyte hyper-responsiveness to mitogenic stimuli coexists with the augmented expression of cytokines indicative of *in vivo* activation of immune cells and with the impaired transcription of TNF- $\alpha$  and IFN- $\gamma$ ; (3) The decline in the lymphocyte nonspecific proliferative responsiveness coincides with the cells increased susceptibility to activation-induced apoptosis; (4) The emergence of virus-specific secondary T cell response after re-exposure to virus is delayed similarly as following primary exposure, and (5) The virus-specific and nonspecific lymphocyte proliferative responses display inverse kinetics during pre-acute and acute phases of infection and after challenge with hepadnavirus.

In regard to characteristics of hepadnavirus-specific T cell response, our study confirmed that self-limited AH is associated with a strong T cell proliferation reactivity directed towards multiple structural and nonstructural hepadnaviral proteins. This finding is consistent with the data from self-limiting AH type B in humans and chimpanzees (Ferrari *et al.*, 1990; Akbar *et al.*, 1993; Bertoletti and Ferrari, 2003), and from woodchucks infected with WHV (Menne *et al.*, 1997). Another feature compatible with the previous observations was the late appearance of WHV-specific T cell response after primary exposure, *i.e.*, from 6 w.p.i. onwards. In this context, virus-specific T lymphocyte proliferative

reactivity became detectable from 8 to 12 w.p.i. in HBV-infected humans (4, 63) and 6-12 w.p.i. in WHV-infected woodchucks (Menne *et al.*, 2002). This characteristic of adaptive T cell response differs from that seen in other viral infections where such a response appears in the first two weeks after primary exposure (Webster *et al.*, 2000). Further, WHV-specific T cell reactivity remained detectable long after resolution of acute infection, albeit at much lower magnitudes than during AH (see Figure 5.2). This finding closely resembles the detection of HBV-specific proliferative and cytotoxic T cell responses in individuals with a history of resolved AH type B (Michalak *et al.*, 1994; Rehmann *et al.*, 1996), who, as woodchucks (Michalak *et al.*, 1999; Cote *et al.*, 2000; Hodgson and Michalak, 2000; Michalak, 2000; Menne *et al.*, 2007), carry low levels of replicating virus for years after apparent complete resolution of AH (Michalak *et al.*, 1994; Rehmann *et al.*, 1996; Weiland *et al.*, 2004). In this regard, it is expected that the trace hepadnavirus replication provides sustained antigenic stimuli maintaining active antiviral immune response keeping the persisting virus under relative control (Menne *et al.*, 2007). However, this control may fail leading to clinically evident reactivation of occult infection (Raimondo *et al.*, 2006; Mulrooney-Cousins and Michalak, 2007).

One of the most intriguing and novel findings in our study was the length of the time required for the WHV-specific T cell response to reappear after challenge with WHV. It has been well documented that immunocompetent hosts previously exposed to a pathogen swiftly mount strong secondary adaptive T cell response

appearing within a week following challenge with the same agent. Classical examples are infections with influenza A virus (Flynn *et al.*, 1998; Doherty and Christensen, 2000; Swain *et al.*, 2006; Rocha and Tanchot, 2006) or lymphocytic choriomeningitis virus (LCMV) (Gallimore *et al.*, 1998; Murali-Krishna *et al.*, 1998; Rocha and Tanchot, 2006). In our study, instead, the "memory" response in the convalescent woodchucks re-exposed to WHV was detected 5 weeks post-challenge. Further, although the magnitude of this secondary response to the majority of WHV antigens was greater than that in the primary infection, there was no difference in regard to the order in the relative strength of this response towards individual WHV antigens. Overall, the results revealed that both primary and secondary exposures to WHV induced delayed virus-specific T cell responses with overall similar kinetics. This finding to our knowledge is the first of this kind and seems to be a unique feature of hepadnaviral infection.

Examination of a lymphocyte response to mitogens is frequently used to assess the fitness and competence of lymphocytes to perform their immunological functions. This type of responsiveness was found to be transiently or permanently impaired in many microbial infections and its analysis frequently provided valuable insights into the capacity of the immune system to control the spread of a pathogen and the progression of infection (Garb *et al.*, 1981; Pedersen *et al.*, 1990; Wallace *et al.*, 1999; Niewiesk *et al.*, 2000). However, this response was only sporadically and fragmentally investigated over the course of HBV infection. In this regard, it has been noticed that during early phase of

serum HBsAg-positive or serum HBsAg-negative HBV infection, lymphocytes displayed increased proliferative capacity after stimulation with PHA, as compared to that observed during the late phase or in healthy controls (Sodomann *et al.*, 1979). The reported data also suggested that acute as well as chronic hepatitis B are associated with diminished lymphocyte proliferative responsiveness to stimulation with ConA (Feighery *et al.*, 1980), PHA (Sodomann *et al.*, 1979) or PWM (De Gast *et al.*, 1976). Our data showed that the proliferative capacity of lymphocytes in response to mitogenic stimuli varied depending on the phase of acute infection, providing a possible explanation for the previously observed variances. The most interesting finding was that this capacity was significantly augmented almost immediately after WHV infection and subsided prior to the appearance of adaptive T cell response (see Figure 5.4). Surprisingly, a similar sequence of events occurred after challenge of the WHV-immune animals with the same dose of the same virus which was done more than a year following the first inoculation.

Our finding of the heightened lymphocyte nonspecific proliferation preceding virus-specific T cell response is not unique and appears to be consistent with findings in some other viral infections. For example, an acute infection with simian/human immunodeficiency virus (SHIV) in macaques is associated with very early, strong polyclonal activation of lymphocytes followed by virus-specific T cell response (Wallace *et al.*, 1999). In this model, the delay in SHIV-specific T cell reactivity was attributed to inappropriately high generalized

activation of lymphocytes leading to the depletion of CD4+ T cells, probably, by activation-induced cell death and direct cell killing by the virus, and diminished virus-specific T cell immunity which, consequently, allowed the virus to spread in the early phase of infection. In this context, it is of note that WHV also is a lymphotropic virus which invariably infects the immune system, even when the liver is not affected, as observed in woodchucks inoculated with WHV doses equal to or below  $10^3$  virions or in offspring born to woodchuck dams convalescent from AH (Coffin *et al.*, 2004; Michalak *et al.*, 2004). Also, WHV invasion of the lymphatic system occurs soon after inoculation, as evidenced by detection of WHV DNA and its replicative intermediate, covalently closed circular DNA, in lymphoid cells as early as 3 days post-inoculation with either liver pathogenic or low, liver non-pathogenic dose of WHV (Guy, C.S. and Michalak T.I., unpublished data).

To gain further insights into the nature of the immune responses accompanying the early phase of hepadnaviral infection, the transcription levels of the cytokines affiliated with activation of immune cells and those of the markers specifying individual immune cell subtypes were quantified in serial samples of circulating lymphoid cells. The cytokine expression patterns revealed were analyzed in the context of the profiles of T cell nonspecific and WHV-specific responses and to the cells susceptibility to activation-induced apoptotic death. In this regard, it is of note that viral infections normally induce immediate type I interferon response, i.e., IFN- $\alpha$  and beta interferon (IFN- $\beta$ ), which precedes

production of other cytokines, such as TNF- $\alpha$ , IL-1, IL-12 and IL-2 by antigen presenting cells (APC) and natural killer (NK) cells (Kawai and Akira, 2006). Together, these cytokines facilitate induction of the effective innate response and the prompt development of adaptive immunity. It has also been shown that during initial phase of infection activated NK cells can eliminate invading virus both by killing infected cells and via a noncytotoxic pathway mediated by IFN- $\gamma$  (Guidotti and Chisari, 2001; Andoniu *et al.*, 2005; Kawai and Akira, 2006). At the same time, around one w.p.i., activated APC acquire ability to promote the virus-specific T cell immune response which inhibits infection onwards (Andoniu *et al.*, 2005). In regard to hepadnaviral infection, investigation of chimpanzees infected with a massive dose of HBV ( $\sim 10^8$  virions) failed to reveal upregulated expression of the genes affiliated with activation of innate immune response for up to 6-10 w.p.i. when measured by microarray analysis in the liver (Weiland *et al.*, 2004). Similarly, intrahepatic expression of IFN- $\gamma$  and TNF- $\alpha$ , along with CD3-positive lymphomononuclear cell infiltration, was found to be delayed until the acute phase of WHV infection, as determined by gene-specific RT-PCR analysis (Hodgson and Michalak, 2001; Nakamura *et al.*, 2001). However, these measurements were initiated not earlier than one w.p.i. and were done, in some instances, by the methods of relatively low sensitivity, raising a concern that the early response or that of a lower magnitude was overlooked. In fact, the recently completed analysis of the expression profiles of the genes affiliated with active innate immune response in serial liver biopsies collected from one hour post

WHV infection and applying highly sensitive real-time RT-PCR assays revealed upregulated transcription of IFN- $\gamma$  and IL-12 and activation of APC and NK cells as early as 3-6 hours and activation of NK T cells at 48-72 hours post-infection with WHV (Guy and Michalak, manuscript in preparation). Therefore, hepadnavirus induces intrahepatic innate response but this response arises almost immediately after infection, is transient, and is not succeeded by the prompt appearance of the local adaptive T cell immunity.

Peripheral lymphoid cells collected weekly from WHV-infected animals in our study demonstrated a transient but significantly augmented expression of IFN- $\alpha$ , along with IL-12, IL-2 and IL-4 and with CD3 and CD56, between one and 3 w.p.i. (see Figure 5.6B). Unexpectedly, the same cells did not display enhanced expression of TNF- $\alpha$  and IFN- $\gamma$  for up to 6 w.p.i., *i.e.*, when AH had fully developed. The identified prolonged absence of TNF- $\alpha$  transcription in immune cells in the early WHV infection may have important consequences due to multiple immunological functions to this cytokine. Among others, TNF- $\alpha$ , together with IFN- $\alpha$ , drives the differentiation of dendritic cells (DC) from precursors (Sousa *et al.*, 1999; Iwamoto *et al.*, 2007), while DC in the presence of IFN- $\alpha$  alone acquire improper mature phenotype characterized by impaired antigen-specific and allo-stimulatory capacities (Dauer *et al.*, 2003; McRae *et al.*, 2000). Furthermore, neutralization of TNF- $\alpha$  by specific antibody administered to LCMV-infected mice abolished the virus-induced activation of DC (Kadowaki *et al.*, 2000), while DC cultured in the presence of both TNF- $\alpha$  and IFN- $\alpha$  acquired

phenotype comparable to that induced *in vitro* by infection with herpes simplex virus (Kadowaki *et al.*, 2000). Taken together, the prompt expression of TNF- $\alpha$  transpires in the appropriate maturation of DC, the effective activation of APC, and the expeditious arise of effective adaptive T cell immunity (Sousa *et al.*, 1999). Nonetheless, along with activation of DC and NK cells, the initiation of effective antiviral T cell immunity also requires synchronous expression of other cytokines, such as IFN- $\alpha$ , IL-12, IL-2, IL-4 and IL-10 (Orange and Biron, 1996; Andoniou *et al.*, 2005). Thus, the absence of TNF- $\alpha$  and nonsynchronous expression of some other cytokines (*e.g.*, IL-10; see Figure 5.6B) during the early phase of WHV infection could translate into inappropriate differentiation and activation of DC, which in turn may fail to promote appropriate presentation of WHV antigens and postpone priming of the anti-viral adaptive T cell response.

On the other hand, early IFN- $\alpha$  response, along with DC-derived cytokines induced by viral infection, initiates proliferation and IFN- $\gamma$  production in NK cells (Biron and Welsh, 1982; Kobayashi *et al.*, 1989). In turn, this cytokine enhances NK cell cytotoxic function, as well as shapes the development of antigen-specific Th1 immune response (Orange and Biron, 1996; Asselin-Paturel *et al.*, 2001; Andoniou *et al.*, 2005; Kawai and Akira, 2006; ). Therefore, the absence of IFN- $\gamma$  transcription in circulating lymphoid cells for up to 6 w.p.i. after administration of WHV further supports the notion of aberrant activation of the innate response in the initial phase of hepadnaviral infection. This defect may further hamper early elimination of hepadnavirus as well as contribute to postponement of virus-

specific T cell response.

We found that lymphoid cells displayed significantly higher susceptibility to undergo activation-induced apoptosis at the time of decreased proliferative responsiveness to mitogenic as well as WHV-specific stimuli. To determine a possible reason behind this rapid decline in lymphoid cell proliferative responsiveness in the early-acute WHV infection, we measured the rates of apoptosis in freshly isolated weekly PBMC samples and in the same samples after *ex vivo* stimulation with ConA or rWHe. The results showed that the rates of apoptosis in unmanipulated lymphoid cells were essentially the same during different phases of the development of acute WHV infection. A comparable observation was reported for unmanipulated, circulating lymphocytes during infection with human immunodeficiency virus (HIV) (Gougeon *et al.*, 1996). In contrast, the same woodchuck cells exposed to Con A or rWHe displayed meaningfully different susceptibility to undergo apoptosis depending upon the phase of acute WHV infection defined by the kinetics of nonspecific and WHV-specific T cell responses (see Figures 5.5 and 5.6B). Taken together, the analysis showed that the decline in the cells proliferative responsiveness to mitogenic stimuli in the early WHV infection coincided with the cells significantly greater susceptibility to activation-induced apoptotic death. Thus, this co-occurrence resembled the mechanism proposed for the depletion of nonspecifically activated lymphocytes in acute SHIV infection (Wallace *et al.*, 1999).

The increased susceptibility to activation-induced cell death in our study was accompanied by reduced IFN- $\alpha$ , IL-2 and IL-12 transcription, and by upregulated expression of IL-10 in circulating lymphoid cells. In this regard, seemingly comparable activation-induced death of lymphoid cells was reported during experimental infection with SHIV (Wallace *et al.*, 1999) and in HIV infection (Gougeon *et al.*, 1996), and was attributed to abnormal expression of cytokines or to defective antigen presentation by APC (Gougeon *et al.*, 1996). It was also observed that CD4+ and CD8+ T cells derived from HIV infection and treated *ex vivo* with PWM or anti-CD3 antibodies in the presence of IL-12 demonstrated the enhanced survival, while those treated in the same way in the presence of IL-10 displayed an increased susceptibility to undergo apoptosis (Gougeon *et al.*, 1996). Further, during acute phase of infection with Epstein-Barr virus, an increased susceptibility of activated CD45RO+ T cells to undergo apoptosis in culture was shown to be reversed by addition of exogenous IL-2 (Akbar *et al.*, 1993). These findings resemble those encountered in the early WHV infection (phase C) where decreased expression of cytokines, especially IL-12 and IL-2, could initiate defective T cell activation with higher susceptibility of the lymphocytes to undergo activation-induced death (see Figures 5.6B and 5.7B). This may represent a mechanism by which improperly activated lymphocytes are eliminated *in vivo*. On the other hand, a contribution of WHV to the cell enhanced susceptibility to apoptotic death was unlikely, since the peak of virus replication occurred in lymphoid cells when acute infection became fully

developed (phase D; see Figure 5.8).

Based on the data acquired in the current study, we postulate that the early aberrant lymphocyte activation followed by apoptotic death of the cells activated, coinciding with a defective expression of the cytokines critical for the prompt initiation of virus-specific T cell response, are responsible for the postponement of adoptive T cell responses in hepadnaviral infection. Identification of a mechanism by which hepadnavirus induces the immediate, defective lymphocyte activation will require further investigation. Similarly, a contribution of the delayed virus-specific T cell response to the intrinsic ability of hepadnavirus to escape from sterilizing elimination by the immune system, leading to establishment of either symptomatic or occult persistent infection, needs to be explained. Overall, the present study throws a new light on the features of immune cell responsiveness accompanying hepadnaviral infection. Because of the high compatibility between virological and pathogenic properties of WHV and HBV and strong parallels in the induced antiviral responses, the current data should contribute to our better understanding of immunological events underlying a prolonged incubation period and the delayed initiation of acute hepatitis in HBV infection, and possibly to design of methods of halting the development of chronic hepatitis.

**CHAPTER 6: PRIMARY OCCULT HEPADNAVIRUS INFECTION INDUCES  
VIRUS-SPECIFIC T CELL PROLIFERATIVE AND ABERRANT CYTOKINE  
RESPONSES IN THE WOODCHUCK MODEL OF HEPATITIS B**

*This study has been submitted in Journal of Virology*

**6.0 SUMMARY**

Although the virological features of asymptomatic, serologically silent hepadnaviral POI have been relatively well recognized in the woodchuck model of hepatitis B, characteristics of accompanying immune responses remain unknown. In this study, the kinetics of both WHV-specific and nonspecific (mitogen-induced) T cell responses and cytokine expression profiles in circulating lymphoid cells and the liver, along with WHV-specific antibody responses and molecular markers of WHV infection, were investigated during experimentally induced POI and subsequent challenge with a liver pathogenic ( $>10^3$  virions) or nonpathogenic (50 virions) dose of the same virus. The data showed that POI, which does not prompt WHV surface antigenemia, antibodies against virus or hepatitis, was accompanied by a strong WHV-specific T cell response directed against multiple virus epitopes that appeared in 8-12 weeks post-infection and intermittently persisted to the end of follow-up. Furthermore, immediately after exposure to a nonpathogenic virus dose, lymphocytes acquired a heightened capacity to proliferate in response to mitogenic stimuli and displayed augmented expression of IFN- $\alpha$ , IL-12 and IL-2, but not tumor necrosis factor alpha. Overall,

the kinetics of WHV-specific and mitogen-induced T cell and cytokine responses accompanying POI or after challenge of animals with POI were closely comparable to those occurring during symptomatic infection caused by a liver pathogenic viral dose. The data revealed that serologically silent POI induced by liver nonpathogenic quantities of hepadnavirus causes early aberrant cytokine expression and delayed virus-specific T cell proliferative response, which closely resemble those accompanying serologically evident infection coinciding with self-limited acute hepatitis.

## 6.1 INTRODUCTION

HBV is a noncytopathic virus causing an infection having several distinctive clinical profiles ranging from symptomatic AH or CH to serologically undetectable, seemingly asymptomatic infection, designated as occult HBV infection (OBI). Following exposure to HBV, more than 90% of adults developing AH resolve liver inflammation (Ferrari *et al.*, 1991; Bertoletti and Gehring, 2006), however they fail to eradicate the virus completely and persistent occult infection follows (Michalak *et al.*, 1994; Mulrooney *et al.*, 2007; Raimondo *et al.*, 2006; Rehmann *et al.*, 1996; Yuki *et al.*, 2003). The remaining ~10% of individuals develop CH type B, which is diagnosed when detection of HBsAg in serum and biochemical and histological indicators of liver inflammation persist for more than 6 months. This form of hepatitis often advances to life-threatening cirrhosis and hepatocellular carcinoma (HCC) (Chisari, 2000; Bertoletti and Ferrari, 2003).

In the last decade, it became apparent that HBV replication commonly persists at low levels after resolution of AH type B in the context of apparent absence of clinical symptoms. It is expected that this form of HBV infection could also be a consequence of resolution of a clinically asymptomatic, but serologically transiently evident (i.e., serum HBsAg-reactive) exposure to virus. The main features of this residual asymptomatic infection, also called secondary occult infection or SOI (Michalak *et al.*, 2004; Mulrooney and Michalak, 2007; Michalak, 2000, Michalak *et al.*, 2007; Raimondo *et al.*, 2006), are: (1) the lack of detectable serum HBsAg, (2) the presence of antibodies to HBV core antigen (anti-HBc), (3) detection of HBV DNA in the circulation at levels usually not exceeding 200 virus genome equivalents (vge) per mL, and (4) the presence of viral genome and its replicative intermediates in the liver and peripheral blood mononuclear cells (PBMC) (Michalak *et al.*, 1994; Murakami *et al.*, 2004; Rehmann *et al.*, 1996). This OBI can be a source of infectious virus available for transmission to healthy individuals through blood and organ donations, as well as a potential cause of diseases of seemingly unknown etiology, including HCC (reviewed in Mulrooney and Michalak, 2007; Brechot, 2004; Ikeda *et al.*, 2007).

The infection of eastern North American woodchucks (*Marmota monax*) with woodchuck hepatitis virus (WHV), a member of the *hepadnaviridae* family (Menne *et al.*, 2007; Michalak, 2007; Michalak, 1998), provides a natural and highly valuable laboratory model of HBV infection. The molecular, virological,

and pathological events which follow WHV invasion are highly compatible to those induced by HBV in humans. Moreover, the understanding of the natural course, virological properties, requirements of transmission and potential pathological consequences of OBI is owed to a large extent to studies in the woodchuck model (reviewed in Michalak *et al.*, 2007). Among others, it was established that replication of hepadnavirus in SOI progresses not only in the liver but also in the immune system (Michalak *et al.*, 1994; Rehemann *et al.*, 1996). In woodchucks, this infection persists for life and virus replicative intermediates, including WHV covalently closed circular DNA (cccDNA) and mRNA, are detectable by highly sensitive assays employing polymerase chain reaction (PCR) and identification of the resulting amplicons by nucleic acid hybridization (NAH), i.e., PCR/NAH (Coffin and Michalak, 1999; Michalak *et al.*, 1999). Moreover, the virus assembled during SOI is infectious, liver pathogenic, can induce HCC, and is transmissible from SOI mothers to offspring (Michalak *et al.*, 1999; Coffin and Michalak, 1999; Hodgson and Michalak, 2001; Michalak *et al.*, 2004). Interestingly, SOI can be reactivated following treatment with an immunosuppressive agent, cyclosporin A, leading to re-appearance of serum WHsAg-positive infection (Menne *et al.*, 2007) and ~20% of woodchucks with SOI finally develop HCC (Michalak *et al.*, 1999, Korba *et al.*, 1989).

Investigating the woodchuck model of hepatitis B, we have recently uncovered yet another form of occult hepadnaviral infection, i.e. primary occult infection (POI) (Michalak *et al.*, 2004; Michalak *et al.*, 2007; Mulrooney and

Michalak, 2007). This form has not yet been identified in humans, however the existence of HBV DNA positive, anti-HBc negative individuals implies its existence (Michalak, 2000; Brechot, 2001; Torbensen and Thomas, 2002; Michalak *et al.*, 2007). Originally, POI was discovered by studying woodchuck dams with SOI which were found to transmit to their offspring a low level WHV infection limited to the lymphatic system that did not engage the liver in the majority of the offspring (Coffin and Michalak, 1999). Subsequently, the same form of occult persistence was experimentally induced by inoculation of immunocompetent, adult woodchucks with WHV doses lower than 1000 virions (Michalak *et al.*, 2004). In this experimental situation, POI again coincided with WHV replication restricted to the lymphatic system which with time in some animals could spread to the liver. In general, POI is characterized by the presence of WHV DNA in serum at levels compatible with those occurring in SOI ( $\leq 200$  vge/mL) and in PBMC ( $\leq 10^3$  vge/ $\mu$ g of total DNA), but not in the liver, the absence of serological (immunovirological) markers of infection, including antibodies against WHV core antigen (anti-WHc), and by normal liver morphology (reviewed in Mulrooney and Michalak, 2007; Michalak *et al.*, 2007). The WHV nucleotide sequence in POI has been found to be wild-type (Michalak *et al.*, 2004; Mulrooney and Michalak, 2008). Further, the virus persisting in POI remains biologically competent, since when WHV from serum or lymphoid cells of animals with POI was administered to naive woodchucks, symptomatic AH was induced (Michalak *et al.*, 2004, Coffin and Michalak, 1999). Most

interestingly, woodchucks with POI are not protected from re-infection with liver pathogenic doses of WHV (i.e.,  $>10^3$  virions) (Michalak *et al.*, 2004) and develop classical AH after the challenge (Coffin and Michalak, 1999; Michalak *et al.*, 1999). Although we have previously documented that POI does not induce WHV-specific humoral immune response (reviewed in Michalak *et al.*, 2007), it is not clear whether the virus-specific T cell responses are also lacking in this form of WHV infection.

In regard to T cell responses accompanying symptomatic HBV infection, the resolution of AH was found to be associated with strong, polyclonal HBV-specific Th1 proliferative and CTL reactivities, while the reverse was demonstrated in chronic hepatitis (Ferrari *et al.*, 1990; Guidotti and Chisari, 2006; Bertoletti and Ferrari, 2003; Chisari, 2000). Hepatic injury in HBV infection is an immune mediated process. It was established that the CTL response generated against HBV epitopes can inhibit replication of intrahepatic virus, both by directly killing infected cells (Maini *et al.*, 1999; Guidotti *et al.*, 1999; Rehermann *et al.*, 1996; Thimme *et al.*, 2003) and by producing anti-viral cytokines, such as gamma interferon (IFN- $\gamma$ ) and tumor necrosis factor alpha (TNF- $\alpha$ ) (Guidotti and Chisari, 2001; Guidotti and Chisari, 2006). In chimpanzees infected with HBV, injection of anti-CD8 antibodies during AH resulted in prolonged viremia and milder hepatic injury, suggesting the dual role of CD8+ T cells in inhibiting HBV replication and mediating liver pathology (Thimme *et al.*, 2003). Further, Th1 cytokine profile, coinciding with a greater expression of IFN- $\gamma$  and TNF- $\alpha$  in HBV-

specific CD4<sup>+</sup> and CD8<sup>+</sup> T cells, was found to be associated with resolution of hepatitis (Ferrari *et al.*, 1990; Guidotti and Chisari, 2001; Bertoletti and Gehring, 2006). On the other hand, the role of the innate immune responses in the pathogenesis and determining the outcome of hepadnaviral hepatitis remains uncertain. It has been shown that activated natural killer (NK) cells (Kimura *et al.*, 2002), NKT cells (Kakimi *et al.*, 2000) and antigen presenting cells (APC) (Kimura *et al.*, 2002), as well as cytokines, such as alpha interferon (IFN- $\alpha$ ) (Weiland *et al.*, 2000), interleukin-12 (IL-12) (Cavanaugh *et al.*, 1997) and IL-18 (Kimura *et al.*, 2002), can independently inhibit virus replication in HBV transgenic mice, implying the role of innate immunity in controlling HBV infection in this model. Moreover, upregulated hepatic expression of IFN- $\gamma$  and TNF- $\alpha$  was found to precede HBV-specific T cell responses and was accompanied by a decrease in HBV replication in the liver in chimpanzees, suggesting that activation of the local innate immunity is, at least partially, successful in limiting virus propagation in acute infection (Thimme *et al.*, 2003; Chisari, 2000). Also, in our recent study, analyzing the expression profiles of the genes affiliated with intrahepatic immune responses in woodchucks immediately after inoculation with a liver pathogenic dose of WHV, clear evidence of very early augmented transcription of the genes indicative of activation of APC, NK cells and NK T cells were found (Guy *et al.*, 2008). However, this early innate response was transient and unable to timely prompt a virus-specific T cell response, unlike other infections induced by many viral pathogens. In patients who resolved AH,

vigorous HBV-specific T cell proliferative and cytotoxic responses were identified for many years after recovery, suggesting the pivotal role of the immune system in controlling virus replication during OBI (Rehermann *et al.*, 1996; reviewed in Bertoletti and Gehring, 2006).

In the present study, the kinetics of WHV-specific and mitogen-induced (generalized) T cell proliferative responses, humoral responses and the profiles of cytokine gene expression in lymphoid cells and in the liver, along with immunovirological (serological) and molecular markers of WHV infection, were analyzed in the animals with experimentally induced POI and after re-exposure of the animals to low (liver nonpathogenic) or high (liver pathogenic) doses of the same virus. Our study shows that POI, despite the absence of serological, biochemical and histological indicators of infection, is accompanied by strong T cell proliferative responses directed towards multiple virus epitopes with kinetics compatible with those observed after infection leading to classical AH. The appearance of WHV-specific T cell responses was preceded by a heightened capacity of lymphocytes to proliferate in response to mitogenic stimuli, as we have recently observed in an symptomatic acute infection (Gujar *et al.*, 2008). Additionally, there was an aberrant expression of cytokines involved in the activation of APC and NK cells. Woodchucks with POI challenged with liver either nonpathogenic or pathogenic dose of WHV demonstrated similar profiles of virus-specific and mitogen-induced T cell proliferative responses as those found after primary infection. However, these strong secondary T cell responses

were unable to provide sufficient help to prevent hepatitis.

## **6.2 MATERIALS AND METHODS**

### **6.2.1 Animals**

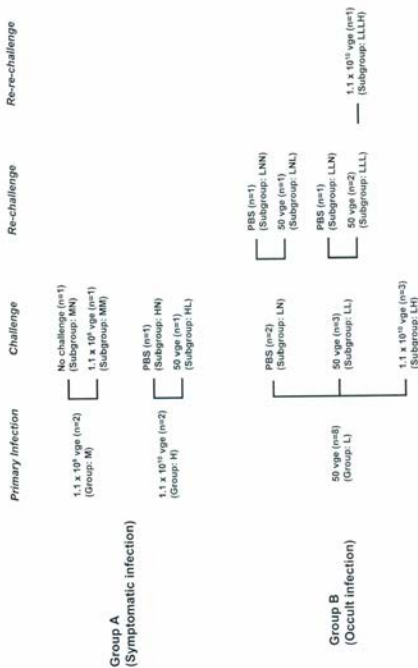
Twelve healthy, adult woodchucks (*Marmota monax*) investigated in this study were housed in the Woodchuck Hepatitis Research Facility at Memorial University, St. John's, Newfoundland, Canada. Their WHV-naive status was confirmed by the absence of WHV DNA in randomly selected liver, peripheral blood mononuclear cells (PBMC) and serum samples analyzed by specific nested PCR-NAH (sensitivity  $\leq 10$  virus genome equivalents (vge)/mL) and by repeated serum negativity for WHsAg and anti-WHc. Experimental protocols were approved by the Institutional President's Committee on Animal Bioethics and Care.

### **6.2.2 Inoculation, challenge and re-challenge with WHV**

Eight woodchucks (Study Group B) were intravenously (i.v.) injected with 50 DNase-protected vge of WHV/tm3 inoculum (Genbank number AY334075) (Michalak *et al.*, 2004) (Figure 6.1). It was previously established that WHV doses below 1000 virions of WHV/tm3 inoculum, as well as other WHV inocula, consistently induce POI in WHV-naive woodchucks (Michalak *et al.*, 2004-

**Figure 6.1** Schematic representation of the experimental protocol used to infect and challenge woodchucks with liver pathogenic (Group A) and liver nonpathogenic (Group B) doses of WHV. In total, 12 WHV-naive, healthy animals were i.v. injected with low (nonpathogenic; 50 vge), medium (liver pathogenic;  $1.1 \times 10^6$  vge) or high (liver pathogenic;  $1.1 \times 10^{10}$  vge) dose of WHV/tm3 inoculum to induce POI or symptomatic infection. (A) Animals in study Group A (n=4) were injected with either high ( $1.1 \times 10^{10}$  vge; n=2) or medium ( $1.1 \times 10^6$  vge; n=2) doses of WHV. Animals developed classical, serologically detectable WHV infection and were challenged with low (50 vge; n=1) or medium ( $1.1 \times 10^6$  vge; n=1) dose of WHV/tm3 or injected with PBS. (B) Animals in experimental Group B (n=8) were initially injected with low (50 vge) dose of WHV. All animals developed serum WHsAg and anti-WHc negative but WHV DNA reactive POI and were challenged or re-challenged with low (50 vge; n=5) or high ( $1.1 \times 10^{10}$  vge; n=4) dose of the same inoculum or injected with PBS. The animals from Groups A and B were divided in to subgroups according to the dose of WHV used to challenge or re-challenge or injection with PBS, as described in detail in Material and Methods. Letter symbols designation: L, low virus dose; M, medium virus dose; H, high virus dose, and N, no virus (injection with PBS).

Figure 6.1



WHV/tm3; Mulrooney and Michalak, 2008- WHV/tm3). After 26 weeks post-primary infection (w.p.p.i.), the animals were challenged with a high dose of WHV/tm3 ( $1.1 \times 10^{10}$  vge; group low-high or LH; n=3), low dose (50 vge; group low-low or LL; n=3) or injected with 0.5 mL of sterile phosphate-buffered saline, pH 7.4 (PBS) as controls (group low-no virus or LN; n=2) (see Figure 6.1). Subsequently, the animals from groups LL and LN were re-challenged at 55 w.p.p.i. with either low WHV dose (50 vge; subgroup low-low-low or LLL; n=2, and subgroup low-no virus-low or LNL; n=1) or injected with PBS (subgroup low-low-no virus or LLN; n=1 or subgroup low-no virus-no virus or LNN; n=1). One animal (9/M) from subgroup LLL was finally challenged at 77 w.p.p.i. with high dose of WHV ( $1.1 \times 10^{10}$  vge; subgroup LLLH) (Figure 6.1).

As controls (Study Group A) , two healthy woodchucks were infected with high dose of WHV/tm3 ( $1.1 \times 10^{10}$  vge) and then injected with PBS (subgroup high-no virus or HN; n=1) (Figure 6.1) at 30 w.p.p.i. or challenged with low dose of WHV/tm3 (50 vge; subgroup high-low or HL; n=1) at 26 w.p.p.i. In addition, two other woodchucks were infected with medium dose of WHV/tm3 ( $1.1 \times 10^6$  vge) and challenged with medium dose of WHV/tm3 ( $1.1 \times 10^6$  vge; subgroup medium-medium or MM; n=1) at 30 w.p.p.i. or left unchallenged (subgroup medium-no virus or MN; n=1).

### 6.2.3 Sample collection and PBMC isolation

Blood samples were collected on sodium-EDTA or without addition of

anticoagulant, weekly up to 10 weeks after each injection with virus, then biweekly up to 20 weeks, and then approximately monthly until challenge or autopsy. Sera were separated from untreated blood and stored at -20 °C. PBMC were isolated from EDTA-treated samples on Ficoll-Paque Plus (Amersham Pharmacia Biotech, AB, Uppsala, Sweden), as described previously (Gujar and Michalak, 2005). The cell viability was measured by the trypan blue dye exclusion method and normally exceeded 98%.

#### **6.2.4 Serological and molecular markers of WHV infection**

Serial serum samples were examined for the presence of WHsAg, anti-WHc and antibodies against WHsAg (anti-WHs) using specific enzyme-linked immunosorbent assays, as reported before (Michalak, *et al.*, 1999; Michalak *et al.*, 2004; Coffin *et al.*, 2004). WHV DNA in serum and liver samples was detected by nested PCR-NAH assays with WHV core (C), surface (S) and X gene-specific primers (sensitivity <10 vge/mL or <10 vge/ $\mu$ g of total DNA) (Michalak, *et al.*, 1999; Michalak *et al.*, 2004; Coffin *et al.*, 2004). As a biochemical measure of liver injury, serum levels of sorbitol dehydrogenase (SDH) were evaluated by an appropriate spectrophotometric assay (Asada and Galambos, 1963, Weisner *et al.*, 1965).

#### **6.2.5 Liver biopsies and histopathology**

Up to seven liver tissue samples were collected from each animal by

surgical laparotomy or at autopsy at time points indicated in Figure 6.2. The samples were routinely processed to paraffin and stained (Michalak *et al.*, 2004). Hepatic lesions were graded on the numerical scale of 0 to 3 and reported as the degree of hepatitis, as described before (Michalak *et al.*, 1990; Michalak *et al.*, 1999; Hodgson and Michalak, 2001).

#### 6.2.6 WHV antigens and T cell mitogens

Recombinant WHV core protein (rWHc), e protein (rWHe) and X protein (rWHx), used to measure WHV-specific T cell proliferative responses, were produced in pET41b(+) *Escherichia coli* expression system (Novagen, Darmstadt, Germany) and purified using histidine-tag affinity chromatography (Qiagen, Mississauga, Canada), as described before (Wang and Michalak, 2007; Gujar *et al.*, 2008). These antigens were extensively tested for nonspecific T cell proliferation against potential bacterial contaminations by using PBMC from WHV-naive animals, including woodchucks prior to injection with WHV investigated in this study, and were found entirely free of such impurities (Wang and Michalak, *et al.*, 2007; Gujar *et al.* 2008). In addition, WHsAg was purified from pooled sera of a woodchuck with chronic WHV infection, as reported (Michalak *et al.*, 2004; Gujar *et al.*, 2008). Also, a synthetic peptide carrying the WHV T cell immuno-dominant epitope located between 97-110 amino acids of WHc protein (WHC<sub>97-110</sub>) (Menne *et al.*, 1997) was synthesized (Synprep Corporation; Dublin, CA). The recombinant WHV antigens and WHsAg were

used at 1 and 2  $\mu\text{g}/\text{mL}$  in the T cell proliferative assays, while WHC<sub>97-110</sub> peptide was used at 5 and 10  $\mu\text{g}/\text{mL}$ .

The generalized (nonspecific) proliferative capacity of the woodchuck lymphocytes was measured by assessing PBMC proliferation in response to stimulation with mitogens, as reported (Gujar *et al.*, 2008). For this purpose, concanavalin-A (ConA; Pharmacia Fine Chemicals, Uppsala, Sweden), pokeweed mitogen (PWM, *Phytolacca americana* agglutinin; ICN Biochemicals Inc., Aurora, Ohio) and phytohemagglutinin (PHA; ICN Biochemicals Inc.) were used in T cell proliferation assays at five serial two-fold concentrations ranging from 1.2 to 20  $\mu\text{g}/\text{mL}$  for ConA and PHA, and from 0.6 to 10  $\mu\text{g}/\text{mL}$  for PWM.

#### 6.2.7 CFSE-based flow cytometry T cell proliferation assay

WHV-specific T cell proliferative response in woodchuck PBMC after stimulation with different WHV antigens or WHC<sub>97-110</sub> peptide was assessed by applying a CFSE-based flow cytometric proliferation assay, as described elsewhere (Gujar and Michalak, 2005). Briefly, freshly isolated PBMC were labeled with 5-and-6-carboxyfluorescein diacetate succinimidyl ester (CFSE; Molecular Probes, Eugene, Oregon) at a final concentration of 1  $\mu\text{M}$  and cultured at a density of  $3 \times 10^5$  cells/well in 48-well tissue culture plates in triplicate with tested concentrations of WHV antigens or WHC<sub>97-110</sub>, as indicated above, or with medium alone as a control. The cells were incubated for 5 days at 37 °C, harvested, and washed in PBS with 1 mM EDTA (PBS-EDTA). The data were

acquired by using a FACSCalibur flow cytometer (Becton Dickinson, Franklin Lakes, NJ). The halving of CFSE fluorescence was deconvoluted using CellQuest Pro software (Becton Dickinson) (Gujar and Michalak, 2005). Cell division index (C.D.I.) was defined by dividing the percentage of cells with halved CFSE fluorescence after stimulation with a test WHV antigen by percentage of cells with halved CFSE-fluorescence cultured in medium only. The C.D.I. values of  $\geq 3.1$  for rWHc, rWHe and rWHx and  $\geq 2.1$  for WHsAg and WHC<sub>97-110</sub> peptide were considered as a measure of WHV-specific T cell proliferative response (Gujar and Michalak, 2005). However, for clarity of the presentation, only the cut off value of  $\geq 3.1$  was marked in the graphs showing WHV-specific T cell response.

### **6.2.8 Adenine incorporation T lymphocyte proliferation assay**

The generalized proliferative capacity of woodchuck lymphocytes in response to virus nonspecific stimulation was evaluated using mitogens and <sup>3</sup>[H]-adenine incorporation assay, as described (Kreuzfelder *et al.*, 1996; Gujar and Michalak, 2005, Gujar *et al.*, 2008). Briefly, freshly isolated woodchuck PBMC were cultured at a density of  $1 \times 10^5$  cells/well of a 96-well tissue culture plate in the presence of different concentrations of mitogens, as indicated above, or medium alone in triplicates. After 5 days in culture, cells were pulsed with 0.1  $\mu$ Ci of <sup>3</sup>[H]-adenine (Amersham Pharmacia Biotech, Uppsala, Sweden) for 12-18 hours, harvested and counts per minute (cpm) in each test and control wells

were measured. The mean cpm values were calculated by averaging the cpm values from the respective triplicate wells. The stimulation index (S.I.) was calculated by dividing mean cpm obtained after a mitogenic stimulation by mean cpm observed without any stimulation (medium only) (Gujar *et al.*, 2008).

### 6.2.9 Real time RT-PCR analysis of gene expression

Sequential liver and PBMC samples collected prior to inoculation with WHV and after challenge with virus were evaluated for the expression of selected cytokine and immune cell marker genes by real time RT-PCR using a LightCycler (Roche Diagnostics, Mannheim, Germany) (Gujar *et al.*, 2008; Guy *et al.*, 2008). In the case of PBMC,  $5 \times 10^5$  to  $1 \times 10^6$  of freshly isolated cells were suspended in 1 mL of Trizol reagent (Invitrogen) and stored at  $-20^\circ\text{C}$ . Liver samples collected at biopsy or autopsy were stored at  $-80^\circ\text{C}$  until RNA isolation with Trizol reagent. After collection of all experimental samples, RNA was extracted simultaneously and reversely transcribed to cDNA, as reported (Gujar *et al.*, 2008; Guy *et al.*, 2008). The expression of woodchuck IFN- $\alpha$ , IFN- $\gamma$ , TNF- $\alpha$ , IL-12, IL-2, IL-4, and IL-10 was quantified using equivalent of 50 ng of total RNA and woodchuck gene-specific primer pairs, and was normalized against expression of woodchuck  $\beta$ -actin as reported in recent works from this laboratory (Gujar *et al.*, 2008; Guy *et al.*, 2008). The expression levels detected after WHV exposure were compared with those determined for the same animal prior to infection to define the fold increase or decrease, as previously described (Gujar

et al., 2008).

### 6.2.10 Statistical analysis

The two-tailed, unpaired Student *t* test, with 95% confidence interval, was used to compare the means of the groups. *P* values of  $\leq 0.05$  were considered to be statistically significant. The differences marked with one asterisk were significant at  $P < 0.05$ , with two at  $P < 0.005$ , and with three at  $P < 0.0001$ .

## 6.3 RESULTS

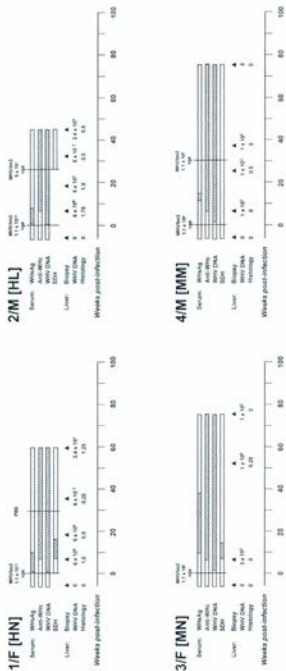
### 6.3.1 Infection with low WHV dose induces serologically silent but WHV DNA evident primary occult infection

Serial serum and liver tissue samples collected from woodchucks inoculated with low (50 vge), medium ( $1.1 \times 10^8$  vge) or high ( $1.1 \times 10^{10}$  vge) doses of WHV were examined for serum WHsAg, anti-WHc and anti-WHs (serological markers) and WHV DNA in serum and hepatic tissue (molecular markers). Animals injected with high WHV dose (1/F and 2/M) showed, as expected, the appearance of WHsAg at 3 - 4 w.p.i. which persisted until 8 - 10 w.p.i. (Figure 6.2). In animals injected with medium dose of WHV (3/F and 4/M), serum WHsAg became reactive at 10 and 12 w.p.i. and the antigen cleared from circulation at 16 w.p.i. in 4/M, while persisted up to 38 w.p.i. in 3/F. All 4 animals developed anti-WHc beginning from 6-8 w.p.i. and remained antibody reactive until the end of follow-up (Figure 6.2). Anti-WHs appeared in

**Figure 6.2** The profiles of serological markers of WHV infection and WHV DNA detection in sera and liver tissue samples in animals belonging to Group A and Group B. Woodchucks were injected with  $5 \times 10^3$ ,  $1.1 \times 10^6$  or  $1.1 \times 10^{10}$  vge of WHV or with PBS at time points indicated by vertical solid lines. For each animal, the appearance and duration of positivity of WHsAg, anti-WHc, WHV DNA and SDH in sequential serum samples are represented by hatched horizontal bars. The liver samples were collected at the time points indicated by solid arrow heads and estimated loads of WHV DNA presented in vge/ $\mu$ g of total liver DNA and histological degree of hepatitis graded on a scale from 0 to 3 in each sample are presented. The liver sample collected at autopsy from 11/M displayed histological features of hepatocellular carcinoma (HCC).

Figure 6.2

## Group A:





1/F and were periodically detectable after 14 w.p.i., while the other 3 woodchucks remained antibody nonreactive (data not shown). There was no difference in the time of the appearance of WHV DNA in serum between animals injected with high or medium doses of WHV and the genome became detectable starting from one w.p.i., and persisted throughout the entire observation period in these animals. The levels of WHV DNA in liver biopsies obtained at 6 w.p.i. were  $6 \times 10^6$  vge/ $\mu$ g and between  $1 \times 10^2$  and  $3 \times 10^2$  vge/ $\mu$ g in animals injected with high and medium WHV doses, respectively. After resolution of acute infection, hepatic load of WHV DNA usually ranged between  $1 \times 10^2$  to  $6 \times 10^3$  vge/ $\mu$ g and persisted to the end of follow-up, however, it transiently elevated to  $1 \times 10^6$  vge/ $\mu$ g in the liver sample of 3/F acquired at 55 w.p.i.

The histological features of AH were found in liver biopsies collected at 6 w.p.i. from woodchuck 1/F and 2/M inoculated with high WHV dose (Figure 6.2). These alterations coexisted with serum WHsAg positivity in both and elevated levels of SDH in 1F (SDH was measured in 2/M after challenge with WHV). In 3/F and 4/M injected with medium WHV dose, liver biopsies obtained at 6 w.p.i. showed normal liver morphology, at the time when serum WHsAg was negative and SDH levels remained normal (Figure 6.2), indicating that these samples were acquired prior to acute phase of infection. Following clearance of WHsAg, minimal to moderate intermittent liver inflammation remained evident in all animals, similarly as it has been observed in previous studies (Michalak *et al.*,

1999; Hodgson and Michalak 2001; Michalak 2004). The challenge of 2/M with 50 vge and 4/M with  $1.1 \times 10^6$  vge did not induce the reappearance of WHs antigenemia nor increased WHV DNA load in serum or liver (Figure 6.2).

In contrast to the woodchucks injected with high or medium doses of WHV, inoculation with 50 vge initiated POI in all 8 animals (Group B), as evidenced by the detection of WHV DNA in serum beginning from one to 2 w.p.i. and its long-term persistence at levels  $\leq 100$  vge/mL in the absence of detectable WHsAg and anti-WHc. This serologically mute infection was accompanied by WHV DNA absence in the liver and entirely normal liver morphology, as was clearly apparent in 5/M followed for up to 96 w.p.i. (Figure 6.2). It is of note that although the liver remained virus genome negative, WHV DNA was detected in the bone marrow collected at autopsy of this animal (data not shown). The above findings were in full agreement with those reported previously for woodchucks with naturally acquired and experimentally induced POI (reviewed in Michalak *et al.*, 2007; Mulrooney and Michalak, 2007; Coffin and Michalak, 1999; Michalak *et al.*, 2004; Gujar *et al.*, 2008).

The animals with POI challenged once or twice with a low, liver nonpathogenic dose of the virus that induced occult infection in the first instance, i.e., 6/M (subgroup LNL), 7/M (subgroup LLL), 8/M (subgroup LLN) and 9/M prior to challenge with high WHV dose (subgroup LLLH), remained WHsAg and anti-WHc nonreactive, did not show an increase in WHV DNA level in serum and their livers remained WHV DNA non-reactive and without histologically evident

alterations (Figure 6.2). The exception was 8/M (subgroup LLN) in which WHV DNA transiently appeared at approximate levels of 100 vge/ $\mu$ g total DNA in two sequential liver biopsies, one collected at 17 w.p.i. and the second at 6 week after first challenge with WHV (Figure 6.2). This intermittent detection of WHV genome was not accompanied by liver injury, as confirmed by histology examination and by normal SDH levels. Further, there was an unexplained appearance of mild liver inflammation in 6/M at 44 w.p.i. that protracted until autopsy, but was not accompanied by elevated SDH levels. As mentioned above, this inflammation also did not coincide with detection of WHV DNA in the liver (Figure 6.2).

As it has been previously observed in either naturally acquired or experimentally induced POI, the challenge with high doses of WHV initiated serum WHsAg-positive infection and hepatitis (Coffin and Michalak, 1999; Michalak *et al.*, 2004). Similarly, all animals with POI which were challenged with high dose of WHV in the current study, *i.e.*, 9/M (subgroup LLLH), 10/F and 12/M (subgroup LH) and 11/M (subgroup LHN) (Figure 6.2), developed WHs antigenemia and became anti-WHc reactive, as well as demonstrated transiently elevated levels of serum SDH. In 9/M, 10/F and 12/M, WHsAg eventually vanished, while it persisted to the end of the observation period in 11/M, *i.e.*, up to 104 weeks after administration of high virus dose (Figure 6.2). This animal developed chronic hepatitis and finally HCC. After challenge of animals with POI with a high dose of WHV, the liver tissue biopsies demonstrated histological

features of hepatitis, except for the sample from 11/M obtained at 6 weeks post-challenge with high WHV dose where only minimal inflammatory alterations were found (Figure 6.2). The same liver samples also became WHV DNA reactive and the livers of these animals remained virus genome positive until the autopsy. In summary, woodchucks infected, challenged or rechallenged with 50 vge of otherwise pathogenic WHV acquired sustained, serologically, biochemically and histologically silent but molecularly evident POI. Furthermore, the animals were not protected from infection with high dose of the same virus and acquired acute hepatitis, as we have previously reported (Coffin and Michalak, 1999; Michalak *et al.*, 2004; Mulrooney *et al.*, 2008).

### **6.3.2 POI is accompanied by delayed WHV-specific T cell response similarly as in symptomatic WHV infection**

To determine features of WHV-specific T cell proliferative response in the course of POI and to compare them with those accompanying serologically evident infection associated with hepatitis, sequential PBMC samples were *ex vivo* stimulated with WHV antigens or WHC<sub>97-110</sub> peptide and their proliferation measured by CFSE-based flow cytometric assay. As illustrated in Figure 6.3A for 1/F and 6/M infected with  $1.1 \times 10^{10}$  vge and 50 vge of WHV, respectively, both virus doses induced strong, multispecific T cell proliferative response of comparable magnitudes between 8-15 w.p.i., which persisted at lower levels to the end of follow-up or until challenge with WHV. In animal 6/M, which was

**Figure 6.3** The kinetics of WHV-specific T cell proliferative responses in woodchucks infected with liver pathogenic and nonpathogenic doses of WHV. The animals were infected with WHV, serial PBMC samples were isolated, stimulated *in vitro* with four different WHV antigens or WHC<sub>97-110</sub> peptide, and analyzed for resultant proliferation using CFSE-based proliferation assay to define cell division index (C.D.I.). The dashed vertical lines and solid arrow heads show the time points at which animals were injected or challenged with WHV, while the dashed horizontal line represents the cutoff value for virus-specific positive T cell response. The duration of POI induced in woodchucks belonging to study Group B is shown with hatched background. (A) Representative profiles of WHV-specific T cell proliferative response in 1/F infected with high, liver pathogenic dose ( $1.1 \times 10^{10}$  vge) and in 6/M inoculated with low, liver nonpathogenic dose ( $5 \times 10^1$  vge) of WHV after stimulation with rWHc, rWHe, rWHx, WHC<sub>97-110</sub> peptide or WHsAg, as determined by CFSE assay. The results are represented as C.D.I. The highest C.D.I. value given by any of the WHV antigens tested or WHC<sub>97-110</sub> peptide at a given time point was considered as a measure of WHV-specific T cell response and is marked by open squares and represented as solid grey shaded area. (B) The profiles of WHV-specific T cell response identified in individual animals infected with high or medium dose of WHV (Group A) or with low WHV dose (Group B). The PBMC collected from these animals were stimulated with rWHc, rWHe, rWHx, WHC<sub>97-110</sub> peptide or WHsAg and the highest C.D.I. value given by any of these antigens for

each time point is represented as WHV-specific T cell response, as explained above.

Figure 6.3A

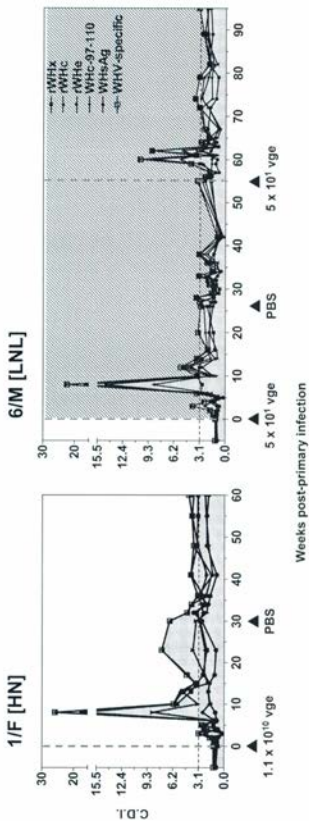
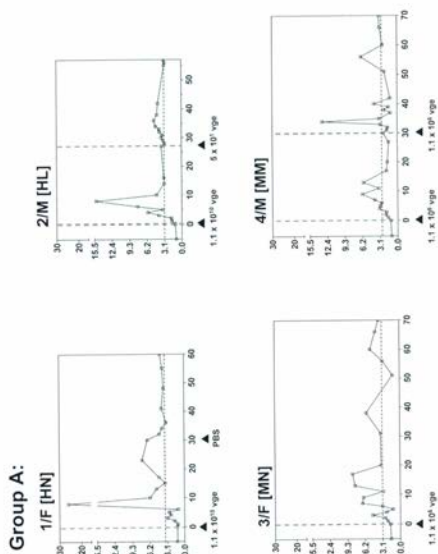
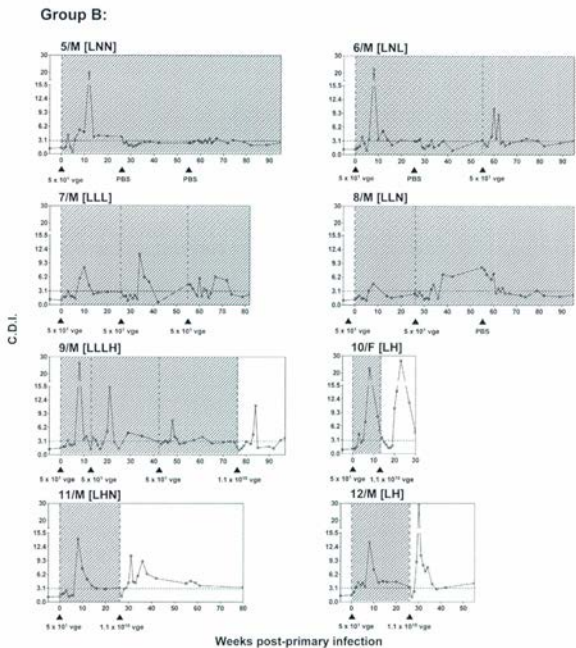


Figure 6.3B



C.D.1

Figure 6.3B (contd.)



challenged with 50 vge at 55 w.p.i., the augmented T cell proliferation in response to WHV antigens reemerged between 59 to 62 w.p.i. (Figure 6.3A).

In animals infected with high or medium WHV dose (Figure 6.3B, Group A), a strong WHV-specific T cell response appeared around 8-15 w.p.i. and remained detectable, although at much lower levels up to the end of the observation period, as in woodchucks 1/F and 3/F, or until challenge with WHV, as in animals 2/M (subgroup HL) and 4/M (subgroup MM). It is of note that the challenge of 2/M with 50 vge did not induce any significant increase in the magnitude of WHV-specific response, while challenge of 4/M with another medium dose ( $1.1 \times 10^6$  vge) again caused strong, but delayed secondary T cell response directed against virus antigens (Figure 6.3B). These findings were closely compatible with those recently reported for woodchucks infected and challenged with large, liver pathogenic doses of WHV (Gujar *et al.*, 2008).

The PBMC samples obtained from animals inoculated with 50 vge of WHV which established POI displayed overall similar profiles of virus-specific T cell response as those encountered in woodchucks injected with high or medium doses of the inoculum. Thus, all animals infected with low virus dose (Figure 6.3B, Group B) responded by generating WHV-specific lymphocyte proliferative reactivity of comparable magnitudes as those observed in the animals infected with liver pathogenic doses between 8-15 w.p.i. Further, the challenge or re-challenge of the woodchucks with POI with a low dose of WHV, *i.e.*, 6/M (subgroups LNL), 7/M (subgroup LLL), 8/M (subgroup LLN) and 9/M before

challenge with high dose (subgroup LLLH), induced similar profiles of WHV-specific T cell responsiveness as in animals injected and then challenged with high or medium doses which peaked between 6-12 weeks after each exposure to virus. In the above animals with POI, including 5/M (subgroup LNN), the virus-specific reactivity was intermittently detectable throughout the entire observation period. Furthermore, the profiles of virus-specific T cell response found in woodchucks infected in the first instance with low dose and then challenged with high dose, *i.e.*, 9/M (subgroup LLLH), 10/F and 12/M (subgroup LH) and 11/M (subgroup LHN), were again similar to those observed during primary infection induced by high, medium or low dose of WHV and then challenged with virus. Taken together, the results clearly showed that both primary and secondary virus-specific T cell proliferative responses in POI are strong and multispecific despite the lack of serological evidence of infection and biochemical and histological signs of hepatitis, and that their kinetics closely follow those occurring after infection with much greater ( $\sim 10^5$  or  $10^{10}$ -fold) doses of the virus.

### **6.3.3 Heightened T cell proliferation in response to mitogenic stimuli follows inoculation with WHV independently of virus dose administered**

Following our previous findings that WHV invasion is almost immediately followed by augmented generalized, nonspecific but not by virus-specific T lymphocyte proliferation response (Gujar *et al.*, 2008), PBMC collected during POI and control symptomatic WHV infection were cultured in the presence of

two-fold serial dilutions of ConA, PHA or PWM and assessed for their ability to proliferate in an adenine incorporation assay. As shown in Figure 6.4A for animals 1/F and 6/M, both high and low doses of WHV induced heightened T cell proliferation after stimulation with all mitogens tested between 1 and 3 w.p.i. This increased responsiveness subsided after 4-6 w.p.i., at the time when virus-specific T cell response appeared, and then rebounded when virus-specific response subsided. A similar pattern of mitogen-induced lymphocyte proliferation was also observed after re-exposure of woodchucks with POI to low dose of WHV (see 6/M in Figure 6.4A). Since the kinetics of proliferative response following ConA, PHA and PWM stimulation were comparable with each other (Figure 6.4A), only ConA-induced profiles are shown for other animals in Figure 6.4B.

As shown in Figure 6.4B and previously reported (Gujar *et al.*, 2008), PBMC collected from animals after injection with high (1/F and 2/M) or medium (3/F and 4/M) WHV dose displayed heightened capacity to proliferate in response to mitogenic stimuli between 1 and 3 w.p.i. This proliferative reactivity subsided between 4-6 w.p.i. when virus-specific T cell response appeared and then rose again when the specific response declined. Further, challenge of 4/M infected with medium dose with another medium dose of the same inoculum induced a similar profile of T cell proliferative response as that observed after primary exposure to WHV (Figure 6.4B, Group A). Interestingly, infection with a low, liver nonpathogenic dose of WHV also induced immediate

**Figure 6.4** The comparative kinetics of mitogen-induced (virus nonspecific) and WHV-specific T cell proliferative responses in woodchucks infected with high (liver pathogenic) and low (liver nonpathogenic) doses of WHV. Freshly isolated PBMC were stimulated with two-fold serial dilutions of ConA, PHA and PWM, and resultant proliferation was measured by adenine incorporation proliferation assay to determine stimulation index (S.I.) for each concentration of mitogens tested. The S.I. values obtained for the five serial concentrations of respective mitogen were averaged to define mean mitogenic stimulation index (M.M.S.I.) which are presented by continued black lines. The dashed vertical lines and solid arrow heads show the time points at which animals were injected or challenged with WHV, while the dashed horizontal line represents the cutoff value for virus-specific positive T cell response. The profile of WHV-specific T cell response for each animal is shown with a shaded area under grey line and the duration of POI is shown with hatched background. The C.D.I. values for WHV-specific T cell response and M.M.S.I. values after mitogenic stimulation are shown on left and right axes, respectively. (A) Representative profiles of lymphocyte proliferative responses induced by ConA, PHA and PWM and WHV-specific T cell response in 1/F infected with liver pathogenic ( $1.1 \times 10^{10}$  vge) dose and in 6/M inoculated with liver nonpathogenic ( $5 \times 10^1$  vge) dose of WHV after stimulation with different mitogens, as explained above. (B) The comparative profiles of ConA-induced and WHV-specific lymphocyte proliferative responses in individual woodchucks infected with high or medium dose of WHV (Group A) or

with low WHV dose (Group B).

Figure 6.4A

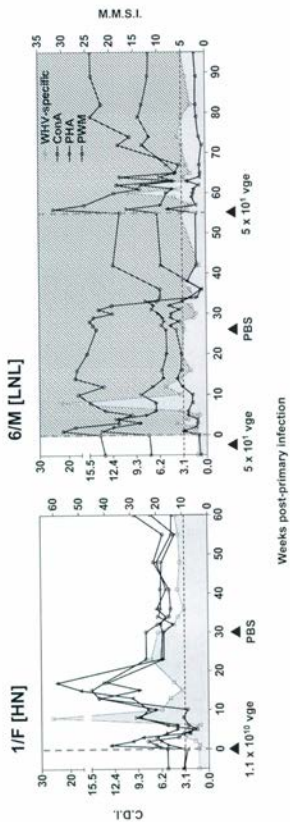
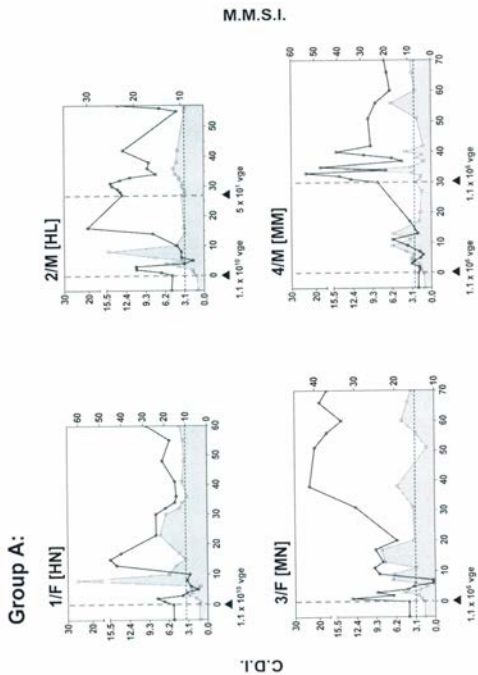
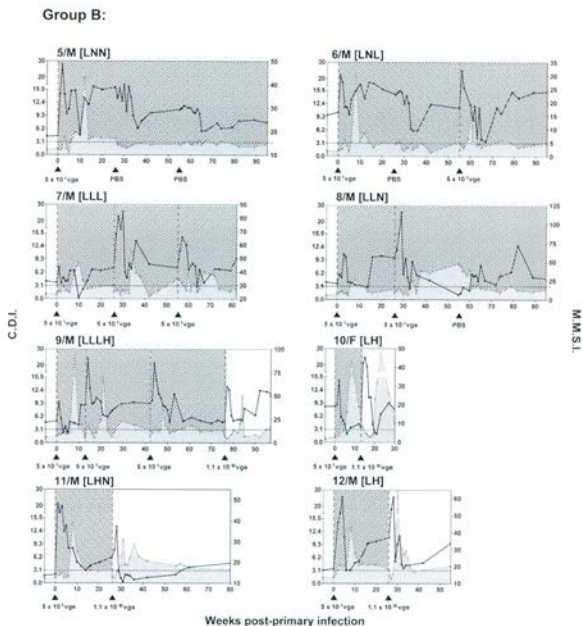


Figure 6.4B



C.D.I.

Figure 6.4B (contd.)



augmentation in lymphocyte proliferation in response to nonspecific stimuli which declined when virus-specific T cell reactivity appeared, and subsequently increased again when specific response declined (Figure 6.4B, Group B). A similar transiently augmented mitogen-induced lymphocyte responsiveness was detected immediately after each challenge or re-challenge of the animals with POI with either low or high dose of WHV. Taken together, the results showed that WHV invasion leading to establishment of either POI or serologically evident infection accompanied by hepatitis coincides with the highly compatible profiles of generalized as well as virus-specific T cell proliferative responses.

#### **6.3.4 Induction of POI and subsequent challenge with WHV are accompanied by aberrant expression of cytokines in peripheral lymphoid cells**

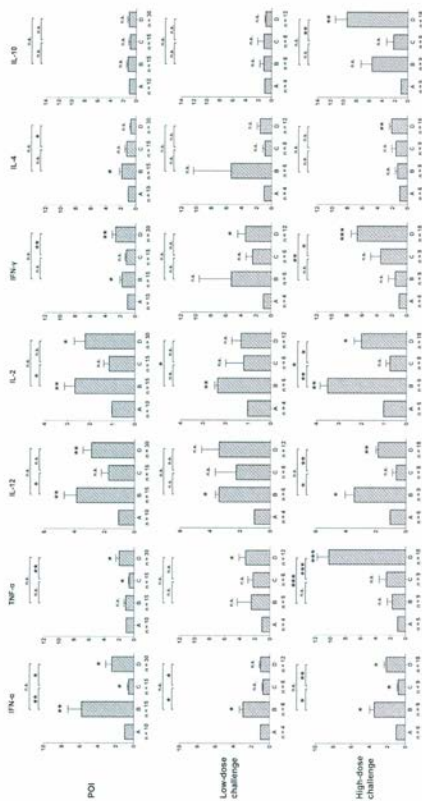
Freshly isolated, unmanipulated PBMC (*i.e.*, not subjected to *ex vivo* stimulation with either mitogens or WHV-specific antigens) collected from woodchucks after infection with a low dose of WHV and subsequent challenge with either a high or low dose of the same virus were quantified for the expression of selected cytokines by real time RT-PCR. Considering the opposing profiles of WHV-specific and mitogen-induced lymphocyte responses observed in this study and taking under consideration previous findings in woodchucks infected and challenged with high ( $\geq 1.1 \times 10^{10}$  vge) doses of WHV (Gujar *et al.*, 2008), the progression of POI was divided into four phases: (1) the

phase before infection (phase A); (2) the phase between 1 and 3 w.p.i. characterized by the heightened mitogen-inducible T cell proliferative reactivity and essentially absent virus-specific T cell response (phase B); (3) the phase between 4 and 6 w.p.i. accompanied by decreasing nonspecific and undetectable virus-specific T cell proliferative responses (phase C), and (4) the phase between 7 and 15 w.p.i. with essentially absent nonspecific T cell proliferative reactivity and arising and then peaking virus-specific T cell response (phase D). Similarly, because of the overall opposing kinetics of the specific and nonspecific T cell responses identified after challenge of animals with POI with WHV, the observation period after the challenge was also divided into phases B to D (see Figure 6.5).

As shown in the top panel of Figure 6.5, the inoculation with a low, liver nonpathogenic dose of WHV induced significantly higher expression of IFN- $\alpha$  ( $P = 0.0092$ ), IL-12 ( $P = 0.0089$ ), IL-2 ( $P = 0.005$ ) along with elevated transcription of IFN- $\gamma$  ( $P = 0.0196$ ) and IL-4 ( $P = 0.0358$ ) during phase B, as compared to the expression levels before infection (phase A). Thus, increased mRNA levels of these genes were detected in intact PBMC at the time when these cells displayed heightened proliferation in response to mitogenic but not to virus-specific stimuli (see Figure 6.4). Subsequently, during phase C, wherein the mitogen-induced T cell proliferative responsiveness subsided, the expression of the cytokines mentioned above, except IFN- $\gamma$  and IL-4, significantly decreased. Most interestingly, the level of transcription of TNF- $\alpha$ , which remained at

**Figure 6.5** A quantitative analysis of cytokine gene expression in circulating lymphoid cells in animals during different phases of WHV POI and their subsequent challenge with either low (liver nonpathogenic) or high (liver pathogenic) dose of WHV. The expression of IFN- $\alpha$ , TNF- $\alpha$ , IL-12, IL-2, IFN- $\gamma$ , IL-4, and IL-10 was analyzed in freshly isolated PBMC collected from animals with POI (n=6) and later after challenge with either low (subgroup LL; n=3) or high (subgroup LH; n=3) dose of the virus. After each primary or subsequent exposure to WHV, the time line of infection was divided into four phases according to the distinct profiles of WHV-specific and mitogen-induced T cell responses, as described in Results. The expression levels of each cytokine were normalized against  $\beta$ -actin and then compared with those observed prior to primary infection with WHV (Phase A) to calculate fold increase or decrease. The *P* values above each bar represented by asterisks were obtained by comparing the mean expression level of a given gene during phase B, C or D with the mean expression determined for this gene in phase A, while the *P* values showed at the top of each panel were obtained by comparing with each other the mean expression level of a given gene determined for phases B, C and D. Differences marked with one asterisk were significant at a *P* value of  $\leq 0.05$ , with two at a *P* value of  $\leq 0.005$ , and with three at a *P* value of  $\leq 0.0001$ .

Figure 6.5



approximately the same level in phases A and B, significantly ( $P = 0.021$ ) declined in phase C (Figure 6.5, top panel). Finally, the expression of IFN- $\alpha$ , TNF- $\alpha$ , IL-12, IL-2 and IFN- $\gamma$ , but not that of IL-4 and IL-10, was synchronously upregulated during phase D, coinciding with the appearance and peaking of WHV-specific T cell response. Following challenge of the animals with POI with low dose (i.e., 50 vge) of WHV (Figure 6.5, middle panel), overall similar patterns of the cytokines' expression were detected during phases B to D as those identified after primary injection with the same low dose, although the differences in transcription levels between different phases were less pronounced for some cytokines after challenge.

When the woodchucks with POI were challenged with high dose (i.e.,  $1.1 \times 10^{10}$  vge) of WHV (Figure 6.5, bottom panel), the expression of IFN- $\alpha$  ( $P = 0.0167$ ), IL-12 ( $P = 0.0296$ ) and IL-2 ( $P = 0.0051$ ) was again elevated during phase B, but then subsided in phase C, while transcription of TNF- $\alpha$  remained unchanged until phase D. Similarly, during phase D, which corresponded to serum WHsAg-positive infection accompanied by histologically evident hepatitis (see Figure 6.2, Group B) and the peaking of WHV-specific T cell response, the expression of TNF- $\alpha$  ( $P = 0.001$ ) and IFN- $\gamma$  ( $P = 0.0063$ ) became significantly augmented (Figure 6.5, bottom panel). Overall, the fold increases in the mRNA levels of the cytokines were much greater than those detected in phase D of POI (Figure 6.5, bottom panel) or in animals with POI which were challenged with low virus dose (see Figure 6.5, middle panel). After challenge with high dose, the

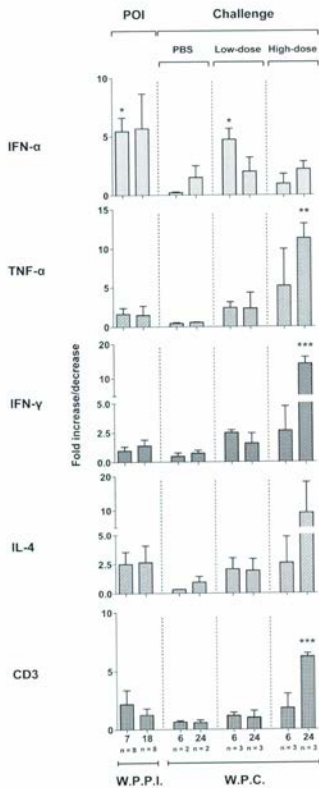
synchronously upregulated expression of IFN- $\alpha$ , TNF- $\alpha$ , IL-12, IL-2, and IFN- $\gamma$  was also accompanied by the significantly greater levels of transcription of IL-4 ( $P = 0.009$ ) and IL-10 ( $P = 0.0097$ ) than those accompanying phase D after primary infection or challenge with low dose of virus (see Figure 6.5 top panel and middle panels, respectively). Collectively, the quantitative analysis of the cytokine expression in circulating lymphoid cells serially acquired during POI revealed that the infection with low, liver nonpathogenic dose of hepadnavirus not only almost immediately enhanced T cell responsiveness to mitogenic stimuli but also upregulated transcription of a number of functionally important cytokines in unmanipulated cells. Although, as in serologically evident infection caused by liver pathogenic doses of the virus (Gujar *et al.*, 2008), POI did not induce TNF- $\alpha$  expression in circulating lymphoid cells that is known to be essential for the activation of APC and NK cells.

### **6.3.5 Hepatic expression of IFN- $\alpha$ but not IFN- $\gamma$ or TNF- $\alpha$ is upregulated during POI**

The liver biopsies obtained at 6 and 18 w.p.i. following primary injection with low dose and after challenge of the animals with POI with either low or high dose of WHV or after control injection with PBS, which were collected at 7 and 24 weeks post-challenge (w.p.c.), were evaluated for the expression of IFN- $\alpha$ , TNF- $\alpha$ , IFN- $\gamma$ , IL-4 and CD3. The results were compared with the transcription levels detected for the same genes in the liver samples obtained from the same

**Figure 6.6** The hepatic expression of selected cytokines and CD3 during POI and after challenge with either high or low dose of WHV or injection with PBS. The levels of IFN- $\alpha$ , TNF- $\alpha$ , IFN- $\gamma$ , IL-4 and CD3 mRNA were measured by real time RT-PCR in liver samples collected during POI (n=8) and after challenge with low (subgroup LL; n=3) or high (subgroup LH; n=3) dose of WHV or after control injection with PBS (subgroup LN; n=2). The mean expression level of a particular gene during POI or after challenge was normalized against  $\beta$ -actin expression and then compared with the mean determined in the liver samples collected prior to infection. Differences marked with one asterisk were significant at a  $P$  value of  $\leq 0.05$ , with two at a  $P$  value of  $\leq 0.005$ , and with three at a  $P$  value of  $\leq 0.0001$ .

Figure 6.6



animals prior to first injection with virus. As shown in Figure 6.6, the liver samples collected at 7 w.p.i. displayed significantly higher mRNA levels of IFN- $\alpha$  ( $P = 0.0001$ ), in the absence of significantly elevated TNF- $\alpha$ , IFN- $\gamma$ , IL-4 or CD3 expression, as compared to the levels detected in the biopsies collected prior to infection (Figure 6.6). Furthermore, the intrahepatic expression of the genes examined, including IFN- $\alpha$ , was not significantly upregulated at 18 w.p.i. as well as after control injection with PBS, as compared to the levels detected in healthy animals prior to injection with WHV. The comparable patterns of cytokine and CD3 expression were also observed in the liver biopsies from the animals with POI after challenge with low dose of WHV (Figure 6.6). Liver samples collected at 24 w.p.c., but not those obtained at 6 w.p.c. with high dose showed strong expression of TNF- $\alpha$  ( $P = 0.0032$ ), IFN- $\gamma$  ( $P = 0.0001$ ) and CD3 ( $P = 0.0003$ ), but not IFN- $\alpha$ . Collectively, these results showed that POI is associated with elevated expression of IFN- $\alpha$  in the absence of TNF- $\alpha$  and IFN- $\gamma$  response and, most intriguingly, in the absence of WHV in the liver.

#### 6.4 DISCUSSION

In this report, we demonstrated that POI experimentally induced by exposure of woodchucks to low, liver nonpathogenic dose of WHV is accompanied by: (1) stimulation of anti-viral T cell proliferative response against multiple epitopes of structural and non-structural proteins of WHV in the absence of virus-specific humoral immunity; (2) induction of a heightened capacity of

lymphoid cells to proliferate in response to mitogenic stimuli soon after exposure to WHV, similarly as in infection induced by a pathogenic dose of the virus, and (3) the aberrant expression in these cells of cytokines mediating early innate immune responses. Also, secondary T cell proliferative immune response induced in woodchucks with POI by their challenge with either liver nonpathogenic or liver pathogenic doses of WHV showed highly comparable kinetics to that observed after primary WHV infection. However, this secondary response failed to protect animals with POI against development of AH following exposure to liver pathogenic dose of the virus.

Findings from studies on other viral infections, such as with hepatitis C virus (HCV) (Quiroga *et al.*, 2006; Kamal *et al.*, 2004, Koziel *et al.*, 1997), human immunodeficiency virus (HIV) (Promadej *et al.*, 2003) and simian immunodeficiency virus (SHIV) (Tasca *et al.*, 2007), parallel the results from our study in regard to the fact that inoculation with a sub-pathogenic quantity of WHV induced virus-specific T cell response without stimulating virus-specific antibody response. In this context, the sexual partners of patients with acute HCV or HIV infections (Langlade-Demoyen *et al.*, 1994; Kamal *et al.*, 2004), individuals seronegative for HCV but with a history of a HCV-contaminated needle stick injury (Koziel *et al.*, 1997), health care workers with occupational exposure to bodily fluids of HIV-infected individuals (Pinto *et al.*, 1995) or infants born to HIV-positive mothers (De Maria *et al.*, 1994), all of whom remain persistently seronegative for anti-viral antibodies display multiepitope-specific CD8+ CTL and

CD4+ T cell antiviral proliferative responses. Similarly, in our study, all 8 animals exposed to a low virus dose established persistent POI in the face of strong WHV-specific T cell proliferative reactivity, without detectable anti-WHc or anti-WHs antibodies, or liver injury. It has been previously hypothesized that following exposure to low doses of hepadnavirus, although T cell response is induced, it is sub-optimal and unable to mediate liver injury or protect from challenge with a pathogenic dose of the virus (Koziel *et al.*, 1997, Coffin and Michalak, 1999). Further, in woodchucks infected with WHV, a virus-specific T cell response during POI was detectable, albeit intermittently and at lower magnitudes than that detected after resolution of AH. This suggests protracted stimulation of this response, probably by low level WHV replication, as it has been observed after recovery from experimental AH in woodchucks (Michalak *et al.*, 1999) and in patients convalescent from acute HBV infection (Rehermann, *et al.*, 1995).

The role of virus-specific T cell responses in the pathogenesis and control of HBV infection is overall well recognized. It has been shown that strong antiviral T cell reactivity directed to multiple epitopes of the virus during the acute phase of infection precedes resolution of hepatitis, while a weak and virus epitope-restricted response is followed by chronic hepatitis. Nonetheless, studies in both humans, chimpanzees and woodchucks have uniformly revealed that T cell responsiveness to hepadnavirus is delayed until 6-12 w.p.i., as compared to the responses observed following invasions with other viral

pathogens, such as lymphocytic choriomeningitis virus (LCMV) (Gallimore *et al.*, 1998), murine cytomegalovirus (MCMV) (Rentenaar *et al.*, 2000) or influenza virus (Flynn *et al.*, 1998; reviewed in Rocha and Tranchot, 2006). This delay in the appearance of hepatitis B virus-specific T cell reactivity was believed to be a consequence of the virus' long incubation period or an inappropriate innate cytokine microenvironment during the pre-acute phase of infection (Bertoletti and Gehring, 2006; Chang and Lewin, 2007). In our most recent study (Gujar *et al.*, 2008), we have shown that this delay in the appearance of virus-specific T cell proliferative response in WHV infection is preceded by virus-induced but nonspecific, aberrant T cell activation occurring between 1 and 6 w.p.i., which is associated with the impaired expression of cytokines, especially that of TNF- $\alpha$  and IFN- $\gamma$ , and followed by apoptotic death of activated cells. In other viral infections, the early and synchronous expression of the above cytokines, together with IFN- $\alpha$ , IL-2 and IL-12, initiate the innate responses leading to the differentiation and maturation of dendritic cells (DC) to professional APCs, as well as to the activation of NK cells to produce IFN- $\gamma$  and acquire cytotoxic capacity (Orange and Biron, 1996; Orange and Biron, 1996; Kawai and Akira, 2006; Kadowaki *et al.*, 2000). The proper activation of this innate response guides the rise of adaptive immunity by stimulating generation of antigen-specific T and B lymphocytes (Andoniou *et al.*, 2005; Kawai and Akira, 2006; Kadowaki *et al.*, 2000). On the other hand, APCs and NK cells generated in the absence of TNF- $\alpha$  or IFN- $\alpha$  have impaired T cell stimulatory capacities and display reduced

anti-viral activity (Dauer *et al.*, 2003; Iwamoto *et al.*, 2007; Mcrae *et al.*, 2000). Thus, similar to our observations made during the period preceding development of acute WHV infection (Gujar *et al.*, 2008), the data from animals with experimentally induced POI suggest that the induction of a strong, nonspecific T cell proliferative response and the aberrant expression of innate cytokines soon after exposure to a low, nonpathogenic dose of hepadnavirus delays the appearance of a virus-specific T cell immune response. It is noteworthy that irrespective of the WHV dose, strong T cell proliferation directed against multiple antigenic epitopes of the virus occurs only after the synchronous expression of IFN- $\alpha$ , TNF- $\alpha$ , IL-12, IFN- $\gamma$  and IL-2 observed from 7 w.p.i. onwards. This provides an indirect validation that the initiation of anti-viral T cell response in WHV infection has to be accompanied by coordinated expression of appropriate cytokines in immune cells. Albeit, the magnitudes of IFN- $\gamma$  and TNF- $\alpha$  transcription in the PBMC from animals with POI was significantly lower ( $P = 0.024$  and  $P = 0.0075$ , respectively) than those detected during respective phase of acute hepatitis.

Despite the fact that hepadnavirus core protein is recognized as a strong T cell independent antigen (Milich and McLachlan, 1986), the absence of anti-WHc antibody responses in the presence of detectable virus-specific T cell reactivity after infection with a low dose of WHV, either following primary exposure or challenge, is difficult to explain. Nonetheless, similar observations have been made in seronegative HCV (Kamal *et al.*, 2004) and HIV infections

(Koziel *et al.*, 1997). Furthermore, infection with a low dose of LCMV, resulting in the inability to detect virus antigens in secondary lymphoid organs, was suggested to hamper the development of T cell-independent antibody response (Ochsenbein *et al.*, 2000), implying that similarly minute quantities of WHcAg might fail to induce specific antibody response in woodchucks with POI. Additionally, the initiation of T cell-dependent B cell activity requires the presence of properly activated CD4+ T cells in the context of the appropriate cytokine milieu enriched with IL-10 and IL-4 (Hosken *et al.*, 1995). The analysis of expression of cytokines in circulating lymphoid cells obtained during POI in our study revealed that after initial exposure to or challenge with low dose of WHV, IL-4 and IL-10 expression remain unchanged, even during phase C (see Figure 6.5), equivalent to acute phase of infection caused by liver pathogenic dose of WHV (Gujar *et al.*, 2008), when expression of IFN- $\alpha$  and TNF- $\alpha$  rebounds. This may imply that the absence of anti-WHc response could also stem from the inappropriate cytokine milieu. This line of reasoning is indirectly supported by the fact that woodchucks with POI challenged with a high dose of WHV, which displayed an increased expression of IL-4 and IL-10 in the PBMC during acute phase of infection, also showed anti-WHc antibody response.

The capacity of lymphoid cells to proliferate in response to *ex vivo* stimulation with non-specific mitogens provided valuable insight into the generalized immune competency of the cells during infections with a variety of microbial pathogens, including HIV (Pedersen *et al.*, 1990), measles virus

(Nieweisk *et al.*, 2000), MCMV (Allan *et al.*, 1982), *Schistosoma japonica* (Garb *et al.*, 1981) and, recently, WHV (Gujar *et al.*, 2008). Similar evaluations using PBMC from patients with CH type B have shown a decreased proliferative capacity of lymphocytes after stimulation with mitogens (Sodoman *et al.*, 1979; Feighery *et al.*, 1980). In our study, irrespective of the quantity of invading virus, each primary or secondary exposure to WHV induced immediately a heightened capacity of lymphocytes to proliferate in response to mitogen stimulation, which eventually declined in magnitude before the virus-specific T cell response appeared. This heightened proliferation was also accompanied by the elevated transcription of genes encoding IFN- $\alpha$ , IL-12 and IL-2 in unmanipulated circulating lymphoid cells. The role of IL-2 in T cell and NK cell growth and in their survival is well acknowledged and the absence of this cytokine is associated with decreased proliferative responsiveness of these cells (Kobayashi *et al.*, 1989; Scitudo *et al.*, 1995; Murphy *et al.*, 1992; Seifer *et al.*, 1993). However, 5-10% of PBMC is comprised of NK cells, which can undergo blastogenesis and incorporate greater amounts of radioactive thymidine *in vitro* in the presence of increased IFN- $\alpha$  expression, as is the case in LCMV and MCMV infections (Orange and Biron, 1996; Su *et al.*, 2001; Biron and Welsh, 1982; Biron *et al.*, 1984). Further, NK cells cultured in the presence of both IFN- $\alpha$  and IL-12 demonstrate greater rates of blastogenesis than those cultured with IFN- $\alpha$  alone, and can promote mitogen-induced proliferation of peripheral T cells, probably due to their increased ability to produce IL-2 (Orange and Biron, 1996; Su *et al.*,

1994) . From this study and from the data on the mitogen-induced lymphocyte hyper-responsiveness and concurrent cytokine expression observed immediately after exposure to WHV, it could be inferred that the elevated expression of cytokines is behind the early, heightened proliferative capacity of T cells in our study.

Although the appearance and the magnitude of T cell responses during POI are similar to those observed during symptomatic WHV infection, these responses do not protect against hepatitis after challenge with large amounts of the virus. It has been postulated that the phenotypic heterogeneity of the cells mediating cellular and humoral immune responses can be dictated by the dose of antigen, with small doses usually favoring the development of cellular immune responses (Hosken *et al.*, 1995; Zannetti *et al.*, 2006). It also is believed that the control of HBV infection is primarily mediated by virus-specific CD8+ T cells (Chisari, 2000; Bertoletti and Gehring, 2006), while the contribution of CD4+ T cell response in this regard is not as well defined. It is of note that in other studies it has been shown that CD4+ T cell responses generated during vesicular stomatitis virus infection induced by low doses tend to inhibit the virus-specific CD8+ T cell response (Cose *et al.*, 2006). This may suggest that infection with low dose of WHV could induce a defective CD8+ T cell response incapable of protecting the host against challenge with liver pathogenic doses of WHV. Nonetheless, patients who recovered from AH type B and those immunized with HBsAg vaccine are protected from development of hepatitis after re-exposure to

HBV, indicating the important role of anti-HBs. As we have established before (Michalak *et al.*, 2004; Coffin and Michalak, 1999) and confirmed in the course of the current study, woodchucks infected with low doses of WHV do not develop detectable anti-WHs or anti-WHc. Taken together, this implies that not only improper activation of T cell responses but also the absence of neutralizing antibodies could fail to render protective immunity in POI.

The analysis of the cytokine gene expression in liver biopsy samples collected during POI and after challenge with a low dose of WHV showed that at 6-7 w.p.i. the transcription of IFN- $\alpha$ , but not IFN- $\gamma$  or TNF- $\alpha$ , was significantly increased. The evidence of IFN- $\alpha$  expression in the liver, along with the absence of lymphocytic infiltrations, as evidenced by histological examination at multiple time points after primary infection or challenge with low WHV dose, indicates that the invasion with such a dose, although unable to prompt immunological responses leading to hepatic injury, was not entirely immunologically inconsequential (neutral) to the liver. Further, elevated transcription of this important cytokine in the context of the absence of detectable WHV replication and immune cell infiltrations suggests that the event might be due to activation of the cells constitutively residing within the liver or circulating throughout the organ after encounter with small quantities of virus. The mechanism of this activation and phenotype of the cells involved will require further investigations. The absence of intrahepatic expression of IFN- $\gamma$  and TNF- $\alpha$  (see Figure 6.6), as well as CD3 (data not shown), at 7 and 18 w.p.i. and following challenge with low

dose of WHV is consistent with the protracted absence of hepadnaviral replication in the liver during POI, as observed in the current study (see Figure 6.1) and also reported previously (Coffin and Michalak, 1999; Michalak *et al.*, 2004; reviewed in Michalak *et al.*, 2007). On the other hand, serologically evident infection induced by high, liver pathogenic doses of WHV (Michalak *et al.*, 1999; Michalak *et al.*, 2004; Gujar *et al.*, 2008; Guy *et al.*, 2008) as well as by challenge of animals with POI with similar high doses (Coffin and Michalak, 1999; Michalak *et al.*, 2004) has been shown to be associated with a significantly greater expression of IFN- $\gamma$ , TNF- $\alpha$  and CD3, indicating the successful generation and recruitment of virus-specific CD8+ CTL and CD4+ Th1 cells to the liver. Taken together, the analysis of gene expression in the hepatic tissue samples performed in our study implies that a low dose of WHV, although it does not initiate infection, induces, by as yet unknown mechanism, a type I interferon response in the liver.

Our study demonstrates that a low dose of hepadnavirus, causing an asymptomatic infection progressing in the absence of liver infection and virus-specific humoral immune response, induces multispecific anti-viral T cell proliferative responses which kinetics are compatible to those accompanying symptomatic infection coinciding with acute hepatitis. Although these virus-specific T cell responses do not protect against hepatitis after challenge with higher doses of the same virus, they represent a reliable immunological correlate of the initiation and progression of occult infection. Similar to our observations, a

recently published study has demonstrated that patients with HBV OBI progressing in the absence of virus-specific antibodies carry circulating HBV-specific CD8+ T cells, as visualized by staining with class I major histocompatibility complex tetramers (Zerbini *et al.*, 2008). The assessment of this cellular response can aid the diagnosis of low dose HBV infection in high risk groups, such as health care workers experiencing contaminated needle stick injuries, family members of infected individuals or intravenous drug users, which otherwise could be underestimated due to the lack of virus-specific antibody responses and the sensitivity of HBV DNA detection assays. Comparative analysis of virus-specific and mitogen-induced T cell proliferative capacities along with cytokine responses during POI and symptomatic infection caused by liver pathogenic doses of hepadnavirus increases our understanding of immunological processes underlying the pathogenesis of HBV infection.

## CHAPTER 7: SUMMARY AND FUTURE DIRECTIONS

### 7.1 SUMMARY

The overall aim of the present study was to investigate the kinetics of cellular and cytokine immune responses following experimental hepadnaviral infection and after re-exposure to the same virus. Specifically, this study was primarily designed: (1) to recognize and understand the reasons behind the delayed appearance of virus-specific T cell response normally observed after exposure to hepadnavirus, (2) to determine the profiles of virus-specific and non-specific T cell proliferative as well as cytokine responses occurring after exposure and re-exposure to a liver nonpathogenic dose of WHV inducing persistent occult infection and, (3) compare those profiles to those induced by a liver pathogenic dose causing serologically evident infection and hepatitis. To aid these investigations in the woodchuck model, the initial studies were designed to develop a CFSE-based flow cytometric T lymphocyte proliferation assay for the detection of virus-specific T cell reactivity with a greater sensitivity than that of the traditional T cell proliferation assays based on incorporation of nucleotide analogues. This CFSE-based T cell proliferation assay was further implemented to assess the kinetics of WHV-specific proliferative reactivities in freshly isolated PBMC samples serially collected beginning from inoculation with WHV, through the pre-acute and acute phases of infection, to seemingly complete recovery. In parallel, the lymphocytes' general capacity to proliferate in response to mitogenic

stimulation and the expression of genes encoding for important antiviral and pro-inflammatory cytokines and immune cell markers were investigated. Further, similar investigations were performed in woodchucks inoculated with a liver nonpathogenic dose of WHV which developed POI, as well as after challenge of these animals with large (liver pathogenic) or low (liver nonpathogenic) doses of WHV. Taken together, the data from our studies indicated that the exposure or re-exposure to hepadnavirus, independent of its dose, induced delayed appearance of virus-specific T cell response, which was preceded by the aberrant activation of lymphocytes following invasion by the virus.

Before the development of the CFSE-based assay during this study, the kinetics of WHV-specific T cell responses in woodchucks were evaluated using adenine or 5-bromo-2-deoxyuridine (BrDU) incorporation T cell proliferation assays. Although, the lower sensitivity of these traditional proliferation assays was able to detect strong WHV-specific T cell proliferative responses, the detection of low magnitude responses required the development of the more sensitive assay. The implementation of a flow cytometric CFSE assay to assess the WHV-specific T cell responses enabled more accurate detection of antigen-specific proliferative reactivities during early pre-acute, AH, resolved and CH phases of WHV infection, which otherwise, in some cases, would have been deemed as not detectable. The data collected during this study clearly demonstrated that the CFSE-based lymphocyte proliferation assay is more sensitive than the traditional nucleotide incorporation T cell assays and, thus,

more efficient in detecting the virus-specific T cell reactivities, such as those observed in woodchucks with CH (see Figure 3.7). Nonetheless, the data obtained using the CFSE-based assay also confirmed some of the basic observations made before using a traditional T cell proliferation assay, regarding the kinetics and strength of virus-specific T cell responses accompanying symptomatic hepadnaviral infection. Among others, it concurred with the previously acknowledged fact that the magnitude of hepadnavirus-specific T cell proliferative response is significantly higher during self-limiting AH that later resolves, than those accompanying CH.

The availability of the more sensitive CFSE-based assay further aided in the determination of the precise kinetics of WHV-specific T cell proliferation responses during primary as well as secondary exposures to either high, medium or low doses of WHV. First, the serial PBMC samples collected from the woodchucks infected with a liver-pathogenic dose of WHV showed that the appearance of consistently detectable WHV-specific T cell proliferative reactivities was delayed until after 7 w.p.i. (see Figures 5.2 and 5.5). The finding of the delayed appearance of virus-specific T cell response was consistent with that reported by others in the woodchuck model (Menne *et al.*, 1997; 1998) and, those found in humans during the natural HBV infection of humans (Webster *et al.*, 2000; Bertoletti and Gehring, 2006). Thus, our study supports the notion that the late arise of the virus-specific T cell proliferative response is a hallmark of the cellular immune response accompanying hepadnaviral infections.

Interestingly, the postponement of the WHV-specific T cell proliferative reactivities was always preceded by the heightened capability of lymphocytes to proliferate after mitogenic stimulation. Similar types of heightened mitogen-induced proliferative capacities of human PBMC were also seen early after HBV infection (Sodoman *et al.*, 1978). This elevated proliferative capability in lymphocytes was equally evident after stimulation with ConA, PHA as well as PWM, indicating that this response was not due to activation of a particular group or sub-type of lymphocytes. These results implied that the exposure to hepadnavirus either directly renders the lymphocytes with an ability to undergo increased cell division, or indirectly orchestrates the lymphoid environment so as to sustain the higher rates of proliferation, after mitogenic stimulations. The implication of this heightened capability of lymphocytes to undergo rapid cell division is not completely understood yet. It is speculated that such an aberrant activation of lymphocytes immediately after exposure to hepadnavirus may render them temporarily insensitive to virus-specific activation. In consequence, this early plasticity of lymphocytes immediately after exposure to hepadnavirus could translate in the failure of prompt development of virus-specific T cell response.

Since, the proliferative capacity of the lymphocytes in response to either antigen-specific or non-specific stimuli is profoundly influenced by the milieu of cytokines as well as constituent cells surrounding it, unmanipulated PBMC were also analyzed for their inherent expression of selected cytokines along with

immune cell markers, to recognize the mechanism underlying the discordant profiles of heightened mitogen-induced and delayed virus-specific T cell proliferative responses. The quantitative analysis of the cytokine and cell marker gene expression suggested that WHV- or non-specific proliferative capacities of lymphocytes found during different phases of WHV infection could be associated with a distinct expression of cytokines. First of all, our results showed that immediately after exposure to WHV, the heightened mitogen-induced proliferative capacities in the lymphocytes were accompanied by upregulated expression of IFN- $\alpha$ , IL-12 and IL-2 in the absence of increased TNF- $\alpha$  expression. IFN- $\alpha$  and IL-12 induce the blastogenesis and increased thymidine incorporation in NK cells (Orange *et al.*, 1996), while IL-2 is a potent T cell growth factor that drives and sustains T cell division. Hence, it is postulated that the higher expression of these cytokines immediately after exposure to virus may endow the higher proliferative capacities to peripheral T and NK cells, which are then evidenced *in vitro* by higher rates of proliferation after mitogenic stimulation. This line of reasoning is supported by the fact that the PBMC collected from HBV-infected patients show increased NK cell frequency during the pre-acute phase of infection (Webster *et al.*, 2000). Similarly, mice infected with MCMV display increased blastogenesis of NK cells *in vivo* that can be inhibited by anti-IFN- $\alpha/\beta$  antibodies (Orange *et al.*, 1996), suggesting the role of IFN- $\alpha$  in driving the expansion of NK cells. Further, NK cells constitute 5-10% of PBMC and are known to undergo proliferation after mitogenic stimulation and enhance by-

stander proliferation of T lymphocytes, most probably through their ability to secrete IL-2 (Callewaert *et al.*, 1978). Our data appears to complement these findings by showing higher CD3 and CD56 expression in the PBMC population immediately after WHV infection. Taken together, our results suggest that, the higher capacity of lymphocytes to undergo proliferation after mitogenic-stimulation during the pre-acute phase coincides with increased expression of pro-growth cytokines, such as IFN- $\alpha$ , IL-12 and IL-2.

Interestingly, the non-specific proliferative capability of PBMC eventually subsided during the early-acute phase of hepatitis (4-6 w.p.i., see Figure 5.5) and was accompanied by the reduced expression of pro-growth cytokines mentioned above. The lymphocytes collected during this phase of WHV infection also displayed elevated expression of IL-10, shown by others to adversely influence mitogen-induced proliferation of lymphocytes from HIV-infected individuals (Clerici *et al.*, 1994). Thus, the absence of IL-2 and IFN- $\alpha$ /IL-12, essential for sustaining lymphocyte growth, in the presence of IL-10, could halt the enhanced proliferative capacities in these cells, as evidenced by lower adenine incorporation and higher rates of apoptosis in woodchuck PBMC during this phase of WHV infection (see Figure 5.6). Further, these non-specific proliferative capacities of the woodchuck lymphocytes further rebound during acute phase, albeit at lower magnitudes than those observed during the pre-acute phase of infection. During this phase, the increased expression of IL-2, IL-12 and IFN- $\alpha$  reappears along with IFN- $\gamma$  and TNF- $\alpha$ . It is well-known that IFN- $\gamma$  has a

potential to impair the proliferation of T lymphocytes, while TNF- $\alpha$  can decrease IFN- $\alpha$ -driven blastogenesis of NK cells (Orange *et al.*, 1996). This type of cytokine milieu during the acute phase of hepadnaviral infection could ensure sub-optimal levels of non-specific proliferative capacities in PBMC, despite the presence of IL-2, IFN- $\alpha$  and IL-12 and, most probably owing to the strong expression of IFN- $\gamma$  and TNF- $\alpha$  (Figure 7.1).

Considering the lack of information on the early events of innate immunity that precede or accompany the initiation of anti-hepadnavirus adaptive immune response, we also investigated the connection between the gene expression profile of cytokines and cell surface markers in PBMC and its possible contribution in shaping the delayed arise of WHV-specific T cell response. This gene expression analysis showed that, immediately after exposure to virus PBMC had transiently elevated IFN- $\alpha$  in the complete absence of TNF- $\alpha$  upregulation up to 6 w.p.i.. The invasion of host with a viral pathogen is known to induce strong expression of type I interferons and TNF- $\alpha$ , which activate NK cells and APCs that, subsequently, aid in the initiation of virus-specific T cell response. Especially, TNF- $\alpha$  expression triggered by virus infection drives the differentiation of immature DCs from its precursors (Res sousa *et al.*, 1999, Iwamoto *et al.*, 2007). On the contrary, the absence of such a TNF- $\alpha$  expression induces improper maturation phenotype and functional impairment in APCs as characterized by impaired antigen-specific and allo-stimulatory capacities of these cells (Dauer et

**Figure 7.1** A proposed model depicting impaired immune responses occurring during hepadnavirus infection. Immediately after exposure to hepadnavirus (pre-acute phase) the expression of pro-growth cytokines, e.g., IFN- $\alpha$ , IL-12 and IL-2, in peripheral lymphoid cells is increased, which can drive and sustain the heightened non-specific proliferative capacities of PBMC observed *in vitro* after stimulation with mitogens. Although, this pre-acute infection fails to induce the expression of TNF- $\alpha$  and IFN- $\gamma$  in lymphoid cells, which can possibly lead to the inappropriate activation of APCs, and transpires in undetectable virus-specific T cell reactivity. This elevated expression of pro-growth cytokines is drastically reduced in PBMC during the early-acute phase, that may endow lymphocytes with impaired capacity to proliferate and an increased susceptibility to undergo apoptosis after either virus-specific or mitogenic stimulation. Finally, during the acute phase of infection, lymphocytes synchronously display the augmented expression of IFN- $\alpha$ , IL-12, TNF- $\alpha$ , IFN- $\gamma$ , IL-2, IL-4 and IL-10, with a potential to initiate antigen-specific immune response and sustain higher proliferative capacities of lymphocytes. The decreased or absence of the expression of a respective cytokine during different phases of hepadnavirus infection is indicated by the grey boxes.

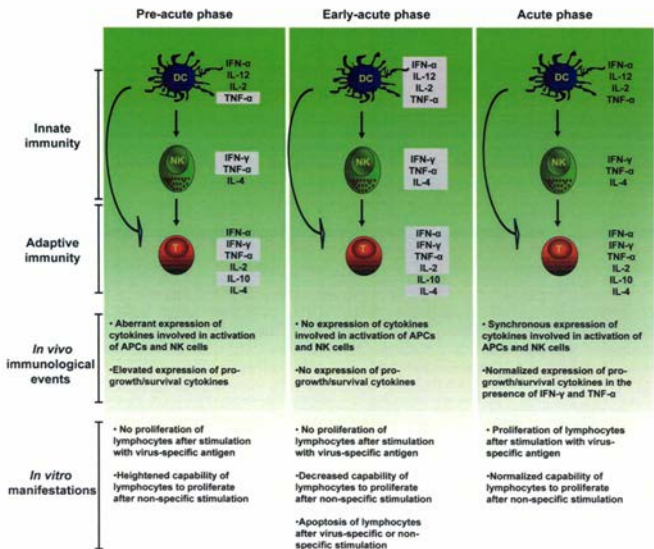


Figure 7.1

al., 2003, McRae *et al.*, 2007). DCs cultured in the presence of IFN- $\alpha$  and TNF- $\alpha$  together, show strong expression of CD80, CD83 and CD86 (Chen *et al.*, 1998; Kadowaki *et al.*, 2000), similar to those generated after *in vitro* herpes simplex virus (HSV) infection, suggesting the synergistic potential of these two cytokines in activating APCs. Similar maturation of DCs initiated after LCMV infection can be abolished by the administration of anti-TNF- $\alpha$  antibodies in infected mice, suggesting the vital role of TNF- $\alpha$  during the differentiation and maturation of DCs (Kadowaki *et al.*, 2000). Thus, the prompt expression of TNF- $\alpha$  after infection is accompanied by proper activation of APCs that is subsequently associated with presence or absence of antigen-specific adaptive immunity. However, along with IFN- $\alpha$  and TNF- $\alpha$  expression, the initiation of effective antiviral immunity also requires synchronous expression of other cytokines such as IL-12, IL-2, IL-4 and IL-10 (Andoniou *et al.*, 2005). Taken together, our data in conjunction with others, suggested that the absence of TNF- $\alpha$ , coupled with non-synchronous expression of other innate cytokines during pre-acute and the early-acute phase of WHV infection (i.e., up to 6 w.p.i., see Figure 5.7) could translate in inappropriate differentiation and activation of DCs, which then fails to prime anti-viral adaptive immunity as evidenced by delayed appearance of WHV-specific T cell reactivity. Interestingly, DCs isolated from healthy individuals and exposed to HBV *in vitro* have impaired functional capacities (Beckebaum *et al.*, 2003), suggesting the inherent potential of hepadnavirus to induce the abnormal immune responses mediated by APCs.

Apart from its immunological role, TNF- $\alpha$  released after pathogen invasion also triggers platelet activation and local blood vessel clotting, that restricts the local dissemination of virus. Thus, the prompt expression of TNF- $\alpha$  is also involved in hampering the pathogen spread by maneuvering the microvasculature-tissue barrier. It is believed that the absence of such a host immune response immediately after exposure to virus represents another possible immune evasion mechanism that may aid in establishing a replication niche and consequent hepadnaviral persistence. In the clinical situation, patients exposed to HBV show lack of TNF- $\alpha$ -induced symptoms during the pre-acute phase of infection, e.g., fever and nausea (Webster *et al.*, 2000; Bertolotti and Gehring, 2006). This observation is consistent with our finding regarding the absence of TNF- $\alpha$  expression in WHV-infected woodchucks immediately after exposure to the virus.

The present study also evaluated whether innate and adaptive immune responses are initiated by WHV POI in the woodchucks infected with low, liver-nonpathogenic doses of virus. Intriguingly, infection of woodchucks with 50 virions triggered a WHV-specific T cell proliferative response, with the kinetics comparable to that observed during symptomatic infection induced by a liver-pathogenic dose of the same virus. The appearance of this virus-specific T cell response initiated after low dose infection was again delayed up to 6-10 w.p.i., as measured in the CFSE-based assay. This observation was in agreement with the previous findings made during asymptomatic HCV (Quiroga *et al.*, 2006;

Kamal *et al.*, 2004, Koziel *et al.*, 1997), HIV (Promadej *et al.*, 2003) and SIV (Tasca *et al.*, 2007) infections, wherein detectable T cell proliferative reactivity was observed in the individuals or animals exposed to virus in the absence of serological or pathological evidence of respective infections. Thus, the results implied that exposure to small quantities of hepadnavirus can induce virus-specific T cell responses with similar profiles of appearance as those observed during symptomatic infection. Nonetheless, the WHV-specific T cell proliferative reactivities detected during POI were sustained at higher magnitudes for a relatively lesser time period than those observed during symptomatic infection. It is possible that during POI, the small amount of invading virus and resultant low level of antigenic stimuli may result in earlier protraction of the stronger WHV-specific T cell proliferative reactivities.

The virus-specific T cell responses observed during WHV POI persisted in the absence of any detectable anti-viral antibody responses. Thus, even though the magnitude of the anti-viral T cell responses was comparable to that during symptomatic infection, the qualitative traits of this response during POI and AH could be different. This hypothesis was further supported by the fact that the virus-specific T cell responses developed during POI failed to protect the animals with established POI against AH after challenge with a liver-pathogenic dose of the same virus. This observation was in contrast to an otherwise well established fact that the virus-specific T cell responses induced after primary exposure to hepadnavirus endows the protection against hepatitis that consequents after

challenge with the same virus. Thus, our results suggested that virus-specific T cell responses accompanying POI may bear differential qualitative features than those accompanying serologically evident hepadnaviral infection.

Additionally, the woodchucks infected with low doses of WHV also displayed similarly discordant profiles of virus-specific and mitogen-induced lymphocyte proliferative reactivities in serially collected PBMC. The comparative analysis of these responses with those observed during symptomatic WHV infection indirectly suggested that such inverse profiles of lymphocyte proliferative responsiveness is a hallmark of hepadnavirus infection in general, and is independent of the dose of invading virus. Also, this type of T cell proliferative responsiveness after mitogenic or virus-specific stimulation is independent of the memory immune response status of the animals, as these discordant responses were equally detectable after the challenge of woodchucks with POI and those recovered from WHV-induced AH. This type of discordant relationship between augmented non-specific and delayed antigen-specific lymphocyte proliferative reactivities following exposure or re-exposure to the virus seems to be a characteristic immunological feature of contact with hepadnavirus, irrespective of virus dose.

Similar to the kinetics of WHV-specific T cell responses, the gene expression profiles of selected innate cytokines in the serial, unmanipulated PBMC collected during POI were comparable to those identified during symptomatic WHV infection. Our data showed that, immediately after exposure

of the woodchucks to low WHV dose, PBMC displayed increased transcription of IFN- $\alpha$ , IL-12 and IL-2 (i.e., between 1-3 w.p.i.), but not that of TNF- $\alpha$ . The elevated expression of these above mentioned cytokines decreased between 4-6 w.p.i., and then increased 7 w.p.i. onwards, accompanied by slightly elevated TNF- $\alpha$  expression. As discussed above for symptomatic infection, such an aberrant expression of innate cytokines, especially IFN- $\alpha$  and TNF- $\alpha$ , early after exposure to hepadnavirus is also believed to result in the postponement of the development of virus-specific T cell response during hepadnaviral POI. Again, such an impaired expression of cytokines immediately after exposure to hepadnavirus seem to be independent of the dose of invading virus.

Nonetheless, the profile of cytokine gene expression during POI also displayed some inherent discrepancies with that observed during infection with high dose. Among others, the expression of TNF- $\alpha$  during POI was quantitatively different than that observed during symptomatic infection. This expression of TNF- $\alpha$  in PBMC collected during POI was only slightly elevated (mean fold increase  $2.0 \pm 0.4$ ) as compared to the robust increase (mean fold increase  $18.5 \pm 4.3$ ) detected during symptomatic infection. It is speculated that this quantitative difference in the TNF- $\alpha$  expression could be associated with the differential potential of virus-specific T cell response developed during POI, since the animals with POI are not protected against AH caused by challenge with high dose of the same virus. Further, in contrast to symptomatic infection, PBMC collected during POI did not show increased expression of IL-4 and IL-10, which may also contribute to the

absence of anti-viral antibody responses.

Another interesting finding made during WHV POI was the induction of the significantly stronger upregulation of the intra-hepatic IFN- $\alpha$  expression, in the absence of elevated expression of IFN- $\gamma$ , TNF- $\alpha$ , IL-4 or CD3, after exposure to low dose as compared to that observed before infection. Such an induction of IFN- $\alpha$  expression in the liver was surprising, considering the fact that after inoculation with low dose of WHV, virus detection is restricted to the lymphatic system, as previously reported (Michalak *et al.*, 1999; Michalak *et al.*, 2004; Mulrooney *et al.*, 2008) as well as observed in this study. The induction of a strong IFN- $\alpha$  response in the liver during POI indicates that this innate anti-viral cytokine response is in fact initiated, and could be sufficient in protecting hepatocytes against the minuscule quantities of invading virus. Further, this elevated intra-hepatic expression of IFN- $\alpha$  was not evident after either infection of WHV-naive animals or challenge of animals with POI with a liver pathogenic dose of the same virus, supporting the previously proposed hypothesis that infection with a liver pathogenic dose of hepadnavirus mediates the impaired activation of innate response in the livers of infected animals. It is possible that, unlike the innate response in the peripheral lymphoid cells, the intrahepatic impairment of IFN- $\alpha$  expression requires the presence of higher loads of virus in the liver.

In conclusion, our study has shown that the exposure to hepadnavirus induces aberrant profiles of virus-specific and mitogen-induced T cell, as well as

innate cytokine responses, irrespective of the dose of invading virus. This type of impaired immune responsiveness may facilitate the establishment of hepadnavirus replication early after infection and may aid in the subsequent virus persistence. In future, it will be imperative to evaluate whether such an impairment of immune responses also occurs during the early phase of natural HBV infection with either liver nonpathogenic or pathogenic dose of the virus. The understanding of the the mechanisms underlying the kinetics of these impaired immune responses should establish a basis for design of prophylactic and therapeutic interventions to prevent development of long-term pathological consequences of HBV infection, including CH, cirrhosis and HCC.

## 7.2 FUTURE DIRECTIONS

The data obtained during this study has unveiled new aspects of immune responses occurring after exposure to hepadnavirus. These novel findings, along with availability of newly generated assays and reagents, have prompted further investigations on other features of WHV infection in the woodchuck model of hepatitis B, such as:

1. Implementation of biologically active wL-2 for the generation of WHV-specific T lymphocyte clones. Since it is known that HBV-specific T cell clones produced using lymphocytes from HBV-infected patients can provide valuable insight into the functional traits of ongoing virus-specific T cell responses, further studies could be aimed at generating WHV antigen-specific T cell clones *in vitro*. This

can be achieved by maintaining long term cultures of T lymphocytes derived from WHV-infected woodchucks in the presence of biologically active rIL-2 and the respective WHV antigenic peptide. This approach will be more beneficial in obtaining woodchuck T cell clones from intrahepatic lymphocytes (IHLs), especially considering the fact that these IHLs are scarcely available for the analysis due to the constraint on the size of the liver sample that can be harvested during biopsy.

2. Comparative analysis of proliferative and functional capabilities of virus-specific lymphocytes during different phases of hepadnavirus infection. The pertinent functional integrity of the antigen-specific T lymphocyte is defined by the ability of these lymphocytes to proliferate, as well as produce cytokines, especially IFN- $\gamma$ , after stimulation with their cognate antigen *in vitro*. The inability of the lymphocytes to either proliferate or produce IFN- $\gamma$  during these *in vitro* evaluations reflects an anergic or functional impairment. Our study has revealed that serial PBMC samples obtained after exposure to different doses of WHV display discordance between WHV-specific proliferation and intracellular IFN- $\gamma$  gene expression. This observation raises the possibility that these virus-specific T cells may have an anergic phenotype, especially during the early phase of infection. Further, current evaluations of IFN- $\gamma$  gene expression in PBMC samples do not identify the particular subset of lymphocytes in which this elevated expression occurs. To address this issue, PBMC samples collected during different phases of WHV infection can be labeled with CFSE, stimulated

with WHV antigens *ex vivo*, stained with newly identified anti-IFN- $\gamma$  antibodies (Jenkins and Michalak, personal communication) and then analyzed simultaneously for proliferation and intracellular expression of IFN- $\gamma$ . Such a comprehensive evaluation of virus-specific lymphocyte response during resolving AH or progressing CH will provide further insight into the role of these immune responses in determining the outcome of hepadnaviral infection.

### 3. Investigation of TNF- $\alpha$ expression immediately after hepadnaviral infection.

The analysis of cytokine gene expression in the serial PBMC samples revealed that the expression of TNF- $\alpha$  is not augmented until later during AH. Since, the PBMC samples were usually collected on a weekly basis during this study, the first sample available for analysis was obtained at 7 days post-exposure. However, IFN- $\alpha$  and TNF- $\alpha$  responses can be triggered very promptly after virus invasion. Hence, PBMC samples collected within the first few hours after exposure to WHV and on a daily basis for 7-10 days post-infection should be analyzed in future, to verify whether the absence of TNF- $\alpha$  expression was an immediate consequence of hepadnaviral infection. Alternatively, the expression of TNF- $\alpha$  as well as other cytokines can also be studied under *in vitro* conditions by exposing PBMC collected from WHV-naïve woodchucks to different doses of WHV.

### 4. Inhibition of the postponement of WHV-specific T cell response in woodchucks using rwTNF- $\alpha$ .

Attempts could be made to over-ride the effects of the absence of TNF- $\alpha$  by injecting biologically active rwTNF- $\alpha$ , immediately after

experimental exposure to WHV. Of course, utmost care should be taken to titrate the dose of rwTNF- $\alpha$  to be administered in order to avoid potential development of systemic shock. It can be anticipated that the presence of artificially provided rwTNF- $\alpha$ , along with inherently expressed IFN- $\alpha$  and IL-12 induced by WHV infection, could induce proper activation of APCs resulting in the prompt arise of virus-specific T cell response and successive resolution of infection. Alternatively, freshly isolated PBMC collected immediately after infection can be treated *ex vivo* with rwTNF- $\alpha$  and transferred back into the same animal. The success of this approach in promoting early development of virus-specific T cell response could translate in an efficient clinical treatment regimen preventing development of CH and HCC.

## REFERENCES

- Akbar A. N., N. Borthwick, M. Salmon, W. Gombert, M. Bofill, N. Shamsadeen, D. Pilling, S. Pett, J. E. Grundy, and G. Janossy. 1993. The significance of low bcl-2 expression by CD45RO T cells in normal individuals and patients with acute viral infections. The role of apoptosis in T cell memory. *J. Exp. Med.* 178:427-438.
- Akira S., K. Takeda, and T. Kaisho. 2001. Toll-like receptors: critical proteins linking innate and acquired immunity. *Nat. Immunol.* 2:675-680.
- Allan J. E., G. R. Shellam, and J. E. Grundy. 1982. Effect of murine cytomegalovirus infection on mitogen responses in genetically resistant and susceptible mice. *Infect. Immun.* 36:235-42.
- Ando K., L. G. Guidotti, S. Wirth, T. Ishikawa, G. Missale, T. Moriyama, R. D. Schreiber, H. J. Schlicht, S. N. Huang, and F. V. Chisari. 1994. Class I-restricted cytotoxic T lymphocytes are directly cytopathic for their target cells in vivo. *J. Immunol.* 152:3245-3253.
- Andoniou C. E., S. L. van Dommelen, V. Voigt, D. M. Andrews, G. Brizard, C. Asselin-Paturel, T. Delale, K. J. Stacey, G. Trinchieri, and M. A. Degli-Esposti. 2005. Interaction between conventional dendritic cells and natural killer cells is integral to the activation of effective antiviral immunity. *Nat. Immunol.* 6:1011-1019.
- Angulo R., and D. A. Fulcher. 1998. Measurement of *Candida*-specific blastogenesis: comparison of carboxyfluorescein succinimidyl ester labeling of T cells, thymidine incorporation, and CD69 expression. *Cytometry* 34:143-151.
- Araki K., J. Miyazaki, O. Hino, N. Tomita, O. Chisaka, K. Matsubara, and K. Yamamura. 1989. Expression and replication of hepatitis B virus genome in transgenic mice. *Proc. Natl. Acad. Sci. USA* 86:207-211.
- Arima S., S. M. Akbar, K. Michitaka, N. Horiike, H. Nuriya, M. Kohara, and M. Onji. 2003. Impaired function of antigen-presenting dendritic cells in patients with chronic hepatitis B: localization of HBV DNA and HBV RNA in blood DC by in situ hybridization. *Int. J. Mol. Med.* 11:169-174.
- Asada M., and J. T. Galambos. 1963. Sorbitol dehydrogenase and hepatocellular injury: An experimental and clinical study. *Gastroenterology* 44:578-587.

- Asselin-Paturel C., A. Boonstra, M. Dalod, I. Durand, N. Yessaad, C. Dezutter-Dambuyant, A. Vicari, A. O'Garra, C. Biron, F. Brière, and G. Trinchieri. 2001. Mouse type I IFN-producing cells are immature APCs with plasmacytoid morphology. *Nat. Immunol.* 2:1144-1150.
- Babinet C., H. Farza, D. Morello, M. Hadchouel, and C. Pourcel. 1985. Specific expression of hepatitis B surface antigen (HBsAg) in transgenic mice. *Science* 230:1160-1163.
- Baron J. L., L. Gardiner, S. Nishimura, K. Shinkai, R. Locksley, and D. Ganem. 2002. Activation of a nonclassical NKT cell subset in a transgenic mouse model of hepatitis B virus infection. *Immunity* 16:583-994.
- Barrault D. V., M. Steward, V. F. Cox, R. A. Smith, A. M. Knight. 2005. Efficient production of complement (C3d)3 fusion proteins using the baculovirus expression vector system. *J. Immunol. Methods* 304:158-173.
- Bazan J. F. 1992. Unraveling the structure of IL-2. *Science* 257:410-413.
- Beasley R. P., L. Y. Hwang, C. C. Lin, and C. S. Chien. 1981. Hepatocellular carcinoma and hepatitis B virus. A prospective study of 22 707 men in Taiwan. *Lancet* 2:1129-1133.
- Beckebaum S., V. R. Cicinnati, X. Zhang, S. Ferencik, A. Frilling, H. Grosse-Wilde, C. E. Broelsch, and G. Gerken. 2003. Hepatitis B virus-induced defect of monocyte-derived dendritic cells leads to impaired T helper type 1 response in vitro: mechanisms for viral immune escape. *Immunology* 109:487-495.
- Behar S. M., and S. A. Porcelli. 2007. CD1-restricted T cells in host defense to infectious diseases. *Curr. Top. Microbiol. Immunol.* 314:215-250.
- Belani R., and G. J. Weiner. 1999. Expression of both B7-1 and CD28 contributes to the IL-2 responsiveness of CTLL-2 cells. *Immunology* 87:271-274.
- Bendelac A., P. B. Savage, and L. Teyton. 2007. The biology of NKT cells. *Annu. Rev. Immunol.* 25:297-336.
- Bendelac A., M. N. Rivera, S. H. Park, and J. H. Roark. 1997. Mouse CD1-specific NK1 T cells: development, specificity, and function. *Annu. Rev. Immunol.* 15:535-562.
- Bernard S., L. Pujo-Menjouet, and M. C. Mackey. 2003. Analysis of cell kinetics using a cell division marker: mathematical modeling of experimental data.

Biophys. J. 84:3414-3424.

Bertoletti A., M. M. D'Elíos, C. Boni, M. De Carli, A. L. Zignego, M. Durazzo, G. Missale, A. Penna, F. Fiaccadori, G. Del Prete, and C. Ferrari. 1997. Different cytokine profiles of intraphepatic T cells in chronic hepatitis B and hepatitis C virus infections. *Gastroenterology* 112:193-199.

Bertoletti A., A. Costanzo, F. V. Chisari, M. Levrero, M. Artini, A. Sette, A. Penna, T. Giuberti, F. Fiaccadori, C. Ferrari. 1994. Cytotoxic T lymphocyte response to a wild type hepatitis B virus epitope in patients chronically infected by variant viruses carrying substitutions within the epitope. *J. Exp. Med.* 180:933-943.

Bertoletti A. and A. J. Gehring. 2006. The immune response during hepatitis B virus infection. *J. Gen. Virol.* 87:1439-1349.

Bertoletti A. and C. Ferrari. 2003. Kinetics of the immune response during HBV and HCV infection. *Hepatology* 38:4-13.

Bertoni R., A. Sette, J. Sidney, L. G. Guidotti, M. Shapiro, R. Purcell, F. V. Chisari. 1998. Human class I supertypes and CTL repertoires extend to chimpanzees. *J. Immunol.* 161:4447-4455.

Bertoni R., J. Sidney, P. Fowler, R. W. Chesnut, F. V. Chisari, and A. Sette. 1997. Human histocompatibility leukocyte antigen-binding supermotifs predict broadly cross-reactive cytotoxic T lymphocyte responses in patients with acute hepatitis. *J. Clin. Invest.* 100:503-513.

Biron C. A. and R. M. Welsh. 1982. Blastogenesis of natural killer cells during viral infection in vivo. *J. Immunol.* 129:2788-2795.

Biron C. A., G. Sonnenfeld, and R. M. Welsh. 1984. Interferon induces natural killer cell blastogenesis in vivo. *J. Leukoc. Biol.* 35:31-37.

Blackman M. A., M. A. Tigges, M. E. Minie, M. A. Koshland. 1986. A model system for peptide hormone action in differentiation: interleukin-2 induces a B lymphoma to transcribe the J chain gene. *Cell* 47:609-617.

Blumberg B. S. 2002. *Hepatitis B. The Hunt for a Killer Virus*, Princeton University Press.

Boni C., A. Bertoletti, A. Penna, A. Cavalli, M. Pilli, S. Urbani, P. Scognamiglio, R. Boehme, R. Panebianco, F. Fiaccadori, C. Ferrari. 1998. Lamivudine treatment can restore T cell responsiveness in chronic hepatitis B. *J. Clin. Invest.* 102:968-975.

- Brechot C. 2004. Pathogenesis of hepatitis B virus-related hepatocellular carcinoma: old and new paradigms. *Gastroenterology* 127: S56-S61.
- Brechot C., V. Thiers, D. Kremsdorf, B. Nalpas, S. Pol, and P. Paterlini-Brechot. 2001. Persistent hepatitis B virus infection in subjects without hepatitis B surface antigen: clinically significant or purely "occult"? *Hepatology* 34:194-203.
- Bruss V., J. Hagelstein, E. Gerhardt, and P. R. Galle. 1996b. Myristylation of the large surface protein is required for hepatitis B virus in vitro infectivity. *Virology* 218:396-399.
- Bruss V., E. Gerhardt, K. Vieluf, and G. Wunderlich. 1996a. Functions of the large hepatitis B virus surface protein in viral particle morphogenesis. *Intervirology* 39:23-31.
- Budkowska A., P. Dubreuil, T. Poynard, P. Marcellin, M. A. Liorot, P. Maillard, J. Pillot. 1992. Anti-pre-S responses and viral clearance in chronic hepatitis B virus infection. *Hepatology* 15:26-31.
- Budkowska A., P. Dubreuil, W. H. Gerlich, Y. Lazizi, and J. Pillot. 1988. Occurrence of pre-S1 antigen in viremic and nonviremic carriers of hepatitis B surface antigen. *J. Med. Virol.* 26:217-225.
- Burk R. D., J. A. DeLoia, M. K. elAwady, and J. D. Gearhart. 1988. Tissue preferential expression of the hepatitis B virus (HBV) surface antigen gene in two lines of HBV transgenic mice. *J. Virol.* 62:649-654.
- Cabatingan M. S., M. R. Schmidt, R. Sen, R. T. Woodland. 2002. Naive B lymphocytes undergo homeostatic proliferation in response to B cell deficit. *J. Immunol.* 169:6795-6805.
- Callan M. F., L. Tan, N. Annels, G. S. Ogg, J. D. Wilson, C. A. O'Callaghan, N. Steven, A. J. McMichael, and A. B. Rickinson. 1998. Direct visualization of antigen-specific CD8+ T cells during the primary immune response to Epstein-Barr virus *In vivo*. *J. Exp. Med.* 187:1395-1402.
- Cardin R. D., J. W. Brooks, S. R. Sarawar, P. C. Doherty. 1996. Progressive loss of CD8+ T cell-mediated control of a gamma-herpesvirus in the absence of CD4+ T cells. *J. Exp. Med.* 184:863-871.
- Carson W. E., T. A. Fehniger, S. Haldar, K. Eckhert, M. J. Lindemann, C. F. Lai, C. M. Croce, H. Baumann, M. A. Caligiuri, 1997. A potential role for interleukin-15 in the regulation of human natural killer cell survival. *J. Clin. Invest.* 99:937-943.

Cavanaugh V. J., L. G. Guidotti, and F. V. Chisari. 1998. Inhibition of hepatitis B virus replication during adenovirus and cytomegalovirus infections in transgenic mice. *J. Virol.* 72:2630-2637.

Cavanaugh V. J., L. G. Guidotti, and F. V. Chisari. 1997. Interleukin-12 inhibits hepatitis B virus replication in transgenic mice. *J. Virol.* 71:3236-3243.

Cerretti D. P., K. McKereghan, A. Larsen, M. A. Cantrell, D. Anderson, S. Gillis, D. Cosman, P. E. Baker. 1986. Cloning, sequence, and expression of bovine interleukin 2. *Proc. Natl. Acad. Sci. USA* 83:3223-3227

Chang J. J., and S. R. Lewin. 2007. Immunopathogenesis of hepatitis B virus infection. *Immunol. Cell Biol.* 85:16-23.

Chang S. F., H. J. Netter, M. Bruns, R. Schneider, K. Frolich, and H. Will. 1999. A new avian hepadnavirus infecting snow geese (*Anser caerulescens*) produces a significant fraction of virions containing single-stranded DNA. *Virology* 262:39-54.

Chemin I., C. Vermot-Desroches, I. Baginski, J. C. Saurin, F. Laurent, F. Zoulim, J. Bernaud, J. P. Lamelin, O. Hantz, and D. Rigal. 1994. Selective detection of human hepatitis B virus surface and core antigens in peripheral blood mononuclear cell subsets by flow cytometry. *J. Viral. Hepat.* 1:39-44.

Chen J. C., M. L. Chang, and M. O. Muench. 2003. A kinetic study of the murine mixed lymphocyte reaction by 5,6-carboxyfluorescein diacetate succinimidyl ester labeling. *J. Immunol. Methods* 279:123-133.

Chen Y., R. Sun, W. Jiang, H. Wei, and Z. Tian. 2007. Liver-specific HBsAg transgenic mice are over-sensitive to Poly(I:C)-induced liver injury in NK cell- and IFN-gamma-dependent manner. *J. Hepatol.* 47:183-190.

Chen H. S., M. C. Kew, W. E. Hornbuckle, B. C. Tennant, P. J. Cote, J. L. Gerin, R. H. Purcell, and R. H. Miller. 1992. The precore gene of the woodchuck hepatitis virus genome is not essential for viral replication in the natural host. *J. Virol.* 66:5682-5684.

Chen Y., H. Wei, R. Sun, and Z. Tian. 2005. Impaired function of hepatic natural killer cells from murine chronic HBsAg carriers. *Int. Immunopharmacol.* 13-14:1839-1852.

Chisari F. V., and C. Ferrari. 1995. Hepatitis B virus immunopathogenesis. *Annu. Rev. Immunol.* 13:29-60.

Chisari F. V. 2000. Viruses, immunity, and cancer: lessons from hepatitis B. *Am J. Pathol.* 156:1117-1132.

Chisari F. V. 1995. Hepatitis B virus transgenic mice: insights into the virus and the disease. *Hepatology* 22:1316-1325.

Chisari F.V. 1997. Cytotoxic T cells and viral hepatitis. *J. Clin. Invest.* 99:1472-1477.

Chisari F. V., P. Filippi, J. Buras, A. McLachlan, H. Popper, C. Pinkert, R. D. Palmiter, and R. L. Brinster. 1987. Structural and pathological effects of synthesis of hepatitis B virus large envelope polypeptide in transgenic mice. *Proc. Natl. Acad. Sci. USA* 84:6909-6913.

Chisari F. V., C. A. Pinkert, D. R. Milich, P. Filippi, A. McLachlan, R. D. Palmiter, and R. L. Brinster. 1985. A transgenic mouse model of the chronic hepatitis B surface antigen carrier state. *Science* 230:1157-1160.

Chisari F. V. 1996. Hepatitis B virus transgenic mice: models of viral immunobiology and pathogenesis. *Curr. Top. Microbiol. Immunol.* 206:149-173.

Chiu Y. H., J. Jayawardena, A. Weiss, D. Lee, S. H. Park, A. Dautry-Varsat, and A. Bendelac. 1999. Distinct subsets of CD1d-restricted T cells recognize self-antigens loaded in different cellular compartments. *J. Exp. Med.* 189:103-110.

Chiu N. M., T. Chun, M. Fay, M. Mandal, and C. R. Wang. 1999. The majority of H2-M3 is retained intracellularly in a peptide-receptive state and traffics to the cell surface in the presence of N-formylated peptides. *J. Exp. Med.* 190, 423-434.

Choo K. B., L. N. Liew, K. Y. Chong, R. H. Lu, and W. T. Cheng. 1991. Transgenome transcription and replication in the liver and extrahepatic tissues of a human hepatitis B virus transgenic mouse. *Virology* 182:785-792.

Clerici M., A. Sarin, R. L. Coffman, T. A. Wynn, S. P. Blatt, C. W. Hendrix, S. F. Wolf, G. M. Shearer, and P. A. Henkart. 1994. Type 1/type 2 cytokine modulation of T-cell programmed cell death as a model for human immunodeficiency virus pathogenesis. *Proc. Natl. Acad. Sci. USA.* 91:11811-11815.

Cochran M. A., B. L. Ericson, J. D. Knell, G. E. Smith. 1987. Use of baculovirus recombinants as a general method for the production of subunit vaccines. *Vaccines* 87:384-388.

Coffin C. S., and T. I. Michalak. 1999. Persistence of infectious hepadnavirus in the offspring of woodchuck mothers recovered from viral hepatitis. *J. Clin. Invest.* 104:203-212.

Coffin C. S., T. N. Pham, P. M. Mulrooney, N. D. Churchill, T. I. Michalak. 2004. Persistence of isolated antibodies to woodchuck hepatitis virus core antigen is indicative of occult infection. *Hepatology* 40:1053-1061.

Cose S., C. Brammer, D. J. Zammit, D. A. Blair, and L. Lefrançois. 2006. CD4 T cells inhibit the CD8 T cell response during low-dose virus infection. *Int Immunol.* 18:1285-1293.

Cote P. J., B. E. Korba, R. H. Miller, J. R. Jacob, B. H. Baldwin, W. E. Hornbuckle, R. H. Purcell, B. C. Tennant, and J. L. Gerin. 2000. Effects of age and viral determinants on chronicity as an outcome of experimental woodchuck hepatitis virus infection. *Hepatology* 31:190-200.

Cote P. J., and J. L. Gerin. 1995. In vitro activation of woodchuck lymphocytes measured by radiopurine incorporation and interleukin-2 production: implications for modeling immunity and therapy in hepatitis B virus infection. *Hepatology* 22:687-699.

Couillin I., S. Pol, M. Mancini, F. Driss, C. Brechot, P. Tiollais, and M. L. Michel. 1999. Specific vaccine therapy in chronic hepatitis B: induction of T cell proliferative responses specific for envelope antigens. *J. Infect. Dis.* 180:15-26.

Coursaget P., P. Adamowicz, C. Bourdil, B. Yvonnet, Y. Buisson, J. L. Barrès, P. Saliou, J. P. Chiron, and I. D. Mar. 1988. Anti-pre-S2 antibodies in natural hepatitis B virus infection and after immunization. *Vaccine* 6:357-361.

Dauer M., K. Pohl, B. Obermaier, T. Meskendahl, J. Röbe, M. Schnurr, S. Endres, and A. Eigler. 2003. Interferon-alpha disables dendritic cell precursors: dendritic cells derived from interferon-alpha-treated monocytes are defective in maturation and T-cell stimulation. *Immunology* 110:38-47.

De Lalla C., G. Galli, L. Aldrighetti, R. Romeo, M. Mariani, A. Monno, S. Nuti, M. Colombo, F. Callea, S. A. Porcelli, P. Panina-Bordignon, S. Abrignani, G. Casorati, and P. Dellabona. 2004. Production of profibrotic cytokines by invariant NKT cells characterizes cirrhosis progression in chronic viral hepatitis. *J. Immunol.* 173:1417-14125.

De Gast G. C., B. Houwen, G. K. van der Hem, and T. H. The. 1976. T-lymphocyte number and function and the course of hepatitis B in hemodialysis patients. *Infect Immun.* 14:1138-43.

- De Maria A., C. Cirillo, and L. Moretta. 1994. Occurrence of human immunodeficiency virus type 1 (HIV-1)-specific cytolytic T cell activity in apparently uninfected children born to HIV-1-infected mothers. *J. Infect. Dis.* 170:1296-1269.
- DeLoia J. A., R. D. Burk, and J. D. Gearhart. 1989. Developmental regulation of hepatitis B surface antigen expression in two lines of hepatitis B virus transgenic mice. *J. Virol.* 63:4069-4073.
- Dengler T. J., D. R. Johnson, and J. S. Pober. 2001. Human vascular endothelial cells stimulate a lower frequency of alloreactive CD8+ pre-CTL and induce less clonal expansion than matching B lymphoblastoid cells: development of a novel limiting dilution analysis method based on CFSE labeling of lymphocytes. *J. Immunol.* 166:3846-3854.
- Devos R., G. Plaetinck, H. Cheroutre, G. Simons, W. Degraeve, J. Tavernier, E. Remaut, W. Fiers. 1983. Molecular cloning of human interleukin 2 cDNA and its expression in *E. coli*. *Nucleic Acids Res.* 11:4307-4323.
- Diao J., N. D. Churchill, and T. I. Michalak. 1998. Complement-mediated cytotoxicity and inhibition of ligand binding to hepatocytes by woodchuck hepatitis virus-induced autoantibodies to asialoglycoprotein receptor. *Hepatology* 27:1623-1631.
- Diao J., A. A. Khine, F. Sarangi, E. Hsu, C. Iorio, L. A. Tibbles, J. R. Woodgett, J. Penninger, and C. D. Richardson. 2001. X protein of hepatitis B virus inhibits Fas-mediated apoptosis and is associated with up-regulation of the SAPK/JNK pathway. *J. Biol. Chem.* 276:8328-8340.
- Doherty D. G., S. Norris, L. Madrigal-Estebas, G. McEntee, O. Traynor, J. E. Hegarty, and C. O'Farrelly. 1999. The human liver contains multiple populations of NK cells, T cells, and CD3+CD56+ natural T cells with distinct cytotoxic activities and Th1, Th2, and Th0 cytokine secretion patterns. *J. Immunol.* 163:2314-2321.
- Doherty P. C. and J. P. Christensen. 2000. Accessing complexity: the dynamics of virus-specific T cell responses. *Annu. Rev. Immunol.* 18:561-92.
- Doherty D. G., and C. O'Farrelly. 2000. Innate and adaptive lymphoid cells in the human liver. *Immunol. Rev.* 174:5-20.
- Domingo D. L., and I. S. Trowbridge. 1988. Characterization of the human transferrin receptor produced in a baculovirus expression system. *J. Biol. Chem.* 263:13386-13392.

- Douglas D. D., H. F. Taswell, J. Rakela, and D. Rabe. 1993. Absence of hepatitis B virus DNA detected by polymerase chain reaction in blood donors who are hepatitis B surface antigen negative and antibody to hepatitis B core antigen positive from a United States population with a low prevalence of hepatitis B serologic markers. *Transfusion* 33:212-216.
- Dumitriu I. E., W. Mohr, W. Kolowos, P. Kern, J. R. Kalden, M. Herrmann. 2001. 5,6-carboxyfluorescein diacetate succinimidyl ester-labeled apoptotic and necrotic as well as detergent-treated cells can be traced in composite cell samples. *Anal. Biochem.* 299:247-252.
- Echevarria S., F. Casafont, M. Miera, J. L. Lozano, F. de la Cruz, G. San Miguel, and F. Pons Romero. 1991. Interleukin-2 and natural killer activity in acute type B hepatitis. *Hepatogastroenterology* 38:307-310.
- Eckenberg R. J. L. Moreau, O. Melnyk, J. Theze. 2000. IL-2R beta agonist P1-30 acts in synergy with IL-2, IL-4, IL-9, and IL-15: biological and molecular effects. *J. Immunol.* 165:4312-4431.
- Elmore L. W., A. R. Hancock, S. F. Chang, X. W. Wang, S. Chang, C. P. Callahan, D. A. Geller, H. Will, and C. C. Harris. 1997. Hepatitis B virus X protein and p53 tumor suppressor interactions in the modulation of apoptosis. *Proc. Natl. Acad. Sci. USA* 94:14707-14712.
- Farza H., M. Hadchouel, J. Scotto, P. Tiollais, C. Babinet, and C. Pourcel. 1988. Replication and gene expression of hepatitis B virus in a transgenic mouse that contains the complete viral genome. *J. Virol.* 62:4144-4152.
- Feighery C., J. F. Grealley, and D. G. Weir. 1980. Mitogen responsiveness in viral hepatitis and chronic active hepatitis: the role of reversible suppressive influences. *Gut* 9:738-744.
- Feitelson M. A., P. L. Marion, and W. S. Robinson. 1983. The nature of polypeptides larger in size than the major surface antigen components of hepatitis B and like viruses in ground squirrels, woodchucks, and ducks. *Virology* 130:76-90.
- Ferrari C., A. Penna, A. Bertoletti, A. Valli, A. D. Antoni, T. Giuberti, A. Cavalli, M. A. Petit, and F. Fiaccadori. 1990. Cellular immune response to hepatitis B virus-encoded antigens in acute and chronic hepatitis B virus infection. *J. Immunol.* 145:3442-3449.
- Ferrari, C., A. Bertoletti, A. Penna, A. Cavalli, A. Valli, G. Missale, M. Pilli, P. Fowler, T. Giuberti, and F. V. Chisari. 1991. Identification of immunodominant T

cell epitopes of the hepatitis B virus nucleocapsid antigen. *J. Clin. Invest.* 88:214-222.

Flynn K. J., G. T. Belz, J. D. Altman, R. Ahmed, D. L. Woodland, and P. C. Doherty. 1998. Virus-specific CD8+ T cells in primary and secondary influenza pneumonia. *Immunity* 8:683-691.

Frauwirth K. A., and C. B. Thompson. 2004. Regulation of T lymphocyte metabolism. *J. Immunol.* 172:4661-4665.

Fujioka H., P. J. Hunt, J. Rozga, G. D. Wu, D. V. Cramer, A. A. Demetriou, A. D. Moscioni. 1994. Carboxyfluorescein (CFSE) labelling of hepatocytes for short-term localization following intraportal transplantation. *Cell Transplant.* 3:397-408.

Fulcher D. A., A. B. Lyons, S. L. Korn, M. C. Cook, C. Koleda, C. Parish, B. Fazekas de St Groth, A. J. Basten. 1996. The fate of self-reactive B cells depends primarily on the degree of antigen receptor engagement and availability of T cell help. *J. Exp. Med.* 183:2313-2328.

Fulcher D., and S. Wong. 1999. Carboxyfluorescein succinimidyl ester-based proliferative assays for assessment of T cell function in the diagnostic laboratory. *Immunol. Cell Biol.* 77:559-564.

Funk A., M. Mhamdi, H. Will, H. Sirma. 2007. Avian hepatitis B viruses: molecular and cellular biology, phylogenesis, and host tropism. *World J. Gastroenterol.* 13:91-103.

Gaffen S. L., S. L. Wang, and M. E. Koshland. 1996. Expression of the immunoglobulin J chain in a murine B lymphoma is driven by autocrine production of interleukin-2. *Cytokine* 8:513-524.

Gaffen S.L. 2001. Signaling domains of the interleukin-2 receptor. *Cytokine* 14:63-77.

Gallimore A., A. Glithero, A. Godkin, A. C. Tissot, A. C. Plückthun, T. Elliott, H. Hengartner, and R. Zinkernagel. 1998. Induction and exhaustion of lymphocytic choriomeningitis virus-specific cytotoxic T lymphocytes visualized using soluble tetrameric major histocompatibility complex class I-peptide complexes. *J. Exp. Med.* 187:1383-1393.

Garb K. S., A. B. Stavitsky, and A. A. Mahmoud. 1981. Dynamics of antigen and mitogen-induced responses in murine Schistosomiasis japonica: in vitro comparison between hepatic granulomas and splenic cells. *J. Immunol.* 127:115-120.

- Gasque P. 2004. Complement: a unique innate immune sensor for danger signals. *Mol. Immunol.* 41:1089-1098.
- Geisse S., H. Gram, B. Kleuser, H. P. Kocher. 1996. Eukaryotic expression systems: a comparison. *Protein Expr. Purif.* 8:271-282.
- Gilles P. N., G. Fey, and F. V. Chisari. 1992. Tumor necrosis factor alpha negatively regulates hepatitis B virus gene expression in transgenic mice. *J. Virol.* 66:3955-3960.
- Gillis S., and K. A. Smith. 1977. Long term culture of tumour-specific cytotoxic T cells. *Nature* 268:154-156.
- Givan A. L., J. L. Fisher, M. G. Waugh, N. Bercovici, P. K. Wallace. 2004. Use of cell-tracking dyes to determine proliferation precursor frequencies of antigen-specific T cells. *Methods Mol. Biol.* 263:109-124.
- Gougeon M. L., H. Lecoœur, A. Dulioust, M. G. Enouf, M. Crouvoiser, C. Goujard, T. Debord, and L. Montagnier. 1996. Programmed cell death in peripheral lymphocytes from HIV-infected persons: increased susceptibility to apoptosis of CD4 and CD8 T cells correlates with lymphocyte activation and with disease progression. *J. Immunol.* 156:3509-3520.
- Granucci F., C. Vizzardelli, N. Pavelka, S. Feau, M. Persico, E. Virzi, M. Rescigno, G. Moro, P. Ricciardi-Castagnoli. 2001. Inducible IL-2 production by dendritic cells revealed by global gene expression analysis. *Nat. Immunol.* 2:882-888.
- Guidotti L. G. and F. V. Chisari. 2006. Immunobiology and pathogenesis of viral hepatitis. *Annu Rev Pathol.* 1:23-61.
- Guidotti L. G., B. Matzke, H. Schaller, and F. V. Chisari. 1995. High-level hepatitis B virus replication in transgenic mice. *J. Virol.* 69:6158-6169.
- Guidotti L. G., S. Guilhot, and F. V. Chisari. 1994. Interleukin-2 and alpha/beta interferon down-regulate hepatitis B virus gene expression in vivo by tumor necrosis factor-dependent and -independent pathways. *J. Virol.* 68:1265-1270.
- Guidotti L. G., K. Ando, M. V. Hobbs, T. Ishikawa, L. Runkel, R. D. Schreiber, F. V. Chisari. 1994. Cytotoxic T lymphocytes inhibit hepatitis B virus gene expression by a noncytolytic mechanism in transgenic mice. *Proc. Natl. Acad. Sci. USA* 91:3764-3768.

- Guidotti L. G., R. Rochford, J. Chung, M. Shapiro, R. Purcell, F. V. Chisari. 1999. Viral clearance without destruction of infected cells during acute HBV infection. *Science* 284:825-829.
- Guidotti L. G., and F. V. Chisari. 2001. Noncytolytic control of viral infections by the innate and adaptive immune response. *Ann. Rev. Immunol.* 19:65-91.
- Guilhot S., T. Miller, G. Cornman, and H. C. Isom. 1996. Apoptosis induced by tumor necrosis factor-alpha in rat hepatocyte cell lines expressing hepatitis B virus. *Am. J. Pathol.* 148:801-814.
- Guilhot S., L. G. Guidotti, and F. V. Chisari. 1993. Interleukin-2 downregulates hepatitis B virus gene expression in transgenic mice by a posttranscriptional mechanism. *J. Virol.* 67:7444-7449.
- Gujar S. A., and T. I. Michalak. 2005. Flow cytometric quantification of T cell proliferation and division kinetics in woodchuck model of hepatitis B. *Immunol. Investig.* 34:215-236.
- Gujar S. A., A. K. Jenkins, C. S. Guy, J. Wang, and T. I. Michalak. 2008. Aberrant Lymphocyte Activation Precedes Delayed Virus-Specific T-Cell Response after both Primary Infection and Secondary Exposure to Hepadnavirus in the Woodchuck Model of Hepatitis B Virus Infection. *J. Virol.* 82:6992-7008.
- Guy C. S., P. M. Mulrooney-Cousins, N. D. Churchill, and T. I. Michalak. 2008. Intrahepatic Expression of Genes Affiliated with Innate and Adaptive Immune Responses Immediately after Invasion and during Acute Infection with Woodchuck Hepadnavirus. 82:8579-8591
- Guy C. S., J. Wang, and T. I. Michalak. 2006. Hepatocytes as cytotoxic effector cells can induce cell death by CD95 ligand-mediated pathway. *Hepatology* 43:1231-1240.
- Hasemann C. A., and J. D. Capra. 1990. High-Level production of a functional immunoglobulin heterodimer in a baculovirus expression system. *Proc. Natl. Acad. Sci. USA* 87:3942-3946.
- Heise T., L. G. Guidotti, V. J. Cavanaugh, and F. V. Chisari. 1999. Hepatitis B virus RNA-binding proteins associated with cytokine-induced clearance of viral RNA from the liver of transgenic mice. *J. Virol.* 73:474-481.
- Ho I. C., J. C. Kim, S. J. Szabo, L. H. Glimcher. 1999. Tissue-specific regulation of cytokine gene expression. *Cold Spring Harb. Symp. Quant. Biol.* 64:573-584.

- Hodgkins P.D., J. H. Lee, and A. B. Lyons. 1996. B cell differentiation and isotype switching is related to division cycle number. *J. Exp. Med.* 184:277-281.
- Hodgson P. D., and T. I. Michalak. 2001. Augmented hepatic interferon gamma expression and T-cell influx characterize acute hepatitis progressing to recovery and residual lifelong virus persistence in experimental adult woodchuck hepatitis virus infection. *Hepatology* 34:1049-1059.
- Hodgson P. D., M. D. Grant, and T. I. Michalak. 1999. Perforin and Fas/Fas ligand-mediated cytotoxicity in acute and chronic woodchuck viral hepatitis. *Clin. Exp. Immunol.* 118:63-70.
- Hoofnagle J. H. and H. J. Alter. 1984. Chronic viral hepatitis. In: *Viral Hepatitis and Liver Diseases*, edited by G. N. Vyas, J. L. Dienstag & J. H. Hoofnagle, Grune and Stratton, Orlando, pp. 97-113.
- Hosken N. A., K. Shibuya, A. W. Heath, K. M. Murphy, and A. O'Garra. 1995. The effect of antigen dose on CD4+ T helper cell phenotype development in a T cell receptor-alpha beta-transgenic model. *J. Exp. Med.* 182:1579-1584.
- Hsu H. M., C. F. Lu, S. C. Lee, S. R. Lin, and D. S. Chen. 1999. Seroepidemiologic survey for hepatitis B virus infection in Taiwan: the effect of hepatitis B mass immunization. *J. Infect. Dis.* 179:367-370.
- Huang C. F., S. S. Lin, Y. C. Ho, F. L. Chen, C. C. Yang. 2006. The immune response induced by hepatitis B virus principal antigens. *Cell Mol. Immunol.* 3:97-106.
- Iizuka H., K. Ohmura, A. Ishijima, K. Satoh, T. Tanaka, F. Tsuda, H. Okamoto, Y. Miyakawa, and M. Mayumi. 1992. Corelation between anti-HBc titers and HBV DNA in blood units without detectable HbsAg. *Vox Sang.* 63:107-111.
- Ikeda K., H. Marusawa, Y. Osaki, T. Nakamura, N. Kitajima, Y. Yamashita, M. Kudo, T. Sato, and T. Chiba. 2007. Antibody to hepatitis B core antigen and risk for hepatitis C-related hepatocellular carcinoma: a prospective study. *Ann. Intern. Med.* 146:649-656.
- Iwamoto S., S. Iwai, K. Tsujiyama, C. Kurahashi, K. Takeshita, M. Naoe, A. Masunaga, Y. Ogawa, K. Oguchi, and A. Miyazaki. 2007. TNF-alpha drives human CD14+ monocytes to differentiate into CD70+ dendritic cells evoking Th1 and Th17 responses. *J. Immunol.* 179:1449-1457.
- Janeway C. A. Jr, and R. Medzhitov. 2002. Innate immune recognition. *Annu. Rev. Immunol.* 20:197-216.

Jin Y. M., N. D. Churchill, and T. I. Michalak. 1996. Protease-activated lymphoid cell and hepatocyte recognition site in the preS1 domain of the large woodchuck hepatitis virus envelope protein. *J. Gen. Virol.* 77:1837-1846.

Kadowaki N., S. Antonenko, J. Y. Lau, and Y. J. Liu. 2000. Natural interferon alpha/beta-producing cells link innate and adaptive immunity. *J. Exp. Med.* 192:219-226.

Kakimi K., L. G. Guidotti, Y. Koezuka, and F. V. Chisari. 2000. Natural killer T cell activation inhibits hepatitis B virus replication in vivo. *J. Exp. Med.* 192:921-930.

Kakimi K., T. E. Lane, S. Wieland, V. C. Asensio, I. L. Campbell, F. V. Chisari, and L. G. Guidotti. 2001. Blocking chemokine responsive to c-2/interferon (IFN- $\gamma$ ) inducible protein and monokine induced by IFN- $\gamma$  activity in vivo reduces the pathogenetic but not the antiviral potential of hepatitis B virus-specific cytotoxic T lymphocytes. *J. Exp. Med.* 194:1755-1766.

Kamal S. M., A. Amin, M. Madwar, C. S. Graham, Q. He, A. Al Tawil, J. Rasenack, T. Nakano, B. Robertson, A. Ismail, and M. J. Koziel. 2004. Cellular immune responses in seronegative sexual contacts of acute hepatitis C patients. *J. Virol.* 78:12252-12258.

Kawai T. and S. Akira. 2006. Innate immune recognition of viral infection. *Nat. Immunol.* 7:131-137.

Kidd I.M., and V. C. Emery. 1993. The use of baculoviruses as expression vectors. *Appl. Biochem. Biotechnol.* 42:137-159.

Kimura K., K. Kakimi, S. Wieland, L. G. Guidotti, and F. V. Chisari. 2002a. Interleukin-18 inhibits hepatitis B virus replication in the livers of transgenic mice. *J. Virol.* 76:10702-10707.

Kimura K., K. Kakimi, S. Wieland, L. G. Guidotti, and F. V. Chisari. 2002b. Activated intrahepatic antigen-presenting cells inhibit hepatitis B virus replication in the liver of transgenic mice. *J. Immunol.* 169:5188-5195.

Klinkert M. Q., L. Theilmann, E. Pfaff, and H. Schaller. 1986. Pre-S1 antigens and antibodies early in the course of acute hepatitis B virus infection. *J. Virol.* 58:522-525.

Kobayashi M., L. Fitz, M. Ryan, R. M. Hewick, S. C. Clark, S. Chan, R. Loudon, F. Sherman, B. Perussia, and G. Trinchieri. 1989. Identification and purification of natural killer cell stimulatory factor (NKSF), a cytokine with multiple biologic

effects on human lymphocytes. *J. Exp. Med.* 170:827-845.

Koike K., K. Moriya, S. Iino, H. Yotsuyanagi, Y. Endo, T. Miyamura, and K. Kurokawa. 1994. High-level expression of hepatitis B virus HBx gene and hepatocarcinogenesis in transgenic mice. *Hepatology* 19:810-819.

Korba B. E., F. V. Wells, B. Baldwin, P. J. Cote, B. C. Tennant, H. Popper, and J. L. Gerin. 1989. Hepatocellular carcinoma in woodchuck hepatitis virus-infected woodchucks: presence of viral DNA in tumor tissue from chronic carriers and animals serologically recovered from acute infections. *Hepatology* 9:461-470.

Koziel M. J., D. K. Wong, D. Dudley, M. Houghton, and B. D. Walker. 1997. Hepatitis C virus-specific cytolytic T lymphocyte and T helper cell responses in seronegative persons. *J. Infect. Dis.* 176:859-866.

Koup R. A., J. T. Safrit, Y. Cao, C. A. Andrews, G. McLeod, W. Borkowsky, C. Farthing, and D. D. Ho. 1994. Temporal association of cellular immune responses with the initial control of viremia in primary human immunodeficiency virus type 1 syndrome. *J. Virol.* 68:4650-4655.

Kreuzfelder E., S. Menne, S. Ferencik, M. Roggendorf, and H. Grosse-Wilde. 1996. Assessment of peripheral blood mononuclear cell proliferation by [2-3H]adenine uptake in the woodchuck model. *Clin. Immunol. Immunopathol.* 78:223-227.

Langlade-Demoyen P., N. Ngo-Giang-Huong, F. Ferchal, and E. Oksenhendler. 1994. Human immunodeficiency virus (HIV) nef-specific cytotoxic T lymphocytes in noninfected heterosexual contact of HIV-infected patients. *J. Clin. Invest.* 93:1293-1297.

Lavanchy D. 2004. Hepatitis B virus epidemiology, disease burden, treatment, and current and emerging prevention and control measures. *J. Viral Hepat.* 11:97-107.

Lew Y. Y., and T. I. Michalak. 2001. In vitro and in vivo infectivity and pathogenicity of the lymphoid cell-derived woodchuck hepatitis virus. *J. Virol.* 75:1770-1782.

Lee T. H., M. J. Finegold, R. F. Shen, J. L. DeMayo, S. L. Woo, and J. S. Butel. 1990. Hepatitis B virus transactivator X protein is not tumorigenic in transgenic mice. *J. Virol.* 64:5939-5947.

Li X., H. Dancausse, I. Grijalva, M. Oliveira, A. D. Levi. 2003. Labeling Schwann cells with CFSE-an in vitro and in vivo study. *Neurosci. Methods* 125:83-89.

Livingston B. D., J. Alexander, C. Crimi, C. Oseroff, E. Celis, K. Daly, L. G. Guidotti, F. V. Chisari, J. Fikes, R. W. Chesnut, and A. Sette. 1999. Altered helper T lymphocyte function associated with chronic hepatitis B virus infection and its role in response to therapeutic vaccination in humans. *J. Immunol.* 162:3088-3095.

Luckow V. A. 1993. Baculovirus systems for the expression of human gene products. *Curr. Opin. Biotechnol.* 4:564-572.

Lyons A. B. 2000. Analysing cell division in vivo and in vitro using flow cytometric measurement of CFSE dye dilution. *J. Immunol. Methods* 243:147-154.

Lyons A. B., and C. R. Parish. 1994. Determination of lymphocyte division by flow cytometry. *J. Immunol. Methods* 171:131-137.

Lyons A.B., J. Hasbold, and P. D. Hodgkin. 2001. Flow cytometric analysis of cell division history using dilution of carboxyfluorescein diacetate succinimidyl ester, a stably integrated fluorescent probe. *Methods Cell Biol.* 63:375-398.

Magnuson N. S., P. M. Linzmaier, R. Reeves, G. An, K. HayGlass, J. M. Lee. 1998. Secretion of biologically active human interleukin-2 and interleukin-4 from genetically modified tobacco cells in suspension culture. *Protein Expr. Purif.* 13:45-52.

Maini M. K., C. Boni, G. S. Ogg, A. S. King, S. Reignat, C. K. Lee, J. R. Larrubia, G. J. Webster, A. J. McMichael, C. Ferrari, R. Williams, D. Vergani, and A. Bertoletti. 1999. Direct ex vivo analysis of hepatitis B virus-specific CD8(+) T cells associated with the control of infection. *Gastroenterology* 117:1386-96.

Maini M. K., and A. Bertoletti. 2000. How can the cellular immune response control hepatitis B virus replication? *J. Viral. Hepat.* 7:321-326.

Maini M. K., C. Boni, C. K. Lee, J. R. Larrubia, S. Reignat, G. S. Ogg, A. S. King, J. Herberg, R. Gilson, A. Alisa, R. Williams, D. Vergani, N. V. Naoumov, C. Ferrari, A. J. Bertoletti. 2000. The role of virus-specific CD8(+) cells in liver damage and viral control during persistent hepatitis B virus infection. *J. Exp. Med.* 191:1269-1280.

Mannering S. I., J. Zhong, and C. Cheers. 2002. T-cell activation, proliferation and apoptosis in primary *Listeria monocytogenes* infection. *Immunology* 106:87-95.

Mannering S. I., J. S. Morris, K. P. Jensen, A. W. Purcell, M. C. Honeyman, P. M.

van Endert, L. C. Harrison. 2003. A sensitive method for detecting proliferation of rare autoantigen-specific human T cells. *J. Immunol. Methods* 283:173-183.

Marion P. L., L. S. Oshiro, D. C. Regnery, G. H. Scullard, and W. S. Robinson. 1980. A virus in beechey ground squirrels that is related to hepatitis B virus of humans. *Proc. Natl. Acad. Sci. USA* 77:2941-2945.

Margalit M., O. Shibolet, A. Klein, E. Elinav, R. Alper, B. Thalenfeld, D. Engelhardt, E. Rabbani, and Y. Ilan. 2005. Suppression of hepatocellular carcinoma by transplantation of ex-vivo immune-modulated NKT lymphocytes. *Int. J. Cancer* 115:443-449.

Maruyama T., F. Schödel, S. Iino, K. Koike, K. Yasuda, D. Peterson, D. R. Milich. 1994. Distinguishing between acute and symptomatic chronic hepatitis B virus infection. *Gastroenterology* 106:1006-1015.

Maschke J., S. Menne, J. R. Jacob, E. Kreuzfelder, B. C. Tennant, M. Roggendorf, H. Grosse-Wilde. 2001. Thymidine utilization abnormality in proliferating lymphocytes and hepatocytes of the woodchuck. *Vet. Immunol. Immunopathol.* 78:279-296.

Mason W. S., G. Seal, and J. Summers. 1980. Virus of Pekin ducks with structural and biological relatedness to human hepatitis B virus. *J. Virol.* 36:829-836.

Matsumoto C., K. Nishioka, T. Oguchi, S. Mitsunaga, N. Nojiri, K. Tadokoro, T. Juji. 1997. Detection and quantitation of HBV DNA by semi-nested PCR in donated blood: comparison with HBV serological markers. *J. Virol. Methods* 66:61-69.

McRae B. L., T. Nagai, R. T. Semnani, J. M. van Seventer, and G. A. van Seventer. 2000. Interferon-alpha and -beta inhibit the in vitro differentiation of immunocompetent human dendritic cells from CD14(+) precursors. *Blood* 96:210-217.

McChesney M. B., J. R. Collins, D. Lu, X. Lu, J. Torten, R. L. Ashley, M. W. Cloyd, and C. J. Miller. 1998. Occult systemic infection and persistent simian immunodeficiency virus (SIV)-specific CD4(+)-T-cell proliferative responses in rhesus macaques that were transiently viremic after intravaginal inoculation of SIV. *J. Virol.* 72:10029-10035.

Menne S. and P. J. Cote. 2007. The woodchuck as an animal model for pathogenesis and therapy of chronic hepatitis B virus infection. *World J. Gastroenterol.* 13:104-124.

- Menne S., and B. C. Tennant. 1999. Unravelling hepatitis B virus infection of mice and men (and woodchucks and ducks). *Nat. Med.* 5:1125-1126.
- Menne S., J. Maschke, M. Lu, H. Grosse-Wilde, M. Roggendorf. 1998. T-Cell response to woodchuck hepatitis virus (WHV) antigens during acute self-limited WHV infection and convalescence and after viral challenge. *J. Virol.* 72:6083-6091.
- Menne S., J. Maschke, T. K. Tolle, M. Lu, M. Roggendorf. 1997. Characterization of T-cell response to woodchuck hepatitis virus core protein and protection of woodchucks from infection by immunization with peptides containing a T-cell epitope. *J. Virol.* 71:65-74.
- Menne S., C. A. Roneker, M. Roggendorf, J. L. Gerin, P. J. Cote, B. C. Tennant. 2002a. Deficiencies in the acute-phase cell-mediated immune response to viral antigens are associated with development of chronic woodchuck hepatitis virus infection following neonatal inoculation. *J. Virol.* 76:1769-1780.
- Menne S., C. A. Roneker, B. C. Tennant, B. E. Korba, J. L. Gerin, P. J. Cote. 2002b. Immunogenic effects of woodchuck hepatitis virus surface antigen vaccine in combination with antiviral therapy: breaking of humoral and cellular immune tolerance in chronic woodchuck hepatitis virus infection. *Intervirology* 45:237-250.
- Menne S., C. A. Roneker, B. E. Korba, J. L. Gerin, B. C. Tennant, and P. J. Cote. 2002c. Immunization with surface antigen vaccine alone and after treatment with 1-(2-fluoro-5-methyl-beta-L-arabinofuranosyl)-uracil (L-FMAU) breaks humoral and cell-mediated immune tolerance in chronic woodchuck hepatitis virus infection. *J. Virol.* 76:5305-5314
- Menne S., P. J. Cote, S. D. Butler, I. A. Toshkov, J. L. Gerin, and B. C. Tennant. 2007. Immunosuppression reactivates viral replication long after resolution of woodchuck hepatitis virus infection. *Hepatology* 45:614-622.
- Michalak T. I. 2004. Immunology of hepatitis B virus. In *Hepatitis Prevention and Treatment*, Colacino, J.M.; Heinz, B.A., Eds.; Birkhäuser Verlag, Switzerland, 87.
- Michalak T.I., C. Pasquinelli, S. Guilhot, F. V. Chisari. 1994. Hepatitis B virus persistence after recovery from acute viral hepatitis. *J. Clin. Invest.* 93:230-239.
- Michalak T. I., P. M. Mulrooney, and C. S. Coffin. 2004. Low doses of hepadnavirus induce infection of the lymphatic system that does not engage the liver. *J. Virol.* 78:1730-1738.

- Michalak T. I. 2007. Characteristics and consequences of experimental occult hepatitis B virus infection in the woodchuck model of hepatitis B. *Curr. Topics Virol.* 6:1-13.
- Michalak T. I. 1998. The woodchuck animal model of hepatitis B. *Viral Hepatitis Rev.* 4:139-165.
- Michalak T. I., B. Lin, N. D. Churchill, P. Dzwonkowski, and J. R. Desousa. 1990. Hepadnavirus nucleocapsid and surface antigens and the antigen-specific antibodies associated with hepatocyte plasma membranes in experimental woodchuck acute hepatitis. *Lab. Investig.* 62:680-689.
- Michalak T. I. 2000. Occult persistence and lymphotropism of hepadnaviral infection: insights from the woodchuck viral hepatitis model. *Immunol. Rev.* 174:98-111.
- Michalak T. I., I. U. Pardoe, C. S. Coffin, N. D. Churchill, D. S. Freake, P. Smith, and C. L. Trelegan. 1999. Occult lifelong persistence of infectious hepadnavirus and residual liver inflammation in woodchucks convalescent from acute viral hepatitis. *Hepatology* 29:928-938.
- Michalak T. I., and B. Lin. 1994. Molecular species of hepadnavirus core and envelope polypeptides in hepatocyte plasma membrane of woodchucks with acute and chronic viral hepatitis. *Hepatology* 20:275-286.
- Michalak T. I., P. D. Hodgson, and N. D. Churchill. 2000. Posttranscriptional inhibition of class I major histocompatibility complex presentation on hepatocytes and lymphoid cells in chronic woodchuck hepatitis virus infection. *J. Virol.* 74:4483-4494.
- Michalak T. I., T. N. Q. Pham, and P. M. Mulrooney-Cousins. 2007. Molecular diagnosis of occult HCV and HBV infections. *Future Virol.* 2:451-465.
- Michalak T. I. 2004. Immunology of hepatitis B virus. In: Colacino, J.M., Heinz, B.A. (eds.), *Hepatitis prevention and treatment*, Birkhäuser Verlag, Switzerland, pp. 87-105.
- Milich D. R., M. Sallberg, and T. Maruyama. 1995. The humoral immune response in acute and chronic hepatitis B virus infection. *Springer. Semin. Immunopathol.* 17:149-166.
- Milich D. R., M. K. Chen, J. L. Hughes, and J. E. Jones. 1998. The secreted hepatitis B precore antigen can modulate the immune response to the nucleocapsid: a mechanism for persistence. *J. Immunol.* 160:2013-2021.

Milich D. R., J. E. Jones, J. L. Hughes, T. Maruyama, J. Price, I. Melhado, and F. Jirik. 1994. Extrathymic expression of the intracellular hepatitis B core antigen results in T cell tolerance in transgenic mice. *J. Immunol.* 152:455-466.

Milich D. R., and A. McLachlan. 1986. The nucleocapsid of hepatitis B virus is both a T-cell-independent and a T-cell-dependent antigen. *Science* 234:1398-1401.

Miller M. J., S. H. Wei, I. Parker, M. D. Cahalan. 2002. Two-photon imaging of lymphocyte motility and antigen response in intact lymph node. *Science* 296:1869-1873.

Miller-Edge M., and G. A. Splitter. 1984. Bovine interleukin 2 (IL-2) production and activity on bovine and murine cell lines. *Vet. Immunol. Immunopathol.* 7:119-130.

Miyazaki T., Z. J. Liu, A. Kawahara, Y. Minami, K. Yamada, Y. Tsujimoto, E. L. Barsoumian, R. M. Permuter, T. Taniguchi. 1995. Three distinct IL-2 signaling pathways mediated by bcl-2, c-myc, and lck cooperate in hematopoietic cell proliferation. *Cell* 81:223-231.

Monsalve-De Castillo F., T. A. Romero, J. Estévez, L. L. Costa, R. Atencio, L. Porto, D. Callejas. 2002. Concentrations of cytokines, soluble interleukin-2 receptor, and soluble CD30 in sera of patients with hepatitis B virus infection during acute and convalescent phases. *Clin. Diagn. Lab. Immunol.* 9:1372-1375.

Morgan D. A., F. W. Ruscetti, and R. Gallo. 1976. Selective in vitro growth of T lymphocytes from normal human bone marrows. *Science* 193:1007-1008.

Moriyama T., S. Guilhot, K. Klopchin, B. Moss, C. A. Pinkert, R. D. Palmiter, R. L. Brinster, O. Kanagawa, F. V. Chisari. 1990. Immunobiology and pathogenesis of hepatocellular injury in hepatitis B virus transgenic mice. *Science* 248:361-364.

Mueller-Stahl K., T. Kofidis, P. Akhyari, B. Wachsmann, A. Lenz, J. Boublik, M. Heine, V. Muehlfait, A. Haverich, H. Mertsching. 2003. Carboxyfluorescein diacetate succinimidyl ester facilitates cell tracing and colocalization studies in bioartificial organ engineering. *Int. J. Artif. Organs* 26:235-240.

Mulrooney-Cousins P. M., and T. I. Michalak. 2007. Persistent occult hepatitis B virus infection: experimental findings and clinical implications. *World J. Gastroenterol.* 13:5682-5686.

Mulrooney-Cousins P. M., and T. I. Michalak. 2008. Repeated Passage of Wild-Type Woodchuck Hepatitis Virus in Lymphoid Cells Does Not Generate Cell

Type-Specific Variants or Alters Virus Infectivity. *J. Virol.* 82: 7540-7550.

Murakami Y., M. Minami, Y. Daimon, and T. Okanoue. 2004. Hepatitis B virus DNA in liver, serum, and peripheral blood mononuclear cells after the clearance of serum hepatitis B virus surface antigen. *J. Med. Virol.* 72:203-214.

Murali-Krishna K., J. D. Altman, M. Suresh, D. Sourdive, A. Zajac, and R. Ahmed. 1998. In vivo dynamics of anti-viral CD8 T cell responses to different epitopes. An evaluation of bystander activation in primary and secondary responses to viral infection. *Adv. Exp. Med. Biol.* 452:123-42.

Murphy W. J., and J. R. Keller, C. L. Harrison, H. A. Young, and D. L. Longo. 1992. Interleukin-2-activated natural killer cells can support hematopoiesis in vitro and promote marrow engraftment in vivo. *Blood* 80:670-677.

Murray K., S. A. Bruce, A. Hinnen, P. Wingfield, P. M. van Erd, A. de Reus, and H. Schellekens. 1984. Hepatitis B virus antigens made in microbial cells immunise against viral infection. *Embo J.* 3:645-650.

Nakamoto Y., L. G. Guidotti, C. V. Kuhlen, P. Fowler, F. V. Chisari. 1998. Immune pathogenesis of hepatocellular carcinoma. *J. Exp. Med.* 188:341-350.

Nakamura I., J. T. Nupp, B. S. Rao, A. Buckler-White, R. E. Engle, J. L. Casey, J. L. Gerin, P. J. Cote. 1997. Cloning and characterization of partial cDNAs for woodchuck cytokines and CD3epsilon with applications for the detection of RNA expression in tissues by RT-PCR assay. *J. Med. Virol.* 53:85-95.

Nakamura I., J. T. Nupp, M. Cowlen, W. C. Hall, B. C. Tennant, J. L. Casey, J. L. Gerin, and P. J. Cote. 2001. Pathogenesis of experimental neonatal woodchuck hepatitis virus infection: chronicity as an outcome of infection is associated with a diminished acute hepatitis that is temporally deficient for the expression of interferon gamma and tumor necrosis factor-alpha messenger RNAs. *Hepatology* 33:439-447.

Niewiesk S., M. Gotzelmann, and V. ter Meulen. 2000. Selective in vivo suppression of T lymphocyte responses in experimental measles virus infection. *Proc. Natl. Acad. Sci. USA* 97:4251-4255.

Nordon R. E., M. Nakamura, C. Ramirez, R. Odell. 1999. Analysis of growth kinetics by division tracking. *Immunol. Cell Biol.* 77:523-529.

Ochsenbein A. F., D. D. Pinschewer, B. Odermatt, A. Ciurea, H. Hengartner, and R. M. Zinkernagel. 2000. Correlation of T Cell Independence of Antibody Responses with Antigen Dose Reaching Secondary Lymphoid Organs: Implications for Splenectomized Patients and Vaccine Design1. *J. Immunol.*

164:6296-6302.

Ogg G. S., X. Jin, S. Bonhoeffer, P. R. Dunbar, M. A. Nowak, S. Monard, J. P. Segal, Y. Cao, S. L. Rowland-Jones, V. Cerundolo, A. Hurley, M. Markowitz, D. D. Ho, D. F. Nixon, and A. J. McMichael. 1998. Quantitation of HIV-1-specific cytotoxic T lymphocytes and plasma load of viral RNA. *Science* 279:2103-2106.

Okada K., I. Kamiyama, M. Inomata, M. Imai, and Y. Miyakawa. 1976. e antigen and anti-e in the serum of asymptomatic carrier mothers as indicators of positive and negative transmission of hepatitis B virus to their infants. *N. Engl. J. Med.* 294:746-749.

Oostendorp R. A., J. Audet, C. J. Eaves. 2000. High-resolution tracking of cell division suggests similar cell cycle kinetics of hematopoietic stem cells stimulated in vitro and in vivo. *Blood* 95:855-862.

Orange J. S., and C. A. Biron. 1996. Characterization of early IL-12, IFN- $\alpha$ , and TNF effects on antiviral state and NK cell responses during murine cytomegalovirus infection. *J. Immunol.* 156:4746-4756.

Parish C. R., and H. S. Warren. 2001. Use of intracellular fluorescent dye CFSE to monitor lymphocyte migration and proliferation. In *Current protocols in immunology*, J. M. Coligan, A. M. Kruisbeek, D. H. Margulies, E. M. Shevach, W. Strober, Eds.; Greene Publishing Associates and Wiley-Interscience, New York, 4.9.1.

Parish C. R. 1999. Fluorescent dyes for lymphocyte migration and proliferation studies. *Immunol. Cell Biol.* 77:499-508.

Pasquetto V., L. G. Guidotti, K. Kakimi, M. Tsuji, and F. V. Chisari. 2000. Host-virus interactions during malaria infection in hepatitis B virus transgenic mice. *J. Exp. Med.* 192:529-536.

Pedersen C., E. Dickmeiss, J. Gaub, L. P. Ryder, P. Platz, B. O. Lindhardt, and J. D. Lundgren. 1990. T-cell subset alterations and lymphocyte responsiveness to mitogens and antigen during severe primary infection with HIV: a case series of seven consecutive HIV seroconverters. *AIDS* 4:523-526.

Penna A., M. Artini, A. Cavalli, M. Levrero, A. Bertoletti, M. Pilli, F. V. Chisari, B. Rehermann, G. Del Prete, F. Fiaccadori, and C. Ferrari. 1996. Long-lasting memory T cell responses following self-limited acute hepatitis B. *J. Clin. Invest.* 98:1185-1194.

Penna A., G. Del Prete, A. Cavalli, A. Bertoletti, M. M. D'Elios, R. Sorrentino, M. D'Amato, C. Boni, M. Pilli, F. Fiaccadori, C. Ferrari. 1997. Predominant T-helper

1 cytokine profile of hepatitis B virus nucleocapsid-specific T cells in acute self-limited hepatitis B. *Hepatology* 1997 25:1022-1027.

Pinto L. A., J. Sullivan, J. A. Berzofsky, M. Clerici, H. A. Kessler, A. L. Landay, and G. M. Shearer. 1995. ENV-specific cytotoxic T lymphocyte responses in HIV seronegative health care workers occupationally exposed to HIV-contaminated body fluids. *J. Clin. Invest.* 96:867-876.

Prince A. M., J. Vnek, W. Stephan. 1983. A new hepatitis B vaccine containing HBsAg in addition to HbsAg. *Dev. Biol. Stand.* 54:13-22.

Promadej N., C. Costello, M. M. Wernett, P. S. Kulkarni, V. A. Robison, K. E. Nelson, T. W. Hodge, V. Suriyanon, A. Duerr, and J. M. McNicholl. 2003. Broad human immunodeficiency virus (HIV)-specific T cell responses to conserved HIV proteins in HIV-seronegative women highly exposed to a single HIV-infected partner. *J. Infect. Dis.* 187:1053-1063.

Quiroga J. A., S. Llorente, I. Castillo, E. Rodríguez-Iñigo, M. Pardo, and V. Carreño. 2006. Cellular immune responses associated with occult hepatitis C virus infection of the liver. *J. Virol.* 80:10972-10979.

Raimondo G., T. Pollicino, I. Cacciola, and G. Squadrito. 2006. Occult hepatitis B virus infection. *J. Hepatol.* 46:160-170.

Reeves R., A. G. Spies, M. S. Nissen, C.D. Buck, A. D. Weinberg, P. J. Barr, N. S. Magnuson, J. A. Magnuson. 1986. Molecular cloning of a functional bovine interleukin 2 cDNA. *Proc. Natl. Acad. Sci. USA* 83:3228-3232.

Rehermann B. and M. Nascimbeni. 2005. Immunology of hepatitis B virus and hepatitis C virus infection. *Nat. Rev. Immunol.* 5:215-29.

Rehermann B., C. Ferrari, C. Pasquinelli, F. V. Chisari. 1996. The hepatitis B virus persists for decades after patients' recovery from acute viral hepatitis despite active maintenance of a cytotoxic T-lymphocyte response. *Nat. Med.* 2:1104-1108.

Rehermann B., P. Fowler, J. Sidney, J. Person, A. Redeker, M. Brown, B. Moss, A. Sette, and F. V. Chisari. 1995. The cytotoxic T lymphocyte response to multiple hepatitis B virus polymerase epitopes during and after acute viral hepatitis. *J. Exp. Med.* 181:1047-1058.

Reifenberg K., J. Lohler, H. P. Pudollek, E. Schmitteckert, G. Spindler, J. Kock, and H. J. Schlicht. 1997. Long-term expression of the hepatitis B virus core-e and X-proteins does not cause pathologic changes in transgenic mice. *J. Hepatol.* 26:119-130.

- Renno T., A. Attinger, S. Locatelli, T. Bakker, S. Vacheron, H. R. MacDonald. 1999. Cutting edge: apoptosis of superantigen-activated T cells occurs preferentially after a discrete number of cell divisions in vivo. *J. Immunol.* 162:6312-6315.
- Rentenaar R. J., L. E. Gamadia, N. van DerHoek, F. N. van Diepen, R. Boom, J. F. Weel, P. M. Wertheim-van Dillen, R. A. van Lier, and I. J. ten Berge. 2000. Development of virus-specific CD4(+) T cells during primary cytomegalovirus infection. *J. Clin. Invest.* 105:541-548.
- Risteovski B., A. J. Young, L. Dudler, R. N. Cahill, W. Kimpton, E. Washington, J. B. Hay. 2003. Tracking dendritic cells: use of an in situ method to label all blood leukocytes. *Int. Immunol.* 15:159-165.
- Rocha B., and C. Tanchot. 2006. The Tower of Babel of CD8+ T-cell memory: known facts, deserted roads, muddy waters, and possible dead ends. *Immunol. Rev.* 211:182-96.
- Robb R. J., A. Munck, and K. A. Smith. 1981. T cell growth factor receptors. Quantitation, specificity, and biological relevance. *J. Exp. Med.* 154:1455-1474.
- Sathiyaseelan T., and C. L. Baldwin. 2000. Evaluation of cell replication by bovine T cells in polyclonally activated cultures using carboxyfluorescein succinimidyl ester (CFSE) loading and flow cytometric analysis. *Res. Vet. Sci.* 69:275-281.
- Sato T., H. Matsui, S. Shibahara, T. Kobayashi, Y. Morinaga, N. Kashima, S. Yamasaki, J. Hamuro, T. Taniguchi. 1987. New approaches for the high-level expression of human interleukin-2 cDNA in *Escherichia coli*. *J. Biochem. (Tokyo)* 101:525-534.
- Schneider S., A. Bruns, B. Moewes, B. Holzknacht, G. Hausdorf, G. Riemekasten, A. Radbruch, F. Hiepe, A. Thiel. 2002. Simultaneous cytometric analysis of (auto)antigen-reactive T and B cell proliferation. *Immunobiology* 206:484-495.
- Sciutto E., G. Fragoso, M. Baca, V. De la Cruz, L. Lemus, and E. Lamoyi. 1995. Depressed T-cell proliferation associated with susceptibility to experimental *Taenia crassiceps* infection. *Infect. Immun.* 63:2277-2281.
- Seeger C., and W. S. Mason. 2000. Hepatitis B virus biology. *Microbiol. Mol. Biol. Rev.* 64:51-68.
- Servet-Delprat C., S. Arnaud, P. Jurdic, S. Nataf, M. F. Grasset, C. Soulas, C.

Domenget, O. Destaing, A. Rivollier, M. Perret, C. Dumontel, D. Hanau, G. L. Gilmore, M. F. Belin, C. Rabourdin-Combe, G. Mouchiroud. 2002. *Fit3+* macrophage precursors commit sequentially to osteoclasts, dendritic cells and microglia. *BMC Immunol.* 3:15-26.

Shanmuganathan S., J. A. Waters, P. Karayiannis, M. Thursz, H. C. Thomas. 1997. Mapping of the cellular immune responses to woodchuck hepatitis core antigen epitopes in chronically infected woodchucks. *J. Med. Virol.* 52:128-135.

Shibolet O., R. Alper, L. Zlotogarov, B. Thalenfeld, D. Engelhardt, E. Rabbani, Y. Ilan. 2003. NKT and CD8 lymphocytes mediate suppression of hepatocellular carcinoma growth via tumor antigen-pulsed dendritic cells. *Int. J. Cancer* 106:236-243.

Siefer A. K., D. L. Longo, C. L. Harrison, C. W. Reynolds, and W. J. Murphy. 1993. Activated natural killer cells and interleukin-2 promote granulocytic and megakaryocytic reconstitution after syngeneic bone marrow transplantation in mice. *Blood* 82:2577-2584.

Siegal F. P., N. Kadowaki, M. Shodell, P. A. Fitzgerald-Bocarsly, K. Shah, S. Ho, S. Antonenko, Y. J. Liu. 1999. The nature of the principal type 1 interferon-producing cells in human blood. *Science* 284:1835-1837.

Sitia G., M. Isogawa, K. Kakimi, S. F. Wieland, F. V. Chisari, and L. G. Guidotti. 2002. Depletion of neutrophils blocks the recruitment of antigen-nonspecific cells into the liver without affecting the antiviral activity of hepatitis B virus-specific cytotoxic T lymphocytes. *Proc. Natl. Acad. Sci. USA* 99:13717-13722.

Sjogren M. H. 2005. Prevention of hepatitis B in nonresponders to initial hepatitis B virus vaccination. *Am. J. Med.* 118 (Suppl 10A):34S-39S.

Smith K. 1988. Interleukin-2: inception, impact, and implications. *Science* 240:1169-1176.

Smith G. E., G. Ju, B. L. Ericson, J. Moschera, H. W. Lahm, R. Chizzonite, M. D. Summers. 1983. Modification and secretion of human interleukin 2 produced in insect cells by a baculovirus expression vector. *Proc. Natl. Acad. Sci. USA* 82:8404-8408.

Sodomann C. P., M. Rother, K. Havemann, and G. A. Martini. 1979. Lymphocyte proliferation to phytohemagglutinin (PHA) in hepatitis B antigen-positive and -negative hepatitis. *Res. Exp. Med. (Berl)* 175:95-107.

Sousa R. C., A. Sher, and P. Kaye. 1999. The role of dendritic cells in the

induction and regulation of immunity to microbial infection. *Curr. Opin. Immunol.* 11:392-399.

Sprengel R., E. F. Kaleta, and H. Will. 1988. Isolation and characterization of a hepatitis B virus endemic in herons. *J. Virol.* 62:3832-3839.

Stacey S. N., A. Ghosh, J. S. Bartholomew, R. W. Tindle, P. L. Stern, M. Mackett, J. R. Arrand. 1993. Expression of human papillomavirus type 16 E7 protein by recombinant baculovirus and use for the detection of E7 antibodies in sera from cervical carcinoma patients. *J. Med. Virol.* 40:14-21.

Stemler M., T. Weimer, Z. X. Tu, D. F. Wan, M. Levrero, C. Jung, G. R. Pape, and H. Will. 1990. Mapping of B-cell epitopes of the human hepatitis B virus X protein. *J. Virol.* 64:2802-2809.

Stern A. S., Y C. Pan, D. L. Urdal, D. Y. Mochizuki, S. DeChiara, R. Blacher, J. Wideman, S. Gillis. 1984. Purification to homogeneity and partial characterization of interleukin 2 from a human T-cell leukemia. *Proc. Natl. Acad. Sci. USA* 81:871-875.

Sternlicht M. D., and Z. Werb. 2001. How matrix metalloproteinases regulate cell behavior. *Annu. Rev. Cell Dev. Biol.* 17:463-516.

Su H. C., J. S. Orange, L. D. Fast, A. T. Chan, S. J. Simpson, C. Terhorst, and C. A. Biron. 1994. IL-2-dependent NK cell responses discovered in virus-infected beta 2-microglobulin-deficient mice. *J. Immunol.* 153:5674-5681.

Su H. C., K. B. Nguyen, T. P. Salazar-Mather, M. C. Ruzek, M. Y. Dalod, and C. A. Biron. 2001. NK cell functions restrain T cell responses during viral infections. *Eur. J. Immunol.* 31:3048-3055.

Summers J., J. M. Smolec, and R. Snyder. 1978. A virus similar to human hepatitis B virus associated with hepatitis and hepatoma in woodchucks. *Proc. Natl. Acad. Sci. USA* 75:4533-4537.

Suri D., R. Schilling, A. R. Lopes, I. Mullerova, G. Colucci, R. Williams, N. V. Naoumov. 2001. Non-cytolytic inhibition of hepatitis B virus replication in human hepatocytes. *J. Hepatol.* 35:790-797.

Swain S. L., J. N. Agrewala, D. M. Brown, D. M. Jelley-Gibbs, S. Golech, G. Huston, S. C. Jones, C. Kamperschroer, W. H. Lee, K. K. McKinstry, E. Román, T. Strutt, and N. P. Weng. 2006. CD4+ T-cell memory: generation and multi-faceted roles for CD4+ T cells in protective immunity to influenza. *Immunol. Rev.* 211:8-22.

Swann J. B., J. M. Coquet, M. J. Smyth, D. I. Godfrey. 2007. CD1-restricted T cells and tumor immunity. *Curr. Top. Microbiol. Immunol.* 314:293-323.

Takashima H., K. Araki, J. Miyazaki, K. Yamamura, and M. Kimoto. 1992. Characterization of T-cell tolerance to hepatitis B virus (HBV) antigen in transgenic mice. *Immunology* 75:398-405.

Taniguchi T., H. Matsui, T. Fujita, C. Takaoka, N. Kashima, R. Yoshimoto, J. Hamuro. 1983. Structure and expression of a cloned cDNA for human interleukin-2. *Nature* 302:305-310.

Tarlinton D. M., F. Batista, and K. G. Smith. 2008. The B-Cell Response to Protein Antigens in Immunity and Transplantation. *Transplantation* 85:1698-1704.

Tasca S., L. Tsai, N. Trunova, A. Gettie, M. Saifuddin, R. Bohm, L. Chakrabarti, and C. Cheng-Mayer. 2007. Induction of potent local cellular immunity with low dose X4 SHIV(SF33A) vaginal exposure. *Virology* 367:196-211.

Tennant B. C., and J. L. Gerin. 2001. The woodchuck model of hepatitis B virus infection. *ILAR J.* 42:89-102.

Tennant B. C., I. A. Toshkov, S. F. Peek, J. R. Jacob, S. Menne, W. E. Hornbuckle, R. D. Schinazi, B. E. Korba, P. J. Cote, and J. L. Gerin. 2004. Hepatocellular carcinoma in the woodchuck model of hepatitis B virus infection. *Gastroenterology* 127:S283-S293.

Testut P., C. A. Renard, O. Terradillos, L. Vitvitski-Trepo, F. Tekaia, C. Degott, J. Blake, B. Boyer and M. A. Buendia. 1996. A new hepadnavirus endemic in arctic ground squirrels in Alaska. *J. Virol.* 70:4210-4219.

Thimme R., S. Wieland, C. Steiger, J. Ghayeb, K. A. Reimann, R. H. Purcell, and F. V. Chisari. 2003. CD8(+) T cells mediate viral clearance and disease pathogenesis during acute hepatitis B virus infection. *J. Virol.* 77:68-76.

Thursz M. R., H. C. Thomas, B. M. Greenwood, A. V. Hill. 1997. Heterozygote advantage for HLA class-II type in hepatitis B virus infection. *Nat. Genet.* 17:11-12.

Torbenson M., and D. L. Thomas. 2002. Occult hepatitis B. *Lancet. Infect. Dis.* 2:479-486.

Tsui L. V., L. G. Guidotti, T. Ishikawa, and F. V. Chisari. 1995. Posttranscriptional clearance of hepatitis B virus RNA by cytotoxic T lymphocyte-activated hepatocytes. *Proc. Natl. Acad. Sci. USA* 92:12398-12402.

- Uprichard S. L., S. F. Wieland, A. Althage, and F. V. Chisari. 2003. Transcriptional and posttranscriptional control of hepatitis B virus gene expression. *Proc. Natl. Acad. Sci. USA* 100:1310-1315.
- Usherwood E.J., G. Crowther, D. L. Woodland. 1999. Apoptotic cells are generated at every division of in vitro cultured T cell lines. *Cell Immunol.* 196:131-137.
- Vidalain P. O., O. Azocar, B. Lamouille, A. Astier, C. Rabourdin-Combe, C. Servet-Delprat. 2000. Measles virus induces functional TRAIL production by human dendritic cells. *J. Virol.* 74:556-559.
- Waldman T. A. 1993. The IL-2/IL-2 receptor system: a target for rational immune intervention. *Immunol. Today* 14:264-270.
- Walker E., T. Leemhuis, and W. Roeder. 1988. Murine B lymphoma cell lines release functionally active interleukin 2 after stimulation with *Staphylococcus aureus*. *J. Immunol.* 140:859-865.
- Wallace M., P. M. Waterman, J. L. Mitchen, M. Djavani, C. Brown, P. Trivedi, D. Horejsh, M. Dykhuizen, M. Kitabwalla, and C. D. Pauza. 1999. Lymphocyte activation during acute simian/human immunodeficiency virus SHIV (89.6PD) infection in macaques. *J. Virol.* 73:10236-10244.
- Wang J., and T. I. Michalak. 2005. Comparison of biological activity of recombinant woodchuck interferon gamma and tumor necrosis factor alpha produced in baculovirus and *Escherichia coli* expression systems. *Cytokine* 30:22-34.
- Wang J., S. A. Gujar, L. Cova, and T. I. Michalak. 2007. Bicistronic woodchuck hepatitis virus core and gamma interferon DNA vaccine can protect from hepatitis but does not elicit sterilizing antiviral immunity. *J. Virol.* 81:903-916.
- Warren H. S. 1999. Using carboxyfluorescein diacetate succinimidyl ester to monitor human NK cell division: analysis of the effect of activating and inhibitory class I MHC receptors. *Immunol. Cell Biol.* 77:544-551.
- Warren H. S., and B. F. Kinnear. 1999. Quantitative analysis of the effect of CD16 ligation on human NK cell proliferation. *J. Immunol.* 162:735-742.
- Webster G. J., S. Reignat, M. K. Maini, S. A. Whalley, G. S. Ogg, A. King, D. Brown, P. L. Amlot, R. Williams, D. Vergani, G. M. Dusheiko, and A. Bertoletti. 2000. Incubation phase of acute hepatitis B in man: dynamic of cellular immune mechanisms. *Hepatology* 32:1117-1124.

- Weijer K., C. H. Uittenbogaart, A. Voordouw, F. Couwenberg, J. Seppen, B. Blom, F. A. Vyth-Dreese, H. Spits. 2002. Intrathymic and extrathymic development of human plasmacytoid dendritic cell precursors in vivo. *Blood* 99:2752-2759.
- Weimer, T., K. Weimer, Z. X. Tu, M. C. Jung, G. R. Pape, and H. Will. 1989. Immunogenicity of human hepatitis B virus P-gene derived proteins. *J. Immunol.* 143:3750-3756.
- Weinberger K. M., T. Bauer, S. Böhm, and W. Jilg. 2000. High genetic variability of the group-specific a-determinant of hepatitis B virus surface antigen (HBsAg) and the corresponding fragment of the viral polymerase in chronic virus carriers lacking detectable HBsAg in serum. *J. Gen. Virol.* 81:1165-1174.
- Wherry E. J., D. L. Barber, S. M. Kaech, J. N. Blattman, and R. Ahmed. 2004. Antigen-independent memory CD8 T cells do not develop during chronic viral infection. *Proc. Natl. Acad. Sci. USA* 101:16004-16009.
- Wieland S., R. Thimme, R. H. Purcell, F. V. Chisari. 2004. Genomic analysis of the host response to hepatitis B virus infection. *Proc. Natl. Acad. Sci. USA* 101:6669-6674.
- Wieland S. F., L. G. Guidotti, and F. V. Chisari. 2000. Intrahepatic induction of alpha/beta interferon eliminates viral RNA-containing capsids in hepatitis B virus transgenic mice. *J. Virol.* 74:4165-4173.
- Wiesner I. S., H. M. Rawnsley, F. P. Brooks, and J. R. Senior. 1965. Sorbitol dehydrogenase in the diagnosis of liver disease. *Am. J. Dig. Dis.* 10:147-151.
- World Health Organization. Hepatitis B. World Health Organization Fact Sheet 204 (Revised October 2000). WHO Website  
<http://www.who.int/mediacentre/factsheets/fs204/en/>
- Yee J. K. 1989. A liver-specific enhancer in the core promoter region of human hepatitis B virus. *Science* 246:658-661.
- Yuki N., Nagaoka, T., Yamashiro, M., Mochizuki, K., Kaneko, A., Yamamoto, K., Omura, M., Hikiji, K., and Kato, M. 2003. Long-term histologic and virologic outcomes of acute self-limited hepatitis B. *Hepatology* 37:1172-1179.
- Zajac A. J., J. N. Blattman, K. Murali-Krishna, D. J. Sourdive, M. Suresh, J. D. Altman, and R. Ahmed. 1998. Viral immune evasion due to persistence of activated T cells without effector function. *J. Exp. Med.* 188:2205-2213.
- Zanetti M. and G. Franchini. 2006. T cell memory and protective immunity by

vaccination: is more better? *Trends Immunol.* 27:511-517.

Zanetti A. R., Mariano, A., Romanò, L., D'Amelio, R., Chironna, M., Coppola, R.C., Cuccia, M., Mangione, R., Marrone, F., Negrone, F.S., Parlato, A., Zamparo, E., Zotti, C., Stroffolini, T., Mele, A. and Study Group. 2005. Long-term immunogenicity of hepatitis B vaccination and policy for booster: an Italian multicentre study. *Lancet* 366:1379-1384.

Zhou J. Y., J. G. Chen, J. Y. Wang, J. X. Wu, H. Gong. 2005. cDNA cloning and functional analysis of goose interleukin-2. *Cytokine* 30:328-338.

Zhang J., S. Zou, and A. Giulivi. 2001. Viral Hepatitis and Emerging Bloodborne Pathogens in Canada: Hepatitis B in Canada Public Health Agency of Canada, Canada Communicable Disease Report 27:10-12.

Zoulim F., J. Saputelli, and C. Seeger. 1994. Woodchuck hepatitis virus X protein is required for viral infection in vivo. *J. Virol.* 68:2026-2030.

**APPENDIX A: Complete cDNA sequence of woodchuck interleukin-2 (wIL-****2) identified during this study**

LOCUS DQ272238 527 bp mRNA linear ROD 20-JUL-2006

DEFINITION *Marmota monax* interleukin-2 mRNA, complete cds.

ACCESSION DQ272238

VERSION DQ272238.1 GI:82592680

## KEYWORDS

SOURCE *Marmota monax* (woodchuck)

ORGANISM *Marmota monax*

Eukaryota; Metazoa; Chordata; Craniata; Vertebrata; Euteleostomi;

Mammalia; Eutheria; Euarchontoglires; Glires; Rodentia;

Sciurognathi; Sciuridae; Xerinae; Marmotini; *Marmota*.

## REFERENCE 1 (bases 1 to 527)

AUTHORS Gujar, S.A. and Michalak, T.I.

TITLE Characterization of bioactive recombinant woodchuck interleukin-2 amplified by RLM-RACE and produced in eukaryotic expression system

JOURNAL *Vet. Immunol. Immunopathol.* 112 (3-4), 183-198 (2006)

PUBMED 16631932

## REFERENCE 2 (bases 1 to 527)

AUTHORS Gujar, S.A. and Michalak, T.I.

TITLE Direct Submission

Submitted (31-OCT-2005) Molecular Virology and Hepatology Research, Faculty of Medicine, Memorial University, 300 Prince Philip Drive, St. John's, NL A1B 3V6, Canada

1 atcacactct ccaatcacta ctccggaac ctgactcta ccgcatgca cccatgccc  
 61 ctgctgtct gctctgcact gactctgca ctggtgac acggtgacc cacctcggc  
 121 tctcgagagg agacaaggca gcagctgaa caactgtgc tggacttga gatgctttc  
 181 agaggtgtca gtaatcaaga gaattccaca ctaccagga tgcgaaatt caaatttac  
 241 atgcccata aggttctga cctggagcat ctctagtc tagaggaaga actcaaacct  
 301 ctgcaggaag tgctgaatgt acctcaaagc aaaaacttc acttgaaga taccaggaac  
 361 ttcatcaga acatcaactg gactgttctg aaactaaagg gatccgccac gacgttcat  
 421 tgtgagtacg ccccgagac agcgaacatt gtagaattc tgaacacatg gatcacctt  
 481 tgccaaagca tcatctgaa gctcactga gaattagtg cctcccg

**APPENDIX B: Frequently used molecular biology buffers and reagents**

**ACK buffer:** 0.15 M  $\text{NH}_4\text{Cl}$ , 1 mM  $\text{KHCO}_3$ , pH 7.3, with 0.1 mM EDTA

**Binding buffer A:** 50 mM Sodium Phosphate (pH 8.0), 300 mM NaCl, 8 M Urea

**Denaturing buffer B:** 50 mM Sodium Phosphate (pH 7.0), 300 mM NaCl, 8 M Urea

**Washing buffer C:** 50 mM Sodium Phosphate (pH 7.0), 300 mM NaCl, 8 M Urea, 7.5 mM Imidazole

**Elution buffer E:** 45 mM Sodium Phosphate (pH 7.0), 8 M Urea, 270 mM NaCl, 150 mM Imidazole.

**GTE (glucose/Tris/EDTA):** 50 mM glucose, 10 mM EDTA in 10 mM Tris-HCl buffer, pH 8.0

**P1 solution:** 50 mM Tris I (pH 8.0), 10 mM EDTA, 100  $\mu\text{g/ml}$  RNase A

**P2 solution:** 200 mM NaOH, 1% SDS (w/v)

**P3 solution:** 3.0 M potassium acetate (pH 5.5)

**QBT buffer:** 750 mM NaCl, 50 mM MOPS (pH 7.0), 15% isopropanol (v/v), 0.15% Triton X-100 (v/v)

**QC buffer:** 1.0 M NaCl, 50 mM MOPS, pH 7.0; 15% isopropanol (v/v)

**QF buffer:** 1.25 M NaCl, 50 mM Tris-HCl (pH 8.5), 15% isopropanol (v/v)

**Superbroth:** 12 g Bacto-tryptone, 24 g Bacto-yeast extract, 4.0 mL glycerol and water to a final volume of 900 ml and autoclave. One liter of superbroth is prepared by adding 100 mL of a sterile solution of 0.17 M  $\text{KH}_2\text{PO}_4$  & 0.72 M  $\text{K}_2\text{HPO}_4$ .

All reagents were obtained from Sigma Chemical Co. unless otherwise noted.



